SMITHSONIAN CONTRIBUTIONS TO THE EARTH SCIENCES • NUMBER 26

Field and Laboratory Investigations of Meteorites from Victoria Land, Antarctica

Ursula B. Marvin
and Brian Mason

EDITORS

SMITHSONIAN INSTITUTION PRESS
City of Washington
1984

ABSTRACT

Marvin, Ursula B., and Brian Mason, editors. Field and Laboratory Investigations of Meteorites from Victoria Land, Antarctica. *Smithsonian Contributions to the Earth Sciences*, number 26, 134 pages, frontispiece, 79 figures, 11 tables, 1984.—This monograph describes the meteorite collecting activities in Victoria Land during the 1980–1981 and 1981–1982 field seasons, and the geodetic measurements of ice motion and ablation at the Allan Hills site. Descriptions and classifications are given for all specimens collected during the 1980–1981 season and for most of those collected during the 1981–1982 season. Review articles are included on the petrology and classification of 145 small meteorites collected in the 1977–1978 season, on Antarctic Type 3 chondrites, and on cosmic-ray-produced nuclides in the Victoria Land meteorites. The first lunar meteorite is described. Chemical analyses of 25 Victoria Land meteorites are published, with a discussion of Antarctic weathering effects. The Appendix lists all of the Victoria Land meteorites classified as of June 1983, by numerical order for each locality and by meteorite class.

OFFICIAL PUBLICATION DATE is handstamped in a limited number of initial copies and is recorded in the Institution's annual report, *Smithsonian Year*. SERIES COVER DESIGN: Aerial view of Ulawun Volcano, New Britain.

Library of Congress Cataloging in Publication Data
Main entry under title:
Field and laboratory investigations of meteorites from Victoria Land, Antarctica.
(Smithsonian contributions to the earth sciences ; no. 26)
Bibliography: p.
1. Meteorites—Antarctic regions. I. Marvin, Ursula B. II. Mason, Brian Harold, 1917–
III. Series.
QE1.S227 no. 26 [QB755.5A] 550s [523.5'1] 83-20087

Contents

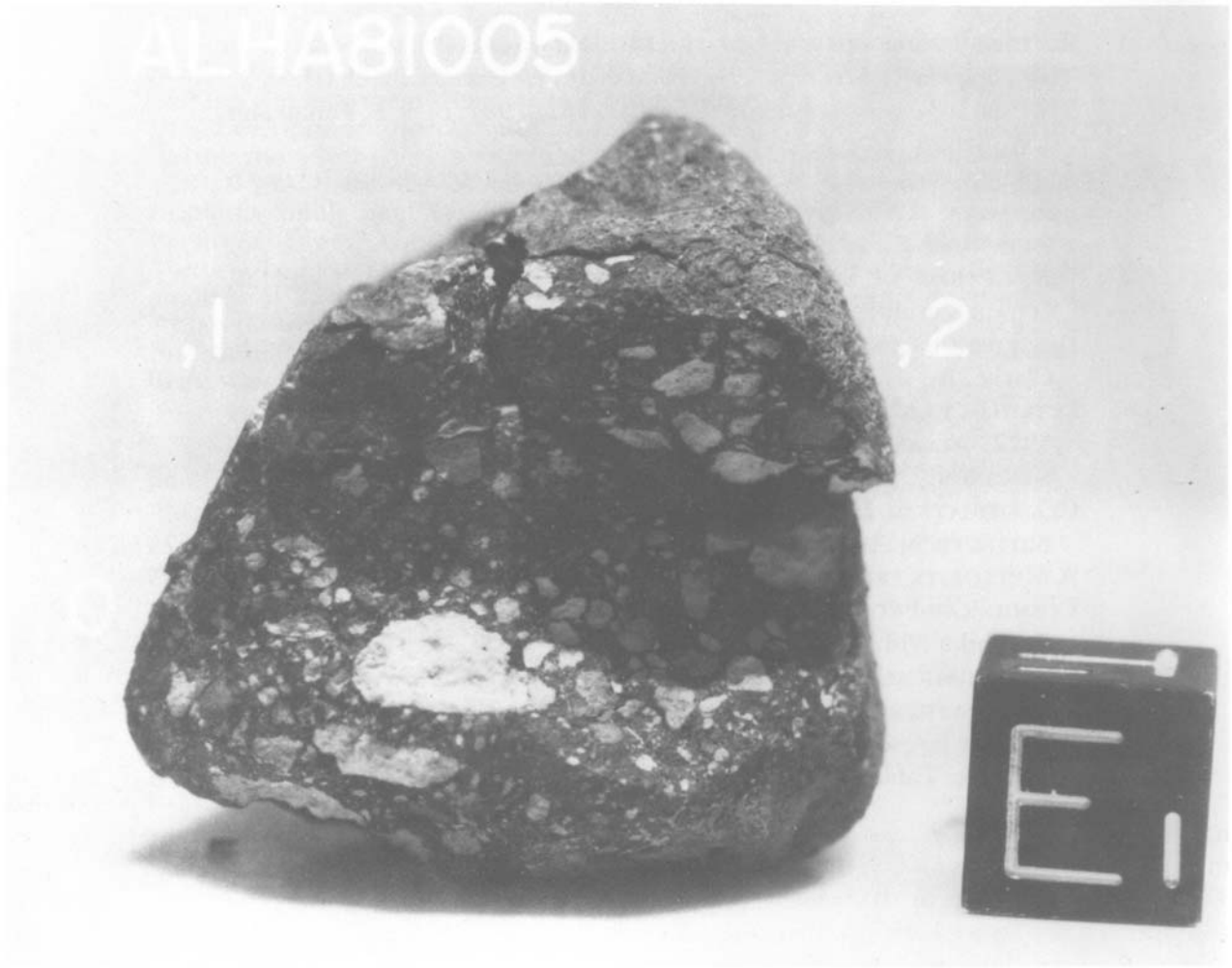

Allan Hills 81005, the first lunar rock to be discovered on the surface of Earth. Photograph taken before processing at the Curatorial Facility in the NASA Johnson Space Center at Houston.

Field and Laboratory Investigations of Meteorites from Victoria Land, Antarctica

Editors' Introduction

Ursula B. Marvin and Brian Mason

This is the third publication in the Smithsonian Contributions to the Earth Sciences series to review the results of the yearly United States expeditions to collect meteorites in Victoria Land, Antarctica. The first two publications were *Catalog of Antarctic Meteorites, 1977–1978* (Marvin and Mason, 1980) and *Catalog of Meteorites from Victoria Land, Antarctica, 1978–1980* (Marvin and Mason, 1982). Both publications were much more than catalogs. They included descriptions of field and laboratory investigations and overview articles on the more interesting types of Antarctic meteorites. This third publication in the series continues this practice and so we have dropped the word "Catalog" from the title.

This issue describes the 1980–1981 and 1981–1982 field seasons in Victoria Land. It contains chapters outlining the results of the first geophysical measurements of ice thickness and the continuing geodetic measurements of ablation and ice motion in the Allan Hills region. All specimens weighing more than 100 grams, collected in those two seasons, are described and classified. In addition, the classifications of several groups of smaller, pebble-sized specimens, collected in the 1977–1978 season, have been added to the updated lists in the Appendices. Appendix Table A lists all of the Victoria Land meteorites, classified by May 1983, for each locality by consecutive numbers; Appendix Table B lists specimens consecutively by meteorite class; and Appendix Table C lists the specimens currently believed to be paired. One chapter reviews new observations on the rare and relatively primitive Type 3 chondrites from Antarctica; another presents the latest measurements of cosmogenic nuclides and terrestrial ages of Antarctic meteorites. A computerized Antarctic Meteorite Bibliography is maintained at the Lunar and Planetary Institute (3303 NASA Road 1, Houston, Texas 77058) and lists of publications from it are available on request.

The highlight of the Antarctic collecting program is the discovery, on the final day of the 1981–1982 field season, of the first lunar sample ever to be found on the surface of the Earth. A brief account is presented of the field

Ursula B. Marvin, Smithsonian Astrophysical Observatory, 60 Garden Street, Cambridge, Massachusetts 02138. Brian Mason, Department of Mineral Sciences, National Museum of Natural History, Smithsonian Institution, Washington, D.C. 20560.

occurrence and initial characterization of this specimen.

The total numbers and classifications of meteorite specimens collected in the 1980–1981 and 1981–1982 seasons are listed in Table 1. After six successive seasons of searches, the Main Icefield at the Allan Hills region still yields new specimens yearly, and exploration has barely begun of the vast reaches of blue ice in the Middle Western and Far Western icefields. (For the configuration of these fields see Marvin, herein, p. 96.) During preparation of this publication, we received news that reconnaissance work in the 1982–1983 season revealed the presence of rich new lodes of specimens in the area of the Thiel Mountains (Figure 1). The fruitfulness of the Antarctic Meteorite Program is thus assured for the foreseeable future.

The field explorations and laboratory research are both increasingly international in

TABLE 1.—Numbers of meteoritic specimens collected in the 1980–1981 and 1981–1982 (in parentheses) seasons.

Class	Allan Hills	Reckling Peak	Outpost Nunatak	Totals
Chondrites	30 (355)	60	1	91
Carbonaceous chondrites	0 (4)	0	0	0
Achondrites	1 (10)	2	0	3
Mesosiderites	0 (2)	4	0	4
Irons	1 (2)	1	0	2
Totals	32 (373)	67	1	100

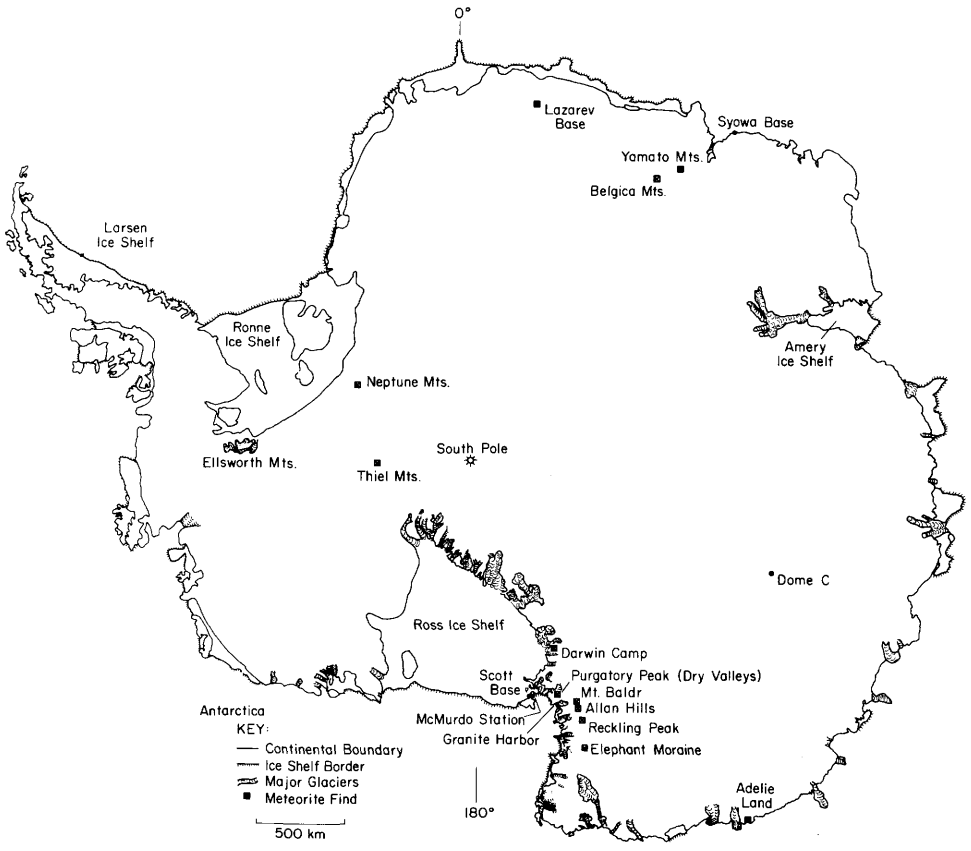

FIGURE 1.—Map of Antarctic meteorite finds. Four meteorites were discovered before the beginning of the current program: Adelie Land, 1912; Lazarev, 1961; Thiel Mountains, 1962; and Neptune Mountains, 1964. Meteorite concentrations were discovered by a United States party in the Thiel Mountains during the 1982–1983 season.

scope. The Japanese program has just completed its eighth season, working out of Syowa Base in the regions of the Yamato and Belgica Mountains. Japanese scientists also spent three seasons with the United States field parties in Victoria Land. The United States program, led by William A. Cassidy of the University of Pittsburgh, began work in Antarctica in 1976 and has spent seven seasons conducting searches along the interior flank of the Transantarctic Range at sites within helicopter range of McMurdo Station. The United States field parties have included members from Japan, West Germany, Denmark, and Switzerland, and future teams are expected to include members from Australia and other countries. Specimens from the United States collections have been distributed to at least ninety research laboratories in thirteen countries.

Approximately 7000 specimens, most of them weighing only a few grams, have been collected in the past ten years by the Japanese and United States scientists. These specimens are important not for their numbers but because they include new varieties of meteorites, which have not been found on other continents, and additional specimens of certain very rare species. Furthermore, isotopic measurements of terrestrial residence times show that the Antarctic specimens landed on the Antarctic ice sheet between 10,000 and 700,000 years ago, with some fall dates clustering between 100,000 and 400,000 years. Most meteorites collected on other continents fell within the past 200 years, although a few stones fell as early as 20,000 years ago. Thus, the Antarctic ice sheet is furnishing us with a somewhat older sample of the stony materials that have followed Earth-crossing orbits. These results have aroused the interest of glacial geologists, who are examining the relationship between meteorite concentrations on bare icefields and the age and flow patterns of the ice in the catchment areas. The Antarctic occurrences have prompted Canadian and Danish scientists to explore for similar meteorite concentrations in the Canadian Arctic and Greenland.

The United States Antarctic Search for Meteorites (ANSMET) is governed by an interagency agreement between the National Science Foundation, the Smithsonian Institution, and the National Aeronautics and Space Administration. Procedures have been developed, based loosely on those followed by the Apollo astronauts, for collecting the specimens by sterile techniques and keeping them frozen until they are processed in nitrogen-filled glove cabinets at the Johnson Space Center in Houston. Details of the field and laboratory procedures are outlined in the first publication in this series (Marvin and Mason, 1980). With the intent of distributing research samples quickly and widely, all newly classified specimens are described in the *Antarctic Meteorite Newsletter* and mailed, on request, to investigators throughout the world. Any scientist wishing to obtain samples may submit a request, describing the proposed research and the numbers, weights, and types of samples required, to the Meteorite Working Group, a committee with a rotating membership responsible for monitoring the program and allocating samples. Requests for the *Antarctic Meteorite Newsletter* or for research samples should be addressed to the Secretary, Meteorite Working Group, Lunar and Planetary Institute, 3303 NASA Road 1, Houston, Texas 77058.

The Antarctic Meteorite Working Group meets twice each year, usually in April and September. Each issue of the newsletter publishes dates of meetings and deadlines for sample requests. Sample requests are welcome from all qualified scientists and are considered on the basis of their merit regardless of whether a scientist is funded for meteorite research. The allocation of Antarctic meteorite samples does not in any way commit a funding agency to support the proposed research.

Libraries of polished thin sections have been established in Washington, Houston, and Tokyo for the use of visitors who wish to make microscopic examinations. The library thin sections are not available for loan. To obtain

meteorite samples from the Japanese collections or to use the thin section library in Tokyo, contact T. Nagata, Director, or K. Yanai, Curator, at the National Institute of Polar Research, 9–10 Kaga 1-chome, Itabashi-ku, Tokyo 173, Japan. To use the thin section library at the Johnson Space Center in Houston, contact the Secretary of the Meteorite Working Group at the address given above. To make arrangements for using the library at the National Museum of Natural History, Smithsonian Institution, Washington, D.C. 20560, contact Brian Mason, Curator.

Literature Cited

Marvin, Ursula B., and Brian Mason, editors
1980. Catalog of Antarctic Meteorites, 1977–1978. *Smithsonian Contributions to the Earth Sciences*, 23: 50 pages.

Marvin, Ursula B., and Brian Mason, editors
1982. Catalog of Meteorites from Victoria Land, Antarctica, 1978–1980. *Smithsonian Contributions to the Earth Sciences*, 24: 97 pages.

The 1980–1981 Field Season

William A. Cassidy

The 1980–1981 field season was the fifth enterprise supported by the National Science Foundation in as many years. Beforehand, we knew that in addition to the Main Icefield (76°42′S, 159°20′E) at Allan Hills, where the existence of a large meteorite concentration had been proved, lesser concentrations of meteorites could be found at the Near Western Icefield (76°40′S, 158°49′E), Reckling Moraine (76°08′S, 158°47′E), and Elephant Moraine (76°14′S, 157°11′E). We were eager to investigate new sites in the hope of locating additional concentrations that could be exploited during future field seasons. We therefore devoted as much time as possible to reconnaissance and as little time collecting meteorites at known sites as was necessary to assure a successful season.

After collecting 32 specimens at Allan Hills we traversed to Reckling Moraine, where we recovered 67 specimens. Reckling Moraine (Figure 2) is an extensive ice-cored detrital rock deposit with no outcropping source in the upstream direction. The source of the moraine rocks therefore may be an elevated segment of an underlying east-west ridge whose surface expression on the ice is a step feature associated with the Reckling Moraine Icefield. This icefield averages 3–5 km in width and extends about 100 km in the east-west direction. Elephant Moraine is located about 50 km to the west, along the same icefield. It may be that the sites of highest meteorite concentration along this icefield are at or near these moraines. These, in turn, could result from a more sluggish flow of ice over the subsurface barriers that produce these moraines. As we have seen at Allan Hills and Yamato Mountains, meteorite concentrations tend to occur at sites where ice flow is sluggish or stagnant.

Approaching the icefield at Reckling Moraine from the south, we had to lower our supply-laden Nansen sledges down the 15°–20° face of the step feature by using snowmobiles in tandem: one at the rear, braking to stabilize the sledge, and one in front, pulling gently to keep its heading true. As in our previous visit, we followed the same route across the step feature as the one first used by the Philip Kyle party in December 1978. At the bottom of the step feature we were on the main part of the Reckling Icefield.

Prevailing wind direction is generally southwesterly across the narrow dimension of the icefield. Most of the 67 specimens we recovered were small (20–100 g) individuals or fragments found near the firn-ice boundary along the northern edge of the icefield. Presumably these are small enough to have been blown across the ice surface by strong winds, then trapped against snow and firn at the northern edge of the ice.

While at Reckling Moraine we received an air-drop of eight drums of snowmobile fuel to enable us to extend our traverse to points farther to the north: these included ice expo-

William A. Cassidy, Department Geology and Planetary Science, University of Pittsburgh, Pittsburgh, Pennsylvania 15260.

FIGURE 2.—Oblique photo looking westward at Reckling Moraine from a point above Reckling Peak. Smooth gray areas are patches of exposed ice. Lighter gray areas are snow. In some places the snow surface appears rough due to the presence of snow dunes (sastrugi). Near the center of the photo is a sinuous feature having the gray of exposed ice but with a rougher surface. This is Reckling Moraine. That part of the exposed ice that looks like a line of low hills and which tends to mimic the irregular boundary of the moraine is the step feature referred to in the text.

sures associated with Griffin Nunatak (Figure 3), Brimstone Peak, Tent Rock, and Sheppard Rocks. We hoped to augment the minimum collection we had made so far with additional recoveries from new concentration areas, but in this we were to be disappointed. A single small specimen was found at Outpost Nunatak, an outlier of Griffin Nunatak, but none were found at the other sites; thus it was well illustrated that not all fields of exposed ice can be expected to produce meteorite concentrations. At these barren localities we were relatively close to an area of fast-moving ice at the head of the David Glacier. In addition, the icefields are located downstream of the outcrops; therefore, the ice probably is migrating toward the head of the David Glacier unimpeded by intervening barriers. In these areas, too, wind direction was such that snow was piled against the upstream sides of the barriers, so that ice ablation was not occurring in the stagnant flow regimes where meteorite stranding would be favored. The net result of our reconnaissance efforts during the 1980–1981 field season was a greater understanding of the conditions under which meteorite surface accumulations occur, and do not occur.

In other activities during the 1980–1981 season, we obtained new measurements of ablation rates at our Allan Hills triangulation network (Cassidy and Annexstad, 1981), and one member of our party devoted considerable time to foot searches for meteorites in Taylor Valley, with negative results. This is of interest because certain surfaces in the Dry Valleys, (77°–78°S, 160°–163°E) are expected to be rather ancient and one would not be surprised to find accumulations of meteorites that had

FIGURE 3.—Camp at Griffin Nunatak, 30 km north of Reckling Peak. Part of the nunatak forms the rock cliff in the background.

fallen on them and been preserved in the dry environment. Mechancial erosion, however, may be more efficient in the Dry Valleys than on the icefields farther inland. Alternatively, the Dry Valley surfaces may be less ancient than has been believed.

TABLE 2.—The 1980–1981 collection.

Class	Allan Hills	Reckling Peak	Outpost Nunatak
Chondrites	30	60	1
Carbonaceous chondrites	0	0	0
Achondrites	1	2	0
Mesosiderites	0	4	0
Irons	1	1	0
Totals	32	67	1

The classification of meteorites recovered during the 1980–1981 season is given in Table 2.

Expedition members were W.A. Cassidy, J.O. Annexstad, J. Schutt, L.A. Rancitelli, L. Schultz, H. McSween, and J. Danielson. This work was supported by NSF/DPP 78-21104 and is Departmental Contribution 572.

Literature Cited

Annexstad, J.O. and W.A. Cassidy
1981. Antarctic Search for Meteorites, 1980–1981. *Antarctic Journal of the United States*, 16(5):61–62.

The Field Season in Victoria Land, 1981–1982

R.F. Fudali and J.W. Schutt

The 1981–1982 field season in Victoria Land was, by any measure, highly successful. Major accomplishments included a second resurvey of the established triangulation network, the recovery of 378 meteorite specimens, and a gravity survey to model the ice-bedrock interface, all at the Allan Hills, South Victoria Land (76°45′S, 159°40′E). Further, advantage was taken of logistic support provided by a season-long field camp in North Victoria Land (72°12′S, 163°50′E) to conduct reconnaissance meteorite searches in this new area and to examine a possible small meteorite crater at Littel Rocks (71°23′S, 162°0′E).

The team was led again by William Cassidy, University of Pittsburgh. Other participants were John Annexstad, NASA Johnson Space Center; Ghislaine Crozaz, Washington University at St. Louis; Ursula Marvin, Smithsonian Astrophysical Observatory; Ludolf Schultz, Max Planck Institute for Chemistry; and the authors.

Annexstad and Schultz spent the period 15 November to 13 December determining horizontal and vertical displacements of their triangulation stations for the second time since their emplacement. They also continued their yearly measurements of ice ablation rates (see Schultz and Annexstad, herein, or Cassidy and Annexstad, 1981). These tasks were accomplished despite long stretches of extremely bad weather, which, however, did prevent them from extending the network further west.

The authors spent 24 November to 15 December at the North Victoria Land (NVL) camp, 600 km north of McMurdo Station near the head of the Canham Glacier. Here the camp scientists were supported by a number of snowmobiles and three HU-1N helicopters. Air photos of the region, on file at USGS Headquarters in Reston, Virginia, were used to delineate a number of promising bare ice areas within helicopter range of the NVL camp. The crater at Littel Rocks was also found during this archival search.

The reconnaissance in NVL was largely by helicopter, but it was necessary to make rather frequent ground checks because of the unanticipated litter of terrestrial rubble on many of the bare ice surfaces. Bare ice patches at the Lonely One Nunataks, Reniere Rocks, Emlen Peaks, Outback Nunataks, Johannsen Nunatak, Frontier Mountan, Onlooker Nunatak, and Monument Nunatak were examined. Icefields in the southern and western regions of the Daniels range were also overflown and a snowmobile traverse to the ice patches near the Gallipoli Heights was undertaken. No meteorites were found during any of these searches; because of the terrestrial rocks littering many of these surfaces we cannot categorically say there are no meteorites present. However, it is clear that there can be no large meteorite concentrations such as those at the Allan Hills and the Yamato Mountains. Most

R.F. Fudali, Department of Mineral Sciences, National Museum of Natural History, Smithsonian Institution, Washington, D.C. 20560. J.W. Schutt, Department of Geology and Planetary Sciences, University of Pittsburgh, Pittsburgh, PA 15260.

of the meteorites found to date in Antarctica have been on ablation surfaces upstream of rock barriers to ice flow. In the areas accessible by helicopter from the NVL camp there appear to be no such upstream icefields. Rather there are a number of fast-moving glacial systems without extensive areas of stagnant ice. The terrestrial rocks littering many of these bare ice surfaces in the vicinity of outcropping bedrock presumably indicates these surfaces are moving away from, rather than toward, the potential rock barriers. In general then, such rock litter may prove to be a strong contraindication of meteorite concentrations, and future reconnaissance in new areas should be conducted with this in mind. Unfortunately, the size range of the rock litter is far too small to be detected on air photos. Whether or not there are other subtle diagnostic features on the air photos that would permit us to distinguish stagnant from moving icefields is a question we have not yet answered. The utility of being able to make such distinctions is obvious; an important step in addressing the question is searching apparently promising icefields and finding *no* meteorite concentrations. So our negative findings at NVL may well prove more useful, in the long run, than if we had found meteorites there.

One day was spent examining the circular "crater" at Littel Rocks. The depression is about 125 m in diameter and has a terrace partially incised inside its bowl, about 5 m above the floor. The depression would be a closed basin of deposition for water, but it has clearly been overidden one or more times in the past by ice. We surmise that the terrace represents the former water level of a shallow lake and was sculpted by moving ice when the lake was frozen. There are other such shallow lakes in the area although none are so circular as this example. In any case we found no evidence of a meteoritic origin—in fact quite the contrary. Littel Rocks is composed of a dolerite intrusion characterized by a very strong, narrowly spaced, vertical joint system. This vertical jointing can be observed, undisturbed, in the floor of the depression; i.e., there is no rubble zone beneath the present floor and the depression is much too shallow (10–15 m) to contemplate the removal of such a rubble zone by eroding ice. We therefore conclude that the depression is not an impact crater and is most likely the result of glacial activity.

The amenities of a season-long Antarctic field camp, such as the NVL establishment, have been described in some detail by Marvin (1982) and will not be repeated herein. Suffice it to say that one of us (RFF) was quite prepared to *not* find meteorites throughout the balance of the field season at NVL until advised that this was not a permissible option.

In contrast to the areas searched in NVL, meteorites were still readily found on the bare ice patches west of the Allan Hills. A party consisting of Cassidy, Crozaz, Marvin, and the authors spent 33 days in this area (22 December 1981 through 23 January 1982).

The Allan Hills icefields comprise five separate bare ice areas (Figure 4). The Main Icefield extends NNW from Peak 2330 for nearly 22 km and contains roughly 75 km^2 of blue ice. The Near Western Icefield, 18 km west of Peak 2330, contains about 14 km^2 of blue ice. The Middle Western Icefield, 31 km WSW of Peak 2330, contains about 30 km^2 of blue ice. The Far Western Icefield (not shown on Figure 4) is a vast area of blue ice, over 40 km long and 2–8 km wide, with an area in excess of 100 km^2. Its southeastern end is some 70 km WSW of Peak 2330. Because of poor weather and insufficient time, a planned reconnaissance of the Far Western Field during the 1981–1982 season was not attempted. The Battlements Icefield, slightly smaller than Middle Western Field, had not been examined previously, primarily because of the very difficult terrain immediately south of Battlements Nunatak. This season our party reached the nunatak and found a passage through it to the icefield. A cursory examination of the ice surface revealed it to be littered with terrestrial rocks. No attempt was made to search for

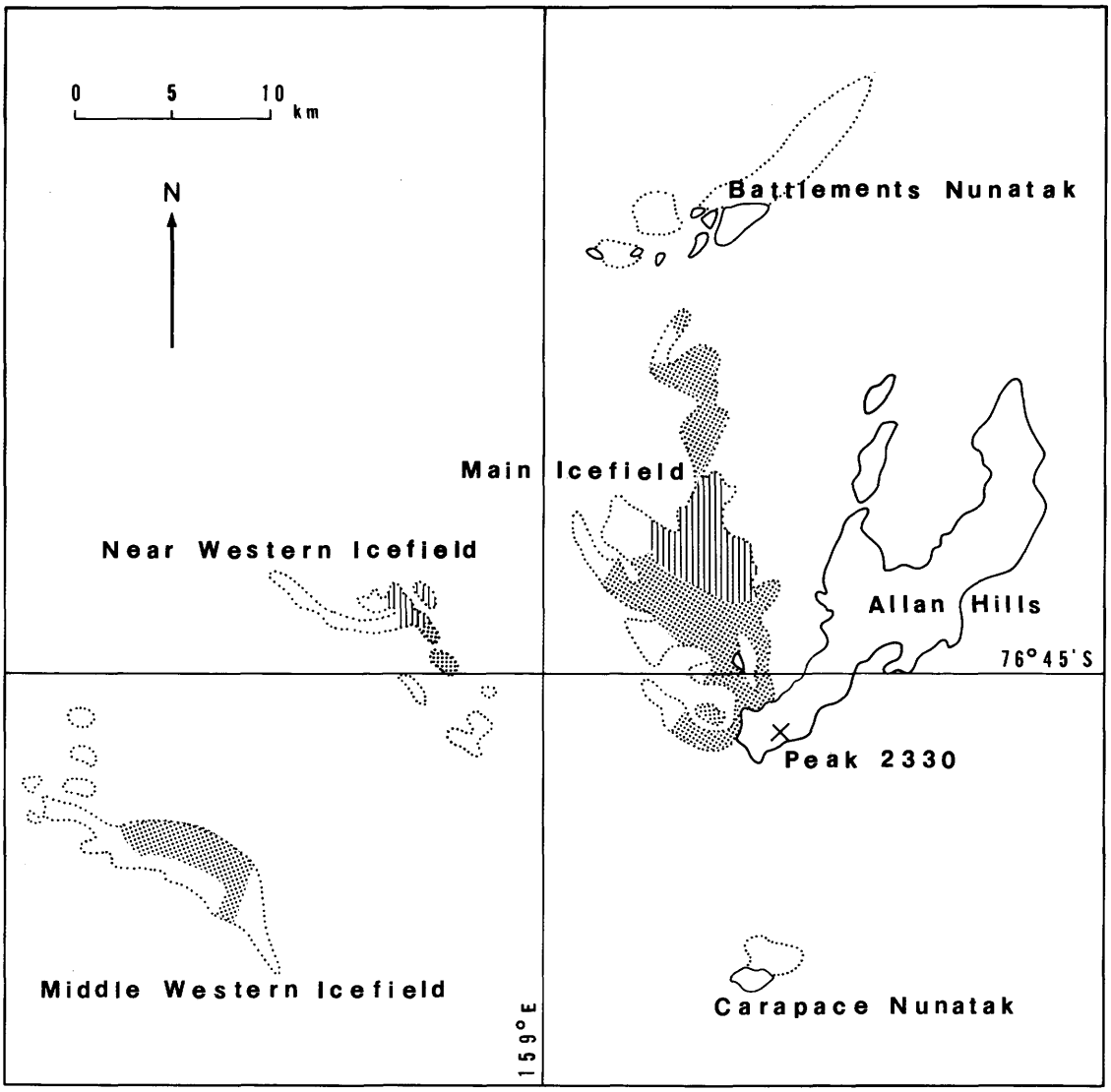

FIGURE 4.—Meteorite collecting areas west of the Allan Hills. Dots outline bare icefields. Stippled areas were searched by a reconnaissance mode. Striped areas were searched systematically during the 1981–1982 field season.

meteorites. Based on our observations at NVL we predict that there is no concentration of meteorites on this icefield. However, it should certainly be searched at a future date to test the predictive power of our NVL experience.

The Main Icefield, searched the longest and most thoroughly, yielded 286 meteorites and meteorite fragments during the 1981–1982 season, bringing the recovered total from this field to 1020. There are at least two reasons why the yield from this field remained high this season despite five previous search efforts. First these so-called "blue or bare ice" patches are not really bare. At any given time there will be a 30–50% snow cover largely in the form of low, N-S trending linear drifts termed sastrugi (Figure 6). As this snow cover shifts from year to year, new, hitherto unobservable ice surfaces, and the meteorites contained thereon, become exposed. Second, and perhaps more importantly, for the first time systematic, steel-cleated snowmobile sweeps were

FIGURE 5.—Helicopter delivering snowmobiles to the Allan Hills camp.

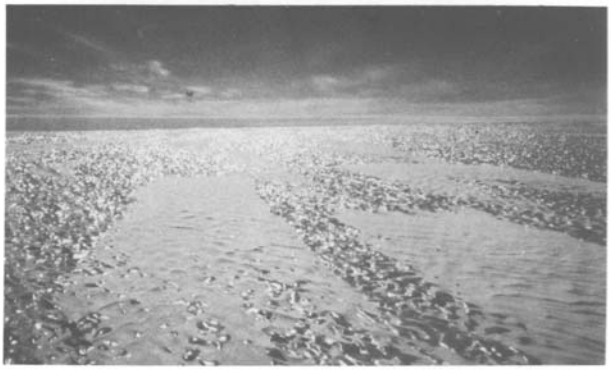

FIGURE 6.—Typical surface of the Main Icefield illustrating partial snow cover.

FIGURE 7.—Snowmobile team preparing to spread out abreast to a 30–50 meter spacing.

conducted over the areas of highest potential (meteorites have been found over nearly the entire Main Icefield but some areas show much higher concentrations than others, nearly barren areas). Typically, once a promising area was found, 4–5 snowmobiles (Figure 7) were aligned abreast, 30–50 m apart, and a disciplined sweep was made in a chosen direction. At the end of a sweep the line pivoted about the "outside" searcher and reversed its direction. The "outside" searcher then became the "inside" searcher following his/her track back to its beginning while the others traversed new ground. This sequence was repeated until the area of interest was completely swept, with a high probability of recovering almost all the exposed meteorites. Meteorites as small as a few millimeters in maximum dimension were recovered by this technique.

Two and a half days were spent systematically searching the Near Western Icefield. Seventy-eight specimens representing a maximum of 24 individuals were recovered. At least 52 weathered fragments appear to be from a single individual and are similar to 30 fragments recovered in previous years from the same area. This icefield yielded the largest meteorite recovered in the 1981–1982 season: the 18 kg hexahedrite described by Roy Clarke (p. 50).

A two-man, one-day reconnaissance at the Middle Western Icefield returned 14 fragments representing 11 individuals. Several other meteorites were found but not collected because of poor weather and insufficient time. These were flagged for collection next season.

From the short times spent at the Near and Middle Western icefields it is clear that a large number of meteorites remain on these surfaces for future collecting. Under the reasonable assumption that we are merely observing the exposed portions of a single concentration system, there must be a very much larger number of meteorites beneath the thin snow cover separating the three icefields (Main, Near, and Middle). Whether or not the meteorite concentration extends to the Far Western Icefields

should be known after the 1982–1983 season.

In summary, a total of 314 field sample numbers were issued for the 378 meteorite individuals and fragments recovered from the Allan Hills icefields during the 1981–1982 season; the discrepancy between the two numbers reflects the obvious pairing of fragments from the same meteorites.

Prior to the 1981–1982 season little effort was made to accurately map the sites of meteorites found on the Allan Hills icefields. This past season we surveyed the positions of the recovered meteorites so that detailed location maps could be produced. The 24 station triangulation network was used as a base for determining meteorite positions on the Main Icefield. The surveying instruments and techniques were rather crude but, we believe, more than adequate for the possible uses of such locality data. Where the triangulation network was not a practical reference, an initial point was established by a three-point resection from prominent landmarks, plotted on the U.S.G.S. *Convoy Range* 1:250,000 scale quadrangle map.

A detailed meteorite location map for the Main Icefield has been produced and has already proven useful for examining the possibility of paired falls of similar meteorites (Marvin, personal communication).

Together with their terrestrial ages, a knowledge of the distribution of the larger meteorites on the icefields may help determine meteorite accumulation rates, ice dynamics, and perhaps other factors bearing on meteorite concentration mechanisms. The locations of meteorites smaller than about 4 cm (maximum dimension) in size are only useful for accurately locating the downwind edge of an icefield. The ever-present katabatic winds are capable of skittering these small meteorites across the ice until they lodge in the snow bordering the bare ice areas.

As part of the on-going effort to delineate the meteorite concentration mechanisms at the Allan Hills, a large number of ice samples were collected at regular intervals along two east-west traverses across the Main Icefield, and the sample positions flagged for future reference. These ice samples were sent directly to Ohio State University for petrographic examination by Ian Whillans, a glaciologist with substantial experience in Antarctica. Dr. Whillans spent the final ten days with our party at the Allan Hills and was most impressed with what he tentatively concluded was an exposed vertical ice section, now running horizontally east-west, that could cover a 600,000 year period. Two large blocks of ice were also collected for radioactive dating and gas content determinations. One of these blocks was excavated from directly beneath the find site of one of the largest chondrites (18 cm, maximum dimension, field number 1556) that we had collected.

Finally, gravity measurements were made at all 24 stations of the previously established triangulation network across the Main Icefield (Figures 8 and 9). Eight additional stations were occupied on bedrock, from the northernmost tip of the Allan Hills south to Carapace Nunatak, to help define any north-south regional gravity trend that might be present. Calibration of the gravity data was provided by a single, direct ice-thickness measurement at station 3 of the network, obtained previously by radio-echo sounding (Kovacs, 1980). With this calibration the gravity values could be used to compute ice thicknesses at all the other stations and so model the shape of the ice/bedrock interface beneath the station network. A detailed description of this survey may be found in the 1982 review issue of the *Antarctic Journal* (vol. 16, no. 5). Only the conclusions are summarized herein.

The calculated east-west profiles are shown in Figure 10. The principal possible error source in constructing these profiles is our ignorance of the east-west regional gravity trend, if any. However, the corrections for any such trend would only rotate the entire profiles up or down about the easternmost points without changing their relative shapes. Thus any conclusions based on a comparison of *relative* bedrock slopes will be valid irrespective of any east-west correction.

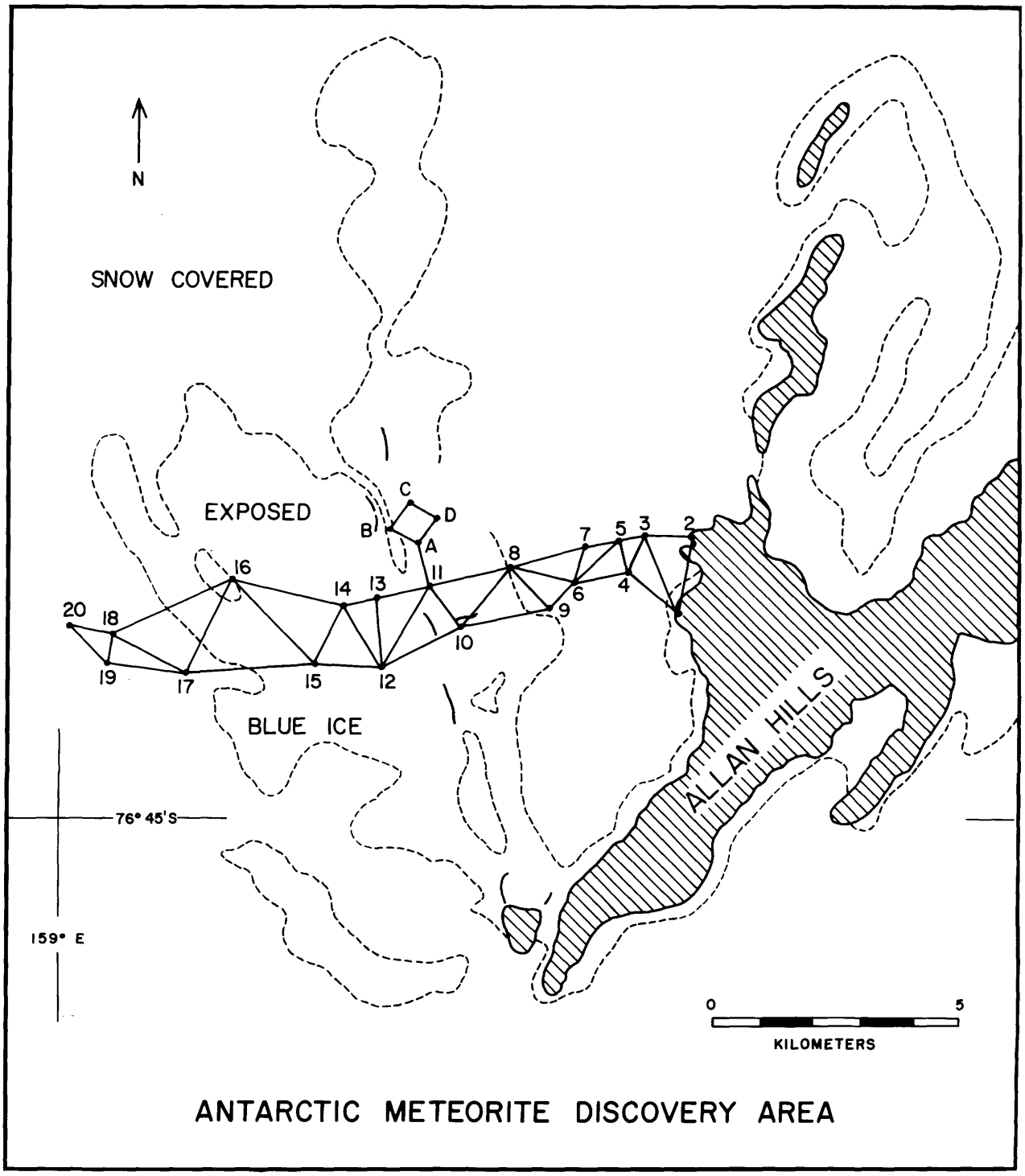

FIGURE 8.—The triangulation network across the Main Icefield at Allan Hills.

FIGURE 9.—Gravity team at work.

A firm conclusion that can therefore be reached is that, if the (exposed) Allan Hills act as a barrier to ice movement, then surely the barrier should begin much further west where comparable bedrock slopes are present. This conclusion is consistent with our 1982 reconnaisance of the Middle Western Icefield, which revealed meteorite concentrations 35 km west of the Allan Hills. It is, however, not consistent with the latest reported triangulation network remeasurements (Schultz and Annexstad, this issue), which indicate a zero horizontal flow rate, 5 km west of the Allan Hills, but an eastward flow of ~ 1 meter/year for the ice 13 km west of the exposed barrier. Although we have no certain explanation for the discrepancy between the two data sets, we do note that the more precise instruments used in the 1981 resurvey lowered the maximum reported horizontal flow rate from 2.5 to 1 meter/year. At the same time, the earlier imprecision causes the retention of high probable errors, which remain on the order of the reported

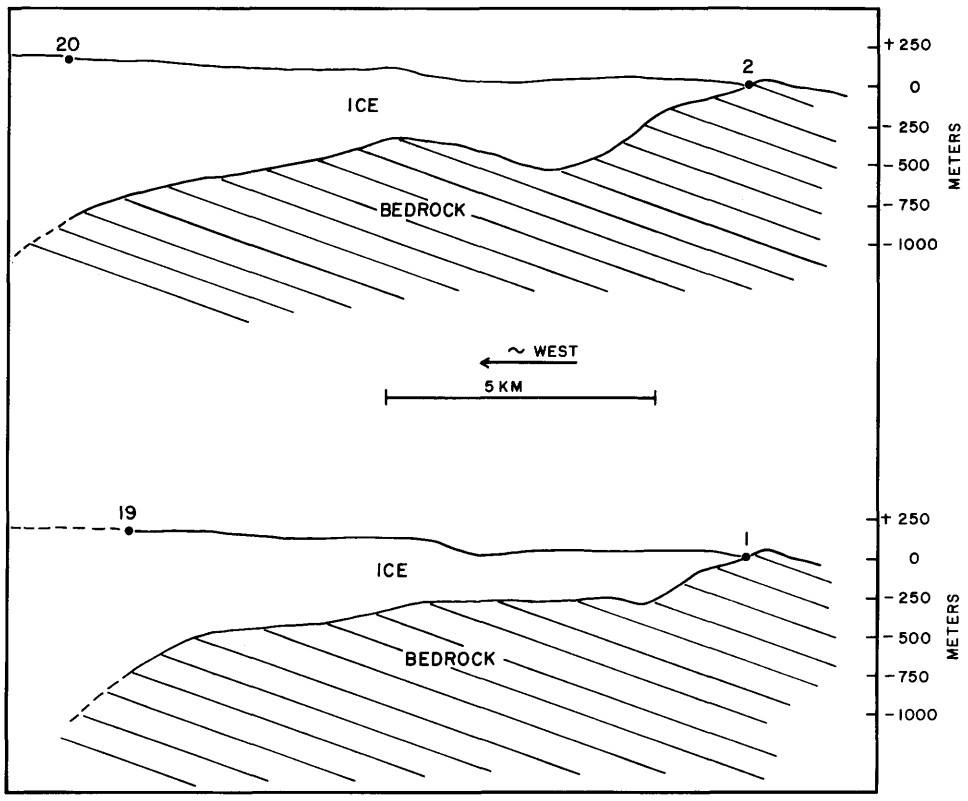

FIGURE 10.—Gravity-deduced bedrock configurations beneath the triangulation network.

rates themselves. The network was surveyed again during the 1982–1983 season and it will be interesting to see whether this data substantiates the latest reported (1981) rates.

Literature Cited

Cassidy, W.A., and J.O. Annexstad
1981. Antarctic Search for Meteorites, 1980–1981. *Antarctic Journal of the United States*, 16(5):61–62.

Kovacs, A.
1980. Radio-Echo Sounding in the Allan Hills, Antarctica, in Support of the Meteorite Field Program. *Special Report 80-23*, U.S. Army Corps of Engineers, Cold Regions Research and Engineering Laboratory, Hanover, New Hampshire.

Marvin, U.B.
1982. The Field Season in Victoria Land, 1978–1979. *In* U.B. Marvin and B. Mason, editors. Catalog of Meteorites from Victoria Land, Antarctica, 1978–1980. *Smithsonian Contributions to the Earth Sciences*, 24:3–8

Ablation and Ice Movement at the Allan Hills Main Icefield between 1978 and 1981

Ludolf Schultz and John O. Annexstad

Introduction

The total number of meteorites found in Antarctica through the southern summer of 1981–1982 exceeds 6000. More than 1000 meteorites have been collected on the icefields near the Allan Hills in South Victoria Land. The United States Antarctic Search for Meteorites (ANSMET), led by W.A. Cassidy, has concentrated in this area not only to search for meteorites but also to study the general phenomenon of meteorite concentrations on blue icefields in the Antarctic. For a general introduction one is referred to Cassidy et al. (1977), Marvin (1981), Schultz (1982), and Cassidy and Rancitelli (1982).

Two factors contribute to the high meteorite concentrations on the surface of some icefields. (1) Small meteorites with weights of a few grams can be detected on bare icefields while in other areas of the Earth similar stones are hidden among terrestrial rocks or vegetation. (2) Weathering is less severe under Antarctic conditions. Without liquid water meteorites are preserved for longer periods of time than in temperate climates. Furthermore, paired meteorite falls contribute to the larger number of meteorite finds. Detailed studies of all meteorite fragments are necessary to recombine multiple falls. Seventy-five meteorites have been tentatively identified as belonging to 13 individual falls in the Allan Hills region (Marvin and Mason, 1982). Even after taking into account all of these effects, a mechanism that concentrates meteorites fallen on large areas is still necessary to explain the high concentrations on some icefields in Antarctica.

Several hypotheses have been proposed to explain these meteorite concentrations (Cassidy et al., 1977; Nagata, 1978; Whillans, 1982). Generally, the process of meteorite concentration is based on the assumption that meteorites entrapped in the ice in the interior of the continent will emerge on the surface of stagnant icefields close to coastal mountain chains where the outward flow of ice is blocked. All hypotheses need three basic parameters to obtain quantitative results: (1) terrestrial ages of meteorites; (2) ablation rates of the ice in regions with high meteorite concentrations; and (3) direction and velocity of the ice movement into these regions.

Terrestrial ages have been determined using radioactive cosmogenic nuclides like ^{14}C, ^{26}Al, ^{36}Cl, and ^{81}Kr. The results show that a large number of Antarctic meteorites have rather high terrestrial ages with values up to 700,000 years (Fireman et al., 1979; Evans et al., 1982; Nishiizumi et al., 1983; Freundel and Schultz, in prep.).

Ludolf Schultz, Max-Planck-Institut für Chemie, D-65 Mainz, West Germany. John O. Annexstad, NASA Johnson Space Center, Houston, Texas, 77058.

To obtain information on ablation and ice movement, a triangular network of 20 stations was established at the Allan Hills icefield in 1978 (Nishio and Annexstad, 1979). Figure 11 shows a map of the Allan Hills area with the triangulation chain, which is based in bedrock and extends more than 13 km westward, crossing the icefield with high meteorite concentrations. Figure 12 shows the Allan Hills with station 1 at the lower left corner and Figure 13 is a view from a helicopter in a southwesterly direction with the 1981 campsite. After the first measurement in 1978, the chain was resurveyed in 1979 (Nishio and Annexstad, 1980; Annexstad, 1982). We report here a summary of another redetermination of the properties of the network in November and December 1981.

The method of the survey was essentially the same as in previous years. However, the instruments used were more modern: a Wild theodolite with 400^g (360°) reading was used for the measurement of horizontal and vertical angles, and the slope distances between adjacent stations were directly observed with a Wild Distomat DI4L (Figure 14). Due to adverse weather conditions in November 1981, in most cases only one side of each of the 18

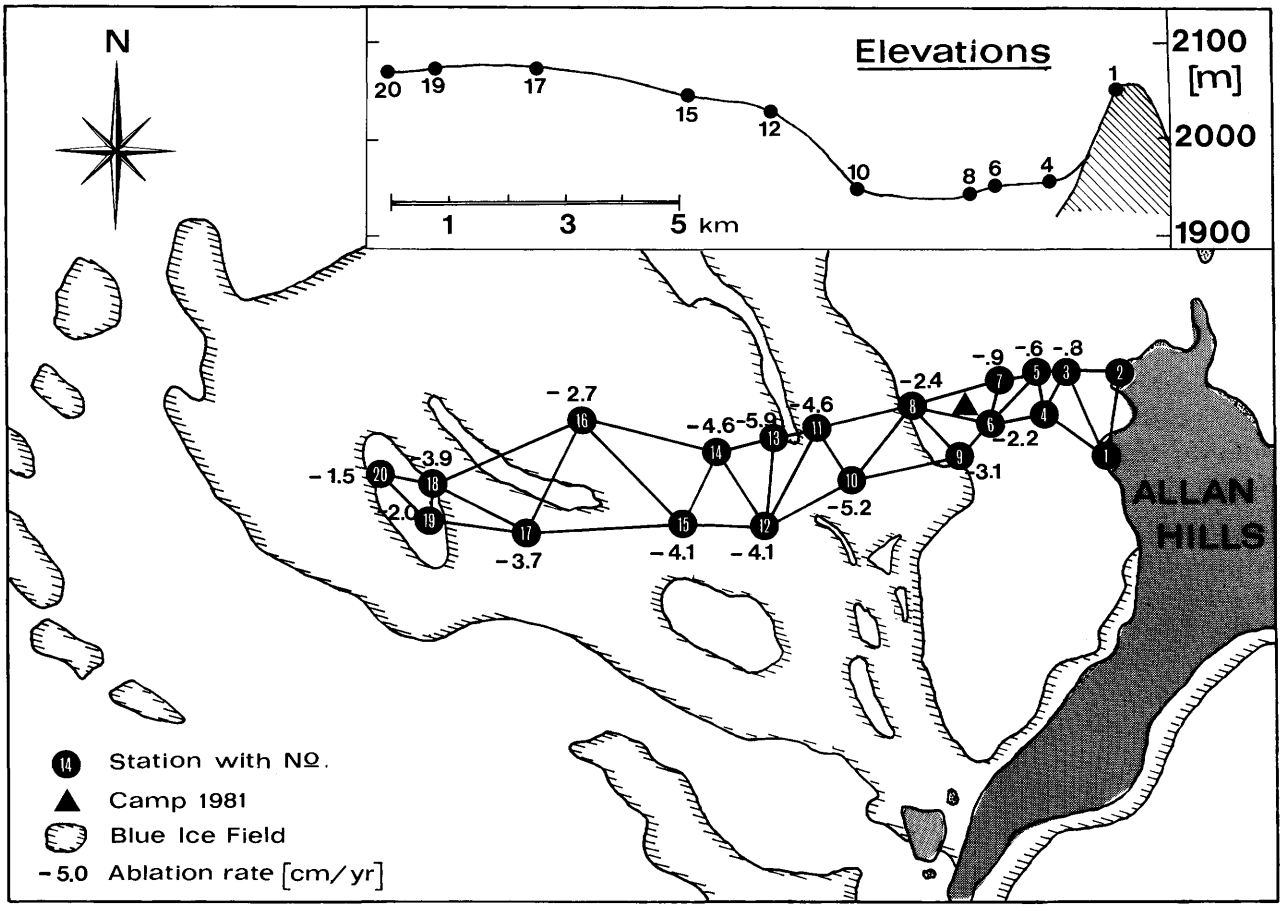

FIGURE 11.—Map of the Allan Hills Main Icefield with the triangulation network. Numbers associated with the stations are measured ablation rates in cm/year. The insert shows calculated elevations along the southern border of the network. The highest meteorite concentrations have been found at the base of the slope that runs through the network between stations 8 and 13.

FIGURE 12.—View along the Allan Hills in a northerly direction. The tripod (left lower corner) has been installed over station 1 (Figure 11).

FIGURE 13.—Helicopter view in a southwesterly direction of the Allan Hills icefield. Visible is the camp site (arrow) and the "monocline" with a moraine, which supplies the icefield with terrestrial rocks to confuse a meteorite hunter.

FIGURE 14.—After removal of the station pole, the survey was carried out from instruments mounted over the hole in the ice. A shelter protects the Wild T2 theodolite and the Wild T14L Distomat from vibrations due to the wind.

triangles (Figure 11) could be measured. The observations from 1981, as well as those from previous measurements, were used to calculate the coordinates of each station relative to stations 1 and 2, which are positioned in the bedrock of the Allan Hills. A standard program of triangulation networks, ARSM, at the Fachhochschule Mainz was used for the data reduction. The attempt to calculate vertical ice movements was done with a computer program developed at the Max-Planck-Institüt in Mainz. Ablation rates of the ice between two measurements are given by the differences of the height of each station pole from the surface of the ice to the top.

Results and Discussion

ABLATION

The mean ablation rate observed for each station over three years is given in Figure 11 (Annexstad and Schultz, 1983). The uncertainty of these numbers is about 1 cm because the ablation rate around the poles is not uniform. Also from year to year the ablation rate may vary due to different wind and temperature conditions. However, a mean ablation rate of about 5 cm/year is well established for the stations on ice close to the areas with high meteorite concentrations. This observation is basic to all models for

the transport and concentration of meteorites. Once buried in the ice, meteorites can emerge to the surface and, assuming a horizontally stagnant icefield over a long period of time, build up dense meteorite concentrations.

Horizontal Movements

Nishio and Annexstad (1980) reported horizontal ice velocities based on observations in 1978 and 1979. Their calculated values have rather large uncertainties because only one year of movement was measured. With the 1981 survey, changes over a three-year period could be observed and, in addition, the use of the Distomat allowed a better determination of the network. For four selected stations the calculated coordinates (in arbitrary units) of the measurements in 1978, 1979, and 1981 are shown in Figure 15. This figure demonstrates that the observational uncertainties could be reduced for the 1979 and 1981 measurements. The errors of the horizontal velocities are based mainly on the uncertainties of the initial measurement.

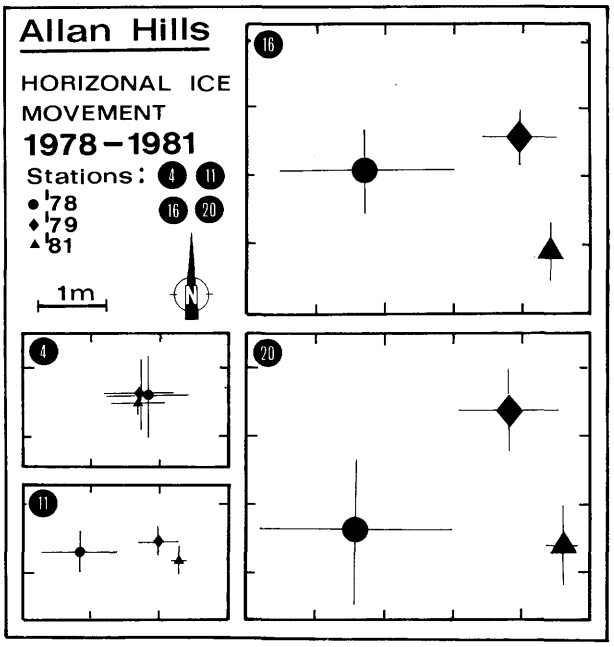

FIGURE 15.—Calculated coordinates (in relative units) of stations 4, 11, 16, and 20 for the measurements in 1978, 1979, and 1981. Due to the application of distance measurements in addition to the angle measurements the uncertainties could be reduced in the 1981 measurement.

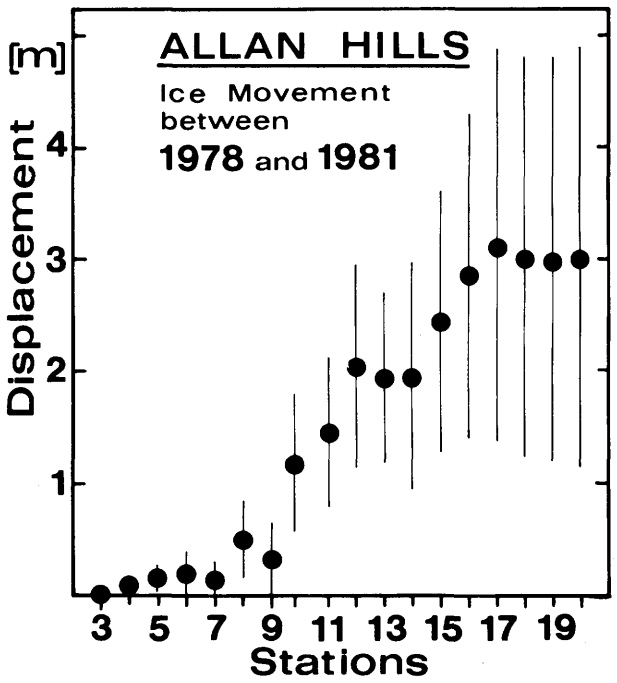

FIGURE 16.—The calculated displacement in an easterly direction of all stations during the period 1978 to 1981.

Figure 16 shows the horizontal displacement of the stations relative to the 1978 measurement. The error bars reflect the sum of the uncertainties of the 1978 and 1981 data. Three different groups can be recognized according to their displacement in an eastward direction between 1978 and 1981. Stations 3 to 7 show, within the limits of error, no movement in three years. This area is the firn-covered icefield closest to the Allan Hills. From stations 8 to 16 the horizontal velocity of the ice increases from about 10±10 cm/year to about 100±70 cm/year. This is the area with many meteorite finds. Stations 17 to 20 have the same rate of movement of about 1 m/year.

These measurements corroborate the suggestion that the ice moves into the Allan Hills region

from the west and becomes stagnant where many meteorites are found. An additional resurvey of the network in future years would enhance the quality of the data, because the 1981 coordinates with rather small errors could then serve as a reference. However, to calculate the ice balance in this region, measurements of the ice thickness are needed.

Vertical Movements

The determination of vertical angles in Antarctica is sometimes more difficult than the measurement of horizontal angles, because atmospheric effects can obscure the top of the poles that are used as targets. Instrumental factors also have more influence on vertical angle measurements. The vertical angles, therefore, have uncertainties that exceed the expected movement of the ice. For example, for stations 9 to 13 the mean error of the calculated elevations from the vertical angle measurements are about 90, 40, and 15 cm for the measurements of 1978, 1979, and 1981, respectively. A resurvey of these parameters in a future field season could result in better data.

Conclusions

The ablation rate of the ice at the Allan Hills meteorite icefield averages about 5 cm/year. The ice from the Eastern Antarctic ice sheet approaching the Allan Hills slows down and becomes stagnant. The ice velocity 13 km west of the Allan Hills is about 1 m/year; at a distance of about 5 km from the Allan Hills it is almost zero. The experimental uncertainties are too high to determine vertical ice velocities; however, due to rather small errors of the 1981 measurement, a resurvey of the network could result in useful values for this parameter.

Literature Cited

Annexstad, J.O.
1982. The Allan Hills Icefield and its Relationship to Meteorite Concentration. *In* U.B. Marvin and B. Mason, editors, Catalog of Meteorites from Victoria Land, Antarctica, 1978–1980. *Smithsonian Contributions to the Earth Sciences*, 24:12–18.

Annexstad, J.O., and L. Schultz
1983. Measurements of the Triangulation Network at the Allan Hills Meteorite Icefield. In *Proceedings of the Fourth International Symposium on Antarctic Earth Sciences*, pages 617–619.

Cassidy, W.A., E. Olsen, and K. Yanai
1977. Antarctica: A Deep-Freeze Storehouse for Meteorites. *Science*, 198:727–731.

Cassidy, W.A., and L.A. Rancitelli
1982. Antarctic Meteorites. *American Scientist*, 70:156–164.

Evans, J.C., J.H. Reeves, and L.A. Rancitelli
1982. Aluminum-26: Survey of Victoria Land Meteorites. *In* U.B. Marvin and B. Mason, editors, Catalog of Meteorites from Victoria Land, Antarctica, 1978–1980. *Smithsonian Contributions to the Earth Sciences*, 24:70–74.

Fireman, E.L., L.A. Rancitelli, and T. Kirsten
1979. Terrestrial Ages of Four Allan Hills Meteorites: Consequences for Antarctic Ice. *Science*, 203:453–455.

Freundel, M., and L. Schultz
In prep. Terrestrial ^{81}Kr Ages of Antarctic Meteorites.

Marvin, U.B.
1981. The Search for Antarctic Meteorites. *Sky and Telescope*, 1981:423–427.

Marvin, U.B., and B. Mason, editors
1982. Catalog of Meteorites from Victoria Land, Antarctica, 1978–1980. *Smithsonian Contributions to the Earth Sciences*, 24: 97 pages.

Nagata, T.
1978. A Possible Mechanism of Concentration of Meteorites within the Meteorite Ice Field in Antarctica. *Memoirs of the National Institute of Polar Research* (Japan), special issue, 8:70–92.

Nishiizumi, K., J.R. Arnold, D. Elmore, X. Ma, D. Newman, and H.E. Gove
1983. ^{36}Cl and ^{53}Mn in Antarctic Meteorites and ^{10}Be-^{36}Cl Dating of Antarctic Ice. *Earth and Planetary Science Letters*, 62:407–417.

Nishio, F., and J.O. Annexstad
1979. Glaciological Survey in the Bare Ice Area near the Allan Hills in Victoria Land, Antarctica. *Memoirs of the National Institute of Polar Research* (Japan), special issue, 15:13–23.

1980. Studies on the Ice Flow in the Bare Ice Area near the Allan Hills in Victoria Land, Antarctica. *Memoirs of the National Institute of Polar Research* (Japan), special issue, 17:1–13.

Schultz, L.

1982. Antarctische Meteorite. *Die Naturwissenschaften*, 69:220–225.

Whillans, I.M.

1982. Meteorite Concentration Mechanism near the Allan Hills and the Age of the Ice. *In* C. Bull and M.E. Lipschutz, editors, Workshop on Antarctic Glaciology and Meteorites. *Lunar and Planetary Institute Technical Report*, 82-03:35. Houston: Lunar and Planetary Institute.

Descriptions of Stony Meteorites

Roberta Score, Carol M. Schwarz, and Brian Mason

This section provides descriptions of the individual specimens, arranged by class. Within the chondrites, the specimens are grouped according to the Van Schmus-Wood (1967) classification, and the descriptions follow the order of increasing petrographic type. The descriptions are based largely on those published in the *Antarctic Meteorite Newsletter*, with additional information as available. The letter-number designation concurs with guidelines recommended by the Committee on Nomenclature of the Meteoritical Society; it carries the following information: ALH (Allan Hills); A80 (Expedition A, 1980); xxx (digits indicating the number of the specimen). The original weight of the specimen is given to the nearest gram (nearest 0.1 gram for specimens weighing less than 100 grams).

This section comprises material on all characterized meteorites collected during the 1980–1981 and 1981–1982 field seasons. Specimens weighing less than 100 grams are listed without descriptions, unless they show distinctive features. A summary account of the petrography of the 1980–1981 collections has been published by Mason and Clarke (1982).

Roberta Score and Carol M. Schwarz, Northrop-Houston, Johnson Space Center, Houston, Texas, 77058. Brian Mason, Department of Mineral Sciences, National Museum of Natural History, Smithsonian Institution, Washington, D.C. 20560.

Chondrites

CLASS C2

FIGURES 17, 18

ALHA81002 (14.0 g).—This is a friable jet black stone (2.5 × 2.5 × 2.5 cm) of pyramidal form, without fusion crust. Chondrules and inclusions can be distinguished on the surface; a minute amount of salt deposit was present on one surface.

ALHA81004 (4.7 g).—Dull black fusion crust, blistery along one edge, covers most of this stone (3 × 1.5 × 1 cm). Small white irregular and rounded inclusions are apparent in the black matrix; several small oxidation halos were noted.

Thin sections of these specimens are very similar to each other and to those of ALHA77306 and 78261, the previously described C2 chondrites from the Allan Hills; these four meteorites may be paired. The sections show numerous small colorless grains (up to 0.1 mm) and irregular aggregates (up to 0.6 mm) mainly of olivine, and a few small chondrules (up to 0.6 mm) in an opaque to translucent brown isotropic matrix. Trace amounts of nickel-iron and troilite are present as widely dispersed minute grains. Microprobe analyses of the olivine show a composition range of Fa_0 to Fa_{52}, mean Fa_{11}, with a strong peak at Fa_0 to Fa_1 characteristic for chondrule

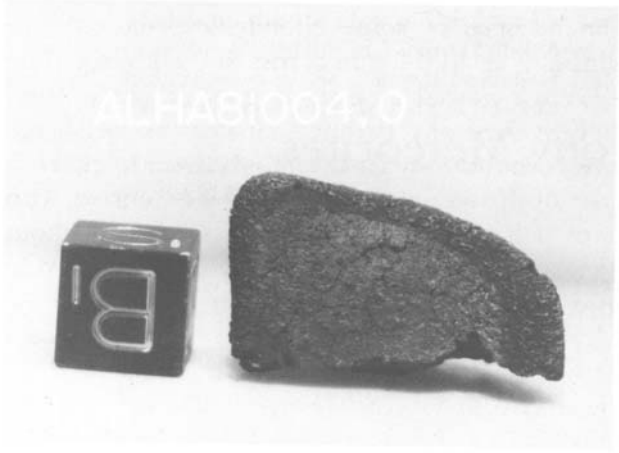

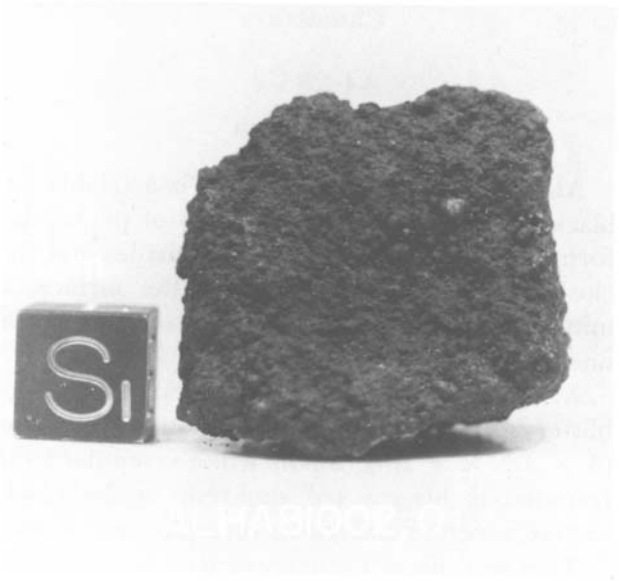

FIGURE 17.—C2 chondrites. Note blistery fusion crust around edge of ALHA81004.

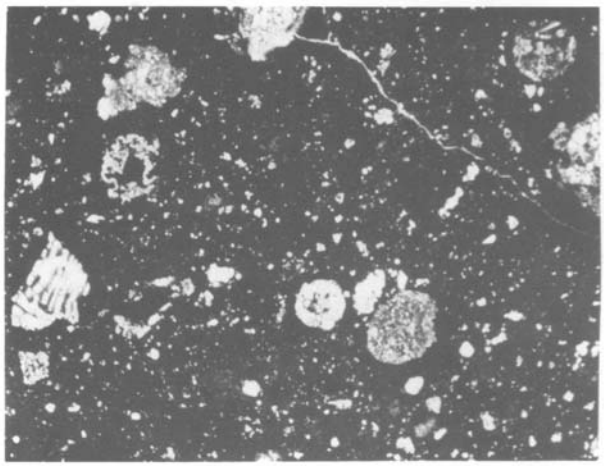

FIGURE 18.—ALHA81004, C2 chondrite. Photomicrograph of thin section (area of field is 3 × 2 mm), irregular grains and rare chondrules, mainly of olivine (white to gray) in translucent to opaque matrix (black).

FIGURE 19.—ALHA81003, C3 chondrite. Note pitted surface, and white inclusions in black matrix.

olivine (isolated olivine grains show a wide composition range). A few grains of clinoenstatite and one grain of diopside were analyzed.

CLASS C3

FIGURES 19, 20

ALHA81003 (10.1 g).—This stone (2.5 × 2.0 × 1.5 cm) from the Allan Hills has only one small area of fusion crust. The exposed surfaces are black and are dotted with abundant irregular white inclusions, some of which are rusty. Sparse metal grains are scattered through the matrix.

The section shows numerous chondrules up to

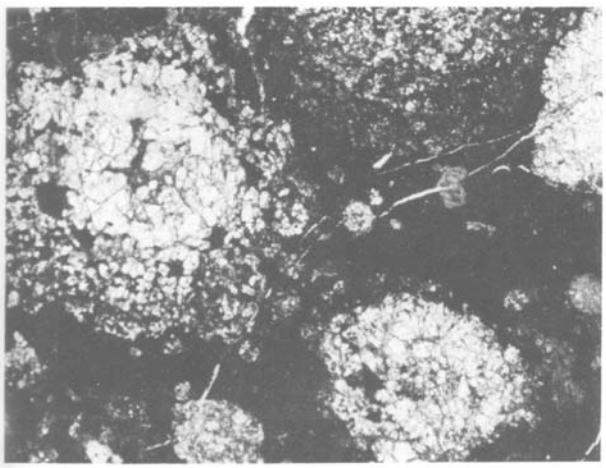

FIGURE 20.—ALHA81003, C3 chondrite. Photomicrograph of thin section (area of field is 3 × 2 mm); note large olivine-rich chondrules in brown to black semi-opaque matrix.

3 mm across and irregular crystalline aggregates up to 2 mm in maximum dimension, set in a minor amount of dark brown to black semi-opaque matrix. The chondrules and aggregates consist mainly of olivine with some polysynthetically twinned pyroxene. Trace amounts of nickel-iron are present as minute grains. Sulfide is present in minor amount, finely dispersed throughout the section. Microprobe analyses of chondrule olivine show a wide compositional range: Fa_0 to Fa_{40}, mean Fa_8; the matrix consists largely of fine-grained iron-rich olivine, Fa_{40} to Fa_{60}. Pyroxene in the chondrules is clinoenstatite, mostly near Fs_1, but with occasional Fe-rich grains. The meteorite is a C3V chondrite; previously described C3 chondrites from the Allan Hills are C3O (Scott et al., 1981).

RKPA80241 (0.6 g).—This small specimen (1.5 × 0.5 × 0.5 cm) from Reckling Peak has a little fusion crust. The thin section shows a close-packed aggregate of chondrules (up to 2.5 mm across) and irregular granular aggregates, set in a small amount of black (probably carbonaceous) matrix. A minor amount of nickel-iron is present, in several forms: as small grains dispersed through some chondrules, concentrated around the margins of some chondrules, and as rare globules up to 0.8 mm across in the matrix. The silicate material consists largely of olivine and polysynthetically twinned clinopyroxene. Well-preserved fusion crust, up to 1.2 mm thick, rims part of the section. Weathering is extensive, with brown limonitic staining pervasive throughout the section. Microprobe analyses show olivine and pyroxene with variable composition; for 30 olivine analyses the Fa range is 0.7–5.5 (except for one of Fa_{36}), and the mean is Fa_3; for 15 pyroxene analyses the range is Wo 0.3–1.5, En 90–98, Fs 1–8, with mean of $Wo_{0.7}En_{95}Fs_4$. The meteorite is tentatively classified as a C3V chondrite.

CLASS H3

FIGURES 21, 22

OTTA80301 (35.5 g).—This rounded stone (3.5 × 3 × 2 cm) from Outpost Nunatak is almost competely covered with brown to black fusion crust, pitted in places. A broken corner reveals abundant chondrules and irregular inclusions. The thin section shows a close-packed aggregate of chondrules and some irregular granular enclaves; the matrix consists of fine-grained silicates with a moderate amount of nickel-iron and a lesser amount of troilite. Chondrules range up

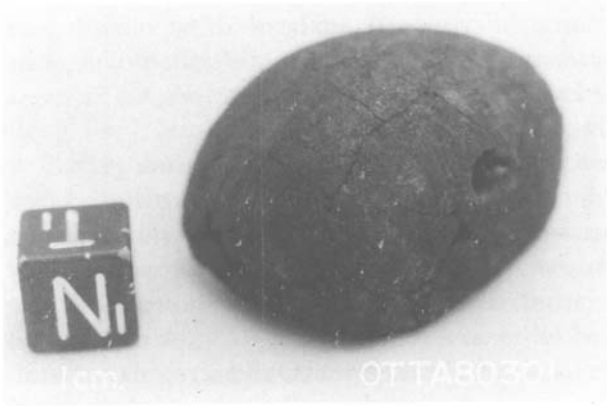

FIGURE 21.—OTTA80301, H3 chondrite, a rounded stone almost completely covered with brown to black fusion crust.

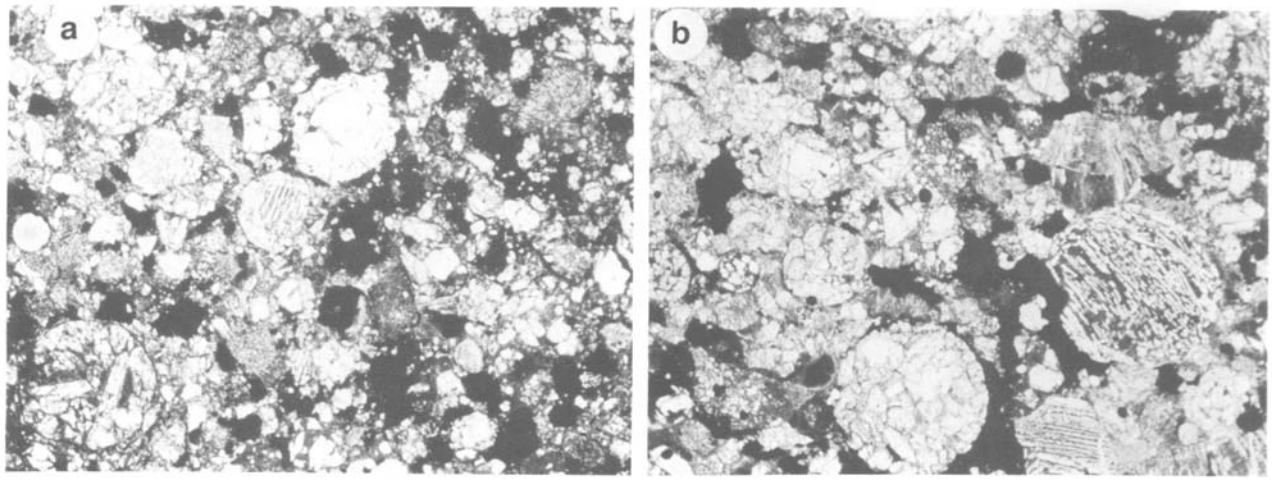

FIGURE 22.—Photomicrographs of thin sections of H3 chondrites (area of each field is 3 × 2 mm): *a*, RKPA80205; *b*, OTTA80301. (Closely packed aggregates of chondrules, irregular enclaves, and mineral grains set in a minor amount of dark matrix.)

to 1.1 mm across, and show a close-packed aggregate of chondrules and some irregular granular enclaves; the matrix consists of fine-grained silicates with a moderate amount of nickel-iron and a lesser amount of troilite. Chondrules range up to 1.1 mm across, and show a variety of types, the commonest being granular olivine and olivine-pyroxene (polysynthetically twinned clinobronzite), porphyritic olivine, and fine-grained pyroxene. Some intergranular glass in the chondrules is clear and transparent, but much of it is turbid and partly devitrified. Minor brown limonitic staining is present around nickel-iron grains. Microprobe analyses show olivine and pyroxene with variable composition: olivine, Fa_{17} to Fa_{19}, average Fa_{18}; pyroxene, Fs_4 to Fs_{11}, average Fs_{10}.

RKPA80205 (53.8 g).—This stone (4 × 3 × 2.5 cm) is partly covered by dull brownish black fusion crust; a weathering rind, 1 mm thick, is present, but the interior is only moderately weathered. The thin section shows a closely packed mass of chondrules (0.2–2.4 mm diameter), chondrule fragments, and irregular crystalline aggregates, with interstitial nickel-iron and troilite and a small amount of dark fine-grained matrix. A considerable variety of chondrules is present; many are granular to porphyritic olivine with transparent to turbid intergranular glass; others consist of granular polysynthetically twinned clinopyroxene with or without olivine, fine-grained pyroxene, or barred olivine. Minor brown limonitic staining is present throughout the section. Microprobe analyses show olivine ranging in composition from Fa_{17} to Fa_{20}, with a mean of Fa_{18}; the pyroxene is low-calcium (CaO 0.1–0.2%) clinobronzite, ranging in composition from Fs_5 to Fs_{13}, with a mean of Fs_{18}.

RKPA80207 (17.7 g).—Dull black fusion crust covers one surface of this specimen (3 × 2.5 × 1.5 cm); other surfaces are deeply weathered. In thin section, chondrules are abundant, ranging from 0.3 to 1.5 mm in diameter; a wide variety is present, the commonest being granular olivine and olivine-pyroxene, and fine-grained pyroxene. The granular chondrules have intergranular glass, sometimes pale brown and transparent but commonly turbid and partly devitrified. Irregular granular clasts and chondrule fragments are also present. Most of the pyroxene is polysynthetically twinned. The matrix consists of fine-grained olivine and pyroxene, with minor subequal amounts of nickel-iron and troilite. Veinlets of limonite and brown limonitic staining

pervade the section. Microprobe analyses show olivine ranging in composition from Fa_{15} to Fa_{29}, with a mean of Fa_{20} (% mean deviation of FeO is 32). Pyroxene composition range from Fs_0 to Fs_{28}, with a mean of Fs_{13}. [This meteorite is reclassified H3 from L3 by Scott (p. 76)].

Class L3

Figures 23, 24, 25, 26, 27

ALHA80133 (3.6 g).—This small stone (2.5 × 1.5 × 1 cm) has no fusion crust but has a reddish brown weathered surface showing rounded inclusions. The thin section shows a close-packed mass of chondrules and chondrule fragments with a small amount of dark fine-grained matrix. Chondrules range from 0.3 to 1.5 mm in diameter and show a diversity of type, the commonest being granular olivine and olivine-pyroxene, barred olivine, and fine-grained pyroxene. Transparent pale brown glass is present in some of the granular chondrules. Much of the pyroxene is polysynthetically twinned clinobronzite. Weathering is extensive, with brown limonitic staining throughout the section. Microprobe analyses show that olivine and pyroxene have highly variable composition: olivine, $Fa_{0.5}$ to Fa_{35}, mean Fa_{14}; pyroxene, Fs_5 to Fs_{30}, mean Fs_{14}. This specimen was originally classified as a C3 chondrite, but Dr. E.R.D. Scott (personal communication) has identified it as an L3 chondrite, paired with ALHA77011 and many other L3 chondrites from the Allan Hills.

Figure 23.—ALHA81024, L3 chondrite, a rounded angular stone with several deep fractures, with a reddish brown weathered surface.

Figure 24.—RKPA80256, L3 chondrite, a fractured stone partly covered with brownish black fusion crust; the fracture surface shows a closely packed aggregate of chondrules and enclaves in dark fine-grained matrix.

ALHA81024 (797 g).—This angular specimen (10 × 8 × 6.5 cm) is covered with reddish brown to black fusion crust on all sides except where eroded away, mainly along fractures. The interior is reddish brown and appears to be extremely weathered. The thin section shows a close-packed aggregate of chondrules, up to 1.5 mm across; a variety of types is present, including porphyritic olivine, barred olivine, granular olivine and olivine-pyroxene, and fine-grained pyroxene. Much of the pyroxene is polysynthetically twinned clinobronzite. Some intergranular glass within the chondrules is pale brown and transparent, but commonly is turbid and partly devitrified. Minor amounts of nickel-iron (largely altered to brown limonite) and troilite are present in the matrix. Olivine and pyroxene have variable composition. Olivine composition ranges from Fa_3 to Fa_{28}, with a mean of Fa_{19} (% mean deviation FeO is 34). Pyroxene composition ranges from Fs_2 to Fs_{24}, with a mean of Fs_{10} (% mean deviation FeO is 79). Transparent chondrule glass has the following mean composition (weight percent): SiO_2 63.3, Al_2O_3 22.5, FeO 0.9, MgO 0.2, CaO 0.2, K_2O 3.3, Na_2O, 8.8,

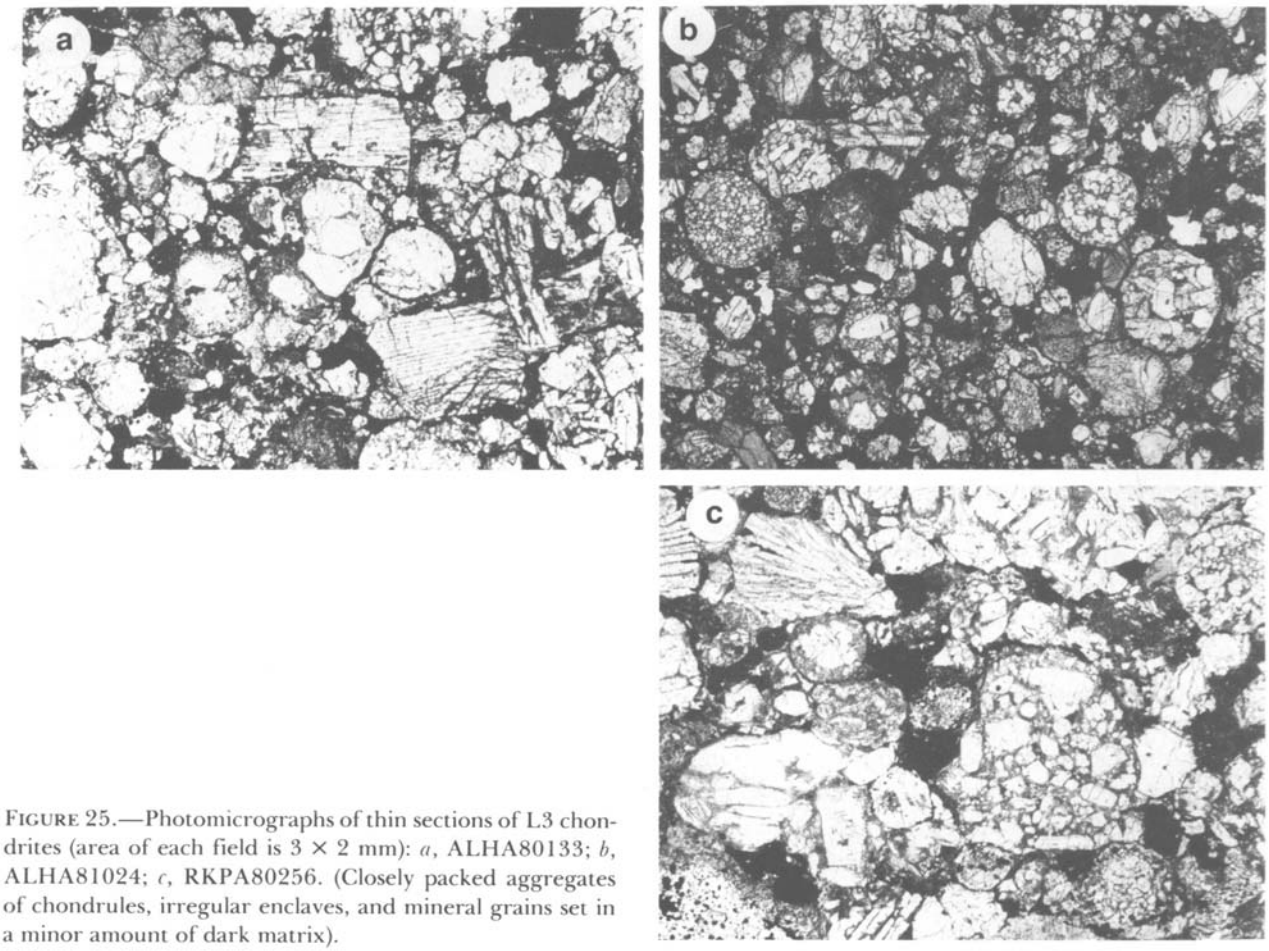

FIGURE 25.—Photomicrographs of thin sections of L3 chondrites (area of each field is 3 × 2 mm): *a*, ALHA80133; *b*, ALHA81024; *c*, RKPA80256. (Closely packed aggregates of chondrules, irregular enclaves, and mineral grains set in a minor amount of dark matrix).

FIGURE 26.—ALHA81031, L3 chondrite, a fractured and weathered stone showing some light-colored angular clasts on the surface.

TiO_2 0.8, MnO 0.03; this composition is close to anorthoclase.

ALHA81025 (379 g).—This stone (9.5 × 8 × 4.5 cm) is extremely weathered; rounded and irregular inclusions (one 7 × 5 mm) are visible on the weathered surfaces.

ALHA81030 (1851 g).—Patchy black fusion crust is present on all surfaces of this angular stone (18 × 9 × 7.5 cm). Several large fractures penetrate the interior. Inclusions can be seen on the exterior and on chipped surfaces.

ALHA81031 (1594 g).—This is an angular specimen (73 × 9 × 9 cm) with small areas of thin lustrous black fusion crust. The surface is weathered dark reddish brown and is penetrated by numerous fractures.

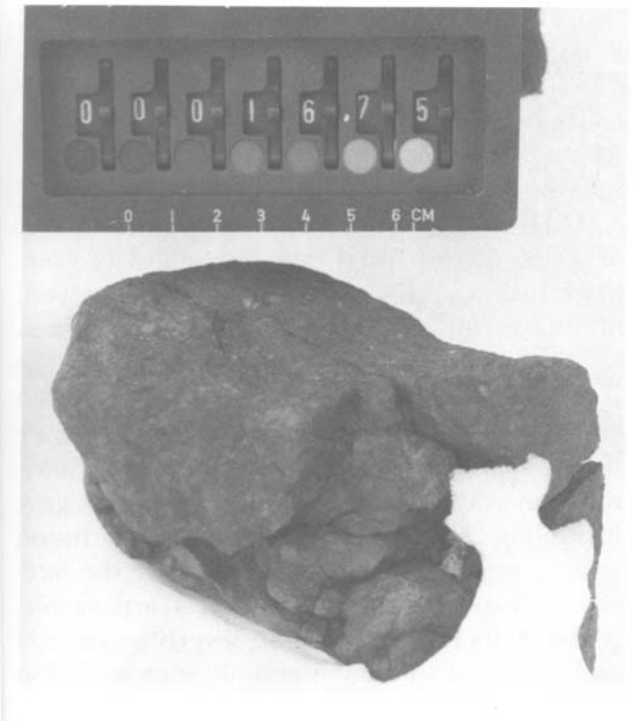

FIGURE 27.—ALHA81031, L3 chondrite, an angular weathered stone partly covered with lustrous black fusion crust; photographed as found.

ALHA81032 (726 g).—Lustrous black fusion crust is present on small areas of this angular stone (9 × 9 × 6 cm). Light colored clasts or chondrules up to 0.5 cm across are visible on weathered surfaces.

The thin section of ALHA81025 shows a close-packed aggregate of chondrules and chondrule fragments up to 3.5 mm across, in a fine-grained matrix of olivine, pyroxene, troilite, and a little nickel-iron. Chondrule types include porphyritic olivine, granular olivine and olivine-pyroxene, barred olivine, and radiating pyroxene. Much of the pyroxene is polysynthetically twinned clinobronzite. Intergranular glass is present in the chondrules, usually turbid but sometimes transparent and purple-brown. Weathering is extensive, with small areas of brown limonite throughout the section. Microprobe analyses show that olivine and pyroxene have variable composition. Olivine composition ranges from Fa_1 to Fa_{41}, with a mean of Fa_{18} (percent mean deviation FeO is 76). Pyroxene composition ranges from Fs_3 to Fs_{40}, with a mean of Fs_{15} (percent mean deviation FeO is 75). Purple glass in a chondrule has the following mean composition (weight percent): SiO_2 56.8, Al_2O_3 24.1, FeO 3.7, MgO 2.4, CaO 0.4, K_2O 4.1, Na_2O 8.8, TiO_2 1.2, MnO 0.09.

Thin sections of ALHA81025, 81030, 81031, and 81032 are so similar in texture, range of mineral composition, and degree of weathering that these meterorites can be paired, together with ALHA77011 (Scott, personal communication).

RKPA80256 (153 g).—This meteorite (7 × 5.5 × 3 cm) is almost totally covered with brownish black fusion crust. Chondrules and white and gray clasts up to 5 mm across are visible on exposed surfaces. The thin section shows a closely packed mass of chondrules (0.3–1.8 mm diameter) and irregular crystalline aggregates. Some of the chondrules have prominent dark rims. The sparse matrix is dark and fine-grained, with a small amount of coarser nickel-iron and troilite scattered throughout. A notable variety of chondrules is present; many are granular or porphyritic olivine and olivine-pyroxene with transparent to turbid interstitial glass. The pyroxene is polysynthetically twinned clinobronzite. There is a little limonitic staining in association with metal grains. Microprobe analyses show olivine ranging in composition from Fa_{20} to Fa_{25}, with a mean of Fa_{22} (% mean deviation of FeO is 8.3). The pyroxene is low-calcium (CaO = 0.1–0.8%), with a composition range of Fs_{10} to Fs_{26} and a mean of Fs_{18}.

CLASS LL3

FIGURE 28

ALHA81251 (158 g).—This meteorite (6.5 × 6 × 2.5 cm) is partly covered with thin lustrous black fusion crust. Broken surfaces show abundant chondrules up to 5 mm in diameter. The interior is weathered a deep reddish brown color.

The thin section of ALHA81251 shows a close-packed aggregate of chondrules and chon-

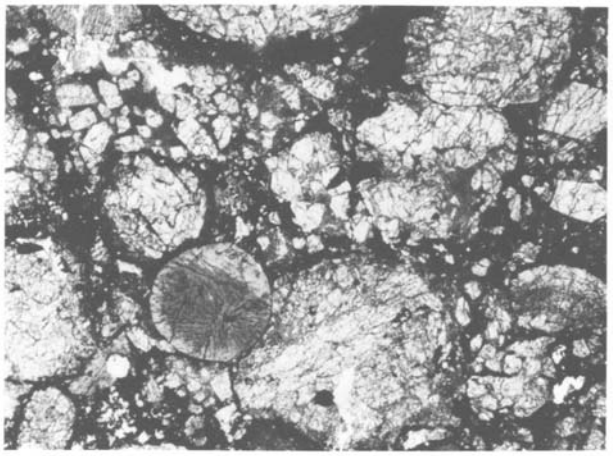

FIGURE 28.—Photomicrograph of a thin section of ALHA81251, an LL3 chondrite (area of the field is 3 × 2 mm). Numerous chondrules, with some angular enclaves and mineral grains, set in a minor amount of dark matrix.

drule fragments, up to 3 mm in maximum dimension. Most of the matrix is black and opaque, with small grains of olivine and pyroxene; the black matrix appears to be carbonaceous, with small amounts of troilite and nickel-iron (largely weathered to limonite). A wide variety of chondrule types is present, including barred olivine, granular olivine and olivine-pyroxene, and fine-grained pyroxene. Clear glass is present in barred olivine chondrules. Microprobe analyses show olivine and pyroxene with variable compositions: olivine, Fa_1 to Fa_{29}, mean Fa_{14} (percent mean deviation FeO is 64); pyroxene, Fs_2 to Fs_{28}, mean Fs_{13} (percent mean deviation FeO is 72). Clear glass in a barred olivine chondrule has the following composition (weight percent): SiO_2 61.4, Al_2O_3 23.5, FeO 1.7, MgO 2.0, CaO 0.4, Na_2O 4.8, K_2O 1.6, TiO_2 1.1, MnO 0.01.

ALHA81251 is tentatively paired with ALHA76004 (Scott, personal communication).

CLASS H4

FIGURES 29, 30

Four H4 chondrites (ALHA80106, 432 g; 80121, 39.1 g; 80128, 138 g; 80131, 19.8 g) were collected at the Allan Hills in 1980–1981, and three (ALHA81022, 912 g; 81044, 386 g; 81048, 190 g) have been identified in the 1981–1982 collection. Three small specimens were collected near Reckling Peak in 1980–1981: RKPA80232, 80.1 g; 80237, 22.2 g; 80267, 24.2 g.

ALHA80106 consists of five fragments, four of which can be fitted together. Areas of shiny black fusion crust are present, but areas devoid of fusion crust are weathered reddish brown, and weathering appears pervasive throughout the fragments. ALHA80128 has dull black fusion crust on all but one surface; several large fractures penetrate the specimen, and the interior is medium gray speckled with white and dark gray inclusions. ALHA81022 has thin black fusion crust over much of the surface; where the interior is exposed many chondrules are visible. ALHA81044 and 81048 are severly weathered and fractured specimens with little or no fusion crust.

In thin sections these specimens show the typical features of Class H4 chondrites: well-developed chondrules, the commonest being granular and porphyritic olivine and olivine-pyroxene, barred olivine, and fine-grained radiating pyroxene (much of the pyroxene is polysynthetically twinned clinobronzite); the groundmass consists

FIGURE 29.—ALHA81022, H4 chondrite, a fractured stone with thin black fusion crust on the original surface; numerous mm-sized chondrules are visible on the fracture surface.

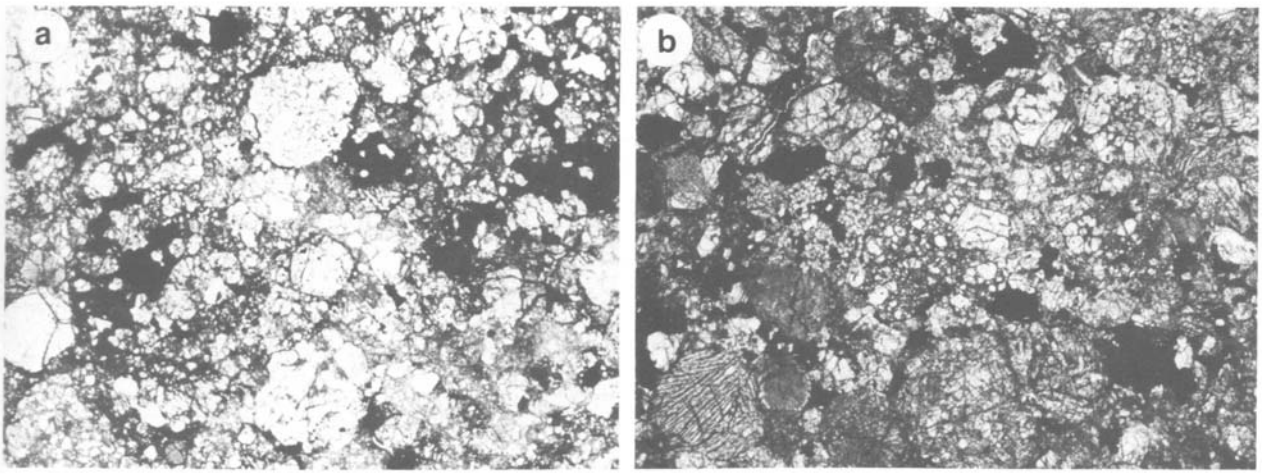

FIGURE 30.—Photomicrographs of thin sections of H4 chondrites (area of each field is 3 × 2 mm): *a*, RKPA80237; *b*, ALHA81044. (Numerous well-defined chondrules are present, but some chondrule margins tend to merge with the granular matrix).

of fine-grained olivine and pyroxene, with minor amounts of nickel-iron and troilite. The Allan Hills specimens have olivine of essentially uniform composition (Fa_{18} to Fa_{19}) and somewhat variable pyroxene (Fs_{15} to Fs_{22}). The ALHA80xxx specimens are possibly paired; ALHA81044 and 81048 are probably pieces of a single meteorite; and ALHA81022 is tentatively paired with ALHA78084 and 77009. The Reckling Peak specimens have olivine (Fa_{18} to Fa_{19}) and pyroxene (Fs_{16}) of essentially uniform composition and are possibly paired.

CLASS L4

FIGURES 31, 32

Two L4 chondrites (RKPA80216, 44.3 g; 80242, 7.3 g) were collected near Reckling Peak in the 1980–1981 season, and one (ALHA81040, 194 g) has been identified in the 1981–1982 collection from the Allan Hills. ALHA81040 is a round stone (5.5 × 5 × 5 cm) with about 75% of its surface covered with dull black fusion crust; where fusion crust is lacking the surface is weathered to a deep reddish brown. The Reckling Peak specimens are small weathered stones completely or almost completely covered with fusion crust.

FIGURE 31.—ALHA81040, L4 chondrite, a rounded stone with much of the surface covered with dull black fusion crust.

Thin sections of these meteorites show the typical features of L4 chondrites. Chondritic structure is well developed, with a variety of chondrule types; irregular granular aggregates, possibly chondrule fragments, are also present. The chondrules are set in a fine-grained matrix consisting largely of olivine and pyroxene, with minor subequal amounts of nickel-iron and troilite. Some of the pyroxene, especially in the chondrules, is polysynthetically twinned clinobron-

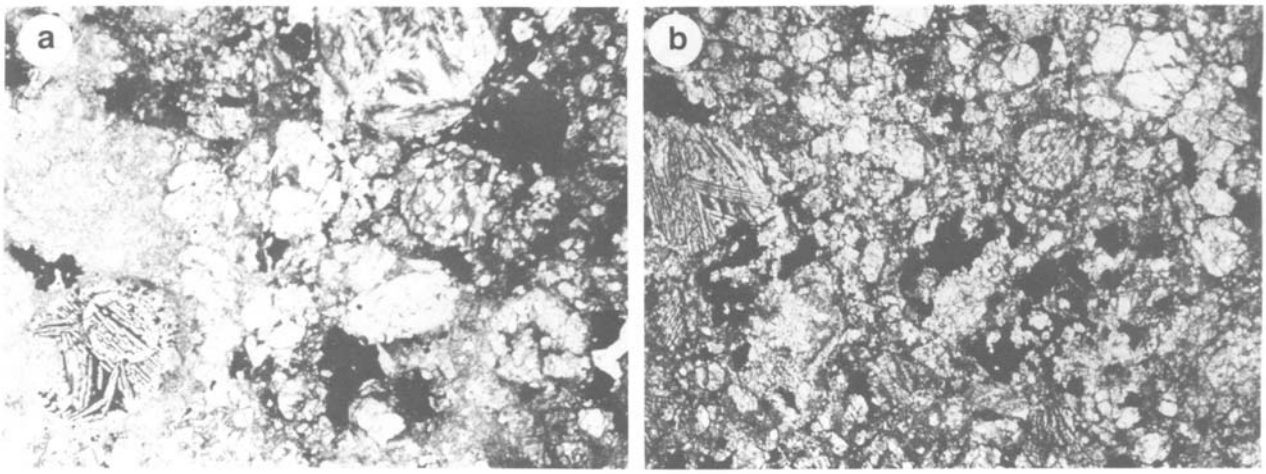

FIGURE 32.—Photomicrographs of thin sections of L4 chondrites (area of each field is 3 × 2 mm): *a*, RKPA80216; *b*, ALHA81040. (Chondritic structure is prominent, but some chondrules show partial integration with the granular matrix; note barred chondrule within barred chondrule in RKPA80216).

zite. Olivine and pyroxene are essentially uniform in composition: olivine, Fa_{23} to Fa_{25}; pyroxene, Fs_{19} to Fs_{21}. The Reckling Peak specimens resemble each other closely in mineralogical compositions, texture, and degree of weathering, and are possibly paired.

CLASS H5

FIGURES 33, 34

Six H5 chondrites were collected at the Allan Hills in the 1980–1981 season, but only one (ALHA80132, 152 g) weighs more than 100 g. ALHA80132 (8 × 4.5 × 3 cm) is a flat stone largely covered with dull brownish black fusion crust with prominent flow bands on one surface; it is considerably fractured and has a thick weathering rind. Nine have been identified in the 1981–1982 collection, all weighing more than 100 g. Nineteen were collected near Reckling Peak in 1980–1981, but most were small specimens; the only ones larger than 100 g are RKPA80220 (124 g) and 80233 (413 g). RKPA80220 is a complete stone (5.4 × 4 × 3 cm) entirely covered with thin patchy fusion crust; several fractures penetrate the interior, which is considerably weathered. RKPA80233

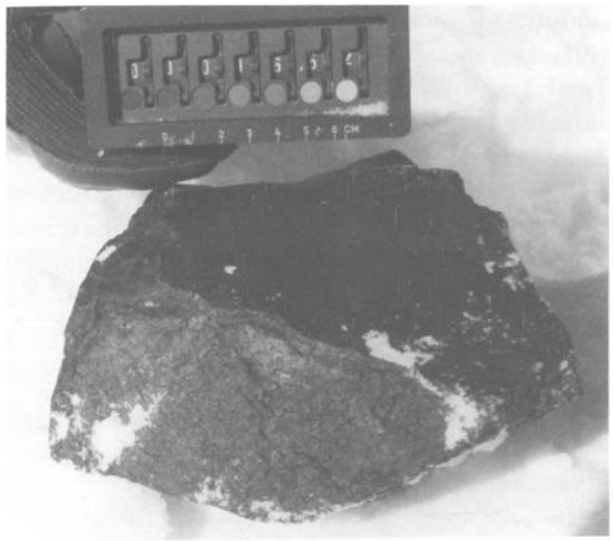

FIGURE 33.—ALHA81015, an H5 chondrite, photographed as found.

(8.5 × 6.5 × 5 cm) has one planar fracture surface, and the rest of the surface is covered with patches of fusion crust; the fracture surface contains numerous chondrules, which can easily be plucked out. Most of the 1981–1982 H5 chondrites from Allan Hills (ALHA81015, 81019, 81020, 81033, 81034, 81036, 81039,

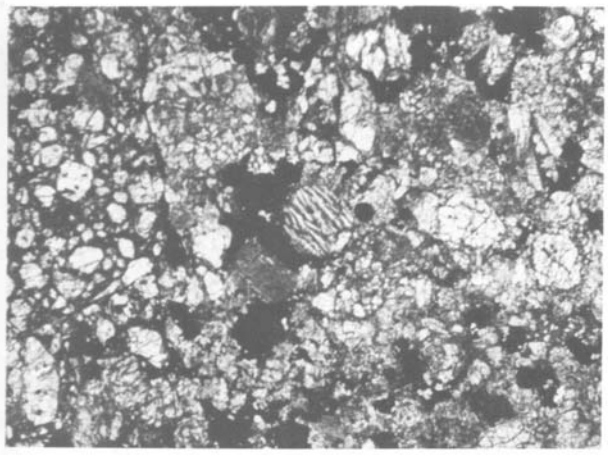

FIGURE 34.—ALHA81033, H5 chondrite, photomicrograph of thin section (area of field is 3 × 2 mm); chondritic structure is well developed, but margins of chondrules tend to merge with the granular groundmass.

81042, 81067) are individual stones partly covered with fusion crust. ALHA81033 consists of six weathered fragments. ALHA81039 (10 × 4.5 × 4 cm) consists of two pieces, which fit together, and a small additional piece; black fusion crust is present on most of the original surface, and a weathering rind is present on fracture surfaces, but the interior is light gray and only slightly weathered. ALHA81067 (7 × 5.5 × 4 cm) was collected as two pieces, which fit together perfectly but do not form a complete stone; some patchy fusion crust is present on original surfaces, and fracture surfaces are deeply weathered to an iridescent red-brown color.

In thin sections all the H5 chondrites show a generally well-developed chondritic structure with a variety of chondrule types, including granular and porphyritic olivine and olivine-pyroxene, barred olivine, and fine-grained pyroxene. Chondrule margins may be somewhat diffuse, tending to merge with the granular groundmass, which consists largely of olivine and pyroxene, with minor amounts of nickel-iron and troilite; minute grains of sodic plagioclase can sometimes be detected. The compositions of the olivine (Fa_{16} to Fa_{19}) and orthopyroxene (Fs_{14} to Fs_{17}) are uniform within the individual specimens.

The Reckling Peak H5 chondrites resemble each other in texture, mineral compositions, and degree of weathering; RKPA80220 and 80223 have been tentatively paired, as have RKPA 80250 and 80251, and further research will probably extend these pairings. The Allan Hills 1980–1981 H5 chondrites, except ALHA 80123, are also very similar in texture, mineral compositions, and degree of weathering, and are tentatively paired; ALHA80123 is more severely weathered and may be a different fall. Possible pairings among the Allan Hills 1981–1982 H5 chondrites remain to be studied.

CLASS L5

FIGURES 35, 36, 37

Three small L5 chondrites were collected near Reckling Peak in the 1980–1981 season: RKPA 80209 (9.7 g), 80228 (11.1 g), 80268 (3.4 g); they are individual stones partly or completely covered with fusion crust. Three L5 chondrites have been identified in the 1981–1982 Allan Hills collection: ALHA81017 (1434 g), 81018 (2236 g), 81023 (418 g). ALHA81017 consists of two pieces (13.5 × 8 × 7 cm and 10 × 9 × 5.5 cm), which do not fit together but are clearly parts of a single stone. Each piece has small areas of dark fusion crust and are somewhat weath-

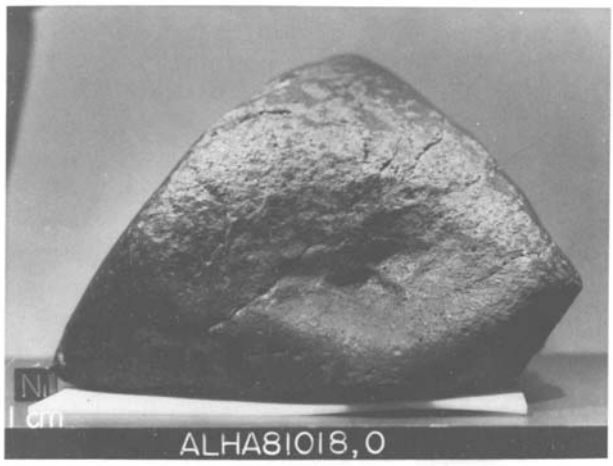

FIGURE 35.—ALHA81018, L5 chondrite, an angular weathered stone partly covered with dull black fusion crust.

FIGURE 36.—ALHA81023, L5 chondrite, found as fragments with remnants of black fusion crust.

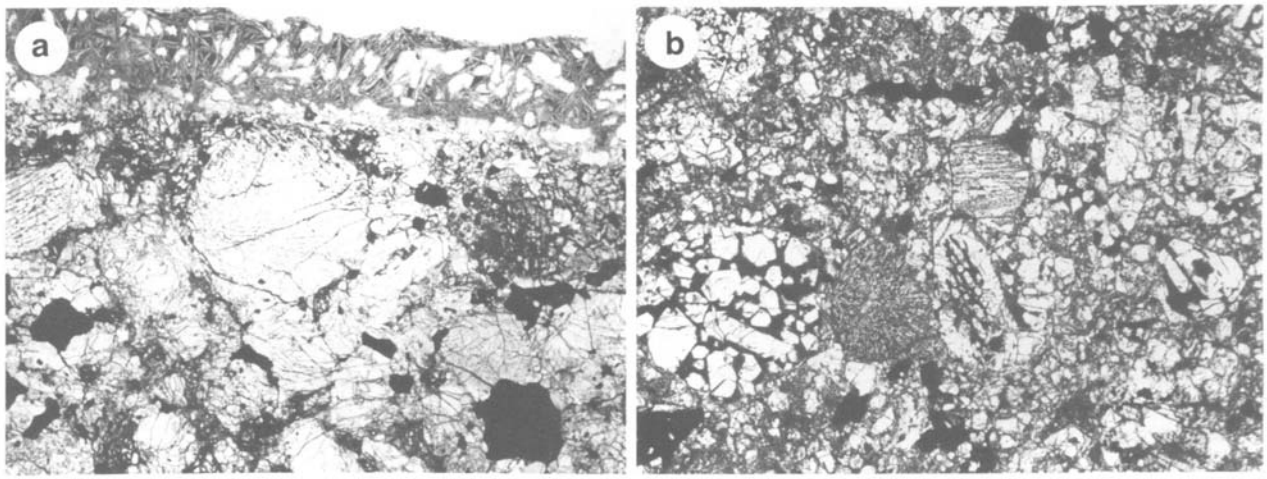

FIGURE 37.—Photomicrographs of thin sections of L5 chondrites (area of fields is 3 × 2 mm): *a*, RKPA80209; *b*, ALHA81023. (Chondrules are prominent, but show some integration with the granular groundmass; note well-preserved fusion crust on RKPA80209).

ered, with oxidation halos around metal grains. ALHA81018 is an angular stone (13.5 × 11 × 10 cm) partly covered with dull black fusion crust; several fractures penetrate the stone, and a weathering rind approximately 10 mm thick is present. ALHA81023 was found as two large pieces, two small pieces, and many tiny chips; none of the pieces fit together, but they are

clearly related. Remnants of fusion crust are present. The interior is light gray and shows many dark colored chondrules and irregular inclusions.

In thin sections the L5 chondrites show a generally well-developed chondritic structure, with a variety of chondrule types, including porphyritic olivine, granular olivine and olivine-pyroxene, and radiating fine-grained pyroxene. Chondrule margins are often diffuse, tending to merge with the granular groundmass, which consists largely of olivine and pyroxene with minor subequal amounts of nickel-iron and troilite. The compositions of the olivine (Fa_{23} to Fa_{25}) and orthopyroxene (Fs_{19} to Fs_{21}) are essentially uniform within the individual specimens.

ALHA81017, 81018, and 81023 are very similar in all respects, and the possibility of their being paired should be considered.

Class LL5

FIGURE 38

Two LL5 chondrites were collected near Reckling Peak during the 1980–1981 field season RKPA80234 (136 g) and RKPA80253 (4.6 g). Although they show some similarities, there are sufficient differences to indicate that they are probably not paired: 80253 is practically unweathered, whereas 80234 is considerably weathered, with extensive brown limonitic staining.

RKPA80234 is a flat stone, 6 × 5 × 2 cm, with fusion crust on one surface; the other surfaces have weathered to a reddish brown color. In thin sections chondritic structure is barely discernible, the sparse chondrules being largely obscured by extensive brecciation. The section shows an aggregate of olivine and pyroxene, with a little troilite and nickel-iron. Microprobe analyses gave the following compositions: olivine, Fa_{26}; orthopyroxene, Fs_{22}.

RKPA80253 is a small flat stone, 2 × 2 × 1 cm, almost totally covered with black fusion crust, blistery in places; the interior has a whitish gray color and contains many dark angular inclusions. In thin section chondrules are fairly abundant, and are relatively large, ranging up to 3 mm in diameter. Brecciation is prominent, and many of the chondrules are fractured and deformed. Only a little nickel-iron is present. Microprobe analyses gave the following compositions: olivine, Fa_{27}; orthopyroxene, Fs_{22} with a few more Mg-rich grains; plagioclase, An_{10}. This

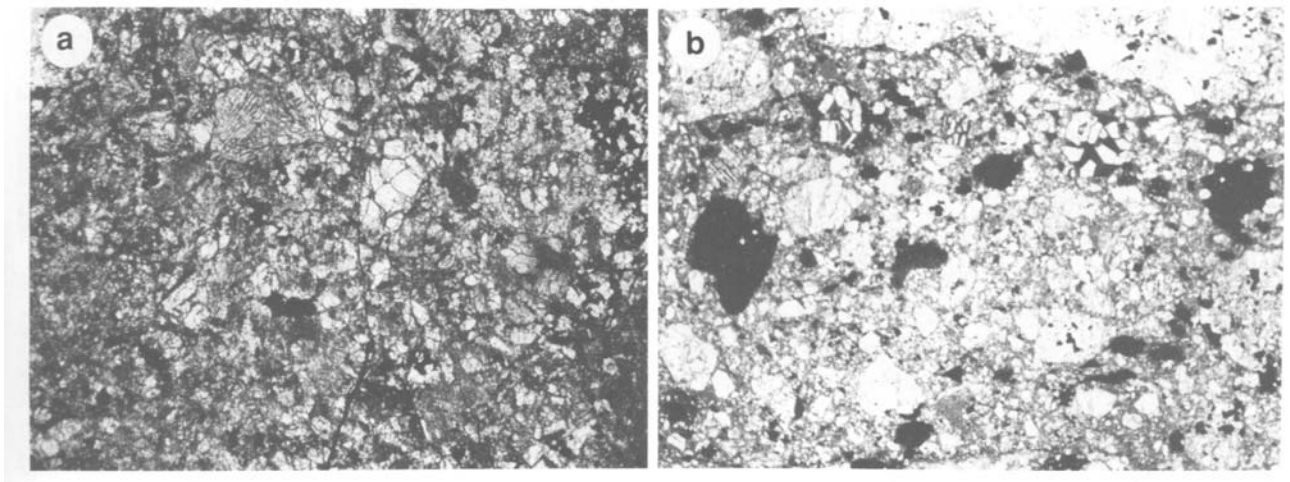

FIGURE 38.—Photomicrographs of thin sections of LL5 chondrites (area of fields is 3 × 2 mm): *a*, RKPA80234; *b*, RKPA80253. (Chondritic structure is somewhat obscured by the extensive brecciation these meteorites have experienced).

meteorite is classified as an LL5 chondrite, but different areas of the brecciated structure show features of higher and lower type.

Class E5

FIGURE 39

RKPA80259 (20.2 g).—Thin iridescent fusion crust covers most of this small stone (2.5 × 1.5 × 1.5 cm). The interior is dark colored and weathered, and shows a small amount of a white evaporite deposit. In thin section chondrules are rare and barely discernible, the meteorite consisting largely of fine-grained enstatite (mean grain size approximately 0.05 mm), with some nickel-iron and troilite. Weathering is very extensive, with much red-brown limonite throughout the section. The silicate material is blackened by the presence of finely dispersed troilite, probably the result of an episode of severe shock. Microprobe analyses showed that the enstatite is almost pure $MgSiO_3$, with minor amounts of Al_2O_3 (0.1–0.3%), FeO (0.1–0.5%), and CaO (0.5–0.8%.).

Class H6

FIGURES 40, 41

Four H6 chondrites were collected at the Allan Hills in the 1980–1981 season: ALHA80118, 80122, 80126, 80130. Each weighs less than 100 g; 81022, 80126, 80130 are very similar and are probably pieces of a single meteorite, but 80118 is less weathered and is probably a different fall. Six H6 chondrites have been identified in the 1981–1982 collection: ALHA81035 (256 g), 81037 (320 g), 81038 (229 g), 81093 (271 g), 81102 (196 g), 81111 (210 g). ALHA81035 is a complete stone, 7.5 × 5.5 × 3 cm, entirely covered with patchy fusion crust; it is extensively weathered. ALHA81037 is an angular specimen, 7.5 × 6 × 4 cm, with fusion crust on all but two sides; it is polygonally fractured, and the interior shows moderate weathering with rusty halos around metal grains. ALHA81038 is a rounded oblong stone, 7 × 4 × 4 cm, with remnants of fusion crust; several fractures penetrate the interior, which is extensively weathered. ALHA 81093 is an equidimensional stone, 6 × 5.5 × 4 cm, completely covered with dull black fusion crust. ALHA81102 is a weathered stone, 7.5 ×

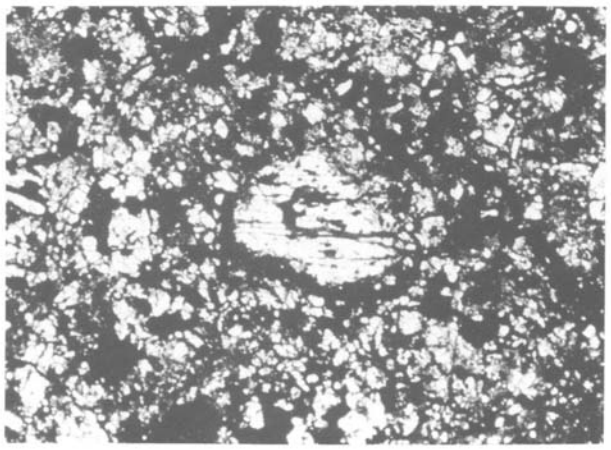

FIGURE 39.—RKPA80259, E5 chondrite, photomicrograph of thin section (area of field is 3 × 2 mm); an enstatite chondrule (center) in a matrix consisting largely of enstatite grains (white) with nickel-iron and sulfide (black).

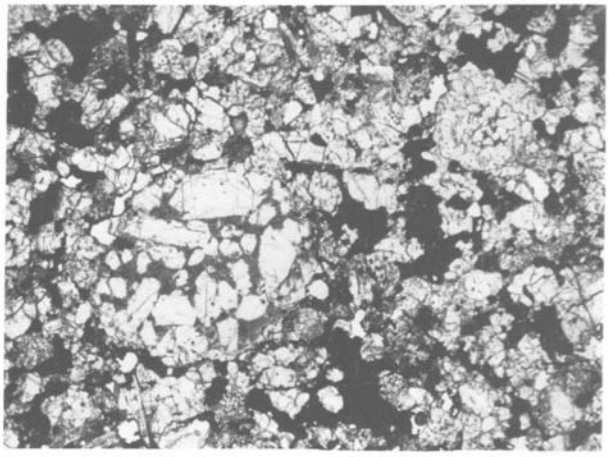

FIGURE 40.—ALHA81035, H6 chondrite, photomicrograph of thin section (area of field is 3 × 2 mm); chondritic structure is barely discernible, the chondrules merging with the granular groundmass.

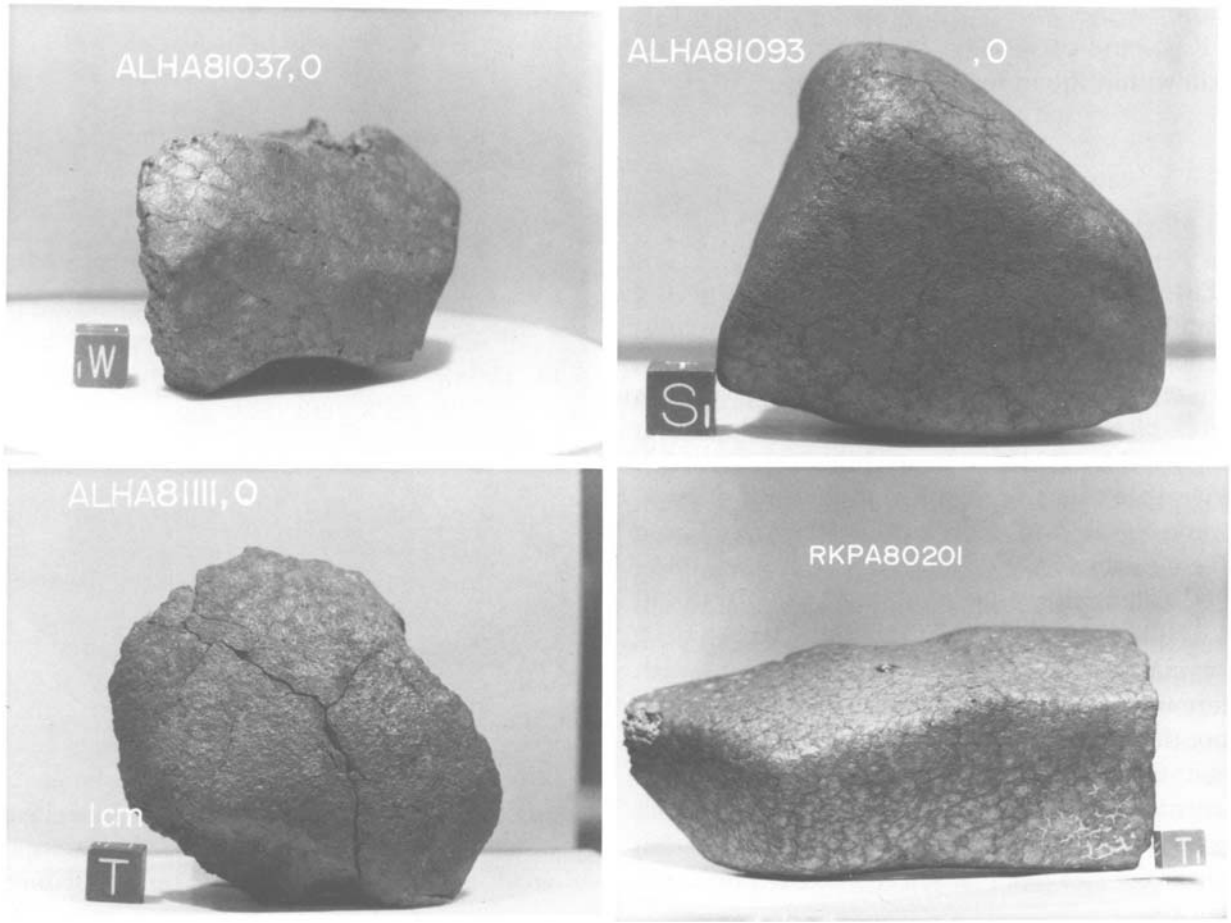

FIGURE 41.—H6 chondrites.

5 × 3 cm, with thin remnant fusion crust; most of the surface is oxidized to a dark red-brown color. ALHA81111 is a rounded stone, 8 × 6 × 4 cm; the upper half is covered with frothy black fusion crust, the lower half is weathered to an iridescent brown color.

Nineteen H6 chondrites were collected near Reckling Peak in the 1980–1981 season; they all weigh less than 100 g except RKPA80201 (813 g) and 80231 (238 g). RKPA80201 is a rectangular stone, 12 × 6 × 5.5 cm, almost completely covered with black fusion crust showing polygonal fractures; minute amounts of white evaporite deposits are present in some of the fractures. RKPA80231 is a weathered and fractured stone, 7 × 5 × 3 cm, with remnants of dull black fusion crust. All the Reckling Peak specimens except RKPA80201 are paired because of their similar and characteristic texture. Specifically they appear to have been considerably fractured and the minerals partly granulated; this feature has been made more prominent by extensive weathering, which has developed numerous thin limonite veinlets throughout the specimens.

All the H6 chondrites show very similar petrographic features. Chondrules are sparse and poorly defined, tending to merge with the granular groundmass, which consists mainly of olivine and pyroxene, with minor amounts of nickel-iron, troilite, and sodic plagioclase. Compositions

of the olivine (Fa_{17} to Fa_{20}) orthopyroxene (Fs_{15} to Fs_{17}), and plagioclase (An_{12} to An_{13}) are uniform within the individual specimens.

Class L6

Figures 42, 43

Fifteen L6 chondrites were collected at the Allan Hills in the 1980–1981 season, 12 weighing more than 100 g each. Macroscopic examination indicated that they might be paired as pieces of a single meteorite, and this has been supported by evidence from thin sections, which shows that they are identical in texture, mineral compositions, and degree of weathering. Three L6 chondrites have been identified in the 1981–1982 Allan Hills collection: ALHA81016 (3850 g), 81026 (515 g), 81027 (3835 g). ALHA81016 is a rounded stone, 15 × 12 × 11 cm, with remnants of fusion crust; most of the surface is smooth and weathered to a dark reddish brown color; the interior is a lighter brown-green color. Mineral grains with cleavage faces and distinct chondrules up to 4 mm across are visible on both

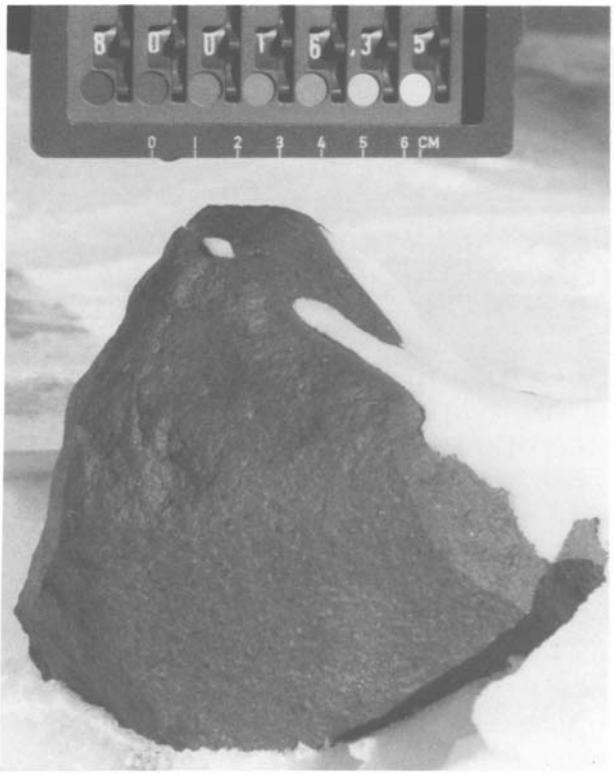

Figure 42.—ALHA81016, an L6 chondrite, photographed as found.

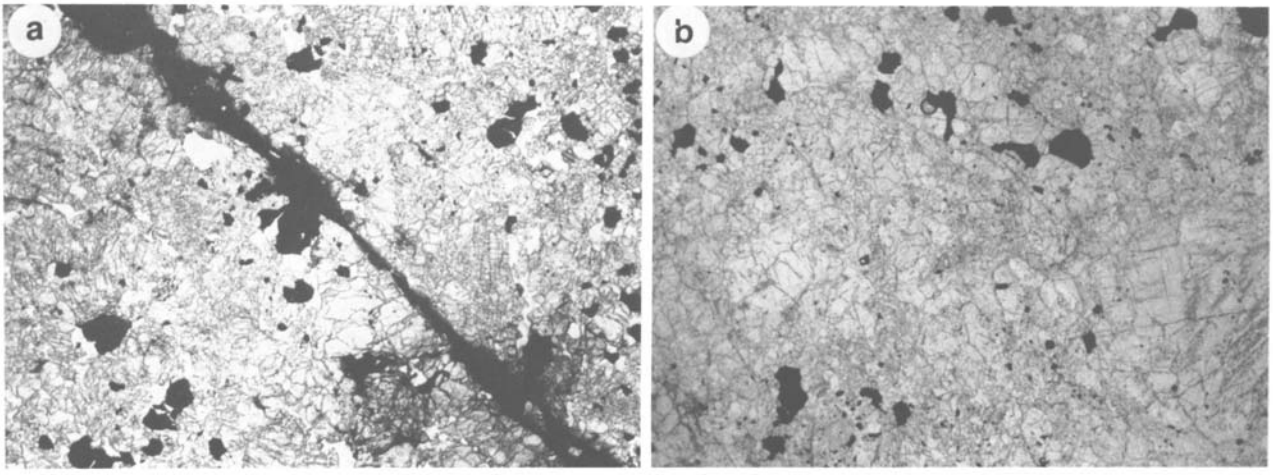

Figure 43.—Photomicrographs of thin sections of L6 chondrites (area of each field is 3 × 2 mm): *a*, RKPA80202, *b*, RKPA80252. (Chondritic structure is barely discernible, the chondrules merging with the granular groundmass; the dark glassy veinlet in RKPA80202 contains clear isotropic material tentatively identified as ringwoodite and majorite).

exterior and interior surfaces. ALHA81026 is a knobby stone, 11 × 6 × 5.5 cm, partly covered with dull black fusion crust; the interior is pale gray, with brown limonitic halos around metal grains. ALHA80127 consists of two pieces that fit together as an incomplete rounded stone, 17 × 11.5 × 10 cm; patchy fusion crust covers much of the surface, and the interior is extensively weathered. This meteorite has been shocked and plagioclase converted to maskelynite, with CaO content equivalent to An_{10} but with Na_2O low and variable, 4.0–5.2%.

Seven L6 chondrites were collected in the Reckling Peak area during the 1980–1981 field season; only one, RKPA80202 (544 g) weighs more than 100 g. All the Reckling Peak specimens except RKPA80215 are identical in texture, mineral compositions, and degree of weathering, and most of them have dark glassy veinlets containing clear isotropic grains tentatively identified as ringwoodite and majorite; these specimens are probably all pieces of a single meteorite and can be paired with RKPA78001, 78003, 79001, and 79002. RKPA80215 is much more weathered than the other Reckling Peak L6 chondrites, and appears to be more heavily shocked, the mineral grains being comminuted and traversed by shock veinlets of troilite.

Class LL6

FIGURE 44

Four LL6 chondrites were collected from the Reckling Peak area in the 1980–1981 field season: RKPA80222 (6.9 g), 80235 (261 g), 80238 (18.4 g), 80248 (11.3 g). RKPA80222, 80238, and 80248 were paired on the basis of macroscopic examination, and this has been confirmed by the evidence from the thin sections. They show the brecciated structure characteristic of many LL chondrites. Chondritic structure is barely discernible, the specimens consisting of a granular aggregate of olivine and pyroxene, with minor amounts of plagioclase and troilite, and a little nickel-iron; some of the nickel-iron is present as unusually large grains, up to 3 mm. A small amount of limonitic staining is present around the metal grains. RKPA80235 differs in being unbrecciated, having less troilite and nickel-iron (without limonitic staining), and having somewhat higher Fa and Fs contents in olivine and pyroxene (Fa_{30} vs. Fa_{28}, Fs_{24} vs. Fs_{23}).

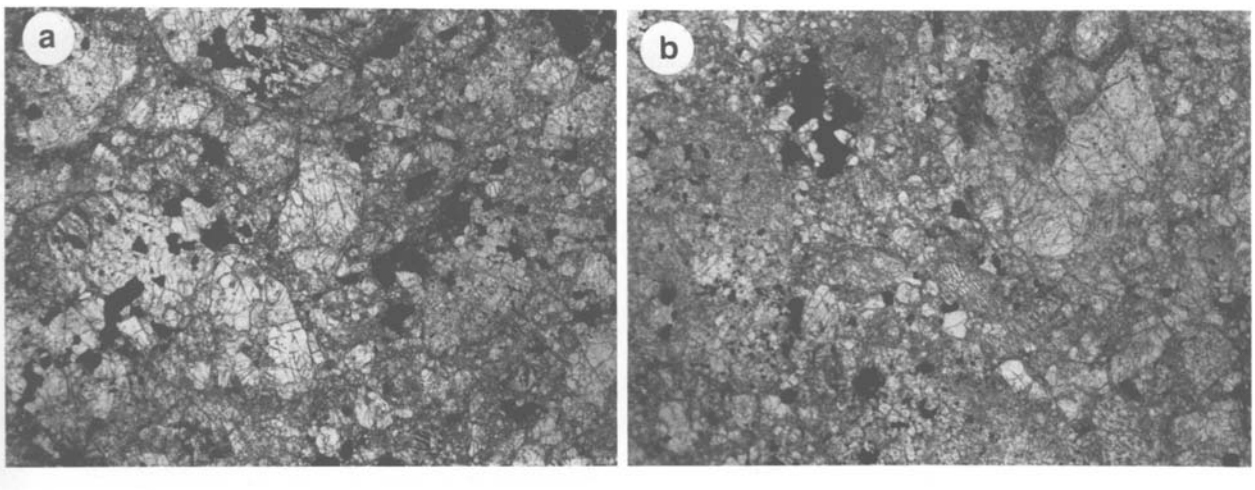

FIGURE 44.—Photomicrographs of thin sections of LL6 chondrites (area of each field is 3 × 2 mm): *a*, RKPA80222; *b*, RKPA80238. (Chondritic structure is barely discernible, being obscured by extenisve brecciation and integration with the granular matrix).

FIGURE 45.—ALHA81021, E6 chondrite, photographed as found; a rounded stone covered with thin black fusion crust showing flow lines.

CLASS E6

FIGURES 45, 46

ALHA81021 (695 g).—This stone (12 × 9 × 3 cm) is smooth and flat, with thin black fusion crust with flow lines on the upper surface; the lower surface is considerably weathered and some of the fusion crust removed, leaving a smooth red-brown surface. Only traces of chondritic structure are visible in a thin section, which consists largely of granular enstatite, with considerable nickel-iron (~20%), minor troilite and plagioclase, and accessory sinoite (Si_2N_2O, identified by its high birefringence). Weathering is extensive, with brown limonitic staining throughout the section. Remnants of fusion crust are present. Microprobe analyses show the enstatite is almost pure $MgSiO_3$ (CaO 0.8%, FeO 0.2%,

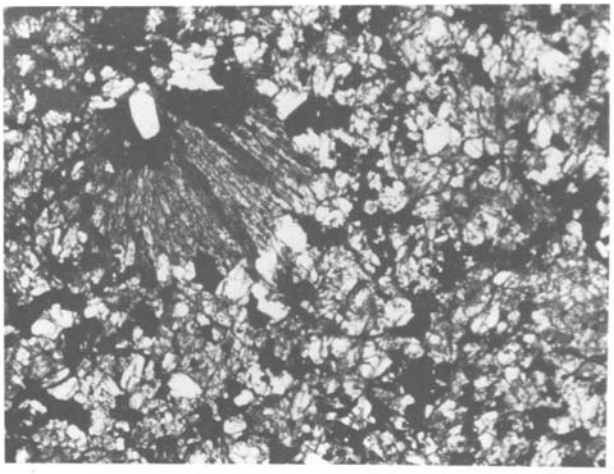

FIGURE 46.—ALHA81021, E6 chondrite, photomicrograph of thin section (area of field is 3 × 2 mm); a radiating enstatite chondrule is enclosed in a field of granular enstatite (white to gray), nickel-iron and sulfides (black).

Al_2O_3 0.2%); plagioclase is $An_{15}Or_4$; the metal contains about 2% Si.

Achondrites

EUCRITES

FIGURES 47, 48, 49

At the Allan Hills in 1980–1981 one eucrite (ALHA80102, 471 g) was collected, and in 1981–1982 several more (ALHA81001, 52.9 g; 81006, 254 g; 81007, 163 g; 81008, 43.8 g; 81009, 229 g; 81010, 219 g; 81011, 405 g; 81012, 36.6 g).

ALHA80102 (12.5 × 8 × 5. cm) has areas of shiny black fusion crust, except on a fracture surface; many vugs, ranging in size from less than 1 mm to greater than 1 cm, are present, typical of Allan Hills polymict eucrites. The interior is medium gray with mm-sized and larger white, yellow, and black clasts throughout. ALHA 81001 is a small stone (4.5 × 4.5 × 4.0 cm) with lustrous black fusion crust on two surfaces; the interior is highly fractured and is quite unlike other eucrites in being glassy and smoky gray in color. ALHA81006 (11 × 4.5 × 3.5 cm) is an elongated stone covered with shiny black fusion crust except on a fracture surface; this surface has mm-size patches of fusion crust, indicating a late breakup in the atmosphere. It is a typical polymict eucrite and has two notably large clasts (7 × 11 mm and 15 × 13 mm). ALHA81007 (8.5 × 6 × 2.5 cm) and 81008 (5 × 3.5 × 3 cm) are similar. ALHA81009 (7 × 5.5 × 3.5 cm) is a hemispherical stone almost completely covered with lustrous black fusion crust. ALHA81010 (8 × 55.5 cm) is similar. ALHA81011 (8 × 65 cm) is a rounded stone with scattered remnants of black fusion crust; it is unusual in containing numerous large clasts up to 2 cm across. Several different types are present—typical eucritic clasts, recrystallized pinkish white clasts, massive gray clasts—and they range in shape from rounded to rectangular to lens-shaped. ALHA81012 (5 × 2 × 3 cm) is a lens-shaped stone typical of the Allan Hills polymict eucrites.

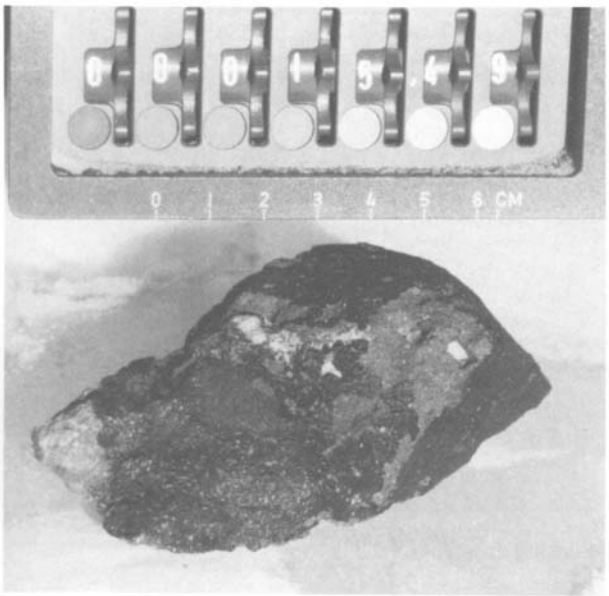

FIGURE 47.—ALHA81006, a polymict eucrite, photographed as found.

ALHA80102, 81006, 81007, 81008, and 81010 are very similar in all respects and are probably paired with previously described Allan Hills polymict eucrites. The following description of the thin section of ALHA81010 is typical of all of them. The meteorite is a microbreccia, consisting largely of angular monomineralic pyroxene and plagioclase clasts up to 4 mm in maximum dimension, and a few lithic clasts, in a matrix of comminuted pyroxene and plagioclase. Transparent brown fusion crust rims part of the section. The pyroxene is light to dark brown pigeonite; a few grains show exsolution lamellae. The lithic clasts have a maximum dimension of 3 mm, and consist of pigeonite and plagioclase with ophitic and gabbroic textures; one clast consists of angular pigeonite and plagioclase grains in a semi-opaque glassy matrix. Microprobe analyses show pigeonite and augite with a wide range of compositions: Wo_5 to Wo_{36}, En_{26} to En_{61}, Fs_{31} to Fs_{57}; plagioclase composition range is An_{78} to An_{93}, mean An_{88}.

ALHA81009 and 81012 resemble each other closely and are tentatively paired. Thin sections consist largely of brown grains of pigeonite up to 1 mm and colorless grains of plagioclase up to

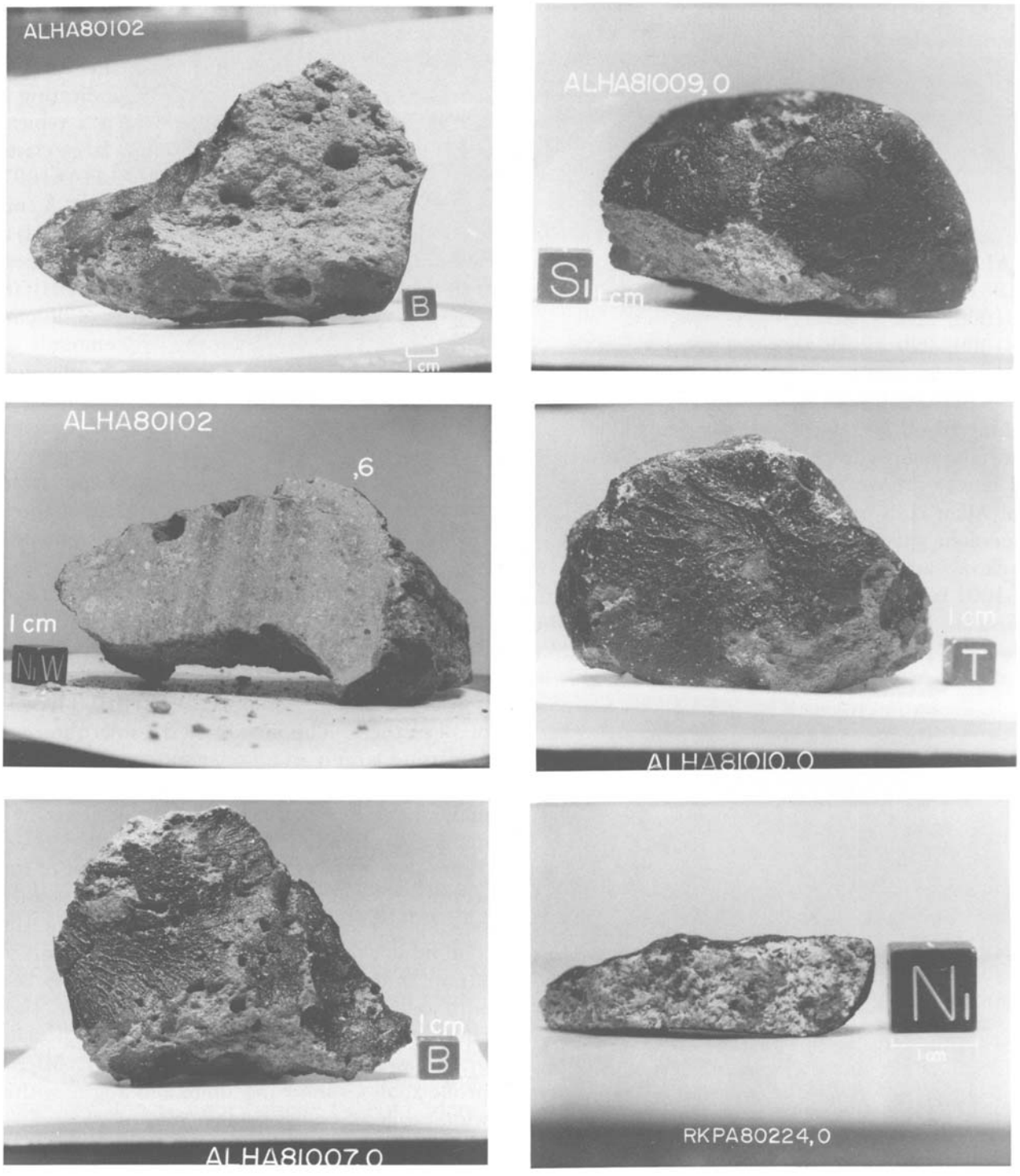

FIGURE 48.—Eucrites.

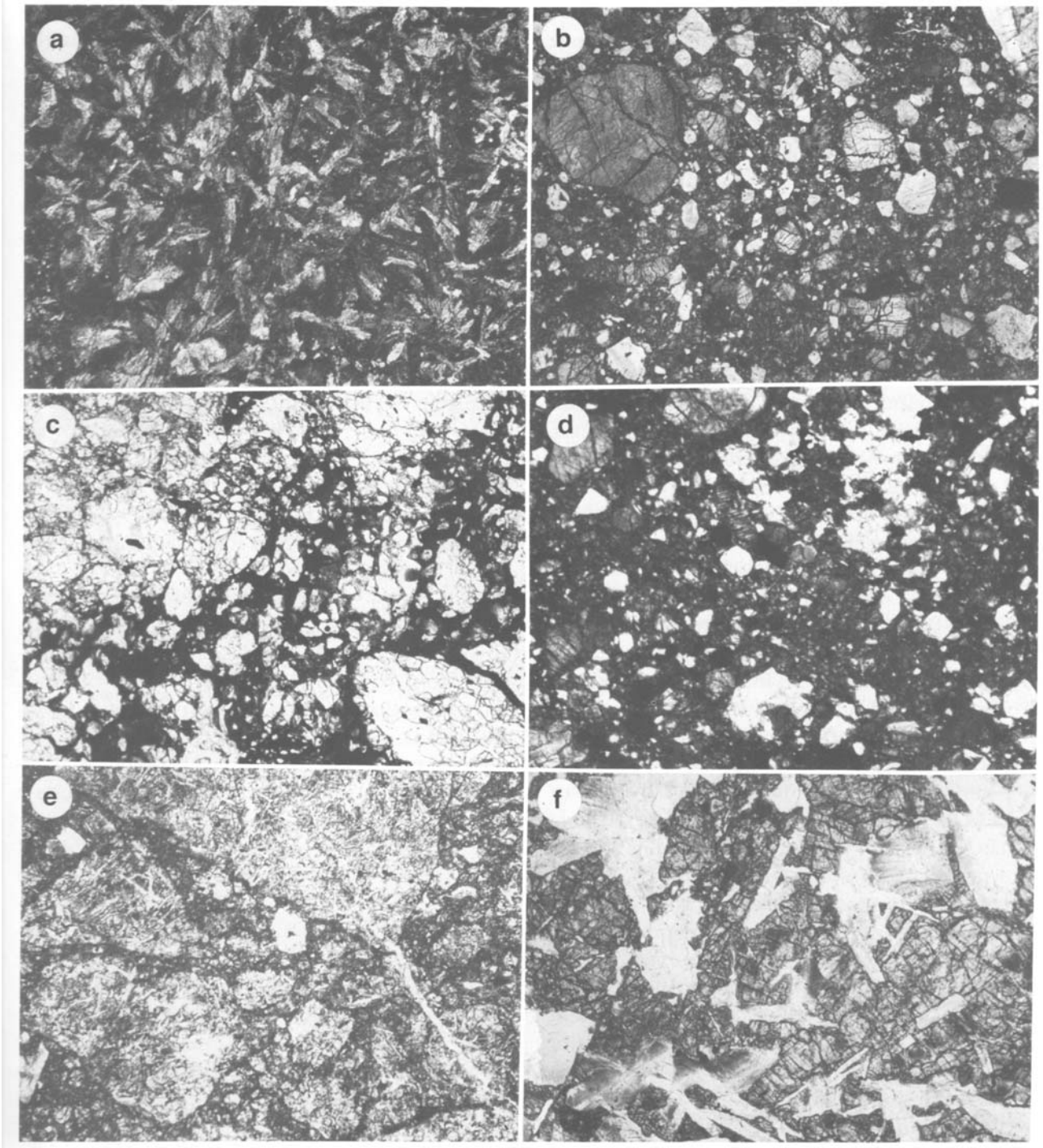

FIGURE 49.—Photomicrographs of thin sections of eucrites (area of each field is 3 × 2 mm): *a*, ALHA81001; *b*, ALHA81006; *c*, ALHA81011; *d*, ALHA81012; *e*, RKPA80204; *f*, RKPA80224.

2 mm in a comminuted groundmass of these minerals. Some lithic clasts, up to 3 mm across, are present; most show fine-grained ophitic textures, but a few have coarse gabbroic textures. Microprobe analyses show pyroxene compositions ranging fairly continuously from $Wo_3En_{35}Fs_{62}$ to $Wo_{40}En_{26}Fs_{30}$, with the En content showing a limited range (26–40). Plagioclase composition range is An_{75} to An_{93}, mean An_{86}. These eucrites differ from previously described polymict eucrites from the Allan Hills in the range and distribution of pyroxene compositions.

ALHA81011 is a breccia of eucritic clasts up to 10 mm in maximum dimension, the clasts sitting in a minor amount of dark glass filled with comminuted grains of pyroxene and plagioclase. The clasts consist of pyroxene and plagioclase and show a variety of textures: finely granular, subophitic, and gabbroic. Microprobe analyses show pyroxene compositions corresponding to pigeonite and augite and clustering around two mean compositions, $Wo_4En_{36}Fs_{60}$ and $Wo_{35}En_{32}Fs_{33}$, with a few intermediate values. Plagioclase has fairly uniform composition, An_{87} to An_{91}, mean An_{88}. The meteorite is a eucritic breccia; although it appears to be polymict, the uniformity of mineral compositions suggests a considerable degree of equilibration, and it may be a genomict breccia.

ALHA81001 appears to be a new type of eucrite. The thin section is translucent in pale brown-gray, with some darker areas, giving a patchy appearance. With crossed polars the material is seen to consist of pyroxene prisms up to 0.5 mm long, mostly with straight extinction, in a glassy groundmass. No opaque minerals are present. Microprobe analyses show the pyroxene has rather uniform composition, averaging $Wo_{1.6}En_{40}Fs_{59}$, with 0.4% Al_2O_3, 0.2% TiO_2, 0.9% MnO, and 0.6% Cr_2O_3. Broad-beam analyses give an approximate bulk composition (weight percent) as follows: SiO_2 (49), Al_2O_3 (14), FeO (18), MgO (6.7), CaO (10), Na_2O (0.2), K_2O (0.1), TiO_2 (0.9), Cr_2O_3 (0.6), MnO (0.7). This composition agrees with that of an average eucrite except that Na_2O is lower (in most eucrites Na_2O is about 0.5%); however, the texture is quite different from any described eucrite. The overall impression from the texture is that the material represents a rapidly quenched melt.

Two eucrites were collected in 1980–1981 near Reckling Peak: RKPA80204 (15.4 g) and 80224 (8.0 g).

RKPA80204 (3 × 2 × 2 cm) is partly covered with black fusion crust. Two texturally distinct lithologies were noted on the surface: one is massive and fine-grained with rounded yellow clasts, the other appears to be coarser-grained, with abundant light and dark grains. Thin (1 mm) black veins extend into both textures. Abundant vugs give the exterior a rough surface. The thin section shows clasts (up to 6 mm in maximum dimension) of subophitic intergrowths of pigeonite and plagioclase, separated by veins of coarser grained pigeonite and plagioclase. The plagioclase laths in the clasts range up to 0.5 mm in length. The pigeonite and plagioclase grains in the veins average about 0.3 mm in maximum dimensions. Microprobe analyses show pigeonite with a limited range of composition ($Wo_4Fs_{57}En_{39}$ to $Wo_{13}Fs_{52}En_{35}$). Plagioclase ranges in composition from An_{85} to An_{94}, with a mean of An_{92}. Accessory ilmenite and titanian chromite (TiO_2 10–13%) are present. The relative uniformity of composition of pyroxene and plagioclase indicates that this specimen may be classified as a monomict eucrite.

RKPA80224 is a small specimen (3.5 × 1.5 × 1.0 cm) partly coated with shiny black fusion crust. The thin section shows an ophitic intergrowth of pigeonite and plagioclase, with accessory amounts of tridymite and opaque minerals; the average grain size of pyroxene and plagioclase is about 1 mm. The pyroxene and plagioclase crystals are somewhat granulated and show undulose extinction. A little limonitic staining is present in one area. Microprobe analyses show pigeonite with an average composition of $Wo_{10}Fs_{54}En_{36}$; some grains show exsolution lamellae of augite with composition $Wo_{44}Fs_{25}En_{30}$. Plagioclase ranges in composition from An_{85} to An_{91}, with a mean of An_{89}. The opaque minerals are troilite, ilmenite and titanian chromite (TiO_2 13–15%). The meteorite is a monomict eucrite.

UREILITES

FIGURES 50, 51

The only ureilite in the 1980–1981 collection (and the first from the Reckling Peak area) is RKPA80239, a 5.6 g specimen. Thin patchy fusion crust is present on all surfaces; areas devoid of fusion crust are crystalline, reddish brown in color, and rough in texture. The thin section shows an aggregate of subhedral to anhedral grains (0.3–1.5 mm across) of olivine with minor amounts of pyroxene. The grains are rimmed with black carbonaceous material. Trace amounts of troilite and nickel-iron are present, the latter largely altered to translucent brown limonite concentrated along grain boundaries. Microprobe analyses show olivine of uniform composition (Fa_{16}) with notably high CaO content (0.3–0.4%); the pyroxene is a pigeonite of composition $Wo_5Fs_{15}En_{80}$. This meteorite appears to be relatively lightly shocked compared to most ureilites.

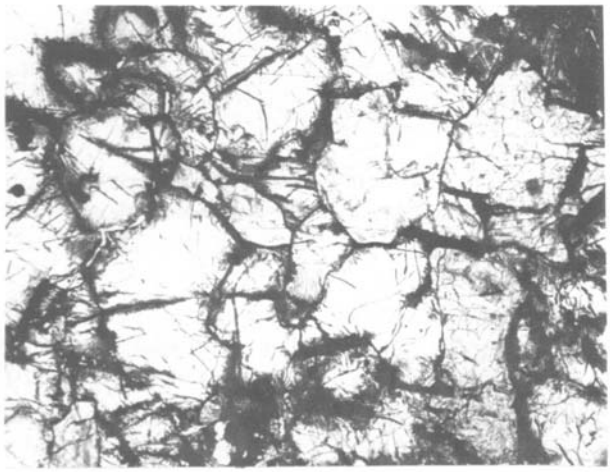

FIGURE 50.—RKPA80239, ureilite, photomicrograph of thin section (area of field is 3 × 2 mm); olivine (white, without cleavage cracks) and pyroxene (light gray, with cleavage cracks), bordered by black material consisting largely of carbon.

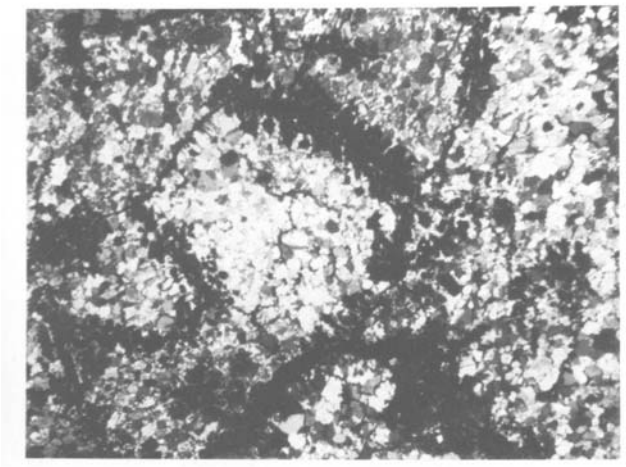

FIGURE 51.—ALHA81101, ureilite, photomicrograph of thin section (area of field is 3 × 2 mm); olivine (white to gray, showing mosaic structure), bordered by black material consisting largely of carbon.

ALHA81101 is a 119 g specimen, 7.2 × 4.5 × 3 cm, with thick black fusion crust on two sides. The section shows an aggregate of subhedral to anhedral crystals of olivine, 1–3 mm across; they are rimmed with dark carbonaceous material. Pyroxene, if present, is in small amount. Accessory nickel-iron is present, as minute grains along crystal boundaries and fractures; it is partly altered to brown limonite. Under crossed polars the olivine crystals are seen as a mosaic of tiny grains averaging 0.05 mm across, evidently a shock effect. Microprobe analyses show olivine of variable composition, Fa_{10} to Fa_{22}, mean Fa_{19}. This urelite differs from previously described ureilites from the Allan Hills in the mosaic texture of the olivine.

ACHONDRITE, UNIQUE

FIGURES 52, 53, 54

ALHA81005 (31.4 g).—At the time of collection this specimen was noted as unusual, because of the greenish glassy fusion crust and the presence of prominent clasts. The stone is rounded, equidimensional (3 × 3 × 2.5 cm) and the crust shows flow markings; the interior consists of abundant angular white clasts up to 8 mm across, set in a dark glassy matrix. In thin sections the matrix is a translucent to semi-opaque dark brown glass and shows flow structure in places; clast:matrix ratio is approximately 40:60. The larger clasts are polymineralic, the smaller (less than 0.3 mm) may be individual mineral grains.

FIGURE 52.—ALHA81005, anorthositic breccia, showing fusion crust and brecciated nature of interior.

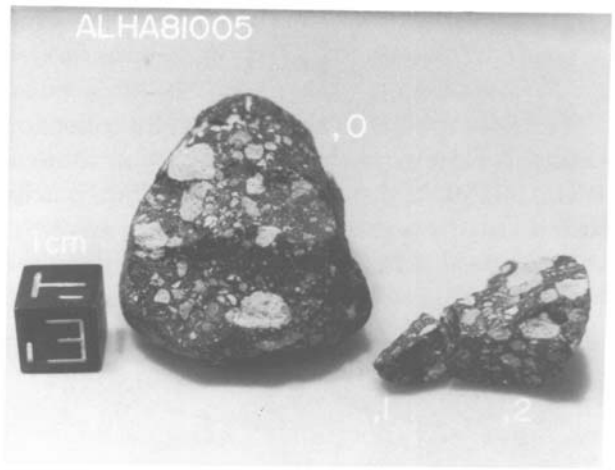

FIGURE 53.—ALHA81005, anorthositic breccia, after laboratory splitting, showing white anorthositic clasts in dark glossy matrix.

The clasts consist largely of plagioclase, together with some pyroxene and occasional olivine; most of the mineral grains are plagioclase. The clasts show a variety of textures, including gabbroic, diabasic, and basaltic; many have been shocked and partly granulated. Some of the clasts resemble eucrites, but many appear to be more feldspathic than most eucrites. The section is notable for the complete absence of opaque minerals, except for a 1 mm metal grain. Microprobe analyses show that the plagioclase is very Ca-rich, averaging An_{97} (range An_{95} to An_{98}); pyroxene is variable in composition, Wo 1–41, En 44–79, Fs 7–47 (richer is En than most eucrite pyroxenes); several grains of olivine, Fa 11–40, were analyzed. The MnO/FeO ratio in pyroxene grains differs from that in eucrite pyroxenes and agrees with that in lunar pyroxenes. The meteorite closely resembles many of the Apollo 16 lunar breccias.

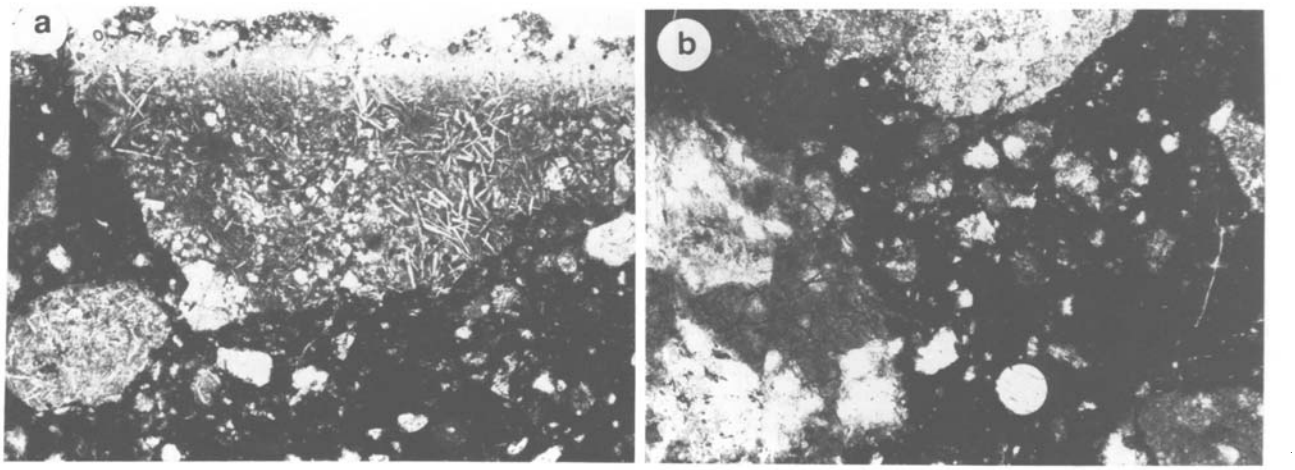

FIGURE 54.—ALHA81005, anorthositic breccia, photomicrograph of thin section (area of field is 3 × 2 mm): *a*, section showing remnants of fusion crust and clasts in dark glassy matrix; *b*, section showing clasts and small clear glass bead.

This specimen has been the object of intensive investigation, the preliminary results of which were presented at the Fourteenth Lunar and Planetary Science Conference in Houston in March 1983. Twenty-two papers were given (the abstracts have been published as LPI Contribution 501 and are available from the Lunar and Planetary Institute, 3303 NASA Road One, Houston, Texas 77058). The results confirmed and extended the preliminary results recorded above, and confirmed a lunar origin for this meteorite. For additional information see Marvin (p. 95).

Literature Cited

Mason, B., and R.S. Clarke, Jr.
1982. Characterization of the 1980–81 Victoria Land Meteorite Collections. *Memoirs of the National Institute of Polar Research* (Japan), special issue, 25:17–33.

Scott, E.R.D., G.J. Taylor, P. Maggiore, K. Keil, S.G. McKinley, and H.Y. McSween
1981. Three CO3 Chondrites from Antarctica—Comparison of Carbonaceous and Ordinary Type 3 Chondrites. *Meteoritics*, 16:385.

Van Schmus, W.R., and J.A. Wood
1967. A Chemical-Petrographic Classification for the Chondritic Meteorites. *Geochimica et Cosmochimica Acta*, 31:747–765.

Descriptions of Iron Meteorites and Mesosiderites

Roy S. Clarke, Jr

This section provides brief descriptions of two octahedrites, a hexahedrite, an ataxite, and a mesosiderite collected during the 1980 and the 1981 field seasons. The descriptions are preliminary and based largely on material prepared for publication in the *Antarctic Meteorite Newsletter.* Also included is a well-studied mesosiderite, RKP A79015, from the 1979 season that was not included in the previous publication in this series.

Octahedrites

RKPA80226 (160 g).—This dark reddish brown specimen (4.3 × 3.2 × 2.8 cm) from the Reckling Peak area is slightly smaller than a hen's egg and is more irregularly shaped. The top surface is covered with pits 2 to 3 mm in length, and it is gently and uniformly convex. Distribution of pits seems to have been controlled in part by the internal Widmanstätten structure. This surface, and the bottom surface, have been strongly affected by terrestrial weathering. The bottom surface is less uniform in shape and more convex. Part of it has a pattern of pits similar to that on the top. However, much of the bottom surface is dominated by a pattern of parallel ridges approximately 1 mm apart standing out in relief, an expression of the Widmanstätten structure of the material.

A median slice of approximately 6 cm^2 was polished and microetched. This revealed a heat-altered zone surrounding the edge of the slice as deep as 3.5 mm in one area. A well-developed Widmanstätten pattern is present with a kamacite band width in the 1.2 mm range. The length/width ratio for these lamellae is about 7. Some Neumann bands are present in the kamacite, as are rhabdites, grain-boundary schreibersites and subgrain boundaries. No epsilon structure or troilite was observed. Taenite bands occupy much of the kamacite grain boundaries, and taenite-kamacite and plessite fields are present. The plessite areas are mainly pearlitic, suggesting the possibility that the entire specimen is heat-altered. It is a medium octahedrite containing 8.5 wt.% Ni.

ALHA81014 (188 g).—This specimen (6.5 × 3 × 2 cm) from the Allan Hills is an irregularly shaped individual somewhat resembling a fish. It is covered with a uniformly pitted, dark reddish brown, iridescent, secondary iron oxide coating.

A surface area of approximately 4.5 cm^3 was microetched. The section was taken perpendicular to the long axis of the specimen near the more massive end. The edge of the section contains a thin, intermittent border of oxide. Below this is a heat-altered zone up to 1 mm thick that is present, with the exception of a few small gaps, around the complete section. Remnant fusion crust was not observed. Kamacite has a rather uniform matte surface at low magnification that can be resolved with higher magnification to a fine epsilon-decomposition structure. A system of wider than average kamacite lamellae, con-

Roy S. Clarke, Jr., Department of Mineral Sciences, National Museum of Natural History, Smithsonian Institution, Washington, D.C. 20560.

taining frequent centered schreibersites in the 100 × 200 μm size range, is a prominent feature. Kamacite lamellae, free of centered schreibersites, have widths in the 0.3 mm range. Plessite fields occupy approximately two-thirds of the surface. Interiors of larger fields contain cellular plessite framed in martensite with taenite borders. Narrow plessite fields have only martensitic areas with taenite borders. Schreibersite is also occasionally present at taenite borders, and as grain boundary schreibersite bridging adjoining plessite areas. Occasional 5 to 10 μm schreibersites are present within plessite fields. Other inclusions were not observed. The specimen is a fine octahedrite distinct from ALHA78252, the previously identified fine octahedrite from the Allan Hills.

Hexahedrite

ALHA81013 (17.75 kg).—The highly distinctive external appearance of this specimen (16 × 16 × 11 cm) from the Allan Hills suggests that it is a fragment that separated during atmospheric breakup from a larger mass with cubic cleavage (Figure 55). Its shape is that of a cube that has been shortened along one axis by severe and irregular ablation-sculpturing of one face. This face is the only one that is deeply sculptured with thumb-size regmaglypts, giving the impression that it was part of the exterior surface prior to fragmentation (Figure 55*a*). Its opposite face is approximately square, with slightly rounded edges, and appears to have been the leading surface during late stage ablation (Figure 55*b*). All surfaces are covered with a thin reddish brown coating of secondary oxides, which are somewhat thicker within the deeper depressions of regmaglypts. Thin cracks several centimeters long are present on all surfaces and tend to parallel the cubic planes of the specimen.

A median slice was removed perpendicular to the square section of the specimen and parallel to opposite sides. One side of the slice was polished and macroetched, resulting in an area of approximately 140 cm^2 available for examination at low magnification. The matrix appears to be single-crystal kamacite that etches to a dull finish, atypical for hexahedrites. Several small troilite-daubreelite inclusions are present, as are a few small schreibersites. Slight variations in kamacite reflectivity appear to be due to tiny schreibersites that are unresolvable at low magnification. The most prominent surface feature is the system of orthogonal cracks mentioned above. They penetrate into the interior of the specimen. Neumann bands are absent. This cursory examination suggests that the meteorite is a hexahedrite of somewhat unusual metallography. It probably represents a separate fall, distinct from the typical hexahedrite ALHA78100.

Ataxite

ALHA80104 (882 g).—This specimen (11 × 7 × 4 cm) from the Allan Hills is an irregularly shaped individual. One prominently rounded surface appears to have been ablation-shaped, and a second fairly large and comparatively smooth surface appears to have been the underside while the specimen was exposed at the surface of the ice. The meteorite is covered with a fairly uniform dark reddish brown iron oxide, and no fusion crust seems to remain. There are several deep linear incisions into the body of the meteorite that are possibly due to either preferential ablation or weathering of schreibersite inclusions exposed at the surface.

A microetched surface area of approximately 7 cm^2 shows a heat-altered zone over part of the external surface of the specimen. The metallographic matrix is a martensitic plessite. Kamacite spindles less than 0.1 mm wide, and generally less than ten times their width in length, are

FIGURE 55.—ALHA81013 is a hexahedrite that appears to have broken out of a larger mass during passage through the atmosphere. (*a*) This view looks straight down on the top surface of the specimen (as it lay on the ice sheet). This single deeply sculptured face was probably ablated prior to separation from a larger mass. The square outline of the specimen is 16 cm on an edge. (*b*) A tilted view of the bottom surface; a somewhat modified cube face is still evident, as is ablation rounding of edges. Cracks following cube directions may be seen in both photographs.

a

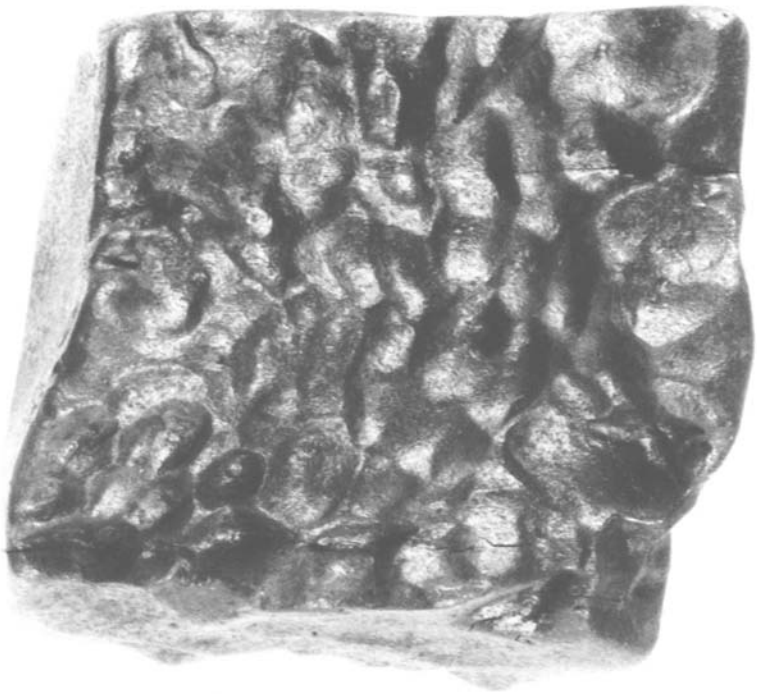

b

moderately uniformly distributed in a vague Widmanstätten pattern orientation. The kamacite spindles frequently enclose small schreibersites. Three large schreibersite areas are enclosed in swathing kamacite as wide as 0.2 mm. The largest such area is 8 mm long. Weathering has penetrated 0.5 cm into the mass in one area. The specimen is an ataxite containing 15.9 wt. % Ni, and it is distinct from ALHA77255, the previously known ataxite from the Allan Hills.

Mesosiderites

RKPA79015 (10.0 kg).—This specimen (26 × 18 × 13 cm) from the Reckling Peak area is a dense mass that has undergone severe external weathering, resulting in an appearance similar to that of many weathered iron meteorites. It is covered with reddish brown iron oxide that is layered in places and thick enough to flake off in centimeter-size pieces. No fusion crust remains, and the original shape of the specimen has undoubtedly been somewhat modified. Occasional cleavage faces of large pyroxene crystals are exposed. It has been described as a mesosiderite by Prinz et al. (1982) and Clarke and Mason (1982). The specimen has been divided into two pieces under clean conditions in a controlled atmosphere at the Antarctic Meteorite Curatorial Lab-

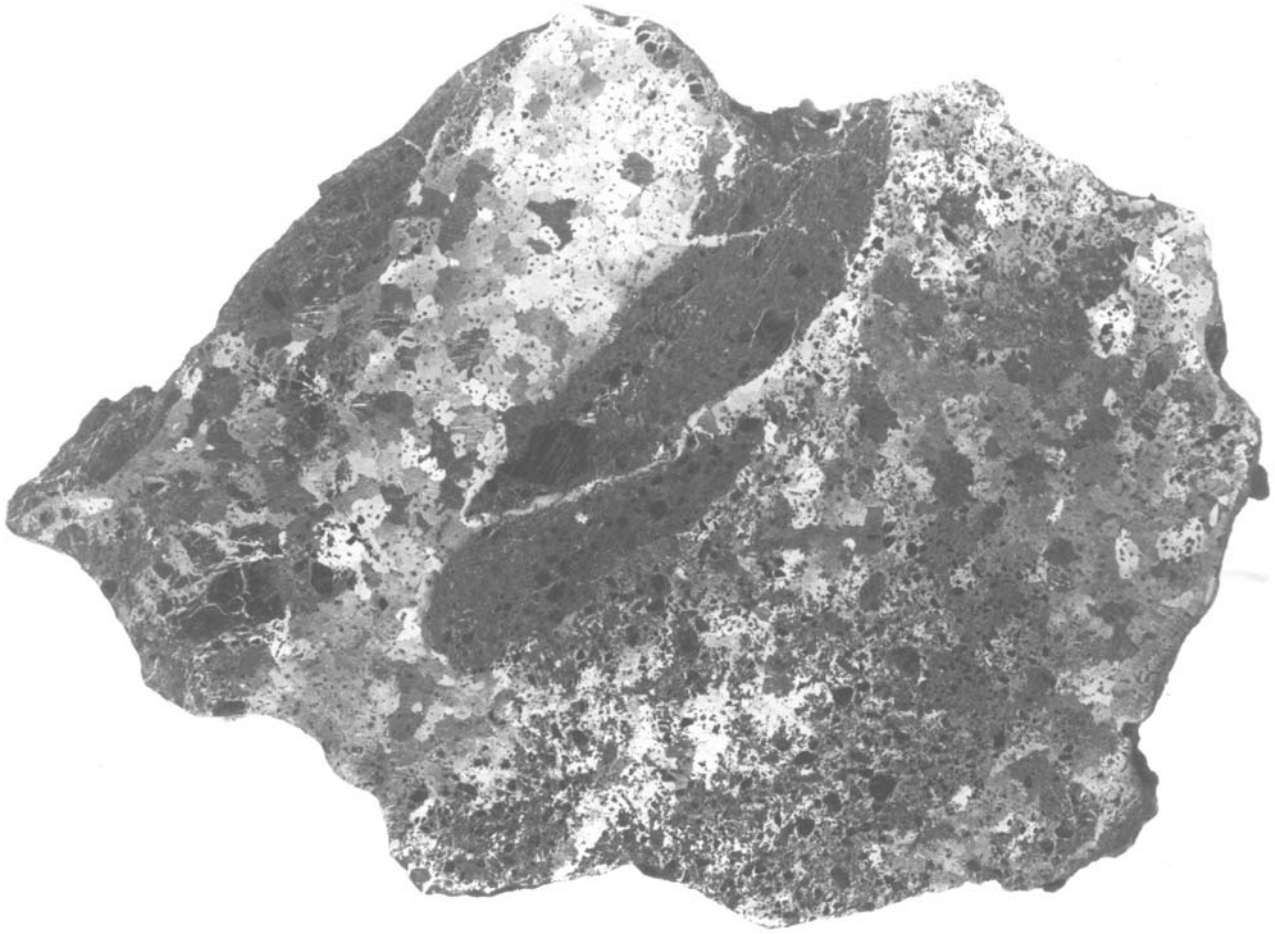

FIGURE 56.—RKPA79015, a median slice 15.5 cm wide revealing heterogeneous distribution of minerals and a brecciated structure. The etched surface reveals large areas of metal and sulfide, large areas of orthopyroxene that contain material that grades from very coarse to finely crystalline, and areas rich in troilite that also contain some metal and pyroxene.

oratory, Lyndon B. Johnson Space Center, Houston. One piece remains in the protective environment in Houston. The other piece weighing 5.52 kg was sent to the Smithsonian Institution for preliminary characterization and distribution to interested scientists.

The brecciated and heterogeneous character of RKPA79015 is shown in Figure 56, a photograph of the polished and etched surface of the slice. The meteorite is composed of major amounts of metal, orthopyroxene, and troilite, each with associated minor or trace minerals. The three major minerals tend to be in close association with each other, even though in given areas one mineral may predominate over the other two.

The silicate minerals present are orthopyroxene of uniform composition ($Wo_2En_{74}Fs_{24}$) and calcium-rich plagioclase of somewhat variable composition (An_{86} to An_{94}). Pigeonite and olivine have been looked for and not found. Chromite containing Al_2O_3 7.0%, MgO 1.8%, MnO 1.6%, and TiO_2 0.5% is present, as is merrillite ($Ca_9MgNa(PO_4)_7$). The bulk metal composition is 9.87% Ni, 0.52% Co, 0.15% P, and 2.14% FeS. Metallic areas consist of polycrystalline kamacite with grain boundaries containing cloudy taenite and schreibersite. Cloudy taenite areas have thick borders of tetrataenite. These metallographic associations indicate a low temperature cooling history identical to that of other well-known mesosiderites. RKPA79015 is apparently paired with four other silicate-rich fragments from the same area: RKPA80229, 80246, 80258, and 80263.

ALHA81059 (539 g).—The exterior of this specimen (9.5 × 5 × 5.5 cm) from the Allan Hills is severely weathered. Close examination revealed cleavage surfaces of large silicate crystals within the secondary oxidation products, suggesting that the specimen is a mesosiderite.

A polished thin section consists largely of orthopyroxene clasts ranging up to 10 mm in maximum dimensions, together with about 30% of nickel-iron in grains up to 0.6 mm; a little troilite is present. The meteorite is extremely weathered and seamed with brown limonite. Microprobe analyses shows that the orthopyroxene is somewhat variable in composition, ranging from Fs_{25} to Fs_{32}, with mean of Fs_{28}; mean weight percent CaO is 1.2, MnO 0.7, Al_2O_3 0.6, TiO_2 0.2. Small amounts of olivine (Fa_{28}), plagioclase (An_{93}), merrillite, and an SiO_2 phase (probably tridymite) were detected with the microprobe. The metal consists largely of kamacite. Tetrataenite-cloudy taenite associations are concentrated mainly at kamacite-silicate boundries. Schreibersite is either enclosed in the tetrataenite-cloudy taenite areas or in contact with them. The meteorite is a mesosiderite, the second from the Allan Hills; it appears to be different from the previous one, ALHA77219 (Agosto et al., 1980; Prinz et al. 1980).

ALHA81098 (60.9 g).—This sample consists of two fragments (4 × 4 × 1.5; 4 × 3.4 × 1 cm) that are similar to ALHA81059 in mineralogy, texture, and weathering, and probably should be paired with it.

Literature Cited

Agosto, W.N., R.H. Hewins, and R.S. Clarke, Jr.
1980. Allan Hills A77219, the First Antarctic Mesosiderite. In *Proceedings of the Eleventh Lunar and Planetary Science Conference*, pages 1027–1045. New York: Pergamon Press.

Clarke, R.S., Jr., and B. Mason
1982. A New Metal-Rich Mesosiderite from Antarctica, RKPA79015. *Memoirs of the National Institute of Polar Research* (Japan), special issue, 25:78–85.

Prinz, M., C.E. Nehru, and J.S. Delaney
1982. Reckling Peak A79015: An Unusual Mesosiderite. In *Lunar and Planetary Science XIII*, page 631. Houston: Lunar and Planetary Institute.

Prinz, M., C.E. Nehru, J.S. Delaney, G.E. Harlow, R.L. Bedell
1980. Modal Studies of Mesosiderites and Related Achondrites, Including the New Mesosiderite ALHA 77219. In *Proceedings of the Eleventh Lunar and Planetary Science Conference*, pages 1055–1071. New York: Pergamon Press.

Petrology and Classification of 145 Small Meteorites from the 1977 Allan Hills Collection

Susan G. McKinley and Klaus Keil

Introduction

We have studied 145 previously undescribed, small meteorites weighing <150 g from the 1977 Allan Hills Antarctica collection. These meteorites are part of the 350 samples collected by scientists from the United States and Japan during the 1977–1978 field season (Cassidy, 1980). Because of their small sizes, these and other specimens in the 1977 collection weighing <150 g were initially set aside and only later allocated to us as a suite of 145 samples. The allocation strategy was as follows: Except for a few meteorites that appeared unusual to the field party and were allocated for preliminary description and classification to B. Mason, each specimen weighing <150 >15 g (although the largest specimen weighed 174.5 g) was equally split between the U.S. Antarctic Meteorite collection curated at the Lyndon B. Johnson Space Center, Houston, Texas, and the Japanese Antarctic Meteorite Collection at the National Institute of Polar Research, Tokyo, Japan. Of each of these specimens, we were allocated a few grams for our studies. Meteorites weighing <15 grams were not split but were divided in equal numbers between the U.S. and Japanese collections. Each of those meteorites remaining in the U.S. collection was allocated to us in total for study and further distribution to interested investigators.

Susan G. McKinley and Klaus Keil, Department of Geology and Institute of Meteoritics, University of New Mexico, Albuquerque, New Mexico 87131.

We carried out mineralogic and petrographic studies of all 145 meteorites. In addition, we initiated studies by others on selected specimens from this suite. P. Signer and co-workers are carrying out noble-gas measurements on four type 3 ordinary chondrites, ALHA77011, 77013, 77176, and 77197, and the enstatite chondrite ALHA77156. Thermoluminescence sensitivity measurements were made by Sears and Weeks (1983) on the same five meteorites. The carbonaceous chondrite (C3O), ALHA77029, was analyzed by INAA (Kallemeyn and Wasson, 1982) and a specimen of ALHA77011 (namely ALHA77050) will be analyzed by J.T. Wasson and co-workers. Several specimens of ALHA 77011 and a pyroxene-rich chondrule from the same meteorite are being analyzed by R.N. Clayton for oxygen isotopic compositions, and 23 equilibrated ordinary chondrites are being studied by J.R. Arnold and co-workers for tracks, radionuclides (^{53}Mn, ^{36}Cl, ^{10}Be, ^{26}Al), and rare gases in a search for objects that may have been in space as small meteoroids. Neon and xenon isotopic compositions of graphite-magnetite inclusions in ALHA77011 (specimen ALHA 77050) were measured by Caffee et al. (1982). We have also loaned polished thin sections of various specimens to several investigators for optical microscopy and electron microprobe studies.

Our mineralogic and petrographic studies show that all 145 meteorites in our suite are chondrites (Table 3). Of those, 120 are equili-

brated (i.e., petrologic types 4 to 6) ordinary chondrites, with two belonging to the LL group, 16 to the L group, and 102 to the H group. The remaining 25 specimens include 19 that are paired with ALHA77011, an unusual L3 chondrite containing a graphite-magnetite matrix in addition to the common silicate ("Huss") matrix (Huss et al., 1981). Three specimens are unpaired L3 chondrites (Table 4), two are paired enstatite chondrites (EH4), and another is a carbonaceous chondrite (C3O).

Here we summarize the classification of all meteorites in our suite and report in more detail on the less common types, namely the carbonaceous chondrite, the four type 3 ordinary chondrites, and the enstatite chondrite. We conclude that study of large suites of small Antarctic meteorites is exceedingly worthwhile and rewarding. Most specimens are relatively fresh and unweathered, and their large numbers increase the likelihood of discovering new, unusual, and rare meteorite types, such as the unique graphite-magnetite bearing L3 ordinary chondrite and the enstatite chondrite (the first from the Allan Hills and only the fourth from Antarctica). Furthermore, these small meteorites may be attractive for special studies, such as the search for objects that travelled in space as small meteoroids. We therefore urge continued collection and study of large suites of small Antarctic meteorites.

ACKNOWLEDGMENTS.—We thank the Antarctic Meteorite Working Group for allocating to us the 145 meteorites studied here; Robbie Score (JSC) for valuable aid in preparing the specimens for us; G. Gomez and Jackie Allen for preparing polished thin sections; and E.R.D. Scott and G.J. Taylor for valuable collaboration, assistance, and discussions throughout the course of this project. This work was supported in part by the National Aeronautics and Space Administration, Grants NGL32-004-064 and NAG-9-30 to K.K.

Method of Study

Each specimen weighing <15 g, which was allocated to us in its entirety, was macroscopically described before cutting. This description includes a sketch of the external shape of the specimen and notes the external appearance of the meteorite, including preservation of the fusion crust, color, degree of weathering, veining, etc. After cutting for preparation of polished thin sections, detailed sketches of the cuts were made and their weights were recorded. A similar brief macroscopic description was also made of the small aliquots we received of meteorites weighing >15 g. Detailed information on their main masses is not available from us but is available from the Curatorial Office at the Johnson Space Center. At least one polished thin section was prepared of each specimen, using special procedures (i.e., no water) in the preparation of sections of meteorites containing water-soluble phases (e.g., the enstatite chondrite). Polished thin sections were studied in the optical microscope in transmitted and reflected light, and olivine and pyroxene compositions of equilibrated ordinary chondrites were determined with an automated ARL EMX-SM electron microprobe. Electron microprobe analyses of these and other phases were carried out using the procedures of Bence and Albee (1968) and Keil (1967), and standards and analytical conditions employed were essentially those listed in Fodor and Keil (1976). Analyzed olivine and pyroxene grains were chosen at random, and ordinary chondrites were then classified on the basis of their ranges and mean olivine and pyroxene compositions and their textural characteristics, using a modified version of the Van Schmus and Wood (1967) scheme (Gomes and Keil, 1980:31–32). More detailed microscopic and electron microprobe studies were made on the carbonaceous chondrite, the type 3 ordinary chondrites, and the enstatite chondrite.

Chondrites

CLASS C3O

ALHA77029 (1.4 g).—This small stone measured 15 × 7 × 4 mm and was covered (except on one flat side) by dark gray, frothy fusion crust. No chondrules were visible on the surface, and

the only external weathering noted was in a small pit in the fusion crust.

Microscopic and electron microprobe studies (Scott, Taylor, et al., 1981) indicate that this meteorite is an unpaired Ornans-type carbonaceous chondrite (C3O). It has the typical texture of C3O meteorites and contains (in the terminology of McSween, 1977) abundant chondrules <0.5 mm in apparent diameter and lithic fragments and inclusions embedded in a dark matrix (Figure 57). These constituents occur in proportions typical for C3O chondrites, except that the matrix to chondrule ratio is the highest (0.79) yet reported (Scott, Taylor, et al., 1981).

Matrix and mineral compositions are typical of C3O chondrites. The matrix is high in FeO and NiO, and olivine and pyroxene compositional histograms obtained on randomly selected grains have the characteristic means and broad ranges of C3O chondrites (Scott, Taylor, et al., 1981). The olivine histogram has no pronounced peak and is similar to that of Ornans (Van Schmus, 1969).

Based on compositional evidence (Scott, Taylor, et al., 1981), we have classified this meteorite as a moderately metamorphosed C3O chondrite of stage II (McSween, 1977). The mean fayalite composition (Fa_{23}) is intermediate between the least and most equilibrated C3O chondrites. Similarly, kamacite has intermediate Cr, Co, and Ni contents, resembling those of the C3O chondrites Felix and Lancé (McSween, 1977).

Class EH4

ALHA77156 (17.7 g); ALHA77295 (141 g), total weight 158.7 g. ALHA77156 is the first enstatite chondrite recovered from the Allan Hills; the second, ALHA81021, an EL6, was found in 1981 (Schwartz and Mason, 1983). Two others from Antarctica are Yamato 69001, an EH4-5 (Okada, 1975) and RKPA80259, an EH5 (Score et al., 1982). We have paired ALHA-77156 with ALHA77295, based on mineral abundances and compositions. Following the recommendations of the Committee on Meteorite Nomenclature of the Meteoritical Society (Graham, 1980), this chondrite should be referred to as ALHA 77156.

ALHA77156 contains well-defined chondrules typical of type 4 chondrites (Figure 58). Silicate phases include clinoenstatite and minor olivine, albite, and silica. Kamacite, niningerite, and zincian daubreelite are present in abundances typical of EH4 chondrites. Troilite, perryite, schreibersite, and oldhamite are more abundant than in other EH4 chondrites. Accessory djerfisherite, sphalerite, and weathered caswellsilverite are also present.

Total Fe concentration (313 mg/g), calculated from mineral compositions and modal abundances, falls within the EH range (Sears, Kallemeyn, et al., 1982). Mineral compositions typically lie within the ranges of EH4 chondrites. Those mineral compositions that are outside of the range are usually close to the mineral compositions in Kota-Kota (EH4) (Keil, 1968). For example, in both ALHA77156 and Kota-Kota, the Ni content is higher in schreibersite and lower in kamacite than the range for these minerals in other EH4 chondrites. Using the niningerite-oldhamite-troilite geothermometer of Skinner and Luce (1971), the calculated equilibration temperatures for niningerite in ALHA77156 and Kota-Kota agree well (475°C and 485°C, respectively). These are the lowest temperatures determined for EH4 chondrites.

Clinoenstatite luminesces in various shades and intensities of red and blue under electron bombardment. Random analyses of enstatite within and outside of chondrules show that the bright blue grains usually have very low (<0.1%) MnO and Cr_2O_3, whereas dull blue and red grains have a broad range of MnO and Cr_2O_3 contents. Our work on minor-element distributions in enstatite of ALHA77156 and other enstatite chondrites (McKinley et al., 1982, 1983) provides convincing evidence against the model of Leitch and Smith (1980, 1981, 1982), in which enstatite chondrites formed by collision of two planetesimals, one consisting of red and the other of blue luminescing enstatites, and mechanical aggregation of the debris.

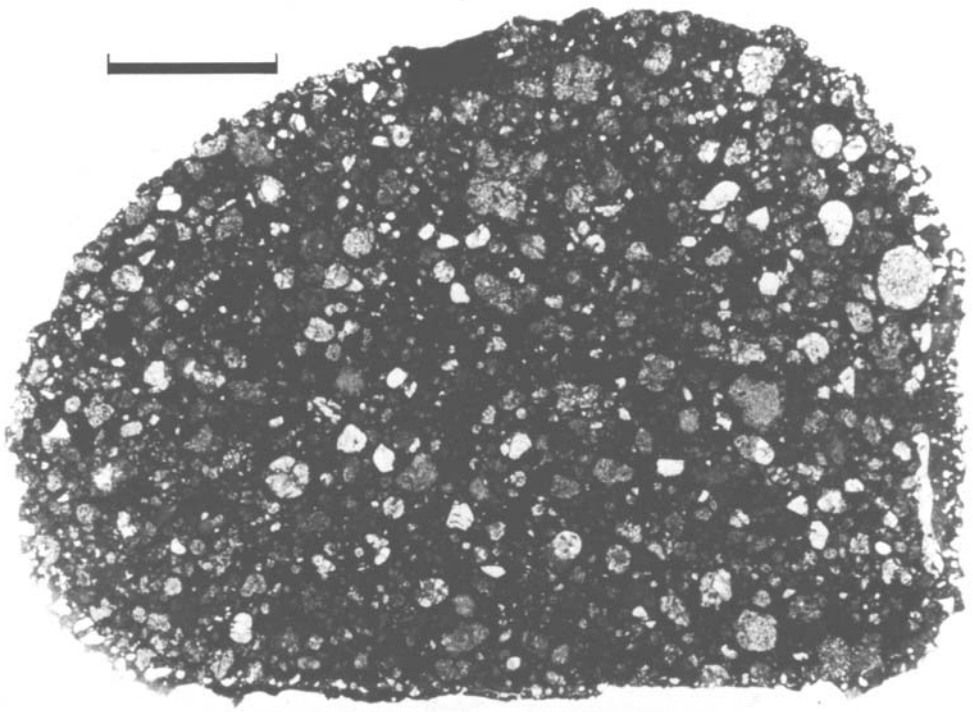

FIGURE 57.—Photomicrograph of the C3O chondrite, ALHA77029, showing chondrules and irregular inclusions in a dark matrix. Transmitted plane-polarized light. Scale = 1.5 mm.

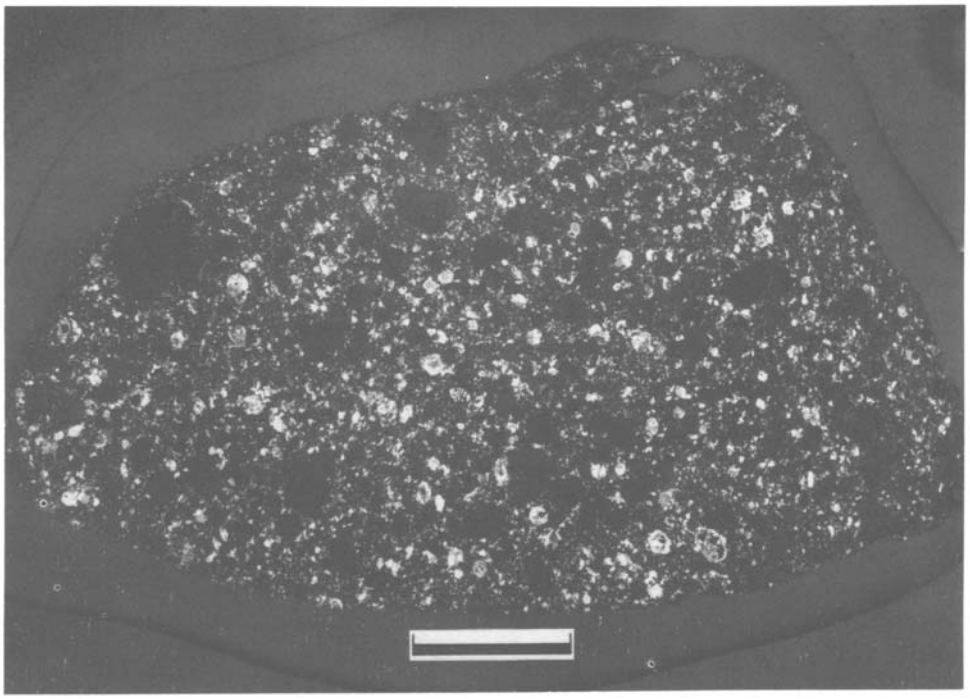

FIGURE 58.—Photomicrograph of the EH4 chondrite, ALHA77156 (paired specimen ALHA77295,8), showing fine-grained opaque phases (light gray and white) and Fe,Ni metal-sulfide aggregates. Reflected light. Scale = 2.7 mm.

Class L3

ALHA77011 (total weight 6338 g).—We have paired 19 of the 145 small meteorites studied here with 15 larger specimens from the 1977–1978–1979 Allan Hills collection, based on the presence of unique graphite-magnetite aggregates (McKinley et al., 1981). Cassidy (1980) had previously suggested that, on the basis of field relationships, nine of the larger specimens may be paired. ALHA77011 is one of the larger specimens and is the lowest-numbered object of the paired specimens. Thus, according to the recommendation of the Committee on Meteorite Nomenclature of the Meteoritical Society (Graham, 1980), this chondrite shower should generically be referred to as ALHA77011, although this specimen is not part of the collection of small meteorites described here.

ALHA77011 is a unique chondrite, characterized by the presence of abundant matrix and inclusions (3.2 vol. %), consisting of aggregates of micron-to-submicron-sized graphite and magnetite, in addition to the typical "Huss" silicate matrix (Huss et al., 1981). This meteorite contains graphite-magnetite in higher amounts than most type 3 ordinary chondrites (which normally have $\leq$0.1 vol. %) but in much lower proportions than the type 3 ordinary chondrite clasts with graphite-magnetite matrices (14–36 vol. %) found in some regolith breccias (Scott, Rubin, et al., 1981). In all other respects, ALHA77011 is typical of type 3 ordinary chondrites. It has sharply defined chondrules embedded into a matrix consisting of about equal amounts of fine-grained opaque and recrystallized silicate matrix (Figure 59). Olivine compositions range from Fa_1 to Fa_{37} (percent mean deviation is 39) and low-Ca pyroxene ranges from Fs_1 to Fs_{40} (percent mean deviation is 56). The percent mean deviation was calculated from FeO weight concentrations in olivine and pyroxene. Metallic Fe,Ni has significant amounts of Cr and Si and widely varying Co contents, indicating that the meteorite is one of the least-metamorphosed type 3 ordinary chondrites (Afiattalab and Wasson, 1980). Using the criteria of Sears, Grossman, et al. (1982), we have classified ALHA77011 as a petrologic type 3.2±0.2 (McKinley et al., 1981), whereas Sears, Grossman et al. (1982) classified it as a petrologic type 3.5± 0.1. Additional mineralogic-petrographic studies of the meteorite have been carried out by Ikeda et al. (1981), Fujimaki et al. (1981), and Nagahara (1981).

Classification of ALHA77011 as an L-group chondrite was originally proposed by King et al. (1980), based on petrographic studies. This classification was confirmed by the bulk analysis of Jarosewich (1980), which yielded total Fe of 20.77 wt.% and an Fe/SiO_2 weight ratio of 0.55, well within the L-group range. The Ni/Mg (0.086), S/Mg (0.15), and Fe/Mg (1.52) ratios also fall within the L fields of Jarosewich and Dodd (1981).

ALHA77013 (23.0 g).—This meteorite contains very well-defined, densely packed chondrules in a matrix of recrystallized Huss silicate matrix and fine-grained silicates (Figure 60). Typical chondrule types are present, including a barred olivine chondrule with interstitial glass.

Olivine composition ranges from $Fa_{9.0}$ to $Fa_{27.6}$ (mean $Fa_{18.7}$), with a standard deviation of the analyses (mole % Fa) of 3.8 and a percent mean deviation of 16.6. Pyroxene ranges from $Fs_{2.2}$ to Fs_{35} (mean $Fs_{13.1}$), with a standard deviation of the analyses (mole % Fs) of 7.9 and a percent mean deviation of 47.3. We classify ALHA77013 as an L3 chondrite, based on its low metallic Fe,Ni content of 3 vol. % and its texture. The olivine and pyroxene compositions (Figure 61) are less conclusive and trend more towards the H group. However, these data suggest that the meteorite is not paired with any other from Victoria Land.

ALHA77013 has been classified as a petrologic type 3.5, based on thermoluminescence sensitivity (Sears and Weeks, 1983). The coefficient of variation of Fa is 20.5, which is within the range for type 3.7 (Sears, Grossman, et al., 1982).

ALHA77176 (54.4 g).—This unpaired meteorite contains very well-defined chondrules in a matrix of opaque and recrystallized Huss silicate matrix (Figure 62). A few large lithic inclusions

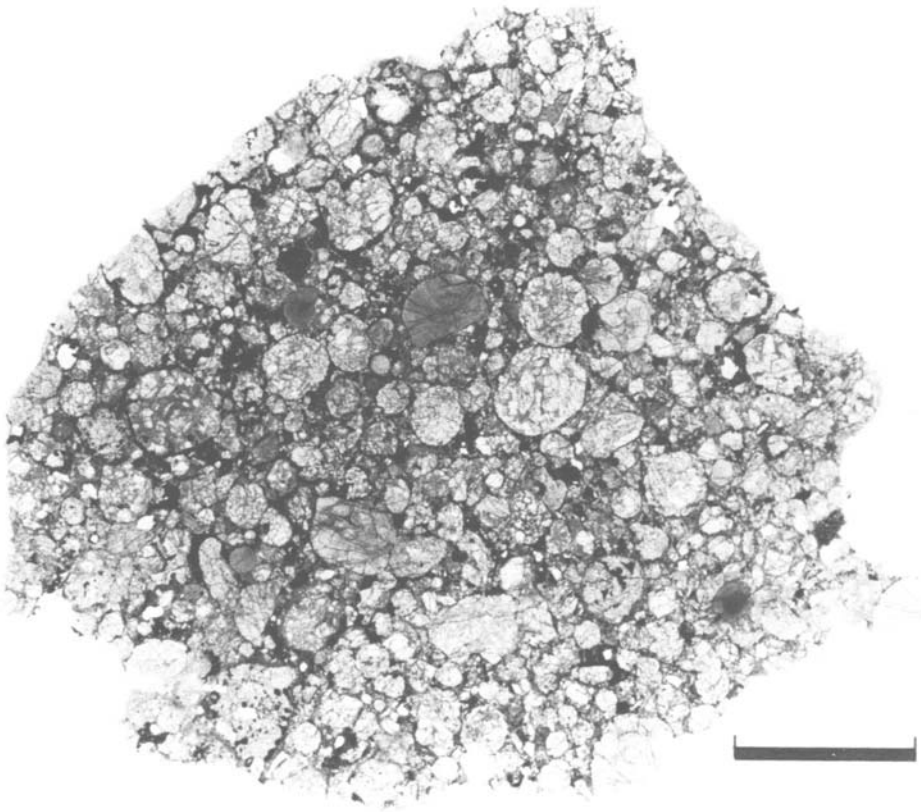

FIGURE 59.—Photomicrograph of the L3 chondrite, ALHA77011 (paired specimen ALHA77052) showing abundant, well-defined chondrules. Transmitted plane polarized light. Scale = 2.5 mm.

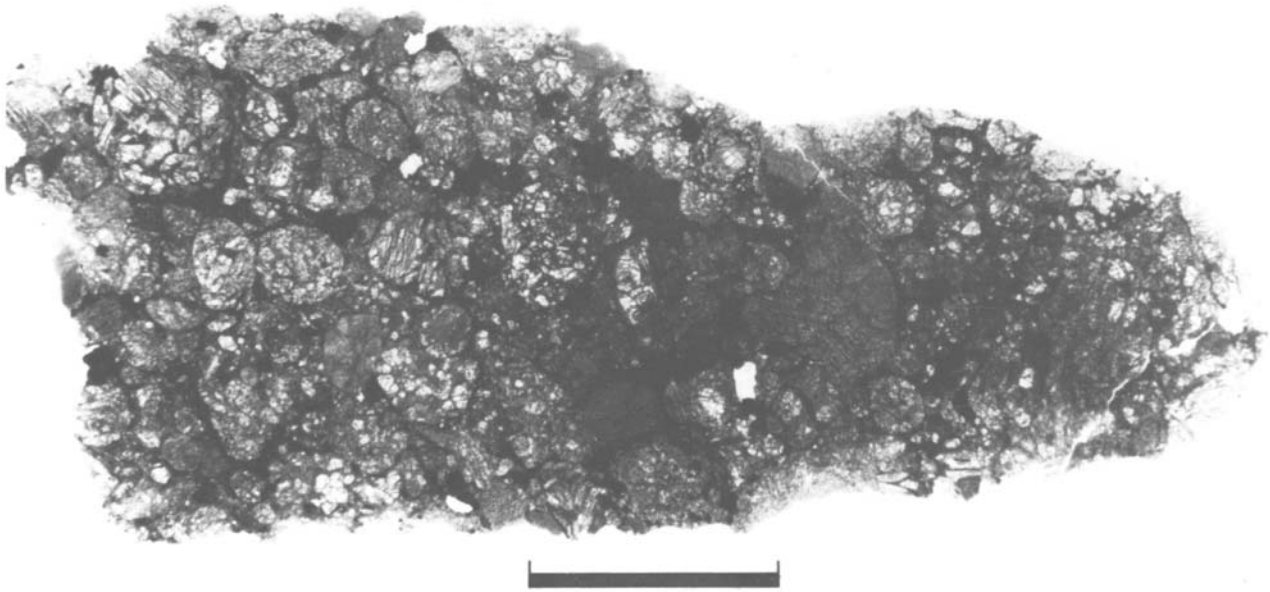

FIGURE 60.—Photomicrograph of the L3 chondrite, ALHA77013, showing abundant, well-defined chondrules. Transmitted plane-polarized light. Scale = 3.0 mm.

are present and the chondrules are commonly irregular in shape. Typical chondrule types are present and clear glass is common in some. Troilite occurs as shock-melted, "fizzed" intergrowths with metallic Fe,Ni and as individual polycrystalline grains.

Olivine and pyroxene in this meteorite are more variable in composition (Figure 61) than in any other Antarctic ordinary chondrite, with the possible exception of ALHA76004 (Scott, this volume), indicating that it is less equilibrated. Olivine ranges from $Fa_{0.3}$ to $Fa_{33.5}$ (mean $Fa_{12.4}$), with a standard deviation of the analyses (mole % Fa) of 8.3 and a percent mean deviation of 54.3. Pyroxene ranges from $Fs_{1.8}$ to $Fs_{36.7}$ (mean $Fs_{12.2}$), with a standard deviation of the analyses (mole % Fs) of 8.9 and a percent mean deviation of 61.2. We have classified the meteorite as an L

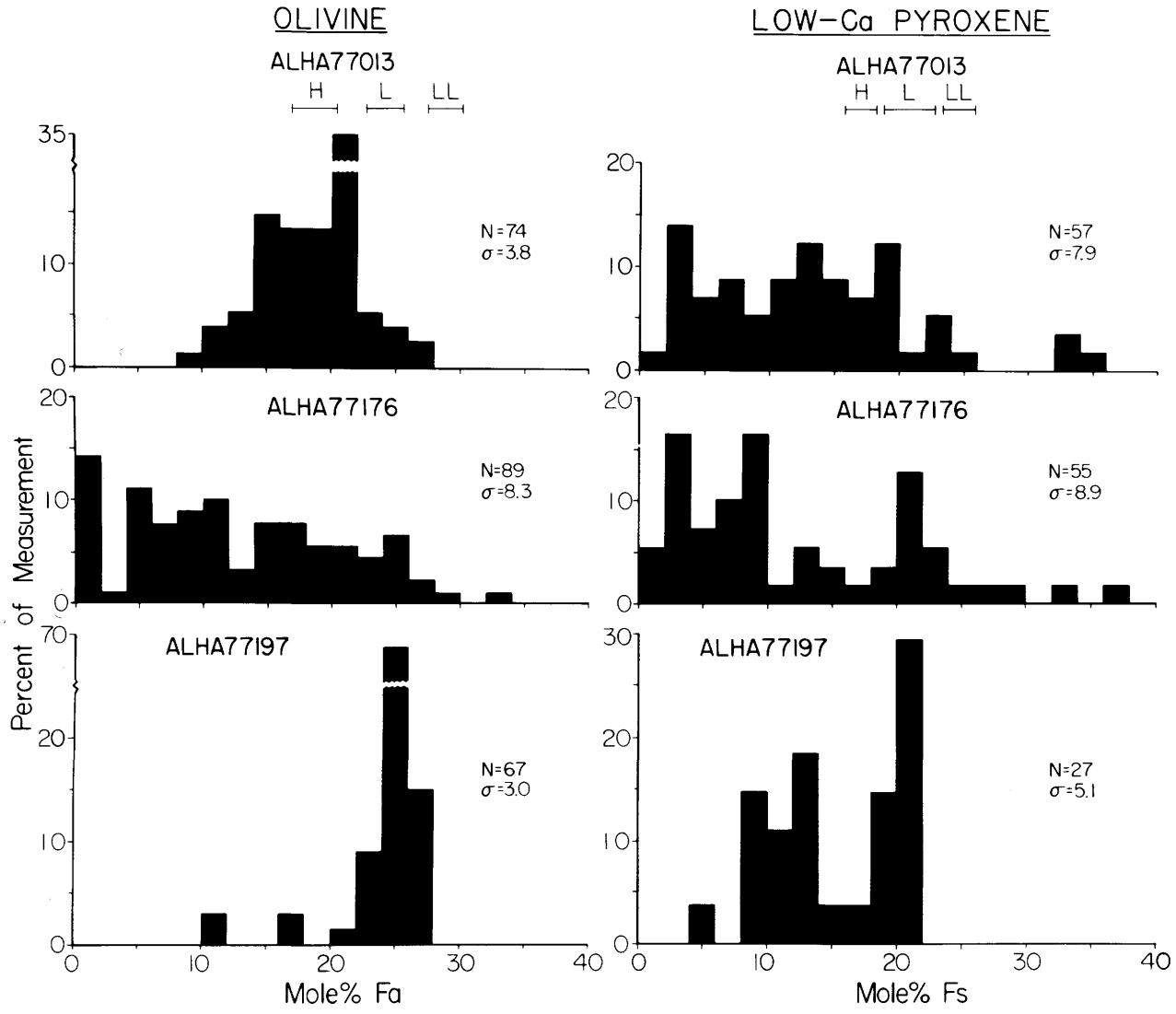

FIGURE 61.—Histograms of electron microprobe analyses of randomly selected olivines (in mole % fayalite), and low-Ca pyroxenes (in mole % ferrosilite), in three L3 chondrites from the Allan Hills. Also given are the number of analyses (N) and their standard deviation (σ). Compositional ranges for equilibrated H, L, and LL group chondrites are from Gomes and Keil (1980).

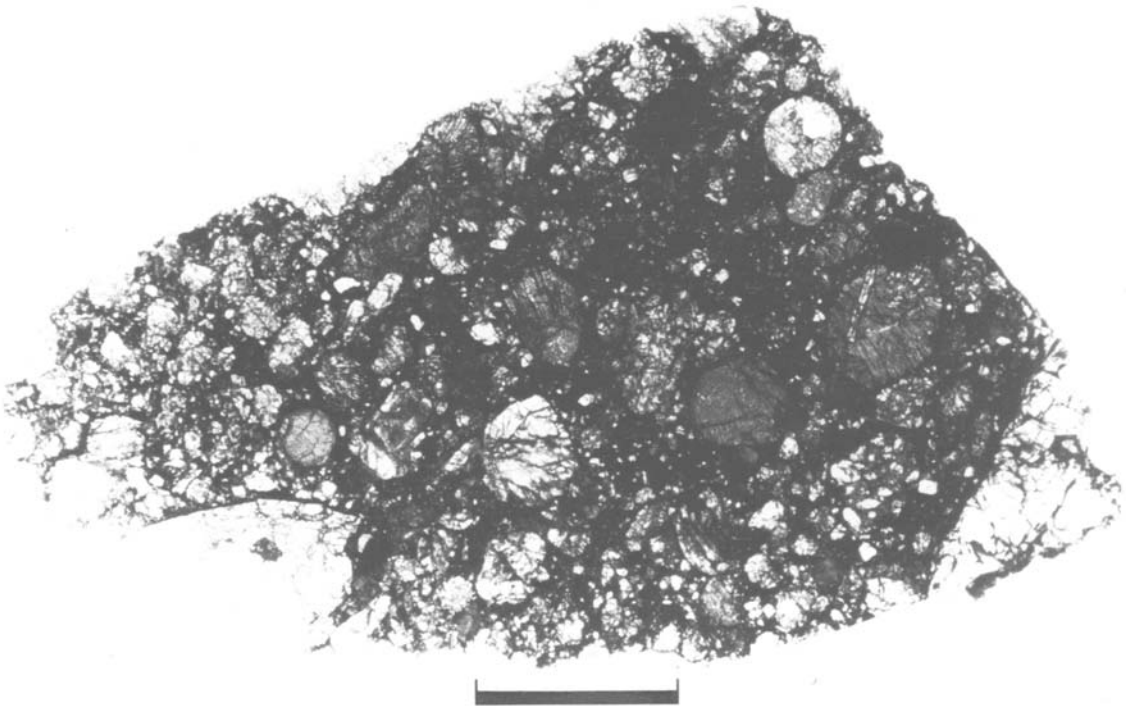

FIGURE 62.—Photomicrograph of the L3 chondrite, ALHA77176, showing well-defined chondrules, a large broken chondrule, and an inclusion. Transmitted plane-polarized light. Scale = 2.0 mm.

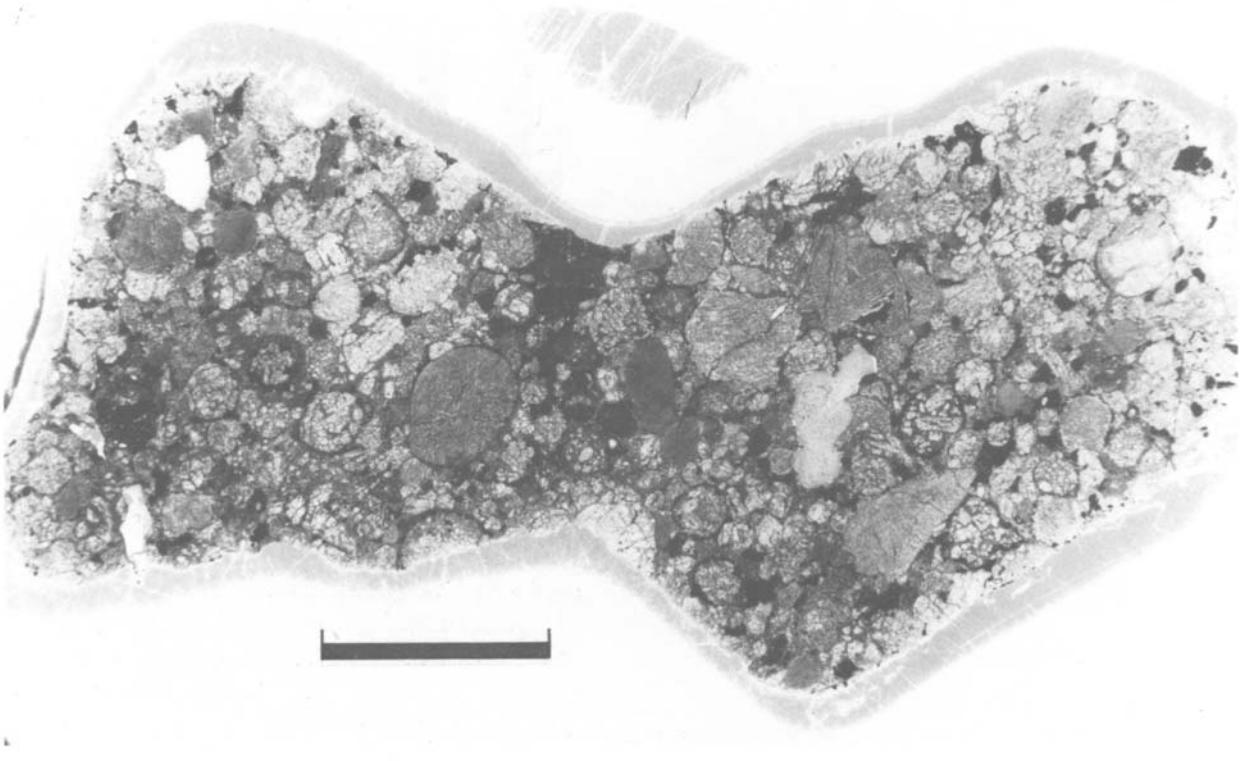

FIGURE 63.—Photomicrograph of the L3 chondrite, ALHA77197, showing abundant, well-defined chondrules. Transmitted plane-polarized light. Scale = 3.0 mm.

group chondrite, based on its low metallic Fe,Ni content (5 vol. %), and as a petrologic type 3, based on its texture and variable olivine compositions. Olivine and low-Ca pyroxene have significantly higher mean MgO and CaO contents than ALHA76004 (see Scott, this volume), indicating less equilibration. ALHA77176 has been classified as a petrologic type 3.2, based on thermoluminescence sensitivity (Sears and Weeks, 1983). The coefficient of variation for Fa in olivine is 67, which indicates a petrologic type ≤3.4 (Sears, Grossman, et al., 1982).

ALHA77197 (20.3 g).—This meteorite contains very well-defined chondrules in a matrix of fine-grained silicates and recrystallized Huss silicate matrix (Figure 63). Typical chondrule types are present, including two with pinkish brown glass.

Olivine composition ranges from $Fa_{10.4}$ to $Fa_{27.4}$ (mean $Fa_{24.4}$), with a standard deviation of the analyses (mole % Fa) of 3.0 and a percent mean deviation of 6.2. Only four of 67 olivine analyses fall outside the range for olivine of L group chondrites (Figure 61); two of these are from the same grain. Pyroxene ranges from $Fs_{4.0}$ to $Fs_{21.0}$, with a standard deviation of the analyses (mole % Fs) of 5.1 and a percent mean deviation of 30.7. We therefore classify ALHA77197 as an L3 chondrite based on low metallic Fe,Ni content, olivine and pyroxene composition, and texture. The meteorite was classified as a petrologic type 3.6, based on thermoluminescence sensitivity (Sears and Weeks, 1983). This classification may be somewhat too low in petrologic grade; the coefficient of variation of Fa is 12.3 %, which falls within the range (10–20%) for petrologic type 3.8 (Sears, Grossman, et al., 1982).

ALHA77197 is not paired with the other eight L3 chondrites from Victoria Land. It is closest in composition to ALHA79022 and RKPA80256. However, the olivine in ALHA77197 is more magnesian than that in ALHA79022 and pyroxene is less variable in composition than that in RKPA80256 (Scott, this volume). Although there are no mineral compositional data available on ALHA77215, the brecciated texture of this regolith breccia (Score, personal communication, 1983) rules out pairing with ALHA77197.

Equilibrated Ordinary Chondrites (Petrologic Types 4 to 6)

The classifications of 120 equilibrated ordinary chondrites (petrologic types 4 to 6) are given in Table 3, together with those of the 22 type 3 ordinary chondrites. The criteria we used in classifying these chondrites are those proposed by Van Schmus and Wood (1967), as modified by Gomes and Keil (1980:31–32). The petrologic characteristics of ordinary chondrites form a continuum from types 3 to 6; thus pigeonholing chondrites into petrologic types is always somewhat arbitrary, particularly for the higher petrologic types. The main diagnostic criteria we used in classifying ordinary chondrites into petrologic types are as follows: type 3, >5 percent mean deviation in the FeO content of olivine; type 4, <5 percent mean deviation in the FeO content of olivine and >20 percent of the total pyroxene is clinopyroxene; type 5, <20 percent of the total pyroxene is clinopyroxene, and plagioclase is common, with grains <50 μm across; and type 6, plagioclase is abundant and grains are >50 μm across.

Discussion

The main motivation for studying this large collection of small meteorites stems from our previous experience with large suites of randomly collected, small rake samples of lunar rocks (e.g., Dowty, Prinz, et al., 1973; Dowty, Conrad et al., 1973; Warner et al., 1975). Our experience is that systematic study of such suites increases the probability of discovering new and rare rock types and that it facilitates comparison of rocks via large data bases obtained in one laboratory. Our optimism was justified. We identified a new meteorite type, ALHA77011, a type 3 ordinary chondrite with a graphite-magnetite

matrix, in addition to the common Huss silicate matrix. Comparison of specimens in this suite enabled us to pair 19 specimens of ALHA77011 from among the 145 meteorites studied here with 15 larger specimens from the 1977–1978–1979 Allan Hills collections. We further discovered a number of rare meteorites, such as the C3O carbonaceous chondrite (ALHA77029), two paired specimens of an EH4 enstatite chondrite (ALHA77156, ALHA77295), and three unpaired petrologic type 3 ordinary chondrites (ALHA77013, ALHA77176, ALHA77197).

Concerns that these small meteorites would be too weathered for scientific study proved to be largely unfounded. Comparison of paired small and large members of a fall indicates that the small objects are not significantly more weathered than the larger ones, at least not in case of the meteorites we studied. Thus, the success in discovering new and rare meteorites in this suite strongly argues for the need to continue to collect very small meteorites in Antarctica, to carefully document their field relationships, and to make them available for study.

In Table 4 we summarize the classification of all 142 ordinary chondrites (petrologic types 3 to 6) studied here. We compare this suite with the classifications of mostly larger types 3 to 6 ordinary chondrites from the 1976–1979 collections from the Allan Hills, Antarctica (Score et al., 1981), the ordinary chondrite falls and finds (Motylewski, 1978), and falls only (Wasson, 1974) from the rest of the world. The purpose of this comparison is to see if there are any similarities or differences in classifications of *small* ordinary chondrites in the 1977 Allan Hills collection when compared to mostly larger meteorites from the same location in Antarctica and from locations around the world, both for falls and finds together and for observed falls only. Such a comparison may allow us to make inferences as to the arrival and collection of generally rather recent arrivals of meteorites to Earth (e.g., as represented among falls and finds from the rest of the world), with the generally older meteorites (in terms of terrestrial residence time), preserved in the deep-freeze of the Antarctic ice (Evans et al., 1982). It should be noted at the outset that such comparisons are considerably affected by many uncertainties due to serious sampling errors and statistical biases. Uncertainties result from biases in the removal of meteorites from their parent bodies, orbital considerations, possible selection effects during atmospheric entry and survival on the ground, pairing of Antarctic finds, and relatively small numbers of meteorites available for comparison. It would appear, however, that the falls summarized by Wasson (1974) would most closely represent the distribution of more recent arrivals to Earth of ordinary chondrites. Furthermore, the ordinary chondrite types represented among the Allan Hills collections (Score et al., 1981) might be expected to be similar to those in the suite of 142 ordinary chondrites studied here. However, as pointed out above, extreme caution must be exercised in such comparisons. Nevertheless, some useful information appears to emerge from the comparison, which is summarized here.

First, the percentage of H5 chondrites in our suite (83%) is much larger than that among the observed falls (47%; Wasson, 1974). Since there are at least 17 paired specimens among the H5 chondrites (*Antarctic Meteorite Newsletter,* 1981) of Score et al. (1981), we conclude that probably many of our H5 chondrites are also paired, thus explaining their preponderance over those among observed falls.

Nomenclature for Shock Facies
(from Dodd and Jarosewich, 1979:340)

a = Olivine fractured; plagioclase at least 50% undeformed; melt pockets not present.

b = Olivine fractured and with undulose extinction; plagioclase at least 50% undeformed; melt pockets not present.

c = Olivine fractured and with undulose extinction; plagioclase at least 50% deformed, but maskelynite and melt pockets absent.

d = Olivine fractured and with mosaic extinction; plagioclase entirely deformed and/or maskelynite; melt pockets present.

TABLE 3.—Characterization of small meteorites from the 1977–1978 Allan Hills collection (n.d. = no data; A = minor; B = moderate; C = severe).

ALHA	Weight (g)	Class and type	Olivine (mole % Fa)	Pyroxene (mole % Fs)	Degree of weathering	Shock facies†
77007	99.3	H5	19.1	16.7	B	a
77008	93.0	L6	24.6	20.6	A	c
77013	23.0	L3	9–28	1–35	B	b
77016	78.3	H5	18.6	17.1	B	c
77017	77.9	H5	18.8	16.3	B	c
77018	51.8	H5	19.0	17.0	B/C	b
77019	59.8	L6	24.9	21.4	B/C	d
77022	16.0	H5	19.1	17.0	A	c
77023	21.4	H5	19.1	16.8	B	c
77026	20.3	L6	24.3	20.7	B/C	b
77027	3.7	L6	25.0	21.5	B/C	d
77029	1.4	C3O	23	2.6	A/B	a
77031*	0.5	L3	n.d.	n.d.	B/C	b
77034*	1.8	L3	n.d.	n.d.	B/C	b
77036*	8.5	L3	n.d.	n.d.	B	b
77038	18.8	H5	19.0	17.1	A/B	c
77039	8.2	H5	18.5	16.3	A/B	c
77041	16.6	LL6	30.7	25.1	A	b
77042	20.4	H5	19.0	16.0	A/B	b
77043*	11.4	L3	1–37	1–28	B/C	b
77045	17.9	H5	18.7	17.0	A	b
77046	7.6	H6	19.0	16.7	A/B	c
77047*	20.4	L3	n.d.	n.d.	C	b
77049*	7.3	L3	n.d.	n.d.	B/C	b
77050*	84.2	L3	n.d.	n.d.	B/C	b
77051	15.0	H5	18.8	16.5	A	b
77052*	112	L3	n.d.	n.d.	B/C	b
77054	10.4	H5	18.5	16.9	B	c
77056	12.3	H4	18.8	16.3	A/B	b
77058	3.7	H5	18.8	16.1	B	b
77060	64.4	LL5	28.1	23.2	A	b
77063	2.9	H5	18.0	16.8	B	c
77066	4.9	H5	19.0	17.4	A	c
77069	0.8	L6	25.4	21.4	B/C	d
77070	18.4	H5	18.4	16.8	B	b
77073	10.1	H5	18.8	17.7	A/B	b
77076	1.7	H5	19.5	16.1	B	b
77078	7.8	H5	19.5	16.7	B	b
77079	7.8	H5	18.2	15.8	A	b
77082	12.0	H5	19.3	16.5	A/B	c
77084	44.1	H5	18.8	16.8	A/B	b
77085	45.9	H5	18.8	17.6	B	b
77087	30.7	H5	19.0	16.7	B	b
77089	7.8	L6	25.5	21.4	B	b
77091	4.2	H5	18.9	16.1	B/C	a
77092	45.0	H5	18.5	16.5	A	b
77094	6.6	H5	18.5	16.2	B	b
77096	2.5	H5	18.7	17.1	A	b

† Nomenclature following Dodd and Jarosewich (1979:340); see accompanying box on p. 64.

TABLE 3.—Continued.

ALHA	Weight (g)	Class and type	Olivine (mole % Fa)	Pyroxene (mole % Fs)	Degree of weathering	Shock facies
77098	8.0	H5	18.7	16.7	B	b
77100	8.5	H5	19.2	16.4	A/B	b
77101	3.8	H5	18.6	17.0	B	b
77104	6.3	H5	18.9	16.9	A	b
77106	7.8	H5	18.8	16.5	A/B	c
77108	0.7	H5	18.5	15.9	A/B	a
77111	52.3	H6	19.0	16.6	A/B	a
77112	21.7	H5	18.7	16.7	A	a
77113	2.0	H5	18.7	17.2	B	a
77114	44.5	H5	19.6	17.2	B	b
77115*	154	L3	n.d.	n.d.	B/C	b
77117	20.8	L5	24.4	21.0	A/B	c
77120	3.9	H5	18.5	16.0	A/B	a
77122	4.6	H5	19.1	16.8	B	b
77125	18.7	H5	17.2	15.5	A/B	a
77126	25.2	H5	18.3	16.2	A/B	a
77127	3.8	L5	25.0	21.1	B	d
77129	1.7	H5	18.9	16.6	B	a
77130	24.8	H5	18.9	16.5	A	a
77131	25.9	H6	19.2	16.8	A/B	b
77132	115	H5	19.0	16.9	A/B	a
77133	18.7	H6	19.0	17.0	A	a
77134	19.1	H6	18.9	16.7	A	c
77136	3.6	H5	19.1	16.4	A/B	a
77138	2.1	H5	19.2	17.0	A	a
77139	65.9	H5	18.6	16.4	A/B	b
77142	3.1	H5	18.9	17.1	A/B	b
77143	39.0	H5	18.7	16.2	A/B	b
77146	18.2	H6	18.9	16.9	A/B	a
77147	18.7	H6	19.0	16.6	A/B	b
77149	25.6	H6	19.1	16.9	A/B	a
77151	16.9	H5	18.9	16.4	A	a
77152	17.8	H5	18.7	16.9	A	b
77153	12.0	H5	19.2	16.7	A	b
77156	17.7	EH4	0.8	1.5	A	b
77157	88.3	H6	18.6	15.7	B	b
77158	19.9	H5	18.9	16.9	A/B	b
77159	17.0	L6	24.4	20.8	A/B	c
77161	6.1	H5	19.3	17.1	B	b
77162	29.0	L6	25.3	20.9	A	d
77163*	24.3	L3	n.d.	n.d.	B/C	b
77166*	140	L3	n.d.	n.d.	C	b
77168	24.7	H5	19.0	16.5	B	b
77170*	12.2	L3	n.d.	n.d.	B/C	b
77171	23.8	H5	18.9	17.0	A/B	a
77173	25.8	H5	19.1	17.0	B	a
77174	32.4	H5	18.3	16.0	A	b
77175*	23.3	L3	n.d.	n.d.	B/C	b
77176	54.4	L3	0.3–34	1–37	B	b

TABLE 3.—Continued.

ALHA	Weight (g)	Class and type	Olivine (mole % Fa)	Pyroxene (mole % Fs)	Degree of weathering	Shock facies
77178*	5.7	L3	1–36	2–40	B/C	b
77181	33.0	H5	20.0	17.3	B	a
77184	128	H5	17.8	15.9	B	b
77185*	28.0	L3	n.d.	n.d.	A/B	b
77186	122	H5	18.8	16.0	A/B	b
77187	52.2	H5	18.1	16.3	A/B	b
77188	109	H5	18.1	16.1	A/B	b
77193	6.7	H5	19.0	15.7	A	b
77195	4.7	H5	18.9	16.4	A	b
77197	20.3	L3	10–27	4–21	A/B	c
77198	7.3	L6	24.4	20.6	B	d
77200	0.9	H6	19.7	17.6	C	a
77201	15.0	H5	18.8	15.3	A	b
77202	2.7	H5	18.6	16.6	B	b
77205	3.1	H5	18.8	16.7	B	b
77207	4.9	H5	17.8	16.7	A/B	b
77209	31.8	H6	18.8	16.4	B	b
77211*	26.7	L3	n.d.	n.d.	B/C	b
77212	16.8	H6	18.9	17.0	A/B	a
77213	8.4	H5	18.6	16.5	A	a
77218	45.1	L5	23.4	19.1	A	c
77220	69.1	H5	17.7	16.0	B	c
77222	125	H4	18.0	15.3	A/B	b
77227	16.0	H5	18.9	16.6	A	a
77228	19.3	H5	18.5	16.3	B	a
77235	4.9	H5	18.9	16.7	A/B	b
77237	4.1	H5	18.5	15.8	A	b
77239	19.0	H6	18.7	15.9	B	a
77240	25.1	H5	18.8	16.0	A	b
77241*	144	L3	n.d.	n.d.	C	b
77242	56.5	H5	18.8	16.2	B	a
77244*	39.5	L3	n.d.	n.d.	B/C	b
77245	33.4	H5	19.2	17.2	A/B	b
77246	41.6	H6	19.2	16.5	B	a
77247	44.2	H5	18.8	16.4	A/B	b
77248	96.1	H6	18.7	16.7	B/C	a
77251	68.8	L6	25.0	21.3	B	d
77253	23.6	H5	19.2	16.9	A/B	c
77265	18.3	H5	17.6	15.9	B	b
77266	108	H5	19.6	17.7	B	a
77267	103	L5	24.7	20.9	A	c
77275	24.9	H5	18.3	15.6	A	a
77279	174	H5	18.8	17.1	A	b
77291	5.8	H5	18.9	15.9	A	b
77293	110	L6	24.7	20.9	B	c
77295**	141	EH4	0.8	1.7	A	b
77301	55.0	L6	24.9	20.9	A	d
77303*	78.6	L3	n.d.	n.d.	B/C	b

* Paired with A77011.

** Paired with A77156.

TABLE 4.—Classification of 142 small ordinary chondrites from the Allan Hills collection compared to classifications of mostly larger specimens recovered from the Allan Hills in 1976, 1977, 1978, and 1979 (Score et al., 1981) as well as meteorite falls and finds (Motylewski, 1978) and falls only (Wasson, 1974) in the rest of the world.

Class	This paper		Score et al. (1981)		Motylewski* (1978)		Wasson (1974)	
	No.	%	No.	%	No.	%	No.	%
H3	0	0	4	3	11	3	6	5
H4	2	2	28	22	86	24	23	20
H5	85	83	68	52	174	49	53	47
H6	15	15	30	23	86	24	32	28
Total H	102	100	130	100	357	100	114	100
L3	22	58	19	25	12	3	9	5
L4	0	0	1	1	30	8	11	7
L5	4	10	3	4	78	20	28	17
L6	12	32	54	70	262	69	117	71
Total L	38	100	77	100	382	100	165	100
LL3	0	0	4	45	6	12	6	18
LL4	0	0	0	0	1	2	1	3
LL5	1	50	3	33	12	25	7	20
LL6	1	50	2	22	30	61	20	59
Total LL	2	100	9	100	49	100	34	100
Total H	102	72	130	60	357	45	114	36
Total L	38	27	77	36	382	49	165	53
Total LL	2	1	9	4	49	6	34	11
Total ordinary chondrites	142	100	216	100	788	100	313	100

* Approximately 2% of these chondrites are from Antarctica.

Second, the percentage of H4 chondrites in our collection (2%) is much lower than in the collection of Score et al. (1981). At least ten of the latter appear to be paired (*Antarctic Meteorite Newsletter*, 1981), but this is still considerably higher than the proportion in our suite. It should be noted that the paired specimens of Score et al. (1981) all weigh more than 1 kg, whereas ours weigh less than 150 g. One is tempted to speculate that the shower of the paired H4 chondrites in the Score et al. (1981) suite yielded predominately large specimens, whereas we studied only small objects. However, Cassidy (1980) states that some of their paired H4 specimens were taken from an area where the smaller objects were removed by wind on the ground.

Third, the proportion of L3 chondrites in our and the Score et al. (1981) suite (58% and 25% of L chondrites, respectively) is biased by the large ALHA77011 shower when compared to falls (5%; Wasson, 1974) and falls and finds (3%; Motylewski, 1978). Our suite contains 19 and the Score et al. (1981) 15 paired specimens of the ALHA77011 L3 shower. Hence, the percentage of L6 chondrites in our L suite (32%) is artificially low when compared to observed falls (71%). The percentage of L6 chondrites in the Score et al. (1981) L suite (70%) is high in spite of the large number of paired L3 chondrites because at least 20 of the L6 chondrites are also paired (*Antarctic Meteorite Newsletter*, 1981). Recalculation, taking into account pairings, would result in approximately 60% L6 chondrites in our L suite and 80% in that of Score et al. (1981),

more in keeping with observed falls (Wasson, 1974).

Fourth, when considering the percentage of H, L, and LL group chondrites, it is apparent that H chondrites dominate over L and LL chondrites in our and the Score et al. (1981) suite. This dominance remains even when taking into account the pairings discussed above. This is contrasted by a domination of L over H chondrites and a higher proportion of LL chondrites among falls (Wasson, 1974) and less so, falls and finds (Motylewski, 1978) in the rest of the world. We conclude that among the generally recent arrivals to the Earth, as represented by observed falls and finds from the rest of the world, L and LL chondrites occur in much greater proportion than among the generally earlier arrivals represented by the Antarctic chondrites.

Summary

Mineralogic and petrographic study of 145 previously undescribed, small meteorites weighing <150 g from the 1977 Allan Hills, Antarctica, collection, indicates that 120 are equilibrated (petrologic types 4 to 6) H(102), L(16), and LL(2) group chondrites. The remaining 25 specimens include 19 that are paired with the graphite-magnetite-bearing L3 chondrite ALHA77011; three unpaired L3 ordinary chondrites; two paired specimens of an enstatite chondrite (EH4); and one carbonaceous chondrite (C3O). The discovery of new and rare meteorites that are generally no more severely weathered than large meteorites strongly argues for continued collection of small meteorites in Antarctica.

Literature Cited

Afiattalab, F., and J.T. Wasson
1980. Composition of the Metal Phases in Ordinary Chondrites: Implications Regarding Classification and Metamorphism. *Geochimica et Cosmochimica Acta*, 44:431–446.

Antarctic Meteorite Newsletter
1981. Paired Meteorites, 4:9–10.

Bence, A.E., and A.L. Albee
1968. Empirical Correction Factors for the Electron Microanalysis of Silicates and Oxides. *Journal of Geology*, 76:382–403.

Caffee, M.W., C.M. Hohenberg, T.D. Swindle, and B. Hudson
1982. Noble Gases in Graphite—Magnetite Inclusions. *Meteoritics*, 17:191–192.

Cassidy, W. A.
1980. Discussion. *In* King et al., Meteorite Descriptions, *in* U.B. Marvin and B. Mason, editors, Catalog of Antarctic Meteorites, 1977–1978. *Smithsonian Contributions to the Earth Sciences*, 23:42–44.

Dodd, R.T., and E. Jarosewich
1979. Incipient Melting in and Shock Classification of L-Group Chondrites. *Earth and Planetary Science Letters*, 44:335-340.

Dowty, E., G.H. Conrad, J.A. Green, P.F. Hlava, K. Keil, R.B. Moore, C.E. Nehru, and M. Prinz
1973. Catalogue of Apollo 15 Rake Samples from Stations 2 (St. George), 7 (Spur Crater) and 9a (Hadley Rille). *Special Publication, Institute of Meteoritics, University of New Mexico*, 8:1–75.

Dowty, E., M. Prinz, and K. Keil
1973. Composition, Mineralogy, and Petrology of 28 Mare Basalts from Apollo 15 Rake Samples. *In* Proceedings of the Fourth Lunar Science Conference. *Geochimica et Cosmochimica Acta*, supplement 4: 423:444.

Evans, J.C., J.H. Reeves, and L.A. Rancitelli
1982. Aluminum-26: Survey of Victoria Land Meteorites. *In* U.B. Marvin and B. Mason, editors, Catalog of Meteorites from Victoria Land, Antarctica, 1978–1980. *Smithsonian Contributions to the Earth Sciences*, 24:70–74.

Fodor, R.V., and K. Keil
1976. Carbonaceous and Non-carbonaceous Lithic Fragments in the Plainview, Texas, Chondrite: Origin and History. *Geochimica et Cosmochimica Acta*, 40:177–189.

Fujimaki, H., M. Matsu-ura, I. Sunagawa, and K. Aoki
1981. Chemical Compositions of Chondrules and Matrices in the ALH-77015 Chondrite (L3). *Memoirs of the National Institute of Polar Research* (Japan), special issue, 20:161–174.

Gomes, C.B., and K. Keil
1980. *Brazilian Stone Meteorites*, 162 pages. Albuquerque, University of New Mexico Press.

Graham, A.L.
1980. Procedures for Naming Antarctic Meteorites. *Meteoritics*, 15:93–103.

Huss, G.R., K. Keil, and G.J. Taylor
1981. The Matrices of Unequilibrated Ordinary Chondrites: Implications for the Origin and History of Chondrites. *Geochimica et Cosmochimica Acta*, 45:33–51.

Ikeda, Y., M. Kimura, H. Mori, and H. Takeda
1981. Chemical Compositions of Matrices of Unequilibrated Ordinary Chondrites. *Memoirs of the National Institute of Polar Research* (Japan), special issue, 20:124–144.

Jarosewich, E.
1980. Appendix 2: Chemical Analyses of Some Allan Hills Meteorites. *In* U.B. Marvin and B. Mason, editors, Catalog of Antarctic Meteorites, 1977–1978. *Smithsonian Contributions to the Earth Sciences*, 23:48.

Jarosewich, E., and R.T. Dodd
1981. Chemical Variations among L-group Chondrites, II: Chemical Distinctions between L3 and LL3 Chondrites. *Meteoritics*, 16:83–91.

Kallemeyn, G.W., and J.T. Wasson
1982. Carbonaceous Chondrites from Antarctica. In *Lunar and Planetary Science XIII*, pages 373–374. Houston: Lunar and Planetary Institute.

Keil, K.
1967. The Electron Microprobe X-Ray Analyzer and Its Application in Mineralogy. *Fortschritte der Mineralogie*, 44:4–66.
1968. Chemical and Mineralogical Relationships among Enstatite Chondrites. *Journal of Geophysical Research*, 73:6945–6976.

King, T.V.V., R. Score, E.M. Gabel, and B. Mason
1980. Meteorite Descriptions. *In* U.B. Marvin and B. Mason, editors, Catalog of Antarctic Meteorites, 1977–1978. *Smithsonian Contributions to the Earth Sciences*, 23:12–44.

Leitch, C.A., and J.V. Smith
1980. Two Types of Clinoenstatite in Indarch Enstatite Chondrite. *Nature*, 283:60–61.
1981. Mechanical Aggregation of Enstatite Chondrites from an Inhomogeneous Debris Cloud. *Nature*, 290:228–230.
1982. Petrography, Mineral Chemistry and Origin of Type I Enstatite Chondrites. *Geochimica et Cosmochimica Acta*, 46:2083–2098.

McKinley, S.G., K. Keil, and E.R.D. Scott
1982. Allan Hills A77156, an EH4 Enstatite Chondrite: Some Evidence against Formation from Red and Blue Luminescing Planetesimals. *Meteoritics*, 17: 251.

McKinley, S.G., E.R.D. Scott, and K. Keil
1983. Chondrules in Enstatite Chondrites—Nature and Source of Enstatite. *Lunar and Planetary Science XIV*, pages 485–486. Houston: Lunar and Planetary Institute.

McKinley, S.G., E.R.D. Scott, G.J. Taylor, and K. Keil
1981. A Unique Type 3 Ordinary Chondrite Containing Graphite-Magnetite Aggregates—Allan Hills A77011. In *Proceedings of the Twelfth Lunar and Planetary Science Conference*, pages 1039–1046. New York: Pergamon Press.

McSween, H.Y. Jr.
1977. Carbonaceous Chondrites of the Ornans Type: A Metamorphic Sequence. *Geochimica et Cosmochimica Acta*, 41:477–491.

Motylewski, K.
1978. *The Revised Cambridge Chondrite Compendium.* Cambridge, Mass.: Smithsonian Astrophysical Observatory.

Nagahara, H.
1981. Petrology of Chondrules in ALH-77015 (L3) Chondrite. *Memoirs of the National Institute of Polar Research* (Japan), special issue, 20:145–161.

Okada, A.
1975. Petrological Studies of the Yamato Meteorites, Part 1: Mineralogy of the Yamato Meteorites. *Memoirs of the National Institute of Polar Research* (Japan), special issue, 5:14–66.

Schwarz, C., and B. Mason
1983. Antarctic Meteorite Descriptions 1981. *Antarctic Meteorite Newsletter*, 6:1–26.

Score, R., C.M. Schwarz, T.V.V. King, B. Mason, D.D. Bogard, and E.M. Gabel
1981. Antarctic Meteorite Descriptions 1976–1977—1978–1979. *Antarctic Meteorite Newsletter*, 4:1–144.

Score, R., C.M. Schwarz, B. Mason, and D.E. Bogard
1982. Antarctic Meteorite Descriptions 1980. *Antarctic Meteorite Newsletter*, 5:1–55.

Scott, E.R.D., A.E. Rubin, G.J. Taylor, and K. Keil
1981. New Type of Type 3 Chondrite with a Graphite-Magnetite Matrix. *Earth and Planetary Science Letters*, 56:19–31.

Scott, E.R.D., G.J. Taylor, P. Maggiore, K. Keil, S.G. McKinley, and H.Y. McSween, Jr.
1981. Three CO3 Chondrites from Antarctica—Comparison of Carbonaceous and Ordinary Type 3 Chondrites. *Meteoritics*, 16:385.

Sears, D.W., J.N. Grossman, and C.L. Melcher
1982. Chemical and Physical Studies of Type 3 Chondrites—I: Metamorphism Related Studies of Antarctic and Other Type 3 Ordinary Chondrites. *Geochimica et Cosmochimica Acta*, 46:2471–2481.

Sears, D.W., G.W. Kallemeyn, and J.T. Wasson
1982. The Compositional Classification of Chondrites, II: The Enstatite Chondrite Groups. *Geochimica et Cosmochimica Acta*, 46:597–608.

Sears, D.W.G., and K.S. Weeks
1983. Thermoluminescence Sensitivity of Sixteen Type 3 Ordinary Chondrites. In *Lunar and Planetary*

Science XIV, pages 682–683. Houston: Lunar and Planetary Institute.

Skinner, B.J., and F.D. Luce
1971. Solid Solutions of the Type (Ca,Mg,Mn,Fe)S and Their Use as Geothermometers for the Enstatite Chondrites. *American Mineralogist*, 56:1269–1296.

Van Schmus, W.R.
1969. Mineralogy, Petrology, and Classification of Type 3 and 4 Carbonaceous Chondrites. *In* P.M. Millman, editor, *Meteorite Research*, pages 480–491. Dordrecht, Holland: D. Reidel Publishing Company.

Van Schmus, W.R., and J.A. Wood
1967. A Chemical-Petrologic Classification for the Chondritic Meteorites. *Geochimica et Cosmochimica Acta*, 31:747–765.

Warner, R.D., K. Keil, M. Prinz, J.C. Laul, A.V. Murali, and R.A. Schmitt
1975. Mineralogy, Petrology, and Chemistry of Mare Basalts from Apollo 17 Rake Samples. *Geochimica et Cosmochimica Acta*, supplement 6, 1:193–220.

Wasson, J.T.
1974. *Meteorites—Classification and Properties.* 316 pages. Heidelberg: Springer-Verlag.

Classification, Metamorphism, and Brecciation of Type 3 Chondrites from Antarctica

Edward R.D. Scott

Introduction

Japanese and United States expeditions to Antarctica are known to have recovered 60 specimens, which probably represent about 21 different type 3 chondrites. About 59 type 3 chondrites have been recovered from outside Antarctica and over two-thirds of these are poorly described or inaccessible. Thus the Antarctic specimens represent a substantial addition to our supply of type 3 chondrites—the least metamorphosed or altered samples of early solar system materials. Interestingly, the ratio of ordinary to carbonaceous type 3 chondrites (Table 5) is much higher for Antarctic (4.2) than non-Antarctic meteorites (2.8) and for meteorite falls (2.1). Reid (1982) has observed similar disparities between Antarctic and non-Antarctic achondrites and speculates that the flux of meteorites reaching the earth may have changed with time, as the Antarctic samples have longer mean terrestrial ages (Evans et al., 1982).

This paper describes the 21 type 3 chondrites that have been identified to date among the 1969–1980 collections, and reviews chemical and petrologic studies relevant to their classification into groups and subtypes. I present new electron-probe analyses of silicates in 11 type 3 and 4 ordinary chondrites, which suggest that several should be reclassified. Seven of these chondrites contain both equilibrated and unequilibrated chondrules, indicating that metamorphism must have preceded lithification of these rocks. I conclude that most type 3 chondrites are probably breccias of materials with differing metamorphic histories.

Edward R.D. Scott, Department of Geology and Institute of Meteoritics, University of New Mexico, Albuquerque, New Mexico 87131.

TABLE 5.—Approximate numbers of Antarctic and non-Antarctic type 3 chondrites described before 1983.

Class	Antarctic	Non-Antarctic
ORDINARY		
H3	5	17
L3	9	13
LL3	3	11
CARBONACEOUS		
C3O	2	6
C3V	1	9
OTHER	1	3
Total	21	59

ACKNOWLEDGMENTS.—I thank A. Bischoff, A.E. Rubin, and C. Williams for technical assistance, K. Keil, S.G. McKinley, D.W. Sears, and G.J. Taylor for useful advice and data, and the Antarctic Meteorite Working Group (USA) and the National Institute of Polar Research (Japan) for the loan of samples. This work was supported in part by NASA grant NGL 32-004-064 to K. Keil.

Techniques

Randomly chosen olivine and low-Ca pyroxene grains in 11 type 3 and 4 chondrites were ana-

lyzed in the electron probe for Fe, Mg, Si, and Ca using crystal spectrometers (Fodor and Keil, 1976). In addition 4 to 10 olivine grains and, where possible, an equal number of pyroxene grains were analyzed in each of 109 chondrules in 8 of these chondrites. Chondrules with heterogeneous silicates were analyzed more thoroughly. These analyses were not made randomly; cores and rims of grains of various sizes both near the center and rim of chondrules were analyzed.

Bulk chemical data for major and minor elements are available for only 7 of the 24 meteorites listed in Table 6. Thus, classifications are based very largely on abundances of metallic Fe, Ni and olivine compositions. Dodd et al. (1967) showed that the most unequilibrated ordinary chondrites do not have peaks in histograms of their olivine compositions. However, in cases where 50% of the analyses lie in a narrow peak, the olivine composition seems to be as accurate a guide for classification as it is for types 4 to 6 chondrites. Jarosewich and Dodd (1981) identify one such chondrite, Carraweena, for which chemical and mineralogical data suggest different classifications (LL and L, respectively).

Type 3 Carbonaceous Chondrites

Four type 3 carbonaceous chondrites are known to have been recovered from Allan Hills (ALH) and Reckling Peak (RKP), Antarctica: ALHA77003, ALHA77029, ALHA77307, and RKPA80241. Yamato 6903 is also discussed below as it has been classified as a C3 chondrite (Okada, 1975), although it is probably a type 4. Data for these chondrites are summarized with those for type 3 ordinary chondrites in Table 6. Classifications, sample weights, and degrees of weathering are taken from the catalogs of Yanai (1979), King et al. (1980), and Score, Schwarz, et al., (1982) and Score, King, et al. (1982), except where noted. (The terms C3O and C3V are used instead of CO3 and CV3 at the request of the volume editors.)

ALHA77003.—This meteorite was described as an H3 chondrite by King et al. (1980), but reclassified as a C3 by Rhodes and Fulton (1981) in accordance with their chemical data. Scott, Taylor, et al. (1981) classified ALHA77003 as a C3O chondrite on the basis of petrologic studies and published chemical data. Ratios of Al/Si, Mg/Si and Ca/Si from Jarosewich's (1980) analysis are appropriate for a CO chondrite, a classification with which Kallemeyn and Wasson (1982a) concur. Its olivines vary widely in composition, 2–45 mole% fayalite, with about half the analyses in the range Fa_{34} to Fa_{40}. Thus it has been metamorphosed more than Ornans but less than Warrenton (Van Schmus, 1969) and is a type II or III on McSween's (1977) metamorphic classification. Analyses of the matrix in ALHA77003 are reported by Ikeda et al. (1981) and of microchondrules by Rubin et al. (1982).

ALHA77029.—This 1.4 g meteorite is one of a suite of small samples described by McKinley and Keil (herein, p. 56). It was classified by Scott, Taylor, et al. (1981) as a C3O chondrite on the basis of its mineralogy. Kallemeyn and Wasson (1982b) analyzed a 72 mg sample by neutron activation and agreed with its classficiation as a CO chondrite. Its olivine compositions vary from 0.2 to 63% Fa with no prominent peak in a histogram of 50 analyses, like those of Ornans (Van Schmus, 1969). It is a metamorphic type II on McSween's (1977) scale and is definitely not paired with any other Antarctic chondrite so far described.

ALHA77307.—This meteorite was classified as a C3 chondrite by King et al. (1980). Scott, Taylor, et al. (1981) likened 77307 to Kainsaz, a very unmetamorphosed C3O, from petrologic studies. Biswas et al. (1981) listed 77307 as a C3V chondrite, as its Cd concentration is typical of C3V chondrites but 30 times higher than any C3O (Takahashi et al., 1978). Kallemeyn and Wasson (1982a) conclude that the bulk chemistry of 77307 partly resembles that of CM and CO chondrites, but they classify it as a unique carbonaceous chondrite. Nagahara and Kushiro (1982) studied the relationships between chondrules, inclusions, and isolated olivines in this

meteorite. They identified a sequence of aggregates and chondrules that increased in grain size and attribute their textural changes to heating below the liquidus. Moore et al. (1981) also analyzed 77307 and identified traces of amino acids.

RKPA80241.—This 0.6 g meteorite is, surprisingly, the only known C3V chondrite from Antarctica. (ALHA80133 was tentatively classified as a C3V chondrite by Score, Schwarz, et al. (1982), but is here paired with ALHA77011 (L3); see Table 8.)

Yamato 6903.—Okada (1975) and Okada et al. (1975) have provided extensive petrologic and chemical data for this meteorite under the name "Yamato (c)," and classified it as a type III carbonaceous chondrite. McSween (1979) lists it as a C3V chondrite, although the published silicate analyses and textural descriptions suggest it may be a type 4 or 5 chondrite. Additional evidence for a higher petrologic grade is provided by Clayton et al. (1979), who found some equilibration of oxygen isotopes between minerals, like that in Karoonda, which is a type 5 (McSween, 1979). The bulk Al/Si, Mg/Si, and Ca/Si ratios

TABLE 6.—Type 3 chondrites from Antarctica and their properties (anom. = anomalous; br = breccia containing more equilibrated clasts or regions; rbr = regolith breccia containing solar-wind noble gases and equilibrated clasts).

Name	Class and type	Subtype[m]	Original weight (g)	Degree of weathering	Olivine composition	
					Mean %Fa	σ/mean %
ALHA76004	LL3[a]	3.3	305[a]	A	17[n]	56[n]
ALHA77003	C3O[b]		779.6	A	25[b]	52[b]
ALHA77011	L3[c]	3.4–3.5	6338[c]	C	17[c]	48[c]
ALHA77013	L3[d]	3.5	23.0	B[d]	19[d]	20[d]
ALHA77029	C3O[b]		1.4	A/B[d]	23[b]	83[b]
ALHA77176	L3[d]	3.2	54.4	B[d]	12[d]	67[d]
ALHA77197	L3[d]	3.6	20.3	A/B[d]	24[d]	12[d]
ALHA77215[l]	L3-rbr[e]	3.8	3046	B	24[e]	
ALHA77278	LL3[f]	3.6	312.9	A	22[g]	44[g]
ALHA77299	H3-br	3.7	260.7	A	17[n]	33[n]
ALHA77304	L4[n]	3.7?	650.4	B	25.5[n]	4[n]
ALHA77307	C3 anom.		181.3	A	13[b]	130[b]
ALHA78084	H4[n]	3.9	14280	B/C	18.7[n]	1.7[n]
ALHA79003	LL3[h]	3.4[h]	5.1	B	26[h]	43[h]
ALHA79022	L3-br[n]	3.7?	31.4	A/B	23.6[n]	4[n]
OTTA80301	H3	3.7	35.5	B/C	18.2[n]	6[n]
RKPA79008	L3	3.7	73.0	B	23[n]	18[n]
RKPA80205	H3	3.7	53.8	B	16[n]	20[n]
RKPA80207	H3[n]	3.2?	17.7	C	19[n]	22[n]
RKPA80241	C3V		0.6	B	3[i]	
RKPA80256	L3	3.6?	153.2	B	23.8[n]	5[n]
Yamato 6903	C4?[jn]		150		30[j]	1[j]
Yamato 74191	L3	3.6	1091.6	A[n]	21[n]	23[n]
Yamato 75028	H3-rbr		6100		19.4[k]	

[l] ALHA77216, 77217, and 77252 are paired with ALHA77215.

REFERENCES (for sources of unreferenced data, see p. 73): [a] Olsen et al., 1978; [b] Scott,Taylor, et al., 1981; [c] McKinley et al., 1981, and Table 8 herein; [d] McKinley and Keil, herein; [e] Score, 1980; [f] McSween and Wilkening, 1980; [g] A. Okada, personal communication; [h] Scott, Taylor, Maggiore, 1982; [i] Score, Schwarz, et al., 1982; [j] Okada, 1975, and Okada et al., 1975; [k] Yanai et al., 1978; [m] Sears et al., 1980, 1982, and Sears and Weeks, 1983; [n] this work.

for Yamato 6903 (Shima and Shima, 1975) are all in the range of carbonaceous chondrites (Wasson, 1974). Ca/Si and Ca/Mn ratios are consistent with those of CV chondrites (Kallemeyn and Wasson, 1981), but Al/Si and Al/Mn appear to be too low. Further studies are obviously needed to establish its classification.

Type 3 Ordinary Chondrites

Seventeen Antarctic type 3 ordinary chondrites and 2 that are reclassified in this paper from type 3 to type 4 are listed in Table 6 with some of their properties. Data for paired specimens are listed under the name of the specimen with the lowest number (Graham, 1980). Histograms of olivine and low-Ca pyroxene analyses in 11 of these chondrites are shown in Figures 64 and 65 (less and more metamorphosed chondrites, respectively). Table 7 lists the number of analyses, mean fayalite and ferrosilite concentrations, and coefficient of variation, which is the standard deviation of the analyses (mole% fayalite or ferrosilite) expressed as a percentage of the mean. Also listed for the olivine analyses is the percent mean deviation (PMD) of the FeO weight concentrations in olivine. This parameter, which was first used by Dodd et al. (1967), is not as convenient as the standard deviation, but it is listed because Van Schmus and Wood (1967) used it to define the boundary between type 3 and 4 chondrites; type 3 chondrites have a PMD that exceeds 5.

For a normal distribution, the mean deviation is $(\pi/2)^{-1/2}$ or 0.80 times the standard deviation. Since mole% Fa and wt.% FeO are not linearly related, this relationship will not hold exactly for PMD (calculated from wt.% FeO) and CV (from mole% Fa or Fs), even neglecting deviations from normal distributions. For eight of the chondrites in Figures 64 and 65, the PMD/CV ratios for low-Ca pyroxene analyses are close to 0.80 (0.76 to 0.82), but for olivine analyses, which are generally far from normally distributed, the PMD/CV ratios average 0.63 ± 0.14.

Of the eight other ordinary chondrites that are listed in Table 6 but not in Table 7, three have already been described in some detail: ALHA77011 (McKinley et al., 1981), ALHA 77278 (McSween and Wilkening, 1980) and ALHA79003 (Scott, Taylor, and Maggiore, 1982). Another three are described for the first time by McKinley and Keil (herein, p. 59). The other two type 3 ordinary chondrites are regolith breccias: ALHA77215 and Yamato 75028; they are the only ones for which thin sections were

TABLE 7.—Electron microprobe analyses of olivines and low-Ca pyroxenes in 11 Antarctic type 3 and 4 ordinary chondrites (br = breccia; PMD = percent mean deviation calculated from FeO wt.% (see Dodd et al., 1967)).

Specimen number, Section	Class	Olivine				Low-Ca pyroxene		
		Anal. No.	Mean % Fa	σ/mean %	PMD	Anal. No.	Mean % Fs	σ/mean %
ALHA76004, 8	LL3	53	17.3	56	40	39	12.1	66
ALHA77299, 40	H3-br	38	17.1	33	24	38	13.7	49
ALHA77304, 35,36	L4	29	25.5	3.6	2.1	22	16.7	38
ALHA78084, 135	H4	64	18.7	1.7	1.6	71	16.7	11.7
ALHA79022, 14	L3-br	49	23.6	4.3	2.5	40	17.7	29
OTTA80301, 13	H3	28	18.2	6.1	2.5	35	11.0	45
RKPA79008, 7	L3	35	22.6	18.1	9.0	35	15.5	39
RKPA80205, 12	H3	36	16.0	19.6	10.5	36	13.0	32
RKPA80207, 11	H3	36	18.7	22.1	12.8	37	15.3	43
RKPA80256, 17	L3	35	23.8	4.7	2.8	35	15.6	30
Yamato 74191, 92	L3	74	21.4	23	17.3	76	11.8	59

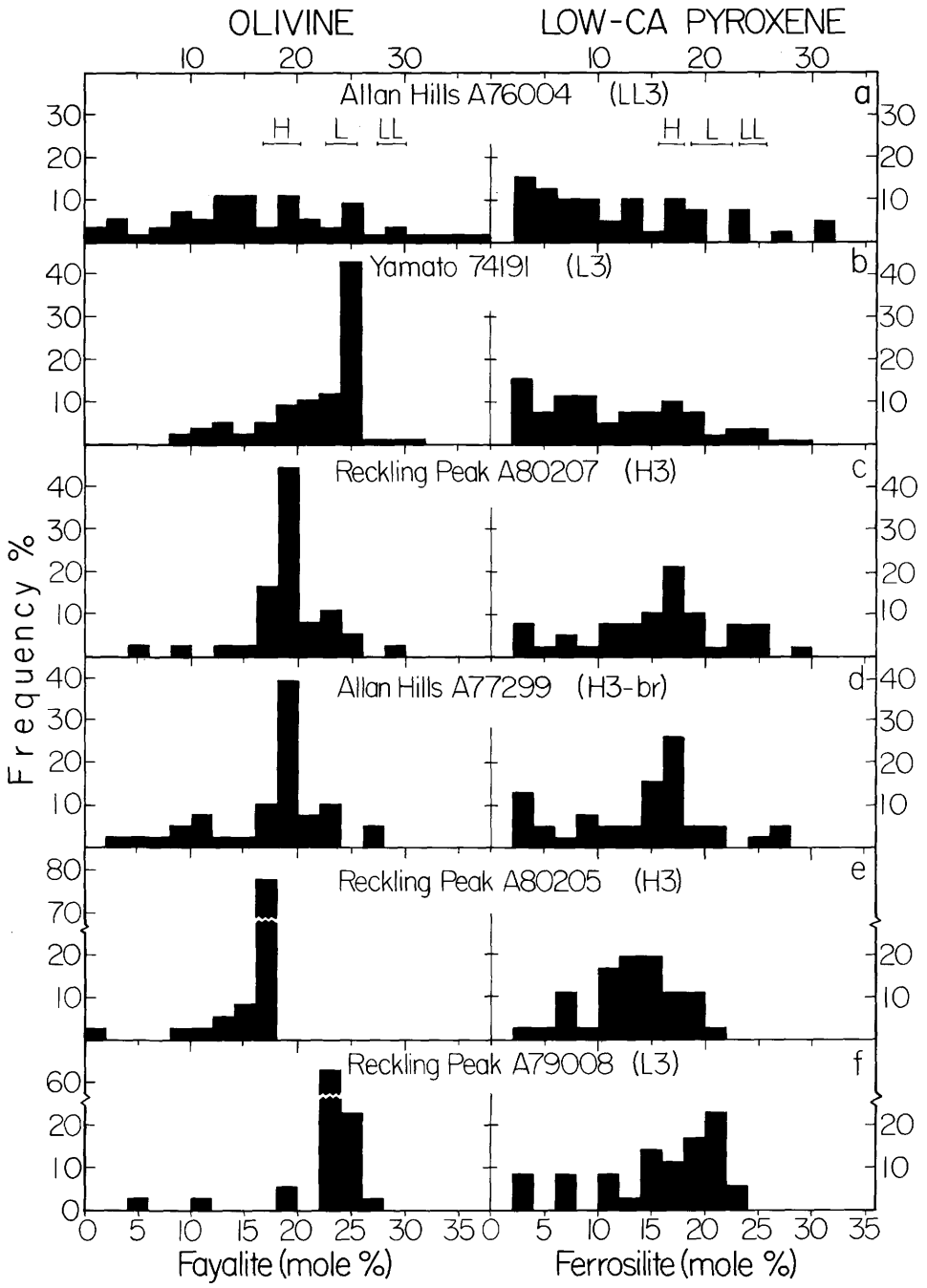

FIGURE 64.—Histograms of electron-probe analyses of randomly chosen olivine and low-Ca pyroxenes in six mildly or moderately metamorphosed type 3 ordinary chondrites from Antarctica (Table 7). Chondrites are arranged in approximately increasing order of their proportion of equilibrated olivines. Compositional ranges for equilibrated H, L, and LL groups are from Gomes and Keil (1980).

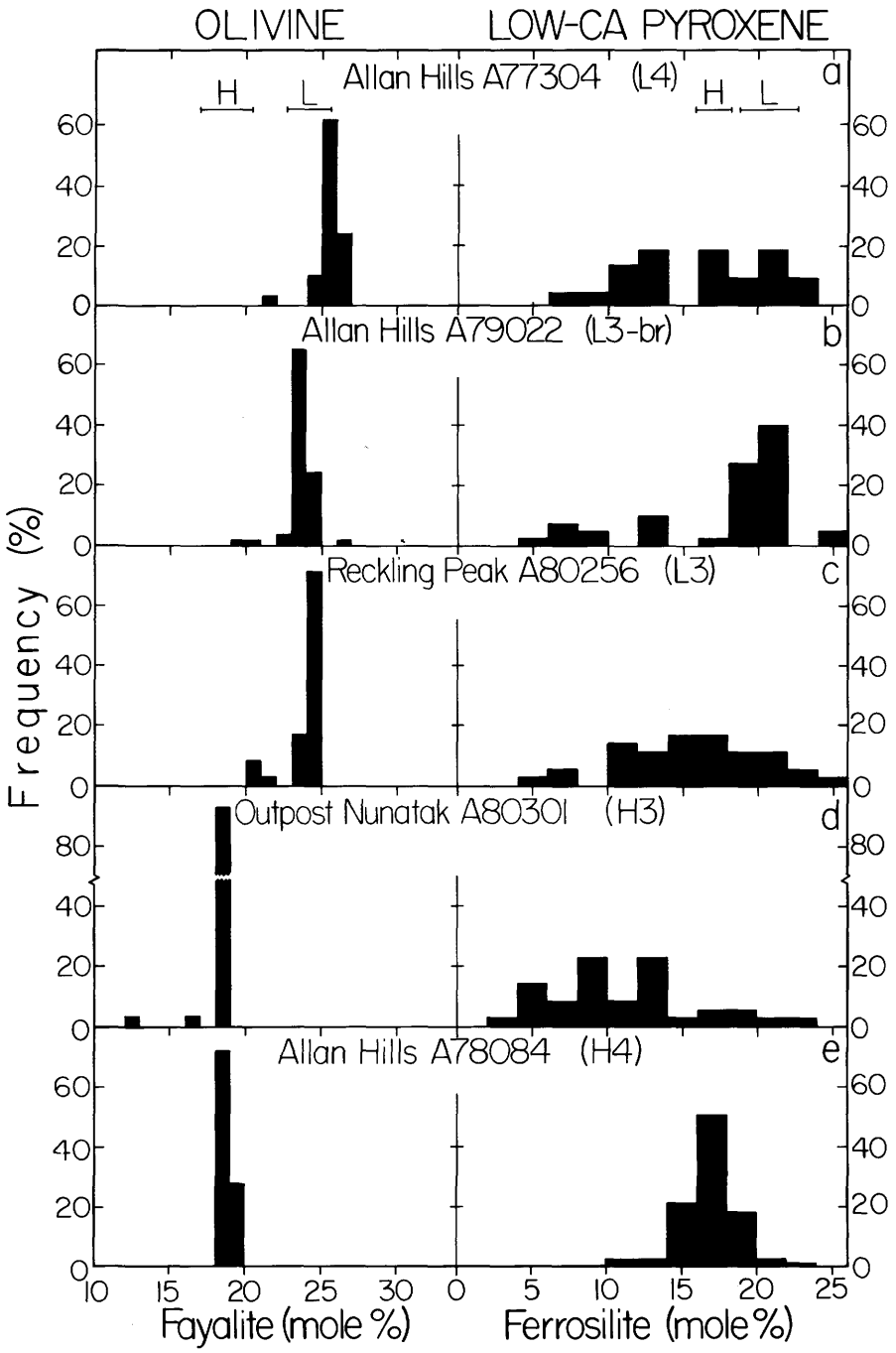

FIGURE 65.—Histograms of olivine and low-Ca pyroxenes in three well metamorphosed type 3 chondrites and two type 4 chondrites, which were previously classified as type 3 (Table 7). In all five chondrites, over 90% of the olivines have compositions in the equilibrated H or L range. However, the proportion of equilibrated low-Ca pyroxenes in each chondrite varies from 5–70%, and, as in Figure 64, these values are not well correlated with the proportion of equilibrated olivines. Metamorphism of chondritic components in diverse locations prior to final lithification accounts for the poor correlations.

not available during the course of the study. Also included in Table 6 are ALHA78084 and 77304, which are here reclassified as type 4 chondrites.

Two ordinary chondrites that have been classified as type 3 chondrites have been omitted from Table 6. Yamato 74065 and the paired specimen 74066 were listed as an L3 chondrite by Yanai (1979) and by Takeda et al. (1979). The section loaned to us (Yamato 74066,73), however, is an L5 chondrite, with olivine $Fa_{23.5}$ to $Fa_{25.5}$ and low-Ca pyroxene $Fs_{19.5}$ to $Fa_{22.0}$. Yanai et al. (1978) found very heterogeneous olivines and pyroxenes in Yamato 74492, and Yanai (1979) listed it as an H3 chondrite. However, section 74492,81 is an H6 chondrite with homogeneous olivine, $Fa_{18.5}$, and low-Ca pyroxene, $Fs_{16.0}$.

In the brief review below of petrologic and chemical studies that are relevant to the classification of these chondrites, the original descriptions and analyses by King et al. (1980), Score, Schwarz, et al. (1982) and Score, King, et al. (1982) are not referred to unless there are conflicting data. However, these papers are the primary source of petrologic information for many of the type 3 ordinary chondrites. Possible specimen pairings are discussed below; except where noted in Tables 6 and 8, it appears that these samples are not paired, but a few cases deserve further study.

ALHA76004.—The first type 3 chondrite to be recovered from Antarctica is one of the least equilibrated. Figure 64*a* shows that its olivines are more heterogeneous than any of the other 10 chondrites analyzed. Like ALHA77176, the other very primitive ordinary chondrite, it contains abundant opaque matrix (Huss et al., 1981), which was analyzed by Ikeda et al. (1981). Detailed petrologic descriptions of ALHA76004 are provided by Olsen et al. (1978), who classified it as an LL3, and Ikeda (1980). Although the oxygen isotopic composition of clasts in ALHA76004 are more extreme than those reported for components in other ordinary chondrites (Mayeda et al., 1980), this chondrite may not be more unusual than other primitive chondrites, such as Bishunpur and Semarkona.

TABLE 8.—List of specimens paired with ALHA77011, L3 chondrite (* = small samples; see Table 3 herein).

77015	77052*	77170*	77260
77031*	77115*	77175*	77303*
77033	77140	77178*	78038
77034*	77160	77185*	78188
77036*	77163*	77211*	79001
77043*	77164	77214	79045
77047*	77165	77241*	80133
77049*	77166*	77244*	
77050*	77167	77249	

ALHA77011.—This meteorite and the paired specimens (Table 8) all contain a few volume percent of graphite-magnetite aggregates (McKinley et al., 1981). These samples are paired with some confidence because other type 3 chondrites contain much less graphite-magnetite, except for Sharps, which has 11 vol.%. However, Sears et al. (1982) believe that the samples may represent two falls, as their thermoluminescence sensitivity values vary by a factor of 3. Extensive sampling of a large type 3 chondrite would be useful to help establish what variation in chemical and physical properties can be expected in a single meteorite.

Chondrules in ALHA77011 (Nagahara, 1981a, 1981b; Fujimaki et al., 1981; data on specimen ALHA77015) do not seem to be different from those in other ordinary chondrites. Ikeda et al. (1981) argue that the opaque matrix in three ALHA77011 specimens *is* different in composition from matrices in three other ordinary type 3 chondrites. Chiefly on the basis of the Na/Al ratio, they find that the matrix of 77011 resembles matrices in C2 and C3 chondrites. However, Na/Al matrix ratios in Sharps and Krymka (Huss et al., 1981) are nearly as low as that of 77011. The bulk composition of this meteorite (Jarosewich, 1980; Rhodes and Fulton, 1981) appears to be typical for L chondrites (McKinley et al., 1981).

ALHA77215.—This is only the sixth L chon-

drite known to contain solar-wind gases (Goswami, 1981). It and the three paired specimens (Table 6) contain 47 vol.% of mineral, lithic, and chondrule fragments (Score, 1980), and solar-flare tracks (Nautiyal et al., 1982). Like many other chondrite regolith breccias, this meteorite also contains graphite-magnetite aggregates (Scott, Rubin, et al., 1981).

ALHA77278.—Although 77278 is very rich in In and Tl (Biswas et al., 1980), McSween and Wilkening (1980) found that its olivine is not as unequilibrated as might be expected. ALHA 76004, for example, has olivines that are more heterogeneous (Figure 64*a*) although its In and Tl concentrations (Biswas et al., 1981) are lower. McSween and Wilkening (1980) and King et al. (1980) classify ALHA77278 as an LL chondrite on the basis of Co concentrations in kamacite and a bulk chemical analysis by Jarosewich (1980). Jarosewich and Dodd (1981) concur with this classification.

This meteorite is only one of four ordinary chondrites (all LL) known to contain carbides and magnetite (Taylor et al., 1981; Scott, Taylor, and Maggiore, 1982). Equilibrated chondrules, but not clasts, were identified by Scott, Taylor, Keil, (1982), and a carbonaceous clast was tentatively identified by King et al. (1980). Weber et al. (1983) found significant excess ^{4}He in ALHA77278, indicative of solar-wind gases. However, its Ne isotopic ratios marginally fail the suggested requirements of Wasson (1974) for a solar-gas-rich meteorite.

ALHA77299.—The mean composition of olivine (Figure 64*d*) and the abundance of metallic Fe,Ni enabled King et al. (1980) to classify 77299 as an H3 chondrite. Analyses by Jarosewich (1980), Rhodes and Fulton (1981), and Biswas et al. (1980) confirm this classification. Additional petrologic descriptions are provided by Haggerty et al. (1979) and Ikeda et al. (1981). An H4 clast is described in the section on breccia properties.

ALHA77304.—This meteorite was classified by King et al. (1980) as an LL3 chondrite, but the data in Table 7 and Figure 65*a* indicate that it should be classified as L4 because of its homogeneous olivine; PMD is 2.1, mostly Fa_{25} to Fa_{26}. Although King et al. (1980) found more heterogeneous olivine (Fa_{18} to Fa_{27}), B. Mason and H. Nagahara (private communications) confirm the L4 classification of ALHA77304. King et al. (1980) note that clasts up to 1 cm in diameter are visible on the surface of this chondrite.

ALHA78084.—This 14 kg meteorite was initially classified as an H3 chondrite (Score, King, et al., 1982), but the homogeneity of its olivine in Figure 65*e* (PMD of olivine is 1.6) is more appropriate to type 4 (Van Schmus and Wood, 1967). Extensive weathering probably made the interchondrule material more opaque, and the chondrules more prominent than normal for a type 4 chondrite. The opaque matrix typical of type 3.0–3.6 ordinary chondrites (Huss et al., 1981) is absent.

ALHA79003.—This tiny meteorite was paired with ALHA79001 by Score, King, et al. (1982) but unpaired by Scott, Taylor, and Maggiore (1982). The latter authors identified 79001 as a specimen of ALHA77011, and reclassified 79003 as the third Antarctic LL3 chondrite. As with non-Antarctic type 3 ordinary chondrites, these three LL3 chondrites are less equilibrated than most Antarctic H3 and L3 chondrites.

ALHA79022.—Score et al. (1981) found heterogeneous olivines with Fa_1 to Fa_{28} and classified this meteorite as an H3, but Figure 65*b* shows that some areas have very homogeneous olivine typical of L4 chondrites (very largely Fa_{23} to Fa_{25}). On the assumption that the more heterogeneous areas represent matrix and that the meteorite does not contain a mixture of H and L material, 79022 is classed as an L3 breccia in Table 6. Limited published data on ALHA77215 are similar to those of this meteorite, suggesting that the possibility of pairing needs more study. ALHA77304, which is another L3–4 breccia, has olivines with significantly higher FeO concentrations (Figure 65*a*) than 79022. However, comparing heterogeneous breccias is clearly a difficult task.

OTTA80301.—Score, Schwarz, et al. (1982)

tentatively classified this meteorite from Outpost Nunatak as an H3 chondrite, and this classification is retained here, even though its olivine composition in Table 7 (PMD of olivine equals 2.5) is too uniform for a type 3. All but two of 28 olivine analyses in Figure 65*d* lie in the range $Fa_{18.2}$ to $Fa_{18.9}$, entirely appropriate for H4 chondrites. However, if one more olivine grain had been encountered that was a little richer in forsterite than the most Mg-rich olivine actually analyzed (Fa_{13}), then the PMD of olivine could have exceeded 5, the upper limit for type 4 chondrites. Thus it may be very difficult to apply this criterion with confidence to distinguish type 3 and 4 chondrites without many hundreds of analyses over a large surface area.

RKPA79008.—Silicate analyses in Figure 64*f* are entirely consistent with those of Score, King, et al. (1982) and their classification of RKPA 79008 as an L3. Olivine compositions in RKPA80256, which is also a moderately equilibrated L3, are slightly more fayalitic (mostly Fa_{22} to Fa_{24}). Although the variation to be expected in a single meteorite is not well known, it seems best to assume that these specimens are not paired.

RKPA80205.—Olivine analyses in Figure 64*e* are consistent with the tentative classification of 80205 as an H3 (Score, Schwarz, et al., 1982). RKPA80207 is an H3 chondrite with similar silicate heterogeneity, which was presumably found in the vicinity of 80205. However, it can be distinguished from 80205 as its olivine is richer in fayalite (Figure 64*c*, *e*), assuming that the sections analyzed are representative of the whole specimens. Thermoluminescence sensitivity results of Sears and Weeks (1983) on the two specimens are also significantly different, although their result for 80207 is not consistent with the silicate analyses in Table 7.

RKPA80207.—The low concentration of metallic Fe,Ni in this chondrite indicated to Score, Schwarz, et al. (1982) that it is an L chondrite. However, the position of the prominent peak in the histogram of olivine analyses (Fa_{16} to Fa_{20}, Figure 64*c*) strongly suggests that it is an H chondrite, especially as severe weathering of this specimen hinders accurate estimates of its metal abundance.

RKPA80256.—Silicate analyses in Figure 65*c* confirm the tentative classification of this meteorite as an L chondrite (Score, Scharz, et al., 1982). However, the olivine PMD of 2.8 (Table 7) is too low for a type 3. Because of the difficulty of measuring PMD accurately (p. 76), the type 3 classification of Score, Schwarz, et al., is retained.

Yamato 74191.—This chondrite is one of the least equilibrated type 3 chondrites from Antarctica (Figure 64*b*). Detailed studies of its chondrules and abundant translucent matrix are provided by Kimura et al. (1979), Ikeda and Takeda (1979), and Ikeda et al. (1981).

Yamato 75028.—This H3 chondrite contains solar-wind gases (Takaoka et al., 1981) and is only the second chondrite regolith breccia found in Antarctica. Petrologic descriptions of the H3 matrix and more equilibrated clasts are given by Takeda et al. (1979), Ohta and Takeda (1982), and Miyamoto et al. (1982).

Petrologic Subtypes

Type 3 ordinary chondrites have recently been subdivided according to the degree of metamorphism that they have experienced (Sears et al., 1980; Huss et al., 1981). The decimal subdivision into types 3.0 to 3.9, which was proposed by Sears and coworkers, has been adopted by most people and is based on measurements of thermoluminescence sensitivity. This parameter appears to be the most useful for classifying type 3 ordinary chondrites. Sears et al. (1980, 1982) have shown that many properties of these chondrites are so well correlated that chondrites can be classified into subtypes by other parameters if thermoluminescence data are not available. The subtypes listed in Table 6 for 18 chondrites are from Sears et al. (1982) and Sears and Weeks (1983), except for ALHA79003, for which thermoluminescence data are not available. Sears and coworkers claim that thermoluminescence data permit subtype classification to a 1σ uncertainty

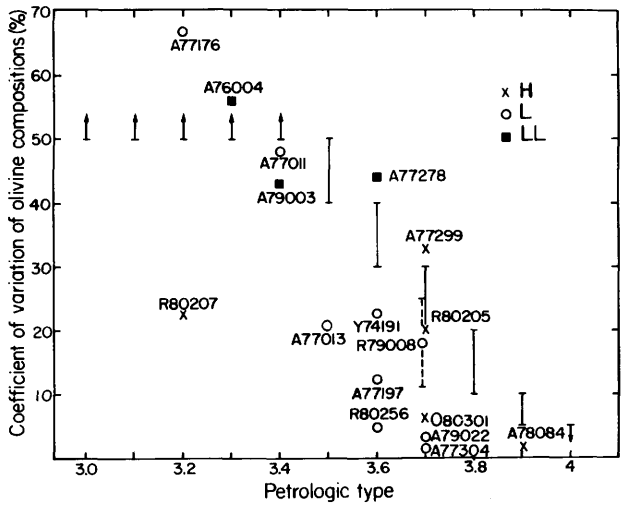

FIGURE 66.—Plot of coefficient of variation of olivine compositions (σFa/mean Fa) from Table 6 against petrologic subtype from Sears et al. (1982) and Sears and Weeks (1983) for 17 Antarctic type 3 and 4 ordinary chondrites. With the exception of RKPA80207 and RKPA80256, and ALHA79022 and ALHA77304, olivine coefficients are close to the ranges shown for the subtypes (Sears, et al., 1982). These four chondrites have much more homogeneous olivine than would be predicted from the thermoluminescence sensitivity data of Sears and coworkers. The dashed line for RKPA79008 is an estimate of the $\pm 2\sigma$ error in its coefficient of variation.

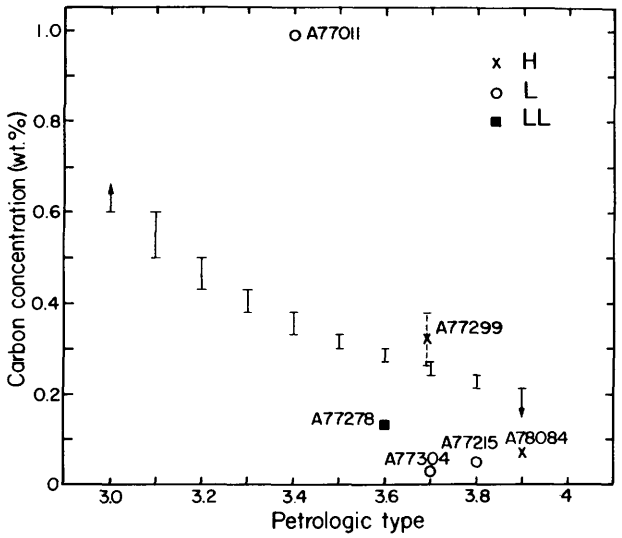

FIGURE 67.—Plot of bulk carbon concentration against subtype for six type 3 ordinary chondrites. The limited C data from Jarosewich (1980), Gibson and Andrawes (1980), and Grady et al. (1982) scatter widely from the ranges predicted by Sears et al. (1980). The dashed line shows the range of C concentrations in ALHA77299 obtained by these authors.

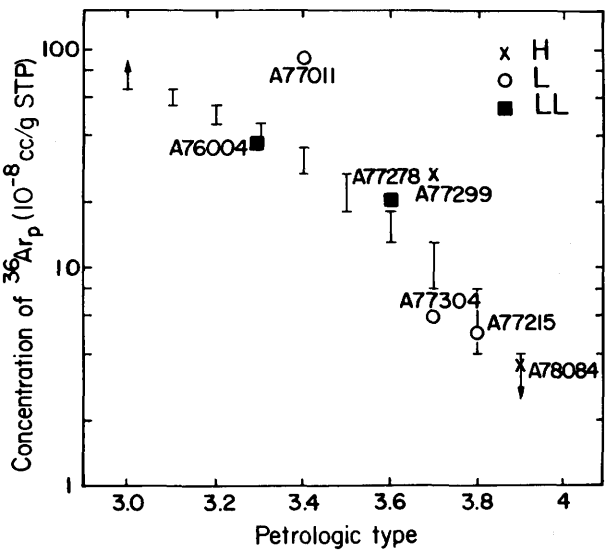

FIGURE 68.—Primordial ^{36}Ar concentrations in Antarctic type 3 ordinary chondrites decrease with increasing subtype and are close to the subtype ranges in Sears et al. (1980). Noble gas analyses are by Weber and Schultz (1980), Takaoka et al. (1981), Nautiyal et al. (1982), Kaneoka (1980), Moniot et al. (1981), and Weber et al. (1983).

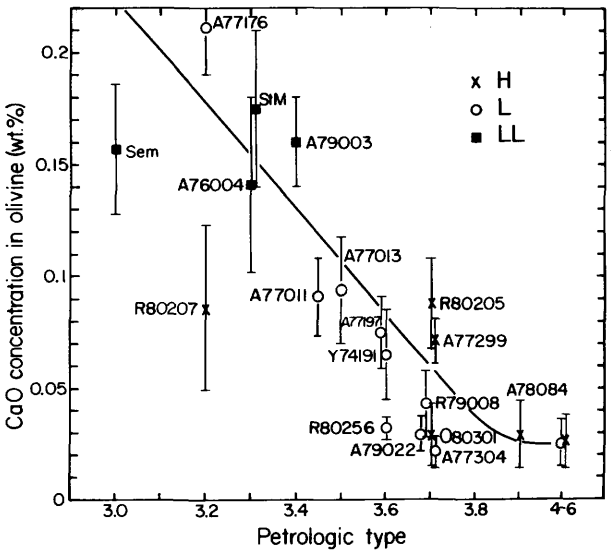

FIGURE 69.—Mean CaO concentrations of randomly chosen olivine grains are inversely correlated with subtype in type 3 ordinary chondrites. Data from Noonan et al. (1977) for St. Mary's Co. (StM); S.G. McKinley (private communication) for ALHA77011, ALHA77013, ALHA77176, and ALHA77197; remainder including Semarkona (Sem), this work. Vertical bars for individual meteorites are $\pm 2\sigma$ of mean values; ranges of types 4–6 from Busche (1975).

of ±0.1, except in cases of extensive weathering, which may lower the thermoluminescence sensitivity and the subtype. Shock may also affect the thermoluminescence sensitivity (Sears, 1980).

Figures 66–68 show data for Antarctic type 3 ordinary chondrites, illustrating the inverse correlations of petrologic subtype with coefficient of variation of olivine (σFa/mean Fa) and the concentration of C and primordial ^{36}Ar. Also marked are the ranges expected within subtypes from Sears et al. (1980, 1982). Unfortunately, bulk C and Ar concentrations have only been measured in about one-third of the Antarctic type 3 ordinary chondrites. However, in general, assignments based on olivine heterogeneity and C and $^{36}Ar_P$ concentrations are within 0.2 of the subtype derived from thermoluminescence sensitivity data.

Dodd (1969, 1981) finds that CaO concentrations in olivine vary according to petrologic type in ordinary chondrites: type 3 olivines have ≥0.1 wt.% CaO, type 4 have 0.06 wt.%, and type 5–6 0.02–0.05 wt.% CaO. Figure 69 shows that even though CaO concentrations in olivine may vary widely within a single type 3 chondrite, the mean value can also be used to classify type 3 chondrites according to subtype with an accuracy better than ±0.2. Chondrites that do not lie on the trends in Figures 66–69 are discussed below.

RKPA80207.—The subtype of 3.2 assigned by Sears and Weeks (1983) is not consistent with the degree of homogeneity of its olivine (Figure 66) and low-Ca pyroxene, which both have peaks in the H range (Figure 64*c*), and its low CaO concentration in olivine (Figure 69). These parameters and the absence of fine-grained, FeO-rich, opaque silicate matrix, or "Huss matrix" (Huss et al., 1981) indicate that type ~3.6 might be a better classification.

ALHA77011.—This L3 chondrite has higher concentrations of C and $^{36}Ar_P$ than expected for its subtype of 3.4–3.5 (McKinley et al., 1981; Sears et al., 1982). Excess C can be attributed to abundant graphite-magnetite.

ALHA79022, ALHA77304 and RKPA 80256.—These three L chondrites have olivines that are too homogeneous and low in CaO to be consistent with their thermoluminescence data. The latter suggest type 3.6 to 3.7 (Sears and Weeks, 1983), whereas olivine compositions suggest type 3.9 or 4.

Although the boundary between types 3 and 4 chondrites is quantitatively defined by Van Schmus and Wood (1967) in terms of olivine heterogeneity (PMD of wt.% Fe is 5), in practice, the distinction is difficult to make. As discussed in the description of OTTA80301, the presence of a few percent of very heterogeneous olivines in a chondrite that contains largely homogeneous olivine can drastically affect the PMD. Thus hundreds of analyses on several sections would be needed to establish the PMD with any confidence. Unfortunately, the thermoluminescence senstivities of type 4 chondrites are largely indistinguishable from type 3.8–3.9 chondrites (Sears et al., 1980). It appears that the boundary between type 3 and 4 chondrites must remain indistinct, like the boundary between type 4 and 5 chondrites.

Another difficulty with the classification scheme of Van Schmus and Wood (1967) concerns the classification of breccias. Regolith breccias, such as Dimmitt (Rubin et al., 1983) and ALHA77215, are defined as type 3 chondrites because their matrices have small amounts of heterogeneous silicates. It seems worthwhile to distinguish breccias, regolith and otherwise, in classification schemes by adding suffixes like those in Table 6.

Some of the above problems in classifying type 3 chondrites according to their subtype may be due to heterogeneities and the presence of equilibrated clasts. Such clasts have been identified in the regolith breccias, ALHA77215 (Score, 1980) and Yamato 75028 (Ohta and Takeda, 1982). During the course of this study of type 3 chondrite thin sections, only one equilibrated clast was identified, an H4 clast in ALHA77299 (Figure 70). However, this clast was found accidentally as a result of random probe analyses of its silicates, and was not prominent in the thin section. King et al. (1980), Score, Schwarz, et al. (1982), and Score, King, et al. (1982) mention clasts in their descriptions of many of the type 3

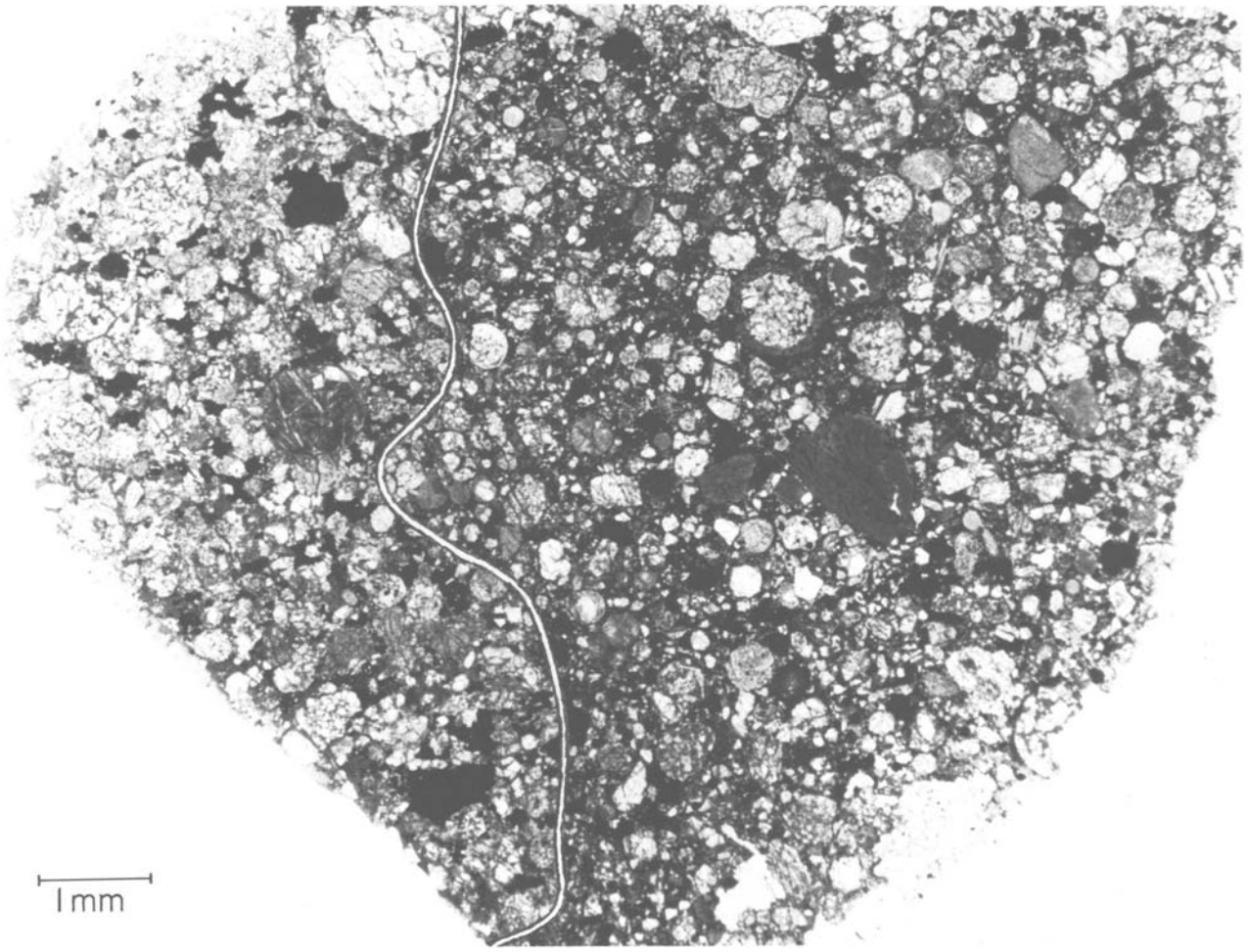

FIGURE 70.—Thin section of ALHA77299 (H3). Line marks approximate boundary between H4 clast on left and H3.7 matrix on right. Clast contains olivine with $Fa_{18.4\pm0.2}$ (1σ of analyses) and 0.03 wt.% CaO, and low-Ca pyroxene with $Fs_{16.1\pm0.4}$. The matrix contains some chondrules like those in the clast, some with equilibrated olivine and unequilibrated low-Ca pyroxene, and others with unequilibrated olivines and pyroxenes (see Figure 71*a*).

chondrites, e.g., inclusions of various colors up to 7 mm in size are present on the surface of ALHA79022. Unfortunately, it is not known whether these are chondritic clasts; some might be large irregular chondrules.

Brecciation and Metamorphism

Dodd et al. (1967) and Dodd (1969) argue convincingly that mineralogic differences among type 3 chondrites are the result of metamorphism. Olivine homogeneity is correlated with the degree of integration of chondrules and matrix, and the glass abundance in chondrules. Similarly, Huss et al. (1981) find that olivine homogeneity is also correlated with the proportion of opaque matrix and its Fe/(Fe+Mg) ratio. They also attribute most of these mineralogic variations in type 3 chondrites to mild metamorphism of the whole rocks.

By contrast, Dodd (1971, 1974) found in Sharps (H3.4) and Hallingeberg (L~3.3) a significant proportion of chondrules with mineralogic features that he attributes to metamorphism *before* the rocks were lithified. These chondrules

are relatively homogeneous in composition, have lower CaO concentrations in olivines, and are commonly zoned with rimward increases in FeO concentration in olivine, with or without concurrent decreases in CaO.

Scott, Taylor, and Keil (1982) studied three moderately metamorphosed type 3 ordinary chondrites, Ngawi (LL3.6), ALHA77278 (LL3.6), and Bremervörde (H3.7), and found in each a significant proportion of chondrules with olivine homogeneity and CaO concentrations appropriate to type 4 chondrites. Because metallic Fe,Ni grains in these three chondrites had cooled at very diverse rates, they argue that chondrules and metal grains were metamorphosed at various depths inside the parent bodies before the three chondrites were lithified.

To check whether any other Antarctic type 3 chondrites are breccias of unequilibrated and equilibrated material, olivine and low-Ca pyroxene grains were analyzed in over 100 chondrules in six chondrites. Figures 71 and 72 show the mean and 1σ ranges of analyses for CaO and fayalite concentrations in 4–10 olivine grains in each chondrule. Yamato 74191 (L3.6), ALHA 77299 (H3.7), RKPA80205 (H3.7) and RKPA 79008 (L3.7) all contain a significant proportion of chondrules that have olivine and low-Ca pyroxene compositions like those in type 4 chondrites (Figure 71). Unequilibrated chondrules have olivines with fayalite ranges and mean CaO concentrations that are generally 5–20 and 2–6 times larger, respectively, than olivines in equilibrated chondrules.

In two of these chondrites, ALHA77299 and RKPA79008, the presence or absence of chondrule rims composed of opaque Huss matrix (Huss et al., 1981) is related to olivine heterogeneity in the chondrules. Most of the unequilibrated chondrules and none of the equilibrated chondrules in these two chondrites have partial rims of opaque Huss matrix (Figure 71*a*, *b*). In Yamato 74191 and RKPA80205, none of the analyzed chondrules have rims of opaque matrix. Yamato 74191 has abundant matrix, but it is all translucent and in parts recrystallized, and it is often difficult to decide which chondrule, if any, is rimmed where matrix material separates adjacent chondrules.

Figure 72*a* shows analyses of olivine in 15 chondrules from ALHA76004 (LL3.3). None of the chondrules have mean olivine compositions appropriate to equilibrated LL chondrites ($Fa_{27.5}$ to $Fa_{30.5}$). All are heterogeneous and have mean CaO concentrations of 0.05–0.3 wt.%, like the unequilibrated chondrules in Figure 71. By contrast, Figure 72*b* shows analyses for 16 chondrules in RKPA80256, which has more equilibrated olivines (Figure 65*c*) than the chondrites described above. Only two chondrules have mean olivine compositions outside the L4–6 range. For comparison, analyses of chondrules in Richardton (H5) and Bjurböle (L4) are shown in Figure 72*c*. Richardton chondrules contain olivine that is more homogeneous and has lower CaO concentrations than Bjurböle chondrules. Both sets of chondrules are more equilibrated than those in RKPA80256.

It might be argued that olivine in some of the chondrules plotted in Figure 71 preserved its heterogeneity and high CaO concentrations from *in situ* equilibration with the matrix or other chondrules because of large crystal or chondrule sizes. However, the unequilibrated chondrules are not on average larger or coarser grained than the equilibrated chondrules. Figure 73 shows photomicrographs of unequilibrated and equilibrated porphyritic-olivine chondrules in each of the three chondrites shown in Figure 71. In two cases the equilibrated chondrule is larger and has larger olivine phenocrysts than the unequilibrated chondrule. In the other case (Figure 73*a*, *b*), chondrule and phenocryst sizes are very similar.

Another possible barrier to equilibration between olivines is the presence of silicates or other phases that have low diffusion rates for Fe and Mg. For example, olivines poikilitically enclosed by low-Ca pyroxene might be expected to lag behind other olivines during metamorphic equilibration. However, none of the analyzed olivines in the unequilibrated chondrules plotted in Figures 71 and 72 are poikilitically enclosed by pyroxene or any other mineral. There do not

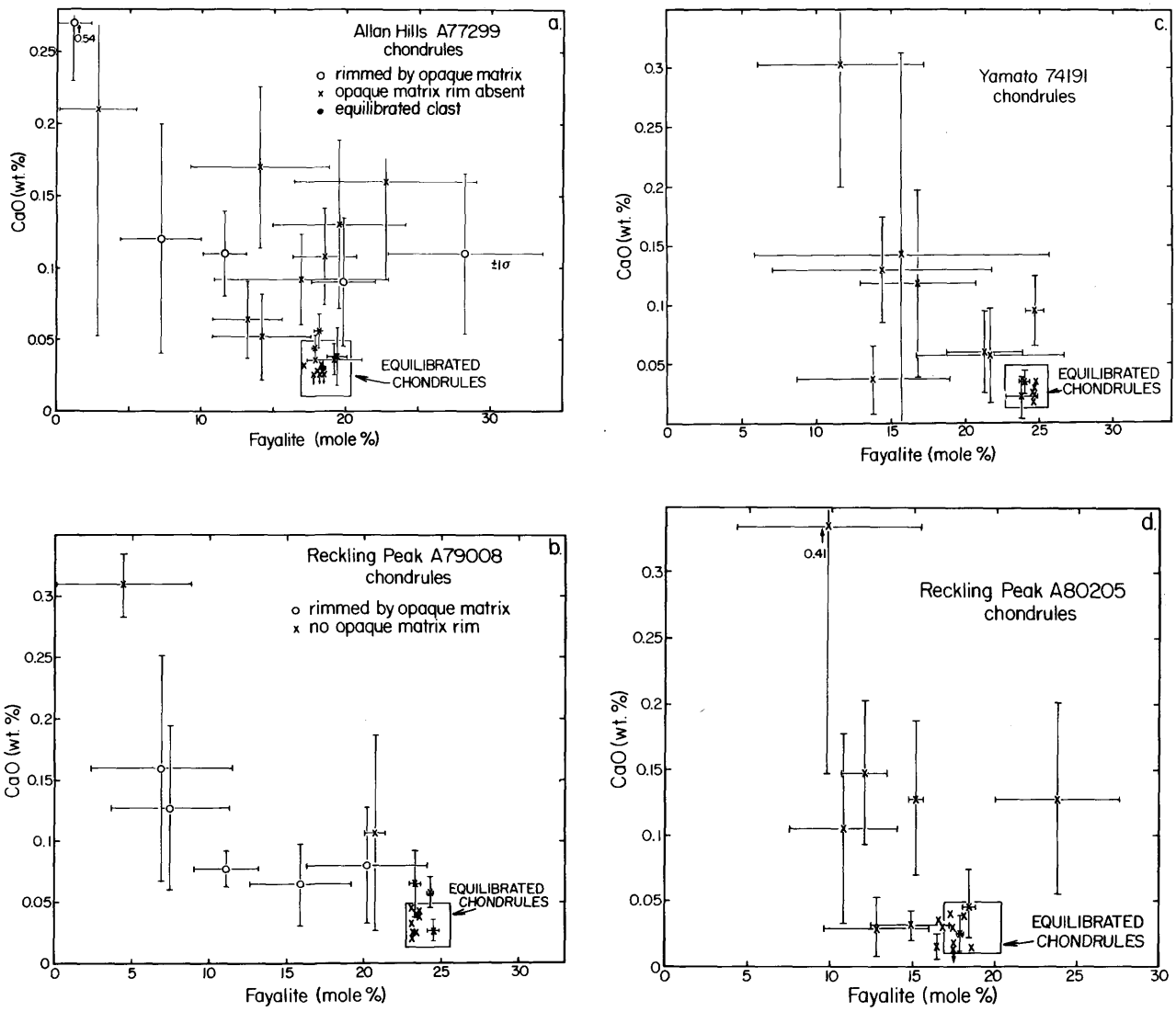

FIGURE 71.—Plots of mean CaO concentration in olivine against mean fayalite concentration for 75 porphyritic-olivine and porphyritic-olivine-pyroxene chondrules in four Antarctic type 3 ordinary chondrites. Bars show $\pm 1\sigma$ values for 4–10 analyses in each chondrule; 1σ values that are not plotted are comparable to the smallest shown. In all four chondrites there are unequilibrated chondrules containing olivine with variable Fa and CaO concentrations and >0.05% CaO, and chondrules with uniform Fa and CaO concentrations and <0.05% CaO in olivine. Chondrules were metamorphosed to different extents before final lithification into chondrites. The boxes showing the compositions of equilibrated chondrules are defined by ranges in type 4–6 H and L chondrites (Gomes and Keil, 1980; Busche, 1975).

appear to be any systematic differences in the mineral textures of unequilibrated and equilibrated chondrules except perhaps in their mesostases, which are generally, but not always, more crystalline in the latter.

The most plausible explanation for the juxtaposition of equilibrated and unequilibrated chondrules in many of the Antarctic type 3.6 to 4 chondrites is that equilibrated chondrules were metamorphosed prior to lithification of the chon-

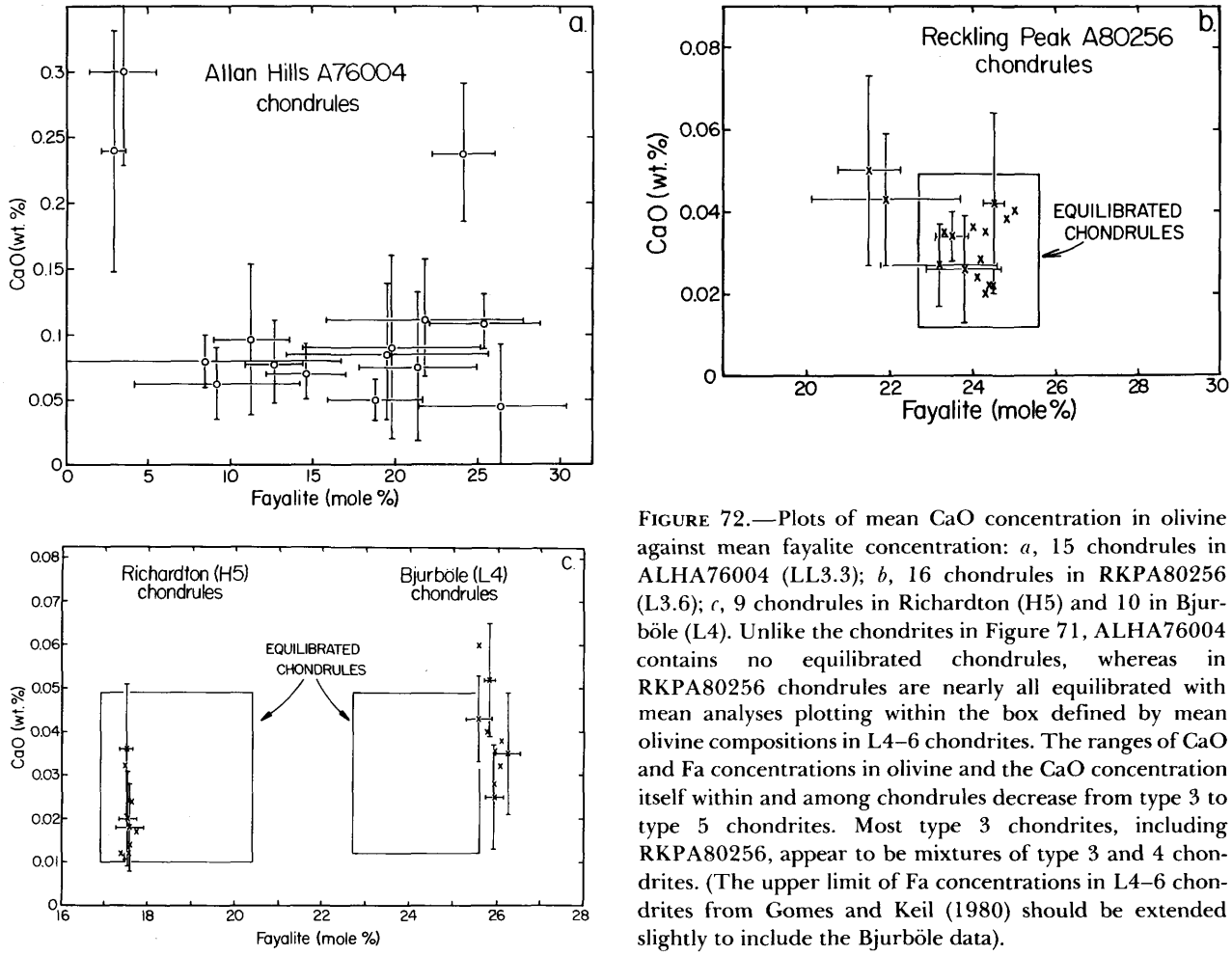

FIGURE 72.—Plots of mean CaO concentration in olivine against mean fayalite concentration: *a*, 15 chondrules in ALHA76004 (LL3.3); *b*, 16 chondrules in RKPA80256 (L3.6); *c*, 9 chondrules in Richardton (H5) and 10 in Bjurböle (L4). Unlike the chondrites in Figure 71, ALHA76004 contains no equilibrated chondrules, whereas in RKPA80256 chondrules are nearly all equilibrated with mean analyses plotting within the box defined by mean olivine compositions in L4–6 chondrites. The ranges of CaO and Fa concentrations in olivine and the CaO concentration itself within and among chondrules decrease from type 3 to type 5 chondrites. Most type 3 chondrites, including RKPA80256, appear to be mixtures of type 3 and 4 chondrites. (The upper limit of Fa concentrations in L4–6 chondrites from Gomes and Keil (1980) should be extended slightly to include the Bjurböle data).

drites. These chondrites are, therefore, breccias composed of materials metamorphosed in diverse locations. The argument is strongest for the chondrites shown in Figure 71. But even for RKPA80256 (Figure 72*b*), it seems probable that some or all of the equilibration between chondrules and matrix occurred before compaction of the chondrite. The two chondrules plotting outside the equilibrated chondrule box in Figure 72*b* are smaller and have smaller grain sizes than many of the equilibrated chondrules. Thus, much of the material in this chondrite may have been metamorphosed to type 4 levels prior to final lithification. However, metamorphism to type 3.6–3.8 levels after compaction cannot be excluded.

Chondrules in RKPA80207 and OTTA 80301, in which olivines are largely equilibrated (Figures 64*c*, 65*d*), were not analyzed in such detail. However, in each chondrite a porphyritic-olivine chondrule with heterogeneous olivine (Fa_{13} to Fa_{19} and Fa_{12} to Fa_{15}, respectively) with appreciable CaO concentrations (0.03–0.21 wt.%) was discovered. Since these chondrules are not especially large or coarse-grained, it is concluded that these two chondrites are also breccias of previously metamorphosed materials.

Figure 64 shows that the proportion of equilibrated chondrules in each of the four chondrites shown in Figure 71 varies considerably. Furthermore, the nature of the equilibrated chondrules in these four chondrites also varies. In

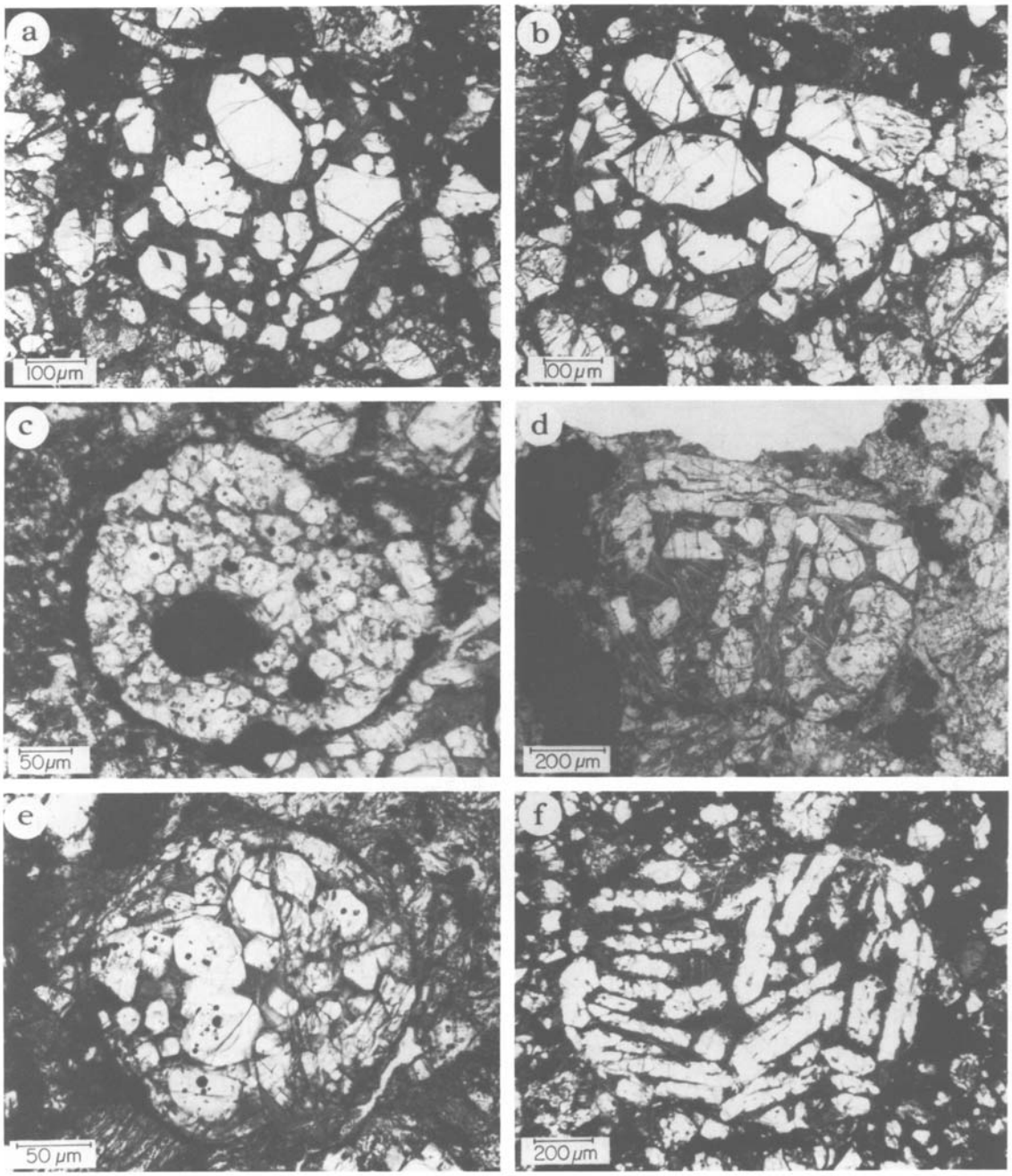

FIGURE 73.—Photomicrographs of six porphyritic-olivine chondrules in type 3.7 ordinary chondrites in transmitted light: *a* and *b*, ALHA77299; *c* and *d*, RKPA79008; *e* and *f*, RKPA80205. Olivine in the three chondrules on the left is heterogeneous (*a*, Fa_{10} to Fa_{20}; *c*, Fa_4 to Fa_{15}; *e*, Fa_{10} to Fa_{14}) and contains high CaO concentrations (0.03–0.31 wt.% CaO), whereas olivine in the three chondrules on the right is more homogeneous (Fa_{18} to Fa_{20} in *b* and *f*, Fa_{23} in *d*) with low CaO concentrations (0.01–0.06 wt.%). Data for these and other chondrules are plotted in Figure 71. Some of the unequilibrated chondrules like *c* have rims of fine-grained, FeO-rich, silicate material ("Huss matrix"), but none of the equilibrated chondrules have such rims. These chondrites and many other type 3 ordinary chondrites are breccias of materials with diverse metamorphic histories.

ALHA77299, many of the equilibrated chondrules have low-Ca pyroxene with compositions appropriate to H4-6 chondrites (Fs_{16} to Fa_{18}). Their presence accounts for the peak at Fs_{16} to Fs_{18} in the histogram of randomly chosen pyroxene grains (Figure 64*d*). For Yamato 74191, however, the low-Ca pyroxene histogram shows no such peak in the equilibrated L range (Fs_{19} to Fs_{23}), and the equilibrated chondrules lack pyroxenes with this composition. In fact, equilibrated chondrules in ALHA77299 seem to be more equilibrated than those in some types 3 and 4 chondrites shown in Figure 65, which overall have much more homogeneous olivines. ALHA77304 and RKPA80256, for example, lack equilibrated low-Ca pyroxenes even though their olivines, in general, appear to be more equilibrated than those of ALHA77299. Thus, various degrees of mixing between materials that have been metamorphosed to various extents can account for the strange lack of coherence between the compositions of olivine and low-Ca pyroxene in the histograms shown in Figures 64 and 65.

Virtually all of the type 3 ordinary chondrites in which mineral compositions have been studied in individual chondrules appear to contain chondrules with diverse metamorphic histories. These include Sharps and Hallingeberg (Dodd, 1971, 1974), Mezö-Madaras (Van Schmus, 1967), Ngawi, ALHA77278, and Bremervörde studied by Scott, Taylor, and Keil (1982) and the seven Allan Hills chondrites discussed above. Van Schmus (1969) argues that components in C3O chondrites also experienced metamorphism prior to compaction of the meteorites. If all type 3 chondrites are mixtures of material with different metamorphic histories, why can they be considered to a good approximation as a sequence of rocks that were metamorphosed to various degrees *after* lithification? Why are their chemical and textural properties that are controlled by metamorphism so well correlated?

Presumably, the answer to these questions is that, in general, the materials mixed do not have very diverse metamorphic histories. Ngawi seems to have the most extreme components; unequilibrated chondrules rimmed with abundant opaque matrix and equilibrated chondrules with homogenous olivine and low-Ca pyroxene (Scott, Taylor, and Keil, 1982). However, in other type 3 chondrites, the range of metamorphic histories represented is much smaller, or else the proportion of material with an unusual thermal history is very small. Brecciation does explain why the properties of type 3 ordinary and carbonaceous chondrites are not better correlated. Ngawi, for example, would be classified as a type 3.3 from the composition of its opaque matrix, but type 3.7 from its bulk C concentration (Sears et al., 1982). Some "measures of metamorphism" are controlled solely by the properties of the least unequilibrated chondrules, whereas others are controlled more by the proportion or nature of the most equilibrated chondrules. Bulk thermoluminescence sensitivity, which varies by a factor of 10^4 in type 3 chondrites, is very sensitive to the amount of equilibrated (type 4) material. Variable degrees of metamorphism may be responsible for some of the spread in the TL sensitivities of individual chondrules in Dhajala found by Sparks et al. (1983).

Some of the results in this paper might be used to argue against the thesis that metamorphism caused equilibration and recrystallization. Kurat (1969) and Fredriksson et al. (1975) suggest that uniform olivine and pyroxene compositions are a result of crystallization, and not metamorphism. However, like Dodd et al. (1967), Huss et al. (1981), and most other workers, I believe that all ordinary chondrites were formed by metamorphism (and brecciation) of materials very similar to the most primitive type 3 ordinary chondrites. Although Fredriksson, Kurat, and coworkers are correct in arguing that constant olivine compositions were not established in situ in these breccias, there is very strong evidence that metamorphism in precursor rocks *was* responsible (Dodd, 1969). Type 3 chondrites contain suites of chondrules that have virtually identical textures (except in their mesostases and rims) but vary widely in silicate heterogeneity. Chondrules may contain heterogeneous olivine and low-Ca pyroxene, homogeneous olivine and

heterogeneous pyroxene or olivine and low-Ca pyroxene that are entirely homogenous. This is consistent with the much higher cation diffusion rates in olivine compared to those in pyroxene; Jones (1983) estimates that olivine diffusion rates are 10^3 times higher.

The presence of some proportion of equilibrated chondrules in many type 3.5–4 chondrites means that it is possible to classify chondrites on the basis of the olivine composition in these chondrules, even when much of the olivine is heterogeneous. Although Dodd (1968) believed he had identified three equilibrated LL chondrules in the H chondrite, Sharps, no such aberrant chondrules were encountered in this study. Mixing of material from different ordinary chondrite groups seems to be very limited, even on parent-body surfaces (Keil, 1982; Rubin et al., 1983).

Of the seven Antarctic type 3 chondrites that have been identified above as breccias, only one, ALHA77299, is known to contain chondritic clasts. Brecciation in type 4–6 chondrites is easier to identify than in type 3 chondrites as more metamorphosed materials are generally better lithified and thus form clasts rather than chondrules when broken. 'Metamorphosed' chondrites that contain a small fraction of minerals with aberrant compositions or textures, e.g., Bhola (Noonan et al., 1978) and Pulsora (Frederiksson et al., 1975), are generally recognizable as breccias of previously metamorphosed material. However, all others, e.g., Morro do Rocio (Wlotzka and Fredriksson, 1980), must be breccias also, unless the aberrant minerals have been isolated from diffusive equilibration by barriers such as large grain size.

Summary

Four carbonaceous type 3 chondrites from Antarctica are known: one C3V, RKPA80241; two C3O, ALHA77003 and 77029, and a unique C3, ALHA77307. Yamato 6903 may be a C4V. ALHA80133 is an L3 chondrite paired with ALHA77011, not a C3V.

Seventeen different ordinary type 3 chondrites from Antarctica are recognized. ALHA77304 is reclassified from LL3 to L4, ALHA78084 from H3 to H4, and RPKA80207 from L3 to H3. Analyses of sections of ALHA79022, OTTA 80301, and RPKA80256 suggest that they are type 4 meteorites, but because of the difficulty of determining PMD olivine when a small percentage of chondrules are heterogeneous, they have not been reclassified from type 3 to type 4. ALHA77299 (H3) contains an H4 clast but is not rich in solar-wind noble gases (Weber et al., 1983). Two type 3 chondrites are regolith breccias, ALHA77215 and Yamato 75028.

In general, silicate analyses are consistent with the subtype classification from thermoluminescence sensitivity data by Sears and coworkers. However, RKPA80207 appears to be a type ~3.6 not a 3.2. ALHA79022, ALHA77304 and RKPA80256 have olivine compositions indicative of type 3.9 or 4, rather than 3.6 to 3.7, as Sears and Weeks (1983) suggest.

The mean concentration of CaO in olivine is another parameter like olivine heterogeneity that is inversely correlated with subtype, decreasing from 0.15 to 0.2 wt.% for type 3.0–3.3 to ≤0.05 wt.% for type 3.7–4.

Seven type 3.5–4 ordinary chondrites contain equilibrated chondrules with CaO and FeO concentrations in their olivines like those of type 4 chondrites, even though some of their chondrules have heterogeneous olivines like those in type 3.0–3.5 chondrites. Metamorphic equilibration must have occurred before lithification of the chondrites. Probably all type 3 chondrites are breccias composed of chondrules with diverse metamorphic histories.

Literature Cited

Biswas, S., H.T. Ngo, and M.E. Lipschutz
1980. Trace Element Contents of Selected Antarctic Meteorites, I: Weathering Effects and ALH A77005, A77257, A77278 and A77299. *Zeitschrift für Naturforschung*, 35a:191–196.

Biswas, S., T.M. Walsh, H.T. Ngo, and M.E. Lipschutz
1981. Trace Element Contents of Selected Antarctic

Meteorites—II: Comparison with Non-Antarctic Specimens. *Memoirs of the National Institute of Polar Research* (Japan), special issue, 20:221–228.

Busche, F.D.
1975. Major and Minor Element Contents of Coexisting Olivine, Orthopyroxene, and Clinopyroxene in Ordinary Chondritic Meteoritics. 75 pages. Doctoral dissertation, University of New Mexico, Albuquerque.

Clayton, R.N., T.K. Mayeda, and N. Onuma
1979. Oxygen Isotopic Compositions of Some Antarctic Meteorites. In *Lunar and Planetary Science X,* pages 221–223. Houston: Lunar and Planetary Institute.

Dodd, R.T.
1968. Recrystallized Chondrules in the Sharps (H3) Chondrite. *Geochimica et Cosmochimica Acta,* 32: 1111–1120.
1969. Metamorphism of the Ordinary Chondrites: A Review. *Geochimica et Cosmochimica Acta,* 33:161–203.
1971. The Petrology of Chondrules in the Sharps Meteorite. *Contributions to Mineralogy and Petrology,* 31:201–227.
1974. The Petrology of Chondrules in the Hallingeberg Meteorite. *Contributions to Mineralogy and Petrology,* 47:97–112.
1981. *Meteorites, A Petrologic-Chemical Synthesis.* 368 pages. England: Cambridge University Press.

Dodd, R.T., W.R. Van Schmus, and D.M. Koffman
1967. A Survey of the Unequilibrated Ordinary Chondrites. *Geochimica et Cosmochimica Acta,* 31:921–951.

Evans, J.C., J.H. Reeves, and L.A. Rancitelli
1982. Aluminum-26: Survey of Victoria Land Meteorites. *In* U.B. Marvin and B. Mason, editors, Catalog of Meteorites from Victoria Land, Antarctica, 1978–1980. *Smithsonian Contributions to the Earth Sciences,* 24:70–74.

Fodor, R.V., and K. Keil
1976. Carbonaceous and Non-Carbonaceous Lithic Fragments in the Plainview, Texas, Chondrite: Origin and History. *Geochimica et Cosmochimica Acta,* 40:177–189.

Fredriksson, K., A. Dube, E. Jarosewich, J.A. Nelen, and A.F. Noonan
1975. The Pulsora Anomaly: A Case against Metamorphic Equilibration in Chondrites. *In* G.S. Switzer, editor, Mineral Sciences Investigations 1972–1973. *Smithsonian Contributions to the Earth Sciences,* 14:41–53.

Fujimaki, H., M. Matsu-ura, I. Sunagawa, and K. Aoki
1981. Chemical Compositions of Chondrules and Matrices in the ALH-77015 chondrite (L3). *Memoirs of the National Institute of Polar Research* (Japan), special issue, 20:161–174.

Gibson, E.K., Jr., and F.F. Andrawes
1980. The Antarctic Environment and Its Effect upon the Total Carbon and Sulfur Abundances in Recovered Meteorites. In *Proceedings of the Eleventh Lunar and Planetary Science Conference,* pages 1223–1234. New York: Pergamon Press.

Gomes, C.B., and K. Keil
1980. *Brazilian Stone Meteorites.* 162 pages. Albuquerque: University of New Mexico Press.

Goswami, J.N.
1981. Solar Flare Irradiation Records in Antarctic Meteorites. *Nature,* 293:124–125.

Grady, M.M., P.K. Swart, and C.T. Pillinger
1982. The Variable Carbon Isotopic Composition of Type 3 Ordinary Chondrites. *Journal of Geophysical Research,* 87(supplement):A289–A296.

Graham, A.L., editor
1980. Meteoritical Bulletin Number 57. *Meteoritics,* 15:93–103.

Haggerty, S.E., S.B. Simon, and J.M. Rhodes
1979. Antarctic Meteorites: Petrology and Chemistry of 77001 (L6), 77002 (L5) and 77299 (H3). In *Lunar and Planteary Science X,* pages 485–487. Houston: Lunar and Planetary Institute.

Huss, G.R., K. Keil, and G.J. Taylor
1981. The Matrices of Unequilibrated Ordinary Chondrites: Implications for the Origin and History of Chondrites. *Geochimica et Cosmochimica Acta,* 45:33–51.

Ikeda, Y.
1980. Petrology of Allan Hills-764 Chondrite (LL3). *Memoirs of the National Institute of Polar Research* (Japan), special issue, 17:50–82.

Ikeda, Y., M. Kimura, H. Mori, and H. Takeda
1981. Chemical Compositions of Matrices of Unequilibrated Ordinary Chondrites. *Memoirs of the National Institute of Polar Research* (Japan), special issue, 20:124–144.

Ikeda, Y., and H. Takeda
1979. Petrology of the Yamato-74191 Chondrite. *Memoirs of the National Institute of Polar Research* (Japan), special issue, 12:38–58.

Jarosewich, E.
1980. Appendix 2: Chemical Analyses of Some Allan Hills Meteorites. *In* U.B. Marvin and B. Mason, editors, Catalog of Antarctic Meteorites, 1977–1978. *Smithsonian Contributions to the Earth Sciences,* 23:48.

Jarosewich, E., and R.T. Dodd
1981. Chemical Variations among L-Group Chondrites, II: Chemical Distinctions between L3 and LL3 Chondrites. *Meteoritics,* 16:83–91.

Jones, J.H.
1983. Mesosiderites: (1) Reevaluation of Cooling Rates and (2) Experimental Results Bearing on the Origin of the Metal. In *Lunar and Planetary Science XIV*, pages 351–352. Houston: Lunar and Planetary Institute.

Kallemeyn, G.W., and J.T. Wasson
1981. The Compositional Classification of Chondrites—I: The Carbonaceous Chondrite Groups. *Geochimica et Cosmochimica Acta*, 45:1217–1230.
1982a. The Compositional Classification of Chondrites; III: Ungrouped Carbonaceous Chondrites. *Geochimica et Cosmochimica Acta*, 46:2217–2228.
1982b. Carbonaceous Chondrites from Antarctica. In *Lunar and Planetary Science XIII*, pages 373–374. Houston: Lunar and Planetary Institute.

Kaneoka, I.
1980. ^{40}Ar-^{39}Ar Ages of L and LL Chondrites from Allan Hills, Antarctica: ALHA77015, 77214 and 77304. *Memoirs of the National Institute of Polar Research* (Japan), special issue, 17:177–188.

Keil, K.
1982. Composition and Origin of Chondritic Breccias. *In* G.J. Taylor and L.L. Wilkening, Workshop on Lunar Breccias and Soils and Their Meteoritic Analogs. *LPI Technical Report*, 82-02:65–83. Houston: Lunar and Planetary Institute.

Kimura, M., K. Yagi, and K. Onuma
1979. Petrological Studies on Chondrules in Yamato-74 Meteorites. *Memoirs of the National Institute of Polar Research* (Japan), special issue, 12:114–133.

King, T.V.V., R. Score, E.M. Gabel, and B. Mason
1980. Meteorite Descriptions. *In* U.B. Marvin and B. Mason, editors, Catalog of Antarctic Meteorites, 1977–1978. *Smithsonian Contributions to the Earth Sciences*, 23:12–44.

Kurat, G.,
1969. The Formation of Chondrules and Chondrites and Some Observations on Chondrules from the Tieschitz Meteorite. *In* P.M. Millman, *Meteorite Research*, pages 185–190. Dordrecht, Holland: D. Reidel Publishing Company.

Mayeda, T.K., R.N. Clayton, and E.J. Olsen
1980. Oxygen Isotopic Anomalies in an Ordinary Chondrite. *Meteoritics*, 15:330–331.

McKinley, S.G., E.R.D. Scott, G.J. Taylor, and K. Keil
1981. A Unique Type 3 Ordinary Chondrite Containing Graphite-Magnetite Aggregates—Allan Hills A77011. In *Proceedings of the Twelfth Lunar and Planetary Science Conference*, pages 1039–1048. New York: Pergamon Press.

McSween, H.Y., Jr.
1977. Carbonaceous Chondrites of the Ornans Type: A Metamorphic Sequence. *Geochimica et Cosmochimica Acta*, 41:477–491.
1979. Are Carbonaceous Chondrites Primitive or Processed? A Review. *Reviews of Geophysics and Space Physics*, 17:1059–1078.

McSween, H.Y., Jr., and L.L. Wilkening
1980. A Note on the Allan Hills A77278 Unequilibrated Ordinary Chondrite. *Meteoritics*, 15:193–199.

Miyamoto, M., H. Takeda, and T. Ohta
1982. "Polymict Chondrite" as Inferred from a Polymict Eucrite Genesis. *Meteoritics*, 17:254.

Moniot, R.K., T.H. Kruse, W. Savin, T. Milazzo, G. Herzog, and R. Warasila
1981. Allan Hills 78084: ^{10}Be and Noble Gas Contents. *Meteoritics*, 16:361–362.

Moore, C.B., J.R. Cronin, S. Pizzarello, M.-S. Ma, and R.A. Schmitt
1981. New Analyses of Antarctic Carbonaceous Chondrites. *Memoirs of the National Institute of Polar Research* (Japan), special issue, 20:29–32.

Nagahara, H.
1981a. Petrology of Chondrules in ALH-77015 (L3) Chondrite. *Memoirs of the National Institute of Polar Research* (Japan), special issue, 20:145–160.
1981b. Evidence for Secondary Origin of Chondrules. *Nature*, 292:135–136.

Nagahara, H., and I. Kushiro
1982. Genetic Relation of Chondrules, Inclusions and Isolated Olivines in ALH-77307 CO3 Chondrite. In *Lunar and Planetary Science XIII*, pages 562–563. Houston: Lunar and Planetary Institute.

Nautiyal, C.M., J.T. Padia, M.N. Rao, T.R. Venkatesan, and J.N. Goswami
1982. Irradiation History of Antarctic Gas-Rich Meteorites. In *Lunar and Planetary Science XIII*, pages 578–579. Houston: Lunar and Planetary Institute.

Noonan, A.F., E. Jarosewich, and R.S. Clarke, Jr.
1977. The St. Mary's County, Maryland, Chondrite. *In* B. Mason, editor, Mineral Sciences Investigations 1974–1975. *Smithsonian Contributions to the Earth Sciences*, 19:96–103.

Noonan, A.F., R.S. Rajan, J. Nelen, and K. Fredriksson
1978. Petrologic and Isotopic Constraints on the Origin of the Bhola Chondrite. *In* Proceedings of the Fourth International Conference on Geochronology, Cosmochronology and Isotope Geology. *U.S. Geological Survey Open File Report*, 78-701:311–313.

Ohta, T., and H. Takeda
1982. H5 Clast and Unequilibrated Host in Yamato 75028 Chondrite Breccia. *In* G.J. Taylor and L.L. Wilkening, Workshop on Lunar Breccias and Soils and Their Meteoritic Analogs. *LPI Technical Report*, 80-02:102–104. Houston: Lunar and Planetary Institute.

Okada, A.
1975. Petrological Studies of the Yamato Meteorites, Part 1: Mineralogy of the Yamato Meteorites. *Memoirs of the National Institute of Polar Research* (Japan), special issue, 5:14–66.

Okada, A., K. Yagi, and M. Shima
1975. Petrological Studies of the Yamato Meteorites, Part 2: Petrology of the Yamato Meteorites. *Memoirs of the National Institute of Polar Research* (Japan), special issue, 5:67–82.

Olsen, E.J., A. Noonan, K. Fredriksson, E. Jarosewich, and G. Moreland
1978. Eleven New Meteorites from Antarctica, 1976–1977. *Meteoritics,* 13:209–225.

Reid, A.M.
1982. Overview of Antarctic Achondrites. *In* U.B. Marvin and B. Mason, editors, Catalog of Meteorites from Victoria Land, Antarctica, 1978–1980. *Smithsonian Contributions to the Earth Sciences,* 24:59–69.

Rhodes, J.M., and C.R. Fulton
1981. Chemistry of Some Antarctic Meteorites. In *Lunar and Planetary Science XII,* pages 880–882. Houston: Lunar and Planetary Institute.

Rubin, A.E., E.R.D. Scott, and K. Keil
1982. Microchondrule-bearing Clast in the Piancaldoli LL3 Meteorite: A New Kind of Type 3 Chondrite and Its Relevance to the History of Chondrules. *Geochimica et Cosmochimica Acta,* 46:1763–1776.

Rubin, A.E., E.R.D. Scott, G.J. Taylor, K. Keil, J.S.B. Allen, T.K. Mayeda, R.N. Clayton, and D.D. Bogard
1983. Nature of the H Chondrite Parent Body Regolith: Evidence from the Dimmitt Breccia. *Journal of Geophysical Research,* 88 (supplement):A741–A754.

Score, R.
1980. Allan Hills 77216: A Petrologic and Mineralogic Description. *Meteoritics,* 15:363.

Score, R., T.V.V. King, C.M. Schwarz, A.M. Reid, and B. Mason
1982. Descriptions of Stony Meteorites. *In* U.B. Marvin and B. Mason, editors, Catalog of Meteorites from Victoria Land, Antarctica, 1978–1980. *Smithsonian Contributions to the Earth Sciences,* 24:19–48.

Score, R., C.M. Schwarz. T.V.V. King, B. Mason, D.D. Bogard, and E.M. Gabel
1981. Antarctic Meteorite Descriptions 1976–1977–1978–1979. *Curatorial Branch Publication 54, JSC 17076,* 144 pages. Houston: Johnson Space Center.

Score, R., C.M. Schwarz, B. Mason, and D.D. Bogard
1982. Antarctic Meteorite Descriptions 1980. *Curatorial Branch Publication 60, JSC 18170,* 55 pages. Houston: Johnson Space Center.

Scott, E.R.D., A.E. Rubin, G.J. Taylor, and K. Keil
1981. New Kind of Type 3 Ordinary Chondrite with a Graphite-Magnetite Matrix. *Earth and Planetary Science Letters,* 56:19–31.

Scott, E.R.D., G.J. Taylor, and K. Keil
1982. Brecciated Type 3 Chondrites and Their Parent Bodies. *Meteoritics,* 17:278.

Scott, E.R.D., G.J. Taylor, and P. Maggiore
1982. A New LL3 Chondrite, Allan Hills A79003, and Observations on Matrices in Ordinary Chondrites. *Meteoritics,* 17:65–75.

Scott, E.R.D., G.J. Taylor, P. Maggiore, K. Keil, S.G. McKinley, and H.Y. McSween, Jr.
1981. Three CO3 Chondrites from Antarctica—Comparison of Carbonaceous and Ordinary Type 3 Chondrites. *Meteoritics,* 16:385.

Sears, D.W.
1980. Thermoluminescence of Meteorites: Relationships with Their K-Ar Age and Their Shock and Reheating History. *Icarus,* 44:190–206.

Sears, D.W., J.N. Grossman, and C.L. Melcher
1982. Chemical and Physical Studies of Type 3 Chondrites—I: Metamorphism Related Studies of Antarctic and Other Type 3 Ordinary Chondrites. *Geochimica et Cosmochimica Acta,* 46:2471–2481.

Sears, D.W., J.N. Grossman, C.L. Melcher, L.M. Ross, and A.A. Mills
1980. Measuring Metamorphic History of Unequilibrated Ordinary Chondrites. *Nature,* 287:791–795.

Sears, D.W.G., and K.S. Weeks
1983. Thermoluminescence Sensitivity of Sixteen Type 3 Ordinary Chondrites, In *Lunar and Planetary Science XIV,* pages 682–683. Houston: Lunar and Planetary Institute.

Shima, Makoto, and Masako Shima
1975. Cosmochemical Studies on the Yamato Meteorites: A Summary of Chemical Studies on Yamato (a), (b), (c), and (d) Meteorites. *Memoirs of the National Institute of Polar Research* (Japan), special issue, 5:9–13.

Sparks, M.H., P.M. McKimmey, and D.W.G. Sears
1983. The Thermoluminescence Carrier in the Dhajala Chondrite. *Journal of Geophysical Research,* 88(supplement):A773–A778.

Takahashi, H., M-J. Janssens, J.W. Morgan, and E. Anders
1978. Further Studies of Trace Elements in C3 Chondrites. *Geochimica et Cosmochimica Acta,* 42:97–106.

Takaoka, N., K. Saito, Y. Ohba, and K. Nagao
1981. Rare Gas Studies of Twenty-Four Antarctic Chondrites. *Memoirs of the National Institute of Polar Reseach* (Japan), special issue, 20:264–275.

Takeda, H., M.B. Drake, T. Ishii, H. Hamamura, and K. Yanai
1979. Some Unique Meteorites Found in Antarctica and Their Relation to Asteroids. *Memoirs of the National Institute of Polar Research* (Japan), special issue, 15:54–76.

Taylor, G.J., A. Okada, E.R.D. Scott, A.E. Rubin, G.R. Huss, and K. Keil
1981. The Occurrence and Implications of Carbide-Magnetite Assemblages in Unequilibrated Ordinary Chondrites. In *Lunar and Planetary Science XII,* pages 1076–1078. Houston: Lunar and Planetary Institute.

Van Schmus, W.R.
1967. Polymict Structure of the Mezö-Madaras Chondrite. *Geochimica et Cosmochimica Acta,* 31:2027–2042.
1969. Mineralogy, Petrology and Classification of Types 3 and 4 Carbonaceous Chondrites. *In* P.M. Millman, *Meteorite Research,* pages 480–491. Dordrecht, Holland: D. Reidel Publishing Company.

Van Schmus, W.R., and J.A. Wood
1967. A Chemical-Petrologic Classification for the Chondritic Meteorites. *Geochimica et Cosmochimica Acta,* 31:747–765.

Wasson, J.T.
1974. *Meteorites—Classification and Properties.* 316 pages. Heidelberg: Springer-Verlag.

Weber, H.W., O. Braun, L. Schultz, and F. Begemann
1983. The Noble Gas Record in Antarctic and Other Meteorites. *Zeitschrift für Naturforschung,* 38a:267–272.

Weber, H.W., and L. Schultz
1980. Noble Gases in Ten Stone Meteorites from Antarctica. *Zeitschrift für Naturforschung,* 35a:44–49.

Wlotzka, F., and K. Fredriksson
1980. Morro do Rocio, an Unequilibrated H5 Chondrite. *Meteoritics,* 15:387–388.

Yanai, K.
1979. *Catalog of Yamato Meteorites in the Collection of National Institute of Polar Research,* 188 pages. Tokyo: National Institute of Polar Research.

Yanai, K., M. Miyamoto, and H. Takeda
1978. A Classification for the Yamato-74 Chondrites Based on the Chemical Compositions of Their Olivines and Pyroxenes. *Memoirs of the National Institute of Polar Research* (Japan), special issue, 8:110–120.

A Meteorite from the Moon

Ursula B. Marvin

On 18 January 1982, John Schutt spotted a small meteorite with a frothy greenish tan fusion crust lying near the edge of the Middle Western Icefield of the Allan Hills region (Figure 74). Large white clasts lying in a dark matrix were clearly visible beneath patches of crust and on a broken surface. After two seasons of collecting Antarctic meteorites, Schutt, who had led the United States search party for the first half of that season, immediately recognized the specimen as unique. Laboratory studies have since shown that the specimen is a meteorite from the Moon; the first one ever found on Earth.

Schutt was not out that day primarily to search for meteorites. He was guiding a visitor, Ian Whillans of Ohio State University, on a reconnaissance trip to examine the regional configuration of the ice sheet. After a 31 km snowmobile ride over long stretches of rough snowdrifts they decided to turn back. A steady wind and blowing snow made visibility poor, so it was by sheerest chance that Schutt saw the plum-sized specimen as they cruised near the edge of the icefield.

Schutt photographed the meteorite in situ (Figure 75) and collected it by the customary sterile procedures. That evening the weather deteriorated so rapidly that further field work became impossible. The lunar rock was the final addition to that season's trove of 373 specimens.

Months later, at the NASA Johnson Space Center in Houston, Roberta Score unpackaged the meteorite in a nitrogen-filled processing cabinet (Frontispiece). She described it as an unusual looking sample with an abundance of angular gray to white clasts, from about 1 to 8 mm in size, set in a black matrix (Score, 1982). It weighed 31.4 grams and measured 3 × 2.5 × 3 centimeters. It was assigned the name Allan Hills 81005 (ALHA81005).

From a thin section, made at the Smithsonian Institution in Washington, Brian Mason classified the rock as an anorthositic breccia. He found the white clasts to consist mainly of Ca-rich plagioclase, making the meteorite much more feldspathic than the eucrites. Mason wrote in the *Antarctic Meteorite Newsletter* that "some of the clasts resemble the anorthositic clasts described from lunar rocks" (Mason, 1982).

News spread quickly of the Antarctic meteorite that looked like a lunar rock, but the story broke too late for sample requests to be submitted in time for the September 1982 meeting of the Meteorite Working Group. Unwilling to wait until the following April, the MWG issued a special *Newsletter* in November announcing the availability of samples for initial characterization. The intent was to obtain sufficient general information from thin sections and matrix chips to guide the formation of a multidisciplinary consortium to study individual clasts. The deadline for submitting sample requests was 1 December 1982. In order to give investigators an equal chance to report their findings, all were asked to delay public announcement of their results until the 14th annual meeting of the Lunar and Plan-

Ursula B. Marvin, Smithsonian Astrophysical Observatory, 60 Garden Street, Cambridge, Massachusetts 02138.

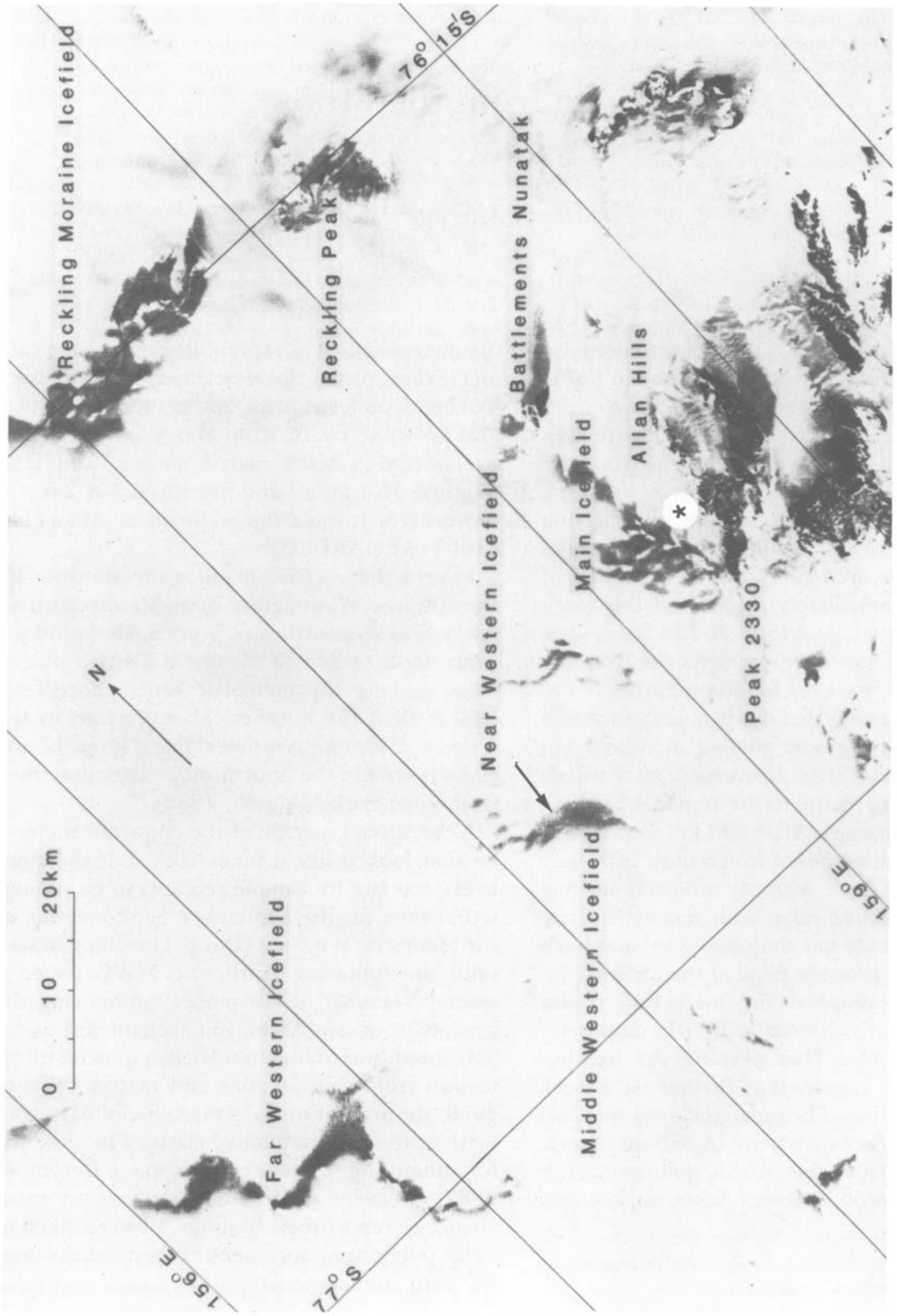

FIGURE 74—Satellite image (Near Infrared Band 7) of the mountains and icefields in the Allan Hills-Reckling Peak region of South Victoria Land. Darkest areas are bedrock; medium-gray patches are bare ice. The star indicates the site of the 1981–1982 campsite at the edge of the Allan Hills Main Icefield; the arrow shows the discovery site of ALHA81005 on the Middle Western Icefield.

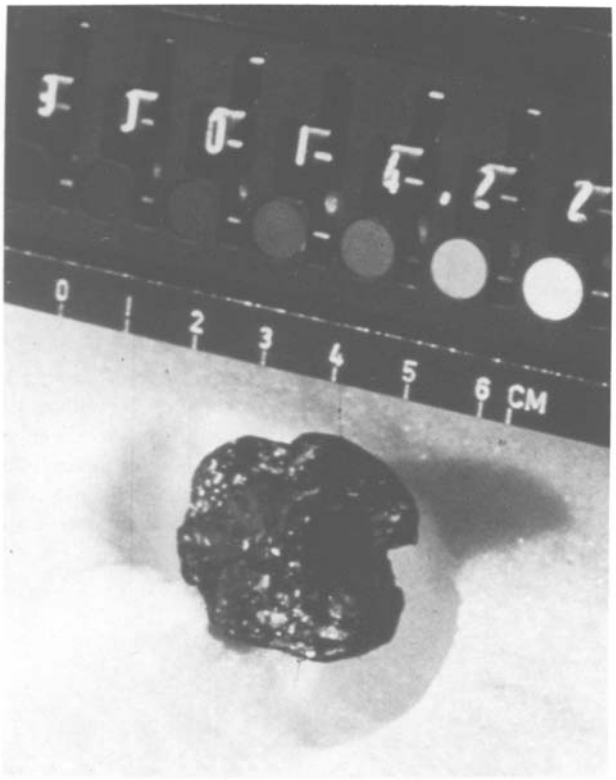

FIGURE 75—An in situ photograph of the meteorite ALHA81005 as it lay on the ice. It is a rounded individual with an angular notch where a piece was broken off. White clasts are visible beneath a thin, frothy fusion crust.

etary Science Conference to be held in Houston in March 1983.

On 4 December, the Meteorite Working Group held a special session at which three-fourths of the participants were conscripts substituting for regular members who had submitted proposals. Twenty-five requests were received and twenty-two were approved. The remaining three were postponed for integration into the consortium. The types of studies authorized for the initial round were electron microprobe analyses of thin sections (with five sections being shared by eight investigators), instrumental and radiochemical neutron activation analyses of bulk and matrix samples, measurements of reflectance spectra, ferromagnetic resonance, noble gas abundances, nuclear particle tracks, oxygen isotopes, and cosmogenic isotopes.

At the special session on Allan Hills 81005, held at the Houston Conference on St. Patrick's Day, a wholly unprecedented degree of unanimity prevailed. All participants agreed that the specimen probably came from the Moon; most said it positively came from the Moon; none said it did not come from the Moon.

The fragmental fabric of the breccia is illustrated in Figure 76, a photomosaic of thin section ALHA81005,22. A heterogeneous array of mineral and rock clasts and masses of devitrified glass are embedded in a dark brown, glassy matrix. The matrix, defined as material with a grain size less than 25 μm, occupies about 60%, and the clasts about 40% of the area. Some clasts show shock effects, such as crushing and partial optical randomization of crystals, but others, including several delicately twinned feldspars, are unshocked.

As first suggested by Mason, the white clasts do indeed resemble those of lunar highlands anorthositic rocks. Plagioclase (An_{94} to An_{98}) is the most abundant component in the clasts and glasses, including the dark brown matrix glass. Colorless, pale yellow, and light orange glass spherules are scattered throughout the breccia, and patches of highly vesicular, swirly glass, formed by the remelting of glass-bonded agglutinates, occur in the matrix (Figure 77). The spherules and reworked agglutinates identify the rock as a soil breccia.

The most common clasts are recrystallized breccias, melt rocks, and devitrified glasses, but the breccia also contains a few clasts of cataclastic ferroan anorthosites, anorthositic gabbros, and troctolites, some of which are probably pristine. The largest clast in thin section ALHA81005,22 is a cataclastic ferroan anorthositic gabbro (Figure 78A) consisting of 87% plagioclase (An_{96}–An_{98}) and 13% pigeonite ($En_{64}Fs_{34}Wo_2$) and ferroaugite ($En_{25}Fs_{32}Wo_{42}$). This rock clearly belongs to the well-established pristine ferroan anorthosites, but it is more Fe-rich than previously analyzed samples.

A different type of anorthositic gabbro consists of chains of pyroxenes and olivines lying in a matrix of granulitic plagioclase (Figure 78B). The plagioclase is An_{97}; the finely exsolved pyroxenes

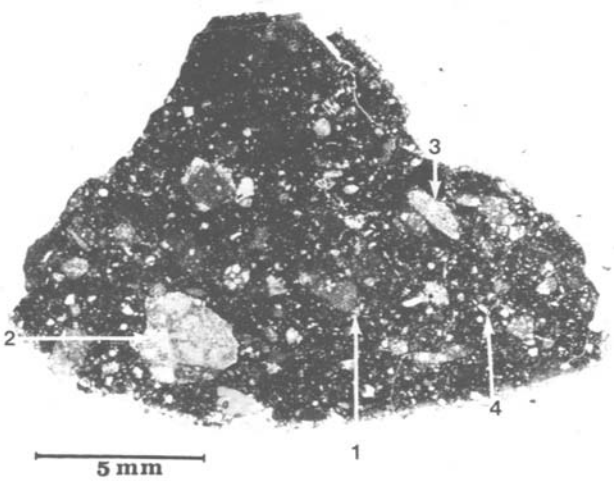

FIGURE 76.—A photomosaic of thin section ALHA81005,22 showing the heterogeneous array of clasts and glasses in the dark glassy matrix. Clasts 1–4 are shown at higher magnifications in Figures 77 and 78.

FIGURE 78.—Three types of lithic clasts in section ALHA81005,22. A, Cataclastic anorthositic gabbro in which the plagioclase is partially optically randomized by shock pressure (clast 2 in Figure 76). B, Anorthositic gabbro with a quasi-cumulate texture. Chains of olivines and pyroxenes lie amid granulitic plagioclase, but large clasts of twinned plagioclase are also present indicating that the rock is a recrystallized breccia (clast 3 in Figure 76). C, Clast consisting of a 430-μm plagioclase lath attached to a mass of black glass. The gray-patterned areas in the lath are patches of glass of the same composition as the plagioclase (clast 4 in Figure 76). (All three clasts photographed in transmitted light). D, Photomicrograph in reflected light of the black glass, showing five phases: rows of opaque crystallites of armalcolite and one larger crystallite of ulvöspinel on edge of glass (lower left), brighter and duller bands of glass, and two minute spherules of metallic Fe (bright dots amid crystallites in lower half of picture). This coarse clast may be a fragment of mare basalt.

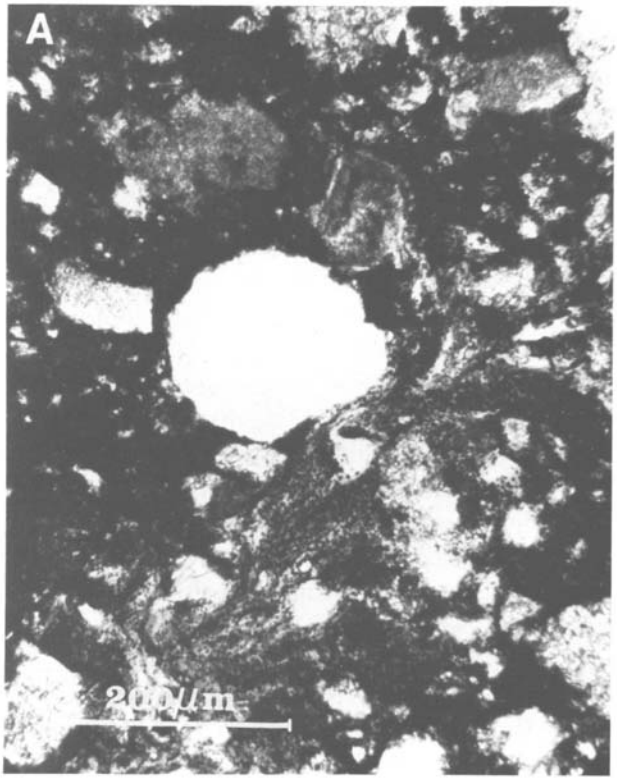

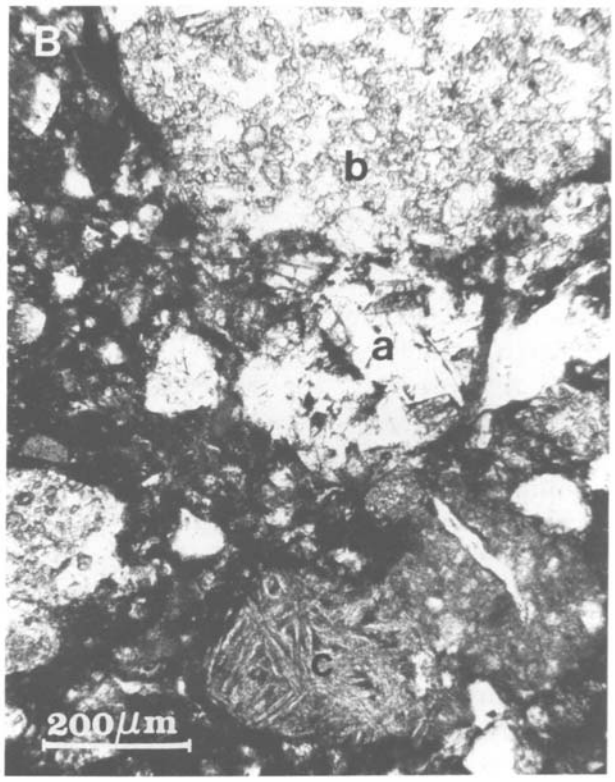

FIGURE 77.—Clasts and matrix textures in thin section ALHA81005,22. A, Lopsided spherule of colorless glass lies adjacent to a swirly mass of tawny-brown glass full of minute vesicles, which appear as black dots. The vesicular glass is a remelted glass-bonded agglutinate, a type of particle that is abundant in lunar soils. B, Small clast (a) of possible low-K mare basalt (Clast 1 in Figure 76) lies between a light-colored granulite (b) formed by the recrystallization of an impact breccia, and a rounded mass of light brown, devitrified glass (c). (Both photomicrographs taken in transmitted light).

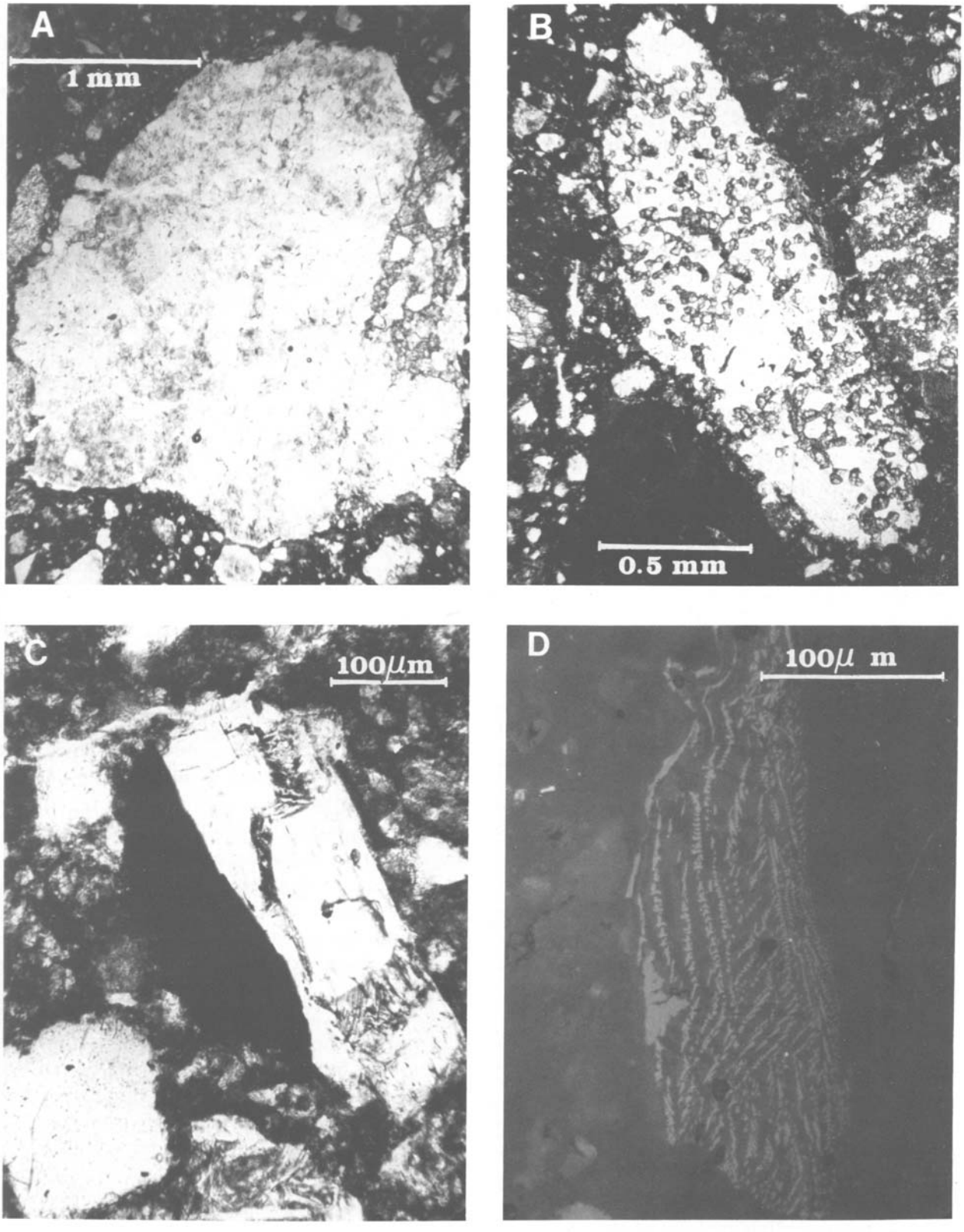
A
1 mm
B
0.5 mm
C
100μm
D
100μ m

are $En_{38-45}Fs_{30-44}Wo_{11-32}$; the olivine is Fo_{40}, by far the most iron-rich mafic mineral reported to date in ALHA81005. Three large crystals of twinned plagioclase (An_{97}) are also present, indicating that the clast is a recrystallized breccia despite the appearance of a cumulate texture.

Several clasts of mare basalts have been found mixed with the predominantly highlands materials in the breccia. Fragments of Very Low Titanium (VLT) mare basalt were discovered in thin sections by Tremaine and Drake (1983) and Ryder and Ostertag (1983). In section ALHA81005,22 a clast consisting of a single 430 μm lath of plagioclase (An_{97}) attached to a mass of black Ti-rich glass may be a fragment of high-titanium mare basalt (Figure 78C,D). The glass is studded with rows of opaque crystallites, chiefly armalcolite, $(Fe,Mg)Ti_2O_5$, and one larger crystallite of ulvöspinel ($FeTi_2O_4$). The black glass contains about 0.22 wt.% K_2O, more than twice the amount measured in the plagioclases of the breccia. The glass appears to be a sample of mesostasis from a medium-grained basalt (Marvin, 1983).

A small diabasic clast (Figure 77B) consisting of 86% bytownite ($An_{85-89}Ab_{10-14}Or_{0.8-1.1}$), augite, and glassy mesostases containing silica glass, K-feldspar, apatite, and ilmenite may represent a low-potassium mare basalt (Marvin, 1983).

A strong indication of lunar origin is provided by the ratios of manganese to iron oxides in the pyroxene minerals of the clasts. Systematic differences in FeO/MnO partitioning in rocks from different sources were first demonstrated by Laul and Schmitt (1973), and subsequent studies have established separate fields for lunar rocks and the various classes of achondritic meteorites. Values for the pyroxenes in ALHA81005 plot in the lunar field as shown in Figure 79.

The major-element composition of the bulk sample closely resembles highland materials from the Apollo 16 and Luna 20 missions. However, the contents of minor and trace elements, particularly potassium, rare earth elements, and phosphorus (KREEP) are markedly lower than those found in the highlands samples previously analyzed. Remote sensing analyses of the lunar surface, by orbiting spacecraft and ground-based telescopes, indicate that areas of KREEP-poor anorthositic crust occur along the far eastern limb of the Earth-facing side, and on the farside of the Moon. Some investigators (e.g., Pieters, 1983) are searching these regions for a youthful impact crater large enough to have been the source of ALHA81005. The site should lie within 100 km or so of mare surfaces of appropriate compositions to account for the basalt clasts that were present in the regolith.

Other lines of evidence for a lunar origin include the oxygen isotopic ratios that bear a distinctly lunar signature (Mayeda et al., 1983), the presence in the matrix of solar wind-implanted noble gases (He, Ne, Ar, Kr, and Xe) in concentrations and relative abundances similar to those in gas-rich lunar soils and breccias (Bogard and Johnson, 1983b), and the absence of galactic particle tracks in the mineral grains, consistent with a short flight time in space (Sutton and Crozaz, 1983). These and additional investigations are reported in a special issue of *Geophysical Research Letters* (1983) devoted to ALHA81005.

This sample was clearly spalled off the Moon into an Earth-crossing orbit from a site not visited by either the United States Apollo missions or the Soviet Union's Luna missions. Thus, that end-of-season snowmobile trip to the Middle Western Icefield of the Allan Hills region has been nicknamed "the Apollo 18 mission" (Korotev, Haskin, and Lindstrom, 1983).

Our examination of ALHA81005 has taught us, once again, that natural events frequently confound the results of all our calculations. Predictions from experimental impacts and computer modeling told us that the only material that could escape the Moon would come from deep below the target area of an impacting projectile and be shock-melted to glass or crushed and dispersed as glassy droplets. But, contrary to these predictions, ALHA81005 is not a rock derived from deep in the lunar crust; it is a welded surface soil, no more highly shocked and glassy than many a sample that the astronauts lifted off the lunar surface with tongs. A new

model is now being constructed (Melosh, 1983), which involves the spalling off of blocks of surface materials at low pressures in front of oblique impacts.

Most of the meteorites collected in the past are believed to have come from asteroids, with a few possibly derived from comets. During the past two centuries nearly 700 meteorite falls have been witnessed and some of the fireballs have been photographed. All of the well-documented trajectories show that the meteorites were following elliptical orbits that originated in the asteroid belt between Mars and Jupiter. Lunar ejecta must also fall on Earth whenever huge meteorites impact the Moon with sufficient energy to accelerate target materials above the lunar escape velocity of 2.4 km per second. Statistical studies have suggested that such impacts happen very infrequently, and it is likely that none has occurred in historic time. We now know, however, that such an event did occur sometime within the past few million years while the great ice sheet has covered Antarctica. Perhaps the fall occurred less than a million years ago. The first attempt to measure the terrestrial age (time since the fall to Earth) of ALHA81005 gave ambiguous results (Evans and Reeves, 1983). However, as shown by Nishiizumi (herein, p. 105), the oldest terrestrial ages yet measured on Antarctic meteorites are in the order of 700,000 years. If meteorite concentrations occur on older patches of ice they have not yet been discovered. We await with much interest age determinations on the other meteorites and, if possible, on ice itself at the Middle Western Icefield.

Systematic searches of the Middle Western Icefield have not yet been made, but that area appears promising not only because of the lunar meteorite but because eight specimens (including a rare enstatite achondrite) were discovered there during two brief helicopter visits in the 1978–1979 season. Present plans call for a camp to be set up nearby and a careful search made in the 1983–1984 season. Meanwhile, the discovery of ALHA81005 has raised many questions. Did this specimen fall on Earth as a single stone, or did it fall as one piece of a great mass of lunar

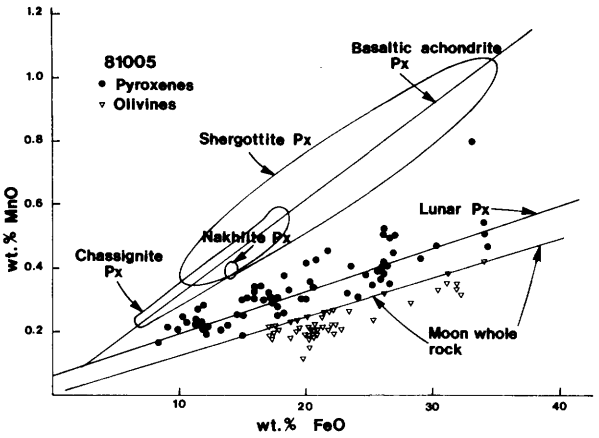

FIGURE 79.—The partitioning of FeO and MnO in lunar samples and achondritic meteorites. The black dots, which represent values measured in pyroxenes of ALHA81005, plot in the lunar field although some of them extend the previously determined range toward achondrite values. The pyroxene ratios plot on and above the lunar whole rock trendline while the olivine ratios (triangles) plot on and below it, thus demonstrating a lunar bulk composition. (The fields for achondrites are taken from Stolper et al., 1979).

debris that was scattered broadcast over our rotating planet? Or did ALHA81005 break off from a larger incoming mass that exploded in the atmosphere and showered fragments over Antarctica? The possibility that this specimen is a shower fragment will inspire the field party to search the area with high hopes of discovering additional pieces of this meteorite from the Moon.

Would we have recognized this unique meteorite as a lunar rock if we had never examined samples from the Moon? Perhaps not, if we had found it much more than a decade ago, because the anorthositic character of the lunar crust came to us as a complete surprise at the time of the Apollo 11 mission. Even then, however, one of the Surveyor modules had sent back analyses indicating a Ca-Al-rich type of crustal rock, and orbital missions have since produced compositional maps of much of the lunar surface. It seems likely that the anorthositic character of ALHA81005 and its marked chemical, mineralogical, and isotopic differences from the basaltic achondrites would have persuaded some scientists to propose a lunar origin for it.

The discovery of a lunar meteorite has given new credibility to the hypothesis, first proposed about five years ago, that the shergottites, a rare class of achondrites represented by nine specimens (two from Antarctica and seven from other continents) may have come from Mars. Originally, this hypothesis was based on isotopic age determinations, which showed that the shergottites crystallized only about 1.3×10^9 years ago. Age determinations on other meteorites show us that the asteroids were already cold and solid about 4.5×10^9 years ago, soon after the solar system formed. Even Earth's moon ceased flooding its basins with basaltic lava flows about 3.1×10^9 years ago. Only a larger body, such as Mars, would be well-insulated enough to retain heat and remain volcanically active to comparatively recent times. Mars has huge volcanic cones on its surface, and crater counts on the surrounding lava flows show them to be young in comparison to the ancient, more heavily cratered terranes. Can the shergottites be samples of these flows?

Recent measurements show that nitrogen, argon, krypton, and xenon trapped in glassy lenses in one of the Antarctic shergottites (EETA 79001) are similar in relative abundances and isotopic ratios to those of the gases in the Martian atmosphere, measured by the Viking Landers (Bogard and Johnson, 1983a; Becker and Pepin, 1983).

The case for Martian shergottites is still highly speculative. The escape velocity from Mars is about 5 km per second, an acceleration that seems prohibitive to many investigators. In the past, many have argued that we could not expect to find Martian rocks on Earth unless we also find samples from our closer neighbor, the Moon. That objection, at least, has now been removed.

Antarctica has proved to be a rich source of meteorites, which lie on certain patches of bare ice awaiting discovery. To journey to Antarctica is an elegant way to add to our collections of planetary samples while we await future missions into space. The discovery of a lunar sample on that windy January day in the Allan Hills has opened an awesome new potential and enhanced immeasurably the excitement of the Antarctic meteorite program.

This work was supported in part by NASA grant NAG 9-29.

Additional papers on this meteorite may be found in a special issue of *Geophysical Research Letters*, 10 (September, 1983).

Literature Cited

Becker, R.H., and R.O. Pepin
1983. Heavy Nitrogen in Glass from Antarctica Meteorite EETA79001 [Abstract]. *EOS*, 64:253.

Bogard, D.D., and P. Johnson
1983a. Martian Atmospheric Gases Trapped in the EETA79001 Shergottite? In *Lunar and Planetary Science XIV: Session on Meteorites from Earth's Moon*, pages 53–54. Houston: Lunar and Planetary Institute.
1983b. Trapped Solar Gases in the ALHA81005 Lunar (?) Meteorite. In *Lunar and Planetary Science XIV: Session on Meteorites from Earth's Moon*, pages 1–2. Houston: Lunar and Planetary Institute.

Evans, J.C., and J.H. Reeves
1983. Aluminum-26 Content of ALHA81005. In *Lunar and Planetary Science XIV: Session on Meteorites from Earth's Moon*, pages 6–7. Houston: Lunar and Planetary Institute.

Korotev, R.L., L.A. Haskin, M.M. Lindstrom
1983. Lunar Highlands Breccia 81005 (ALHA): So Apollo 18 Flew, but Where Did It Sample? In *Lunar and Planetary Science XIV: Session on Meteorites from Earth's Moon*, pages 12–13. Houston: Lunar and Planetary Institute.

Laul, J.C., and R. Schmitt
1973. Chemical Composition of Apollo 15, 16, and 17 Samples. In Proceedings of the Fourth Lunar Science Conference. *Geochimica et Cosmochemica Acta*, supplement 4, 2:1349–1367.

Marvin, Ursula B.
1983. The Discovery and Initial Characterization of Allan Hills 81005: The First Lunar Meteorite. *Geophysical Research Letters*, 10:775–778.

Mason, Brian
1982. In *Antarctic Meteorite Newsletter*, 5 (4).

Mayeda, T.K., R.N. Clayton, and C.A. Molini-Velsko
1983. Oxygen and Silicon Isotopes in ALHA 81005. *Geophysical Research Letters*, 10:799–800.

Melosh, H.J.
1983. Impact Ejection, Spallation and the Origin of Cer-

tain Meteorites. *Lunar and Planetary Science XIV: Session on Meteorites from Earth's Moon*, pages 21–22. Houston: Lunar and Planetary Institute.

Pieters, Carle

1983. If ALHA81005 Came from the Moon, Can We Tell from Where? In *Lunar and Planetary Science XIV: Session on Meteorites from Earth's Moon*, pages 27–28. Houston: Lunar and Planetary Institute.

Ryder, G., and R. Ostertag

1983. ALHA 81005: Petrographic Components of the Target. In *Lunar and Planetary Science XIV: Session on Meteorites from Earth's Moon*, pages 29–30. Houston: Lunar and Planetary Institute.

Score, Roberta

1982. *In Antarctic Meteorite Newsletter 5* (4).

Stolper, E., H.Y. McSween, Jr., and J.F. Hays

1979. A Petrogenetic Model of the Relationship between Achondritic Meteorites. *Geochimica et Cosmochimica Acta*, 43:589–592.

Sutton, S.R., and G. Crozaz

1983. Thermoluminescence and Tracks: Constraints on the History of This Unusual Meteorite. In *Lunar and Planetary Science XIV: Sessions on Meteorites from Earth's Moon*, pages 33–34. Houston: Lunar and Planetary Institute.

Tremaine, A.H., and M.J. Drake

1983. Meteorite from the Moon: Petrology of Terrae Clasts and One Mare Clast in ALHA 81005,9. In *Lunar and Planetary Science XIV: Session on Meteorites from Earth's Moon*, pages 35–36. Houston: Lunar and Planetary Institute.

Cosmic-Ray-Produced Nuclides in Victoria Land Meteorites

Kunihiko Nishiizumi

In the last few years measurements of cosmic-ray-produced nuclides in Antarctic meteorites have been carried out by several groups. At the present time, we have measured ^{53}Mn ($t_{1/2} = 3.7 \times 10^6$ y) in 153 meteorites (62 Victoria Land meteorites and 91 Yamato meteorites) by the destructive neutron-activation method (Nishiizumi, Imamura, et al., 1979; Nishiizumi et al., 1981; Nishiizumi, Arnold, Imamura, et al., 1982; Nishiizumi, Arnold, Elmore, et al., 1983; Imamura et al., 1979, Goswami and Nishiizumi, 1983) and ^{36}Cl ($t_{1/2} = 3.0 \times 10^5$ y) in 62 Antarctic meteorites by Accelerator Mass Spectroscopy (Nishiizumi, Arnold, et al., 1979, Nishiizumi et al., 1981, 1983, and Nishiizumi, unpublished). ^{26}Al ($t_{1/2} = 7.2 \times 10.5$ y) has been measured in 129 Victoria Land meteorites by the Battelle group using nondestructive gamma-ray analysis (Evans et al., 1979, 1982). In addition to the above data, nine ^{10}Be ($t_{1/2} = 1.6 \times 10^6$ y), and eighteen ^{14}C (5730 y) measurements, and twenty-six sets of noble gas data are also available for our study.

Cosmogenic nuclide concentrations in a meteorite give us the cosmic-ray exposure age in space and terrestrial age on the earth, if we know the expected equilibrium concentrations and half-lives. It is important to measure two or more cosmogenic nuclides in the same meteorite.

Table 9 is a compilation of published and unpublished data for Victoria Land meteorites for which measurements of more than one nuclide are available. This table also includes the exposure age and terrestrial age of these meteorites. The exposure age was calculated from the cosmogenic ^{21}Ne content; the shielding condition was corrected by the $^{22}Ne/^{21}Ne$ ratio or from cosmogenic ^{40}K content. The terrestrial age of the meteorite was calculated from ^{36}Cl or ^{14}C content, comparing it with the saturated activity level that was expected at the time of fall on Antarctica. The details are discussed in a recent paper (Reedy et al., 1983).

The measurement of terrestrial age is an important subject for Antarctic meteorites. The terrestrial ages of non-Antarctic stone meteorites are less than 3×10^4 years, usually much less. However the terrestrial ages of Allan Hills meteorites range from 1×10^4 (ALHA77256) to 7×10^5 years (ALHA77002). This age not only gives us information on the accumulation mechanism of meteorites and the history of the Antarctic ice sheet, but also about ancient meteorite influx rates. Our interest was focused on Allan Hills meteorites for terrestrial age measurements. So far, several features have appeared. Meteorites found on the northwest part of the Allan Hills blue ice region have shorter terrestrial ages than meteorites found on the southeast part. Probably this feature gives key information for the accumulation mechanism of Allan Hills meteorites and glaciology. On the other hand there is no clear correlation between the terres-

Kunihiko Nishiizumi, Department of Chemistry, B-017, University of California, San Diego, La Jolla, California 92093.

TABLE 9.—Activity (dpm/kg), exposure age, and terrestrial age of meteorites in which more than one nuclide has been measured (numbers in parentheses indicate half-life of each nuclide).[1]

Specimen number	Class	Activity[2]					Exposure age	Terrestrial age
		^{53}Mn (3.7×10^6y)	^{10}Be (1.6×10^6y)	^{26}Al (7.2×10^5y)	^{36}Cl (3.0×10^5y)	^{14}C (5730y)	10^6y	10^3y
ALLAN HILLS								
ALHA76001	L6	443±33					45	
ALHA76002	IA	556±21			14.1±0.5		410	200±80
ALHA76003	L6	431±25					53	
ALHA76004	LL3			58±2			26	
ALHA76005	Eu	390±36		89±9		<1.0	10	>34
ALHA76006	H6	453±33		51±1		<1.7	28	>32
ALHA76007	L6	332±26		45±4		<1.2	33	>34
ALHA76008	H6	22±3	3.9±0.5	11±1	9.4±1.0	<1.7	(1.5)	100±70
ALHA76009	L6	477±34					20	
ALHA77001	L6	422±13		52±5	20.1±1.2			<120
ALHA77002	L5	255±8		30±3	4.6±1.1			700±160
ALHA77003	C3	317±13	19±2	45±5	18.4±1.2	0.62±0.06	20	110±70
ALHA77004	H4	326±13		52±5	15.2±0.5	0.65±0.02		170±70
ALHA77009	H4			32±2	10.7±0.2			320±70
ALHA77015	L3	162±8		36±4			3.1	
ALHA77081	H?			42±4			5.6	
ALHA77167	L3	137±7		37±2			2.4	
ALHA77214	L3	151±6	15±1	56±6	17.0±0.8	0.35±0.03	3.3	120±80
ALHA77216	L3	348±14		40±3			30	
ALHA77230	L4	362±15		51±3				
ALHA77249	L3	181±9		37±2	14.9±0.5			180±70
ALHA77250	IA	565±22			15.6±0.2			160±70
ALHA77255	Anom	385±15			19.2±0.2			<130
ALHA77256	Di	400±21				16.0±1.5		11±1
ALHA77257	Ur	181±8			9.8±0.8		10	360±90
ALHA77258	H6	434±18		29±2	12.2±0.4			270±70
ALHA77260	L3	150±8		37±2			1.8	
ALHA77261	L6	302±13		36±4	11.1±0.6			310±80
ALHA77262	H4	327±13		47±5				
ALHA77270	L6	494±20		40±3	6.7±0.1			530±70
ALHA77272	L6	213±11	18±2	35±4	6.6±0.3	<0.5	4.6	530±80
ALHA77273	L6	224±11		31±2	6.2±0.3			560±80
ALHA77278	LL3	264±11		28±3	10.9±0.7		21	320±90
ALHA77280	L6	325±16			12.2±0.3			270±70
ALHA77282	L6	384±17		49±3	12.1±0.4	1.07±0.24		270±70
ALHA77283	IA	437±17			17.5±0.3			110±70
ALHA77285	H6	394±16		38±4	13.6±0.5			220±70
ALHA77289	IA	534±21			15.3±0.3			170±70
ALHA77290	IA	504±20			15.1±0.3			170±70
ALHA77294	H5	433±17		67±4	20.8±0.6	1.6±0.3		30±2
ALHA77297	L6	428±17		70±7	19.6±0.2	<0.60		80±40
ALHA77299	H3	317±19		43±4	18.9±0.8		36	80±80
ALHA77304	L4	211±9		50±3				
ALHA78043	L6	457±22		33±3	7.3±0.3			490±80

[1] Average saturated activity: ^{53}Mn: 414±50; ^{10}Be: 20±2; ^{26}Al: 60±7(L), 56±7(H); ^{36}Cl: 22.8±3.1; ^{14}C: 60.

[2] Activity: ^{53}Mn: dpm/kg (Fe+⅓ Ni); ^{10}Be, ^{26}Al, ^{14}C: dpm/kg meteorite; ^{36}Cl: dpm/kg metal.

TABLE 9.—Continued.

Specimen number	Class	Activity[2]					Exposure age 10^6y	Terrestrial age 10^3y
		^{53}Mn (3.7×10^6y)	^{10}Be (1.6×10^6y)	^{26}Al (7.2×10^5y)	^{36}Cl (3.0×10^5y)	^{14}C (5730y)		
ALHA78076	H6	427±18		52±4	16.9±0.5			130±70
ALHA78084	H4	318±13	18±2		16.4±0.5	1.41±0.24	37	140±70
ALHA78102	H5			35±3	14.0±0.6			210±80
ALHA78105	L6	462±21		61±7	12.5±0.3			260±70
ALHA78109	LL5	444±28		46±3	12.4±0.5			260±70
ALHA78112	L6	347±16	21±2	42±3	13.4±0.5			230±70
ALHA78114	L6	360±14	14±2	38±2	7.8±0.3			460±80
ALHA78115	H6	334±14	16±2	43±3	21.6±0.6			<90
ALHA78128	H5			34±2	15.2±0.4			170±70
ALHA78130	L6	380±15	18±2	51±4	20.7±0.5			<110
ALHA78131	L6	402±19		40±3	9.3±0.4			380±80
ALHA78132	Eu			68±4			11	
ALHA78232	IVA	376±14			9.9±0.2			360±70
ALHA81005	A		4.1±0.5	46±3				
BATES NUNATAK								
BTNA78002	L6	424±18			19.5±0.4			<130
DERRICK PEAK								
DRPA78008	IIB	2.7±0.2			0.032±0.004			
DRPA78009	IIB	65±3			0.20±0.01			
METEORITE HILLS								
META78001	H4	429±17		53±3	20.5±0.8			<120
META78002	L6			47±3	21.0±0.5			<100
META78005	L6			44±3	20.0±0.4			<120
META78006	H6			60±4	20.9±0.5			<100
META78010	H5			56±3	21.8±0.5			<90
META78028	L6			56±3	21.3±0.6	1.01±0.03		32±1
MOUNT BALDR								
MBRA76001	H6	394±34				1.19±0.30	6	31±3
MBRA76002	H6	355±26					7	
PURGATORY PEAK								
PGPA77006	IA	569±23			18.4±0.5			90±70
RECKLING PEAK								
RKPA78003	L6	363±16		50±3	19.8±0.4			<130

References:

Column 1: Imamura et al., 1979; Nishiizumi et al., 1979, 1981, 1983; Nishiizumi, Arnold, Imamura, et al., 1982; Goswami and Nishiizumi, 1983.

Column 2: Moniot et al., 1982; Nishiizumi, Arnold, Imamura, et al., 1982; Nishiizumi, Arnold, Klein, et al., 1982; Tuniz et al., 1983.

Column 3: Evans et al., 1979, 1982; Evans, personal communication; Tuniz et al., 1983.

Column 4: Nishiizumi, Arnold, et al., 1979; Nishiizumi et al., 1981, 1983.

Column 5: Fireman, 1979, 1980, 1983; Fireman and Norris, 1981; Andrews et al., 1982, Nishiizumi, unpublished data.

Column 6: Nagao and Takaoka, 1979; Nitoh et al., 1980; Schultz et al., 1980; Weber and Schultz, 1980; Takaoka et al., 1981; Nautiyal et al., 1982; Nagao et al., 1983; Weber et al., 1983.

Column 7: Nishiizumi, herein.

trial age of a meteorite and its weathering features. This indicates that many meteorites stayed in the ice for a long time and weathering only began when the specimen was exposed at the ice surface. Allan Hills meteorites have a wide range of terrestrial ages and are generally older than other Victoria Land meteorites and Yamato meteorites.

Although the cosmogenic noble-gas data are important for meteorite bombardment history in space, relatively small amounts of data are available for Allan Hills meteorites compared to Yamato meteorites. Based on both cosmogenic stable (noble gas) and radioactive nuclide data, at least four Antarctic meteorites showed clearly multistage irradiation records. They are ALHA76008, Yamato 7301, 74028, and 74116 (Nishiizumi et al., 1978, 1979, Nishiizumi, Arnold, Imamura, et al., 1982; Imamura et al., 1979). The multistage irradiation model asserts that the meteorite was irradiated in a heavily shielded position in the parent body for a long time. During this period most of the cosmogenic stable nuclides (noble gas and ^{40}K) were produced. The parent body was then fragmented, initiating the second-stage irradiation by exposing the small preatmospheric bodies to cosmic rays for a short time so that the long-lived radioactive nuclides were not saturated. Except for Antarctic meteorites, Jilin (Kirin) is the only stony meteorite definitely known to have had a multistage irradiation record.

An iron meteorite, Derrick Peak A78008, contains the lowest concentration of cosmogenic radionuclides yet measured among Antarctic meteorites. This object is known to be a shower fragment of DRPA78001-78009 (Clarke, 1982). Based on a low ^{53}Mn result of (2.7±0.2 dpm/kg), the preatmospheric size of this group of Derrick Peak meteorites was more than 3.3 m in diameter, or more than 150 tons in weight.

Combined analysis of cosmogenic nuclides and cosmic-ray track data in an aliquot sample provides information on size and location of a meteorite in the preatmospheric body. Such analysis is extremely useful to check on pairing of Antarctic meteorites. For example, L3 chondrites ALHA77015, 77167, and 77260 could be fragments from a single meteorite with radius ~25 cm (Goswami and Nishiizumi, 1983). On the other hand L6 chondrites ALHA77273 and 77280, which were previously suggested to be a single fall of a meteorite, could not be fragments from a single meteorite (Goswami and Nishiizumi, 1983).

This research was supported in part by NASA Grant NGL 005-009-148.

Literature Cited

Andrews, H.R., R.M. Brown, G.C. Ball, N. Burn, Y. Imahori, J.C.D. Milton, W.J. Workman, and E.L. Fireman
1982. ^{14}C Content of Antarctic Meteorites Measured with the Chalk River MP Tandem Accelerator. *In* Abstracts, *Fifth International Conference on Geochronology, Cosmochronology, and Isotope Geology, Nikko, Japan*, pages 8–9.

Clarke, R.S., Jr.
1982. The Derrick Peak, Antarctica, Iron Meteorites. *Meteoritics*, 17:129–134.

Evans, J.C., L.A. Rancitelli, and J.H. Reeves
1979. ^{26}Al Content of Antarctic Meteorites: Implications for Terrestrial Ages and Bombardment History. In *Proceedings of the Tenth Lunar and Planetary Science Conference*, pages 1061–1072. New York: Pergamon Press.

Evans, J.C., J.H. Reeves, and L.A. Rancitelli
1982. Aluminum-26: Survey of Victoria Land Meteorites. *In* U. B. Marvin and B. Mason, editors, Catalog of Meteorites from Victoria Land, Antarctica, 1978–1980. *Smithsonian Contributions to the Earth Sciences*, 24:70–74.

Fireman, E.L.
1979. ^{14}C and ^{39}Ar Abundances in Allan Hills Meteorites. In *Proceedings of the Tenth Lunar and Planetary Science Conference*, pages 1053–1060. New York: Pergamon Press.
1980. Carbon-14 and Argon-39 in ALHA Meteorites. In *Proceedings of the Eleventh Lunar and Planetary Science Conference*, pages 1215–1221. New York: Pergamon Press.
1983. Carbon-14 Ages of Antarctic Meteorites. In *Lunar and Planetary Science XIV*, pages 195–196. Houston: Lunar and Planetary Institute.

Fireman, E.L., and T. Norris
1981. Carbon-14 Ages of Allan Hills Meteorites and Ice. In *Proceedings of the Twelfth Lunar and Planetary*

Science Conference, pages 1019–1025. New York: Pergamon Press.

Goswami, J.N., and K. Nishiizumi
1983. Cosmogenic Records in Antarctic Meteorites. *Earth and Planetary Science Letters*, 64:1–8.

Imamura, M., K. Nishiizumi, and M. Honda
1979. Cosmogenic ^{53}Mn in Antarctic Meteorites and Their Exposure History, *Memoirs of the National Institute of Polar Research* (Japan), special issue, 15:227–242.

Moniot, R.K., T.H. Kruse, W. Savin, C. Tuniz, T. Milazzo, G.S. Hall, D. Pal, and G.F. Herzog
1982. Beryllium-10 Contents of Stony Meteorites and the Neon-21 Production Rate. *Lunar and Planetary Science XIII*, pages 536–537. Houston: Lunar and Planetary Institute.

Nagao, K., and N. Takaoka
1979. Rare Gas Studies of Antarctic Meteorites. *Memoirs of the National Institute of Polar Research* (Japan), special issue, 12:207–222.

Nagao, K., N. Takaoka, and K. Saito
1983. Rare Gas Studies of the Antarctic Meteorites. In *Eighth Symposium on Antarctic Meteorites*, pages 83–84. Tokyo: National Institute of Polar Research.

Nautiyal, C.M., J.T. Padia, M.N. Rao, T.R. Venkatesan, and J.N. Goswami
1982. Irradiation History of Antarctic Gas-Rich Meteorites. In *Lunar and Planetary Science XIII*, pages 578–579. Houston: Lunar and Plantary Institute.

Nishiizumi, K.
1978. Cosmic-Ray-Produced ^{53}Mn in Thirty-one Meteorites. *Earth and Planetary Science Letters*, 41:91–100.

Nishiizumi, K., J.R. Arnold, D. Elmore, R.D. Ferraro, H.E. Gove, R.C. Finkel, R.P. Beukens, K.H. Chung, and L.R. Kilius
1979. Measurements of ^{36}Cl in Antarctic Meteorites and Antarctic Ice using a Van de Graaff Accelerator. *Earth and Planetary Science Letters*, 45:285–292.

Nishiizumi, K., J.R. Arnold, D. Elmore, X. Ma, D. Newman, and H.E. Gove
1983. ^{36}Cl and ^{53}Mn in Antarctic Meteorites and ^{10}Be-^{36}Cl Dating of Antarctic Ice. *Earth and Planetary Science Letters*, 62:407–417.

Nishiizumi, K., J.R. Arnold, M. Imamura, T. Inoue, and M. Honda
1982. Cosmogenic Radionuclides in Antarctic Meteorites. In *Seventh Symposium on Antarctic Meteorites*, pages 52–54. Tokyo: National Institute of Polar Research.

Nishiizumi, K., J.R. Arnold, J. Klein, and R. Middleton
1982. ^{10}Be and Other Radionuclides in Antarctic Meteorites and in Associated Ice. *Meteoritics*, 17:260–261.

Nishiizumi, K., M. Imamura, and M. Honda
1978. Cosmic Ray Induced ^{53}Mn in Yamato-7301(j), -7305(k) and -7304(m) Meteorites. *Memoirs of the National Institute of Polar Research* (Japan) special issue, 8:209–219.
1979. Cosmic Ray Produced Radionuclides in Antarctic Meteorites. *Memoirs of the National Institute of Polar Research* (Japan), special issue, 12:161–177.

Nishiizumi, K., M.T. Murrell, J.R. Arnold, D. Elmore, R.D. Ferraro, H.E. Gove, and R.C. Finkel
1981. Cosmic-Ray-Produced ^{36}Cl and ^{53}Mn in Allan Hills-77 Meteorites. *Earth and Planetary Science Letters*, 52:31–38.

Nitoh, O., M. Honda, and M. Imamura
1980. Cosmogenic K-40 in Antarctic Meteorites. *Memoirs of the National Institute of Polar Research* (Japan), special issue, 17:189–201.

Reedy, R.C., J.R. Arnold, and D. Lal
1983. Cosmic-Ray Record in Solar System Matter. *Science*, 219:127–135.

Schultz, L., H. Palme, B. Spettel, H. Wänke, and H.W. Weber
1980. Chemistry and Noble Gases of the Unusual Stony Meteorite Allan Hills A77081. In *Lunar and Planetary Science XI*, pages 1003–1005. Houston: Lunar and Planetary Institute.

Takaoka, N., K. Saito, Y. Ohba, and K. Nagao
1981. Rare Gas Studies of Twenty-Four Antarctic Chondrites. *Memoirs of the National Institute of Polar Research* (Japan), special issue, 20:264–275.

Tuniz, C., D.K. Pal, R.K. Moniot, W. Savin, T.H. Kruse, G.F. Herzog, and J.C. Evans
1983. Recent Cosmic Ray Exposure History of ALHA 81005. *Geophysical Research Letters*, 10:804–806.

Weber, H.W., O. Braun, L. Schultz, and F. Begemann
1983. The Noble Gas Record in Antarctic and Other Meteorites. *Zeitschrift für Naturforschung*, 38a:267–272.

Weber, H.W., and L. Schultz
1980. Noble Gases in Ten Stone Meteorites from Antarctica. *Zeitschrift für Naturforschung*, 35a:44–49.

Bulk Chemical Analyses of Antarctic Meteorites, with Notes on Weathering Effects on FeO, Fe-metal, FeS, H_2O, and C

Eugene Jarosewich

In addition to a large number of ordinary chondrites, the discovery and subsequent collection of a large number of the Antarctic meteorites has yielded a considerable selection of rare types. Among these rare types are achondrites, carbonaceous chondrites, a unique "moon meteorite," and several type 3 chondrites, to name a few. Since these meteorites are rare, they are the object of extensive studies by researchers from various disciplines, and their data are compared with the data from existing specimens in our collections.

The bulk chemical analysis of some of these rare meteorites was undertaken as a part of a broader study of Antarctic meteorites; particularly, the type 3 chondrites, because of the importance of the chemical data in their classification.

The bulk chemical analyses of these meteorites were performed using a modified chemical method published by Jarosewich (1966). Between 2 and 20 g of sample were made available for the analyses of these Antarctic meteorites, but for actual analysis only between 1.5 and 3.5 g was used. Most of the samples were prepared in a clean environment with a special automatic agate mortar, where the whole sample was ground, homogenized, and then split for other studies, including those for trace elements.

As a convenient summary of bulk analyses, Table 10 gives the data for 17 newly analyzed chondrites and for 8 meteorites published earlier by Marvin and Mason (1980). The data in this table give primarily basic geochemical information and indicate the degree of weathering. Six of the L3 type severely weathered chondrites (indicated by an asterisk in Table 10) are paired and their chemical data are given. The chemical analyses of these L3 types were undertaken before they were identified as paired. The agreement of the data, considering that they were obtained on different specimens, is remarkable, although it is somewhat disappointing that these rare meteorites are paired rather than separate specimens. All the data of these meteorites for FeO, Fe-metal, FeS, H_2O and C do not give true values for these components; nevertheless, with some corrections, the nature of chemical composition of the meteorites can be approximated. The weathering of the Antarctic meteorites was described in a general manner by Lipschutz (1982). Gibson and Andrawes (1980) described specifics of C and S content and possible condition of weathering processes, and Marvin and Motylewski (1980) described the mineralogy of weathered meteorites.

Eugene Jarosewich, Department of Mineral Sciences, National Museum of Natural History, Smithsonian Institution, Washington, D.C. 20560.

TABLE 10.—Chemical composition of Antarctic meteorites (nd = not determined; * = paired L3 meteorites; H_2O = H_2O total; Fe,M = Fe-metal; Fe,T = Fe total)

Name and type	SiO_2	TiO_2	Al_2O_3	Cr_2O_3	FeO	MnO	MgO	CaO	Na_2O	K_2O
ALHA77003 C3	34.19	0.14	2.89	0.49	21.78	0.31	23.53	2.22	0.56	0.06
ALHA77005 Sh	42.40	0.46	3.14	1.05	19.85	0.46	28.16	3.39	0.48	0.04
*ALHA77011 L3	38.21	0.14	2.29	0.57	20.07	0.27	23.89	1.78	0.92	0.12
*ALHA77015 L3	38.23	0.14	2.29	0.57	19.63	0.26	23.97	1.71	0.74	0.10
ALHA77155 L6	39.99	0.13	2.21	0.54	16.33	0.32	24.70	1.79	0.95	0.11
*ALHA77167 L3	37.94	0.13	2.18	0.58	19.64	0.26	23.85	1.64	0.91	0.11
*ALHA77214 L3	37.73	0.11	2.30	0.49	19.63	0.33	22.69	1.70	0.82	0.07
ALHA77216 L3	39.43	0.10	2.25	0.49	15.85	0.32	24.57	1.67	0.90	0.12
ALHA77219 M	32.27	0.16	3.93	0.63	15.84	0.41	12.56	3.14	0.15	0.03
ALHA77231 L6	39.43	0.11	2.18	0.49	16.07	0.31	24.47	1.75	0.91	0.12
*ALHA77249 L3	36.96	0.12	2.21	0.53	21.28	0.26	22.91	1.60	0.86	0.11
ALHA77256 Di	52.15	0.16	1.56	1.06	16.07	0.47	26.48	1.50	0.04	0.01
ALHA77257 Ur	41.12	0.04	<0.1	0.70	13.57	0.38	39.66	1.07	0.03	0.01
*ALHA77260 L3	37.53	0.13	2.15	0.56	21.45	0.24	23.82	1.75	0.83	0.11
ALHA77270 L6	40.15	0.12	2.49	0.53	15.46	0.32	24.92	1.79	0.96	0.11
ALHA77271 H6	36.88	0.11	1.97	0.50	13.43	0.28	23.36	1.60	0.83	0.10
ALHA77278 LL3	41.03	0.12	2.26	0.50	16.79	0.34	24.08	1.90	0.82	0.10
ALHA77284 L6	40.43	0.12	2.30	0.48	14.50	0.32	25.17	1.78	0.91	0.10
ALHA77294 H5	37.75	0.14	2.31	0.57	8.76	0.33	23.66	1.83	0.72	0.07
ALHA77296 L6	40.21	0.14	2.36	0.57	15.53	0.35	25.00	1.96	0.80	0.09
ALHA77297 L6	40.13	0.14	2.41	0.52	15.43	0.36	25.02	1.93	0.80	0.08
ALHA77299 H3	35.94	0.11	2.27	0.41	13.15	0.30	22.50	1.81	1.08	0.12
ALHA77304 L4	40.49	0.14	2.35	0.57	16.36	0.28	25.10	1.81	1.01	0.13
ALHA77078 L6	38.64	0.13	2.34	0.58	15.57	0.35	24.49	1.86	0.74	0.07
ALHA78106 L6	39.70	0.13	2.36	0.51	14.31	0.36	25.13	1.96	0.75	0.07

The degree of weathering in the Antarctic meteorites is accurately reflected in the preliminary petrographic description of the meteorites in the *NASA Newsletters*. Severely weathered meteorites denoted as "C" condition and two "A" (minor weathering) were selected from Table 10 and are listed in Table 11; in this table the degree of weathering is quantitatively expressed for FeO, H_2O, FeS, Fe-metal, and C. It can be seen that the values for H_2O, C, and FeO (which includes weathered metal) are higher and Fe-metal and FeS are lower than the averages for their class of meteorites. There are some exceptions to this general trend; FeS in ALHA77214 and C in ALHA77271 are very close to the average amounts of these two components for their type, and two meteorites in Table 10, ALHA77278 and ALHA77299, classified as "A" (minor weathering) show considerable amounts of H_2O and a slight increase in C, and ALHA77299 shows high FeO and low Fe-metal. These few variations in an otherwise definite trend in weathering of different constituents in meteorites, high FeO, H_2O, C, and low Fe-metal and FeS, would indicate that the weathering is a very selective process, one dependent on variety of conditions, the processes of which are little understood.

The contamination of the Antarctic meteorites, especially those of "A" condition, at this point, is not a serious problem for most elements that have been studied (Lipschutz, 1982). However, it is evident that the carbon contamination in "C" condition meteorites is significant and its source is of importance. The suggestion of the presence of CO_2 in secondary minerals was verified, using classical CO_2 determination in "C" condition meteorite, ALHA77214 (for which

TABLE 10.—Continued.

P_2O_5	H_2O	Fe,M	Ni	Co	FeS	C	Total	Fe,T	Ref[1]	Degree of weathering[2]
0.23	1.89	4.50	1.37	0.07	4.85	0.28	99.36	24.51	2	A
0.41	0.02	ND	0.01	<0.01	<0.1	0.02	99.89	15.43	2	A
0.25	2.74	1.94	1.02	0.06	4.47	0.97	99.71	20.38	1	C
0.25	2.55	2.30	1.12	0.06	4.69	0.98	99.59	20.54	1	C
0.20	0.49	6.09	1.34	0.06	4.32	0.04	99.61	21.53	1	A/B
0.24	2.74	2.44	1.13	0.06	4.55	0.99	99.36	20.60	1	C
0.21	3.29	2.02	1.18	0.06	5.73	1.08	99.44	20.77	2	C
0.20	0.75	6.40	1.13	0.06	5.75	0.04	100.03	22.37	1	A/B
0.30	1.63	23.63	2.86	0.10	1.10	0.15	98.89	36.64	2	B
0.23	0.75	6.37	1.20	0.06	4.88	0.03	99.36	21.96	1	A/B
0.24	3.34	2.25	1.17	0.07	4.41	1.08	99.40	21.59	1	C
0.01	0.02	nd	0.01	<0.01	0.15	0.03	99.72	12.49	2	A/B
0.06	0.18	nd	0.08	<0.01	<0.01	3.34	100.24	10.55	2	A
0.27	2.99	1.53	1.11	0.06	3.43	1.07	99.03	20.39	1	C
0.26	0.31	5.99	1.12	0.07	5.34	0.01	99.95	21.40	1	A/B
0.22	1.25	12.90	1.69	0.09	4.42	0.04	99.67	26.15	1	C
0.20	1.58	2.23	1.03	0.05	6.17	0.16	99.36	19.20	2	A
0.18	0.79	5.90	1.20	0.06	5.16	0.01	99.41	20.45	1	A/B
0.25	0.23	16.00	1.84	0.06	5.62	0.02	100.16	26.38	1	A
0.22	0.20	6.00	1.26	0.06	4.80	0.01	99.56	21.12	1	A/B
0.24	0.14	6.39	1.11	0.07	5.24	0.01	100.02	21.72	1	A
0.22	1.71	12.26	1.67	0.08	5.23	0.38	99.24	25.80	2	A
0.22	0.99	4.36	1.16	0.07	4.80	0.01	99.85	20.13	1	B
0.25	0.71	6.48	1.32	0.07	6.03	0.02	99.65	22.41	1	A/B
0.22	0.11	6.78	1.29	0.07	5.87	0.01	99.63	21.64	1	A/B

[1] References: 1 = herein; 2 = Marvin and Mason, 1980, appendix 2.
[2] Degree of weathering: A = minor; B = moderate; C = severe.

TABLE 11.—Amounts of most weathered components of weathered meteorites (A = minor, C = severe).

Name and type	FeO	H_2O	Fe,M	FeS	C	Degree of weathering
ALHA77011 L3	20.07	2.74	1.94	4.47	0.97	C
ALHA77015 L3	19.63	2.55	2.30	4.69	0.98	C
ALHA77167 L3	19.64	2.74	2.44	4.55	0.99	C
ALHA77214 L3	19.63	3.29	2.02	5.73	1.08	C
ALHA77249 L3	21.28	3.34	2.25	4.41	1.08	C
ALHA77260 L3	21.45	2.99	1.53	3.43	1.07	C
ALHA77271 H6	13.43	1.25	12.9	4.42	0.04	C
ALHA77278 LL3	16.79	1.58	2.23	6.17	0.16	A
ALHA77299 H3	13.15	1.71	12.26	5.23	0.39	A

sufficient sample was available), giving 0.19% CO_2, clearly within the range estimated by Gibson and Andrawes (1980) from 5% to 10% of total carbon but still not accounting for the remainder of carbon.

Weathering is not a major concern in the study of these meteorites; however, the contamination or depletion of elements is. The relationship between weathering, which can be readily observed, and contamination is an area to be explored. This work establishes for a group of Antarctic meteorites that the presence of H_2O and low Fe-metal with resulting high FeO and depletion of FeS is accompanied by an increase of C, which is clearly a contaminant.

The analyses of weathered Antarctic meteorites, especially those of rare types, will be the source of important additional data, provided the necessary precautions are exercized in the acquisitions of these data.

The analyses of carbon in the Antarctic Meteorite samples was done by J. Nelen.

Literature Cited

Gibson, E.K., Jr., and F.F. Andrawes
1980. The Antarctic Environment and Its Effect upon the Total Carbon and Sulfur Abundances in Recovered Meteorites. In *Proceedings of the Eleventh Lunar and Planetary Science Conference,* pages 1223–1234. New York: Pergamon Press.

Jarosewich, E.
1966. Chemical Analyses of Ten Stony Meteorites. *Geochimica et Cosmochimica Acta,* 30:1261–1265.

Lipschutz, M.E.
1982. Weathering Effects in Antarctic Meteorites. *In* U.B. Marvin and B. Mason, editors, Catalog of Meteorites from Victoria Land, 1978–1980. *Smithsonian Contributions to the Mineral Sciences,* 24:67–69.

Marvin, U.B., and B. Mason, editors
1980. Catalog of Antarctic Meteorites, 1977–1978. *Smithsonian Contributions to the Earth Sciences,* 23: 50 pages.

Marvin, U.B., and K. Motylewski
1980. Mg-Carbonates and Sulfates on Antarctic Meteorites. *Lunar and Planetary Science XI,* pages 669–670. Houston: Lunar and Planetary Institute.

Appendix

Tables of Victoria Land Meteorites

Terminology

Class and type: A = achondrite, unique; Au = aubrite; C = carbonaceous chondrite; Di = diogenite; E = enstatite chondrite; Eu = eucrite; H = high-iron chondrite; Ho = howardite; I = iron (IA, IIA, IIB, IVA = iron groups); L = low-iron chondrite; LL = low-iron low-metal chondrite; M = mesosiderite; Sh = shergottite; Ur = ureilite. Chondrite type is indicated by the digit following the letter.

Olivine composition in mole percent Fe_2SiO_4(Fa).

Pyroxene (orthopyroxene or low-Ca clinopyroxene) composition in mole percent $FeSiO_3$(Fs).

Degree of weathering: A = minor; metal flecks have inconspicuous rust halos, oxide stain along cracks is minor. B = moderate; metal flecks show large rust halos, internal cracks show extensive oxide stain. C = severe; specimen is uniformly stained brown, no metal survives.

Degree of fracturing: A = slight; specimen has few or no cracks and none penetrate the entire specimen. B = moderate; several cracks extend across the specimen, which can be readily broken along the fractures. C = severe; specimen has many extensive cracks and readily crumbles.

Locations: ALH = Allan Hills; BTN = Bates Nunatak; DRP = Derrick Peak; EET = Elephant Moraine; MBR = Mount Baldr; MET = Meteorite Hills; OTT = Outpost Nunatak; PCA = Pecora Escarpment; PGP = Purgatory Peak; RKP = Reckling Peak; TIL = Thiel Mountains.

Classification: by S.J.B. Reed and S.O. Agrell (*); by S.G. McKinley and K. Keil (**).

Abbreviations: n.d. = no data.

NOTE: While this monograph was in press PCA82500 was reclassified from LL6 to C4.

TABLE A.—Meteorites listed by source area in numerical sequence (fractions of grams in weight dropped unless total weight is less than 1 gram).

Specimen number	Weight (g)	Class and type	%Fa in olivine	%Fs in pyroxene	Degree of weathering
ALHA					
76001	20151	L6	25	21	A
76002	1510	I			
76003	10495	L6	25	21	A
76004	305	LL3	0–34	0–53	A
76005	1425	Eu		37–57	A
76006	1137	H6	18	16	C
76007	410	L6	24	21	B
76008	1150	H6	19	17	B/C
76009	407000	L6	24	21	B
77001	252	L6	25	21	B
77002	235	L5	25	22	B
77003	779	C3	4–48	2–25	A
77004	2230	H4	17–20	15–27	C
77005	482	Sh	28	23	A
77007**	99	H5	19.1	16.7	B
77008**	93	L6	24.6	20.6	A
77009	235	H4	18	16	C
77010	295	H4	18	15–18	C
77011	291	L3	4–36	1–33	C
77012	180	H5	18	16	C
77013**	23	L3	9–28	1–35	B
77014	308	H5	18	17	C
77015	411	L3	1–21	4–24	C
77016**	78	H5	18.6	17.1	B
77017**	77	H5	18.8	16.3	B
77018**	51	H5	19.0	17.0	B/C
77019**	.59	L6	24.9	21.4	B/C
77021	16	H5	18	17	C
77022**	16	H5	19.1	17.0	A
77023**	21	H5	19.1	16.8	B
77025	19	H5	18	17	C
77026**	20	L6	24.3	20.7	B/C
77027**	3	L6	25.0	21.5	B/C
77029**	1	C3	23.0	2.6	A/B
77031**	0.5	L3	n.d.	n.d.	B/C
77033	9	L3	8–38	8–9	C
77034**	1	L3	n.d.	n.d.	B/C
77036**	8	L3	n.d.	n.d.	B
77038**	18	H5	19.0	17.1	A/B
77039**	8	H5	18.5	16.3	A/B
77041**	16	LL6	30.7	25.1	A
77042**	20	H5	19.0	16.6	A/B
77043**	11	L3	1–37	1–28	B/C
77045**	17	H5	18.7	17.0	A
77046**	7	H6	19.0	16.7	A/B
77047**	20	L3	n.d.	n.d.	C
77049**	7	L3	n.d.	n.d.	B/C
77050**	84	L3	n.d.	n.d.	B/C
77051**	15	H5	18.8	16.5	A
77052**	112	L3	n.d.	n.d.	B/C
77054**	10	H5	18.5	16.9	B
77056**	12	H4	18.8	16.3	A/B
77058**	3	H5	18.8	16.1	B
77060**	64	LL5	28.1	23.2	A
77061	12	H5	18	17	B
77062	16	H5	18	17	B
77063**	2	H5	18.0	16.8	B
77064	6	H5	18	17	B
77066**	4	H5	19.0	17.4	A
77069**	0.8	L6	25.4	21.4	B/C
77070**	18	H5	18.4	16.8	B
77071	10	H5	18	17	B
77073**	10	H5	18.8	17.7	A/B
77074	12	H5	18	17	B
77076**	1	H5	19.5	16.1	B
77078**	7	H5	19.5	16.7	B
77079**	7	H5	18.2	15.8	A
77081	8	H?	11	11	B
77082**	12	H5	19.3	16.5	A/B
77084**	44	H5	18.8	16.8	A/B
77085**	45	H5	18.8	17.6	B
77086	19	H5	19	17	C
77087**	30	H5	19.0	16.7	B
77088	51	H5	19	17	C
77089**	7	L6	25.5	21.4	B
77091**	4	H5	18.9	16.1	B/C
77092**	45	H5	18.5	16.5	A
77094**	6	H5	18.5	16.2	B
77096**	2	H5	18.7	17.1	A
77098**	8	H5	18.7	16.7	B
77100**	8	H5	19.2	16.4	A/B
77101**	3	H5	18.6	17.0	B
77102	12	H5	19	15	B
77104**	6	H5	18.9	16.9	A
77106**	7	H5	18.8	16.5	A/B
77108**	0.7	H5	18.5	15.9	A/B
77111**	52	H6	19.0	16.6	A/B
77112**	21	H5	18.7	16.7	A
77113**	2	H5	18.7	18.4	B
77114**	44	H5	19.6	17.2	B
77115**	154	L3	n.d.	n.d.	B/C
77117**	20	L5	24.4	21.0	A/B
77118	7	H5	19	17	C

TABLE A.—Continued.

Specimen number	Weight (g)	Class and type	%Fa in olivine	%Fs in pyroxene	Degree of weathering
77119	6	H5	18	17	C
77120**	3	H5	18.5	16.0	A/B
77122**	4	H5	19.1	16.8	B
77124	4	H5	19	16	C
77125**	18	H5	17.2	15.5	A/B
77126**	25	H5	18.3	16.2	A/B
77127**	3	L5	25.0	21.1	B
77129**	1	H5	18.9	16.6	B
77130**	24	H5	18.9	16.5	A
77131**	25	H6	19.2	16.8	A/B
77132**	115	H5	19.0	16.9	A/B
77133**	18	H6	19.0	17.0	A
77134**	19	H6	18.9	16.7	A
77136**	3	H5	19.1	16.4	A/B
77138**	2	H5	19.2	17.0	A
77139**	65	H5	18.6	16.4	A/B
77140	78	L3	8–44	2–17	C
77142**	3	H5	18.9	17.1	A/B
77143**	39	H5	18.7	16.2	A/B
77144	7	H6	19	17	B
77146**	18	H6	18.9	16.9	A/B
77147**	18	H6	19.0	16.6	A/B
77148	13	H6	18	16	C
77149**	25	H6	19.1	16.9	A/B
77150	58	L6	25	22	C
77151**	16	H5	18.9	16.4	A
77152**	17	H5	18.7	16.9	A
77153**	12	H5	19.2	16.7	A
77155	305	L6	24	20	A/B
77156**	17	E4	0.8	1.5	A
77157**	88	H6	18.6	15.7	A/B
77158**	19	H5	18.9	16.9	B
77159**	17	L6	24.4	20.8	A/B
77160	70	L3	3–46	6–40	C
77161**	6	H5	19.3	17.1	B
77162**	29	L6	25.3	20.9	A
77163**	24	L3	n.d.	n.d.	B/C
77164	38	L3	6–39	3–41	C
77165	30	L3	8–33	6–35	C
77166**	138	L3	n.d.	n.d.	C
77167	611	L3	2–41	3–17	C
77168**	24	H5	19.0	16.5	B
77170**	12	L3	n.d.	n.d.	B/C
77171**	23	H5	18.9	17.0	A/B
77173**	25	H5	19.1	17.0	B
77174**	32	H5	18.3	16.0	A
77175**	23	L3	n.d.	n.d.	B/C
77176**	54	L3	0.3–34	1–37	B
77177	368	H5	18	16	C
77178**	5	L3	1–36	2–40	B/C
77180	190	L6	24	20	C
77181**	33	H5	20.0	17.3	B
77182	1134	H5	19	17	C
77183	288	H6	19	16	C
77184**	127	H5	17.8	15.9	B
77185**	28	L3	n.d.	n.d.	A/B
77186**	122	H5	18.8	16.0	A/B
77187**	52	H5	18.1	16.3	A/B
77188**	109	H5	18.1	16.1	A/B
77190	387	H4	17–19	15–22	C
77191	642	H4	16–18	14–16	C
77192	845	H4	16–18	15–21	C
77193**	6	H5	19.0	15.7	A
77195**	4	H5	18.9	16.4	A
77197**	20	L3	10–27	4–21	A/B
77198**	7	L6	24.4	20.6	B
77200**	0.9	H6	19.7	17.6	C
77201**	15	H5	18.8	15.3	A
77202**	2	H5	18.6	16.6	B
77205**	3	H5	18.8	16.7	B
77207**	4	H5	17.8	16.7	A/B
77208	1733	H4	17	14	C
77209**	31	H6	18.8	16.4	B
77211**	26	L3	n.d.	n.d.	B/C
77212**	16	H6	18.9	17.0	A/B
77213**	8	H5	18.6	16.5	A
77214	2111	L3	1–49	4–23	C
77215	819	L3	22–26	9–21	B
77216	1470	L3	15–35	14–23	A/B
77217	413	L3	17–25	9–26	B
77218**	45	L5	23.4	19.1	A
77219	637	M	26	24–28	B
77220**	69	H5	17.7	16.0	B
77221	229	H4	15	13–15	C
77222**	125	H4	18.0	15.3	A/B
77223	207	H4	17	15–23	C
77224	786	H4	19	17	C
77225	5878	H4	17	16	C
77226	15323	H4	18	16	C
77227**	16	H5	18.9	16.6	A
77228**	19	H5	18.5	16.3	B
77230	2473	L4	22–25	18–29	C
77231	9270	L6	24	21	A/B
77232	6494	H4	17	15	C
77233	4087	H4	14–21	15–17	C
77235**	4	H5	18.9	16.7	A/B
77237**	4	H5	18.5	15.8	A
77239**	19	H6	18.7	15.9	B

TABLE A.—Continued.

Specimen number	Weight (g)	Class and type	%Fa in olivine	%Fs in pyroxene	Degree of weathering
77240**	25	H5	18.8	16.0	A
77241**	144	L3	n.d.	n.d.	C
77242**	56	H5	18.8	16.2	B
77244**	39	L3	n.d.	n.d.	B/C
77245**	33	H5	19.2	17.2	A/B
77246**	41	J6	19.2	16.5	B
77247**	44	H5	18.8	16.4	A/B
77248**	96	H6	18.7	16.7	B/C
77249	503	L3	7–35	2–25	C
77250	10555	I			
77251**	68	L6	25.0	21.3	B
77252	343	L3	22–28	2–22	B
77253**	23	H5	19.2	16.9	A/B
77254	245	L5	23	20	A/B
77255	765	I			
77256	676	Di		23	A/B
77257	1995	Ur	13	12	A
77258	597	H6	18	16	B/C
77259	294	H5	18	15	C
77260	744	L3	7–23	1–28	C
77261	411	L6	24	21	B
77262	861	H4	15–19	13–16	B/C
77263	1669	I			
77264	11	H5	19	16	A/B
77265**	18	H5	17.6	15.9	B
77266**	108	H5	19.6	17.7	B
77267**	103	L5	24.7	20.9	A
77268	272	H5	18	16	C
77269	1045	L6	24	22	B
77270	588	L6	24	21	A/B
77271	609	H6	18	16	C
77272	674	L6	24	20	B/C
77273	492	L6	24	20	B
77274	288	H5	18	16	C
77275**	24	H5	18.3	15.6	A
77277	142	L6	24	20	A/B
77278	312	LL3	11–29	9–21	A
77279**	174	H5	18.8	17.1	A
77280	3226	L6	24	21	B
77281	1231	L6	24	20	B
77282	4127	L6	24	20	B
77283	10510	I			
77284	376	L6	25	21	A/B
77285	271	H6	18	16	C
77286	245	H4	17	12–16	C
77287	230	H5	18	16	C
77288	1880	H6	19	17	C
77289	2186	I			
77290	3784	I			
77291**	5	H5	18.9	15.9	A
77292	199	L6	24	20	B
77293**	109	L6	24.7	20.9	B
77294	1351	H5	17	15	A
77295**	141	E4	0.8	1.7	B
77296	963	L6	24	21	A/B
77297	951	L6	24	20	A
77299	260	H3	11–21	15–20	A
77300	234	H5	18	16	C
77301**	55	L6	24.9	20.9	A
77302	235	Eu		37–64	A
77303**	78	L3	n.d.	n.d.	B/C
77304	650	L4	18–27	13–19	B
77305	6444	L6	24	21	B/C
77306	19	C2	1–45	1	A
77307	181	C3	1–30	1–12	A
78004*	35	H5	19.2		
78006	8	Ho		25–61	A
78015*	34	LL(?L)3	8–35		
78019	30	Ur	22	18	B/C
78027*	29	H5	19.3		
78038	363	L3	4–42	2–19	C
78039	299	L6	24	21	B
78040	211	Eu		33–52	A
78042	214	L6	24	20	B
78043	680	L6	25	21	B
78044	164	L4	23–25	19–24	B/C
78045	396	L6	25	21	B/C
78047*	130	H5	18.8		B
78048	190	L6	24	21	A/B
78050	1045	L6	23	20	B
78052*	97	H5	17.9		C
78053	179	H4	17	16	C
78074	200	L6	24	21	B
78075	280	H5	18	16	B/C
78076	275	H6	18	16	B
78077	330	H4	19	15–18	C
78078	290	L6	24	20	A/B
78081*	17	H5	19.1		
78084	14280	H4	18	8–24	B/C
78085	219	H5	18	16	B
78086*	9	H6	19.0		
78088*	5	H5	18.8		
78090*	7	H5	18.7		
78092*	16	H5	19.0		
78094*	4	H5	19.1		
78096*	7	H5	18.9		
78098*	2	H5	18.9		

TABLE A.—Continued.

Specimen number	Weight (g)	Class and type	%Fa in olivine	%Fs in pyroxene	Degree of weathering
78100	85	I			
78102	336	H5	18	17	B/C
78103	589	L6	24	20	B
78104	672	L6	24	20	B
78105	941	L6	23	20	B
78106	464	L6	24	20	A/B
78107	198	H5	18	17	C
78108	172	H5	18	16	B
78109	233	LL5	28	23	A/B
78110	160	H5	18	16	B/C
78111	126	H5	18	16	B/C
78112	2485	L6	25	20	B
78113	298	Au	0	0	A/B
78114	808	L6	25	20	B/C
78115	847	H6	18	16	B
78116*	127	H5	18.7		B
78121*	30	H5	19.2		
78125*	18	L6	25.0		B
78126	606	L6	25	21	B
78127	194	L6	24	20	B/C
78128	154	H5	19	17	C
78130	2733	L6	25	21	B/C
78131	268	L6	25	21	B/C
78132	656	Eu		40–68	A
78134	458	H4	18	15–20	B/C
78135*	130	H6	19.0		B
78139*	17	H5	19.3		
78142*	31	L5	24.2		
78147*	30	H5,6	19.4		
78153	151	LL6	29	24	B/C
78158	15	Eu		40–68	A
78160*	16	H5	19.3		
78165	20	Eu		37–61	A
78188	0.9	L3	1–34	5–29	C
78193	13	H4	18	16	B/C
78196	11	H4	18	16	B/C
78209	12	H5	18	15	B/C
78211	11	H6	18	16	B
78213	9	H6	18	15	B
78215	6	H6	18	16	B/C
78221	5	H5	18	16	B
78223	6	H4	18	16	B
78225	4	H5	18	16	B
78227	2	H5	18	16	B/C
78229	1	H6	18	15	B
78231	1	H6	18	16	B/C
78233	1	H5	18	16	B/C
78251	1312	L6	23	20	B
78252	2789	I			
78261	5	C2	0–50	1–8	A
78262	26	Ur	22	19	B/C
79001	32	L3	6–39	2–31	C
79002	222	H6	16	18	C
79003	5	LL3	10–38	5–26	B
79004	34	H5	16	14	B/C
79005	60	H6	18	16	B
79006	40	H5	18	15	B/C
79007	142	L6	23	19	A/B
79008	12	H5	17	15	B
79009	75	H5	18	15	C
79010	25	H5	17	15	B/C
79011	14	H5	18	16	B/C
79012	191	H5	17	15	C
79013	28	H5	18	16	C
79014	10	H5	18	16	B
79015	64	H5	17	15	B
79016	1146	H6	17	15	B/C
79017	310	Eu		28–53	A
79018	120	L6	23	20	B/C
79019	12	H6	17	15	B
79020	4	H6	17	15	B/C
79021	29	H5	18	17	B
79022	31	L3,4	1–28	9–22	A/B
79023	68	H4	17	14–17	B/C
79024	21	H6	17	15	C
79025	1208	H5	17	15	C
79026	572	H5	18	16	B
79027	133	L6	24	20	B
79028	16	H6	18	16	B
79029	505	H5	18	16	C
79031	2	H5	16	14	C
79032	2	H5	16	14	C
79033	208	L6	24	20	B
79034	12	H6	18	16	B
79035	37	H4	17	14–18	B
79036	20	H5	18	16	B
79037	14	H6	18	16	B
79038	49	H5	17	15	C
79039	108	H4	16	15	B
79040	13	H5	18	15	B
79041	20	H5	18	16	B
79042	11	H5	18	16	B
79043	62	L6	23	20	C
79045	115	L3	2–38	2–29	C
79046	89	H5	18	15	B
79047	19	H5	18	15	B
79048	36	H5	18	16	B

TABLE A.—Continued.

Specimen number	Weight (g)	Class and type	%Fa in olivine	%Fs in pyroxene	Degree of weathering
79049	54	H6	18	16	C
79050	27	H5	18	15	C
79051	24	H5	18	15	C
79052	22	L6	23	20	B/C
79053	86	H5	17	15	B/C
79054	36	H5	18	16	B
79055	15	H6	18	16	B/C
80101	8725	L6	24	20	B
80102	471	Eu		34–52	A
80103	535	L6	24	20	B
80104	882	I			
80105	445	L6	24	20	B
80106	432	H4	19	16–19	C
80107	177	L6	24	20	B
80108	124	L6	24	20	B
80110	167	L6	24	20	B
80111	42	H5	18	16	B
80112	330	L6	24	20	B
80113	312	L6	24	20	B
80114	232	L6	24	20	B
80115	306	L6	24	20	B
80116	191	L6	24	20	B/C
80117	89	L6	24	20	B
80118	2	H6	17	15	B
80119	33	L6	24	20	B
80120	60	L6	24	20	B
80121	39	H4	19	17	B/C
80122	49	H6	18	16	B/C
80123	27	H5	18	16	C
80124	11	H5	18	16	B
80125	139	L6	24	20	B/C
80126	34	H6	19	17	A/B
80127	47	H5	18	16	B
80128	138	H4	18	15–20	B
80129	93	H5	18	15	B
80130	5	H6	18	16	B/C
80131	19	H4	19	16–22	B
80132	152	H5	18	16	B
80133	3	L3	1–35	5–30	B
81001	52	Eu		59	A
81002	14	C2	0–52	0–2	A
81003	10	C3	0–60	1	A/B
81004	4	C2	0–52	0–2	A/B
81005	31	A	11–40	7–47	A/B
81006	254	Eu		35–60	A
81007	163	Eu		38–55	A/B
81008	43	Eu		32–59	A/B
81009	229	Eu		30–63	A
81010	219	Eu		31–57	A
81011	405	Eu		33–60	A/B
81012	36	Eu		33–62	A/B
81013	17727	I			
81014	188	I			
81015	5489	H5	19	16	B
81016	3850	L6	25	21	B
81017	1434	L5	25	21	B
81018	2236	L5	24	21	B
81019	1051	H5	19	16	B/C
81020	1352	H5	19	16	B
81021	695	E6		0–1	A
81022	912	H4	19	17	B/C
81023	418	L5	25	21	B
81024	797	L3	3–28	2–24	C
81025	379	L3	1–41	3–40	C
81026	515	L6	25	21	B
81027	3835	L6	25	21	C
81028	80	L6	25	21	B
81029	153	L6	25	21	C
81030	1851	L3	1–49	5–33	B/C
81031	1594	L3	1–43	3–35	C
81032	726	L3	0–42	2–14	C
81033	252	H5	18	16	C
81034	254	H5	19	17	B
81035	256	H6	19	17	C
81036	252	H5	19	17	C
81037	320	H6	20	17	B
81038	229	H6	19	17	C
81039	205	H5	19	17	A/B
81040	194	L4	25	21	B/C
81041	728	H4	18	15–23	C
81042	534	H5	19	17	C
81043	106	H4	18	15	B/C
81044	386	H4	18	16	C
81045	90	H4	18	16	C
81046	16	H4	18	16	C
81047	81	H4	18	16	B/C
81048	190	H4	18	16	B/C
81049	8	H4	18	16	B/C
81050	25	H4	18	16	C
81051	43	H4	18	16	B/C
81052	28	H4	18	16	C
81053	2	L3	1–29	1–42	C
81054	2	H6	19	17	B
81055	4	H6	19	16	B
81056	1	H4	19	17	B
81057	8	H4	19	13–21	B
81058	66	H4	18	15	C

TABLE A.—Continued.

Specimen number	Weight (g)	Class and type	%Fa in olivine	%Fs in pyroxene	Degree of weathering
81059	539	M	28	25–32	C
81060	28	L3	2–28	5–27	C
81061	23	L3	3–33	5–27	B/C
81062	0.5	H5	18	16	C
81063	4	H5	18	16	B/C
81064	191	H5	18	15	C
81065	13	L3	10–41	5–24	B/C
81066	8	L3	1–44	1–25	C
81067	227	H5	19	17	C
81068	23	H4	19	16	B
81069	7	L3	4–38	1–31	B/C
81070	3	H5	19	17	B/C
81071	2	H5	19	17	B
81072	3	H5	19	17	B/C
81073	3	H4	19	8–18	B/C
81074	7	H4	19	16	B
81075	15	H5	19	17	B
81076	10	H6	19	16	B
81077	4	H5	19	17	B
81078	5	H6	19	16	B/C
81079	7	H6	19	16	C
81080	16	H5	19	17	A/B
81081	5	H5	19	17	B
81082	5	H5	19	17	B
81083	6	H5	19	16	B
81084	15	H5	19	16	B
81085	16	L3	1–39	2–25	C
81086	5	H6	19	16	B
81087	8	L3	2–29	3–31	B/C
81088	3	H5	19	17	B
81089	11	H5	19	17	B
81090	9	H5	19	16	B
81091	12	H5	19	16	B
81092	15	H4	19	17	B
81093	271	H6	20	17	A/B
81094	152	H6	19	16	C
81095	58	H4	18	16	B/C
81096	83	H6	19	17	B
81097	79	H4	18	16	B
81098	70	M		28	C
81099	151	L6	25	21	A/B
81100	154	H5	19	17	B
81101	119	Ur	10–22		A/B
81102	196	H6	19	17	B/C
81103	136	H6	19	17	B/C
81104	183	H4	19	17	C
81105	92	H4	18	16	C
81106	48	L6	24	20	B
81107	139	L6	24	21	B
81108	69	H5	18	16	B
81109	1	H4	19	17	B
81110	3	H5	19	17	B/C
81111	210	H6	19	17	B/C
81112	150	H6	19	17	B/C
81113	111	H5	18	16	B/C
81114	79	H4	18	16	B/C
81115	154	H5	19	17	C
81116	1	H5	19	17	B
81117	32	H4	18	14–21	B
81118	84	H5	19	16	B/C
81119	107	L4	24	21	B
81120	13	H5	18	16	B/C
81121	88	L3	8–40	1–24	B
81122	20	L6	25	21	B
81123	2	LL6	30	25	B
81124	9	H5	19	17	B
81125	10	H5	19	17	B
81126	21	H5	19	16	B
81127	15	H6	19	17	B/C
81136	1	H5	20	17	B
81153	4	L5	24	21	B
81154	1	H6	19	17	B
81158	2	H5	19	17	B/C
81251	158	LL3	1–29	2–28	B/C
82100	24	C2	1–47	1–2	A
82101	29	C3	1–50	1–10	A
BTNA					
78001	160	L6	24	21	B
78002	4301	L6	24	20	B
78004	1079	LL6	30	24	B
DRPA					
78001	15200	I			
78002	7188	I			
78003	144	I			
78004	133	I			
78005	18600	I			
78006	389	I			
78007	11800	I			
78008	59400	I			
78009	138100	I			
EETA					
79001	7942	Sh	23–27	16–67	A
79002	2843	Di	24–25	22	B
79003	435	L6	24	20	B
79004	390	Eu		30–61	B
79005	450	Eu		30–61	A

TABLE A.—Continued.

Specimen number	Weight (g)	Class and type	%Fa in olivine	%Fs in pyroxene	Degree of weathering
79006	716	Ho		19–57	B
79007	199	H5	18	16	B
79009	140	L5	24	20	B
79010	287	L6	24	20	B
79011	86	Eu		30–61	B
82600	247	Ho		22–53	A
MBRA					
76001	4108	H6	18	16	B
76002	13773	H6	18	16	B
META					
78001	624	H4	17	14–21	B/C
78002	542	L6	23	20	B
78003	1726	L6	24	21	B
78005	172	L6	24	20	B
78006	409	H6	18	15	C
78007	174	H6	19	17	B/C
78010	233	H5	19	17	B
78028	20657	L6	25	21	B
OTTA					
80301	35	H3	17–19	4–19	B
PCA					
82500	90	LL6	31		B
82501	54	Eu		41–57	A
82502	890	Eu		36–61	A
PGPA					
77006	19068	I			
RKPA					
78001	234	L6	23	20	C
78002	8483	H4	18	15	B
78003	1276	L6	23	20	C
78004	166	H4	17	14–21	A
79001	3006	L6	23	20	B
79002	203	L6	24	20	B
79003	182	H6	18	16	B
79004	370	H5	18	16	B/C
79008	73	L3	1–29	2–28	B
79009	55	H6	18	16	C
79012	12	H6	18	16	B
79013	11	L5	23	20	B/C
79014	77	H5	18	16	B/C
79015	10022	M		24	A/B
80201	813	H6	19	16	B
80202	544	L6	24	20	B
80203	3	H6	19	17	C
80204	15	Eu		52–57	A
80205	53	H3	17–20	5–13	B
80206	46	H6	19	17	C
80207	17	H3	15–29	6–28	C
80208	10	H6	19	17	B
80209	9	L5	25	21	C
80210	10	H5	19	16	B/C
80211	2	H6	19	17	C
80213	19	H6	19	17	B/C
80214	4	H6	19	17	C
80215	9	L6	24	20	C
80216	44	L4	23	20	B
80217	7	H5	18	15	C
80218	6	H5	18	15	C
80219	21	L6	25	21	B
80220	124	H5	18	16	B/C
80221	51	H6	19	17	C
80222	6	LL6	28	23	B
80223	25	H5	18	16	C
80224	8	Eu		54	A/B
80225	8	L6	25	21	C
80226	160	I			
80227	7	H5	19	16	B/C
80228	11	L5	23	19	C
80229	14	M		24	C
80230	58	H5	18	16	B
80231	238	H6	18	16	C
80232	80	H4	18	16	B
80233	413	H5	18	16	B/C
80234	136	LL5	26	22	B
80235	261	LL6	30	24	A/B
80236	15	H5	18	16	B/C
80237	22	H4	18	16	C
80238	18	LL6	28	23	A/B
80239	5	Ur	16	15	B
80240	61	H5	18	16	C
80241	0.6	C3	1–6	1–8	B
80242	7	L4	22	19	B/C
80243	3	H5	18	16	C
80244	14	H5	18	16	C
80245	36	H5	18	16	B/C
80246	5	M		24	C
80247	1	H5	18	16	C
80248	11	LL6	27	23	A/B
80249	9	H5	17	15	B/C
80250	3	H5	17	15	B/C
80251	29	H5	17	15	B
80252	11	L6	24	20	A/B
80253	4	LL5	27	22	A/B

TABLE A.—Continued.

Specimen number	Weight (g)	Class and type	%Fa in olivine	%Fs in pyroxene	Degree of weathering	Specimen number	Weight (g)	Class and type	%Fa in olivine	%Fs in pyroxene	Degree of weathering
80254	68	H6	19	17	C	80263	16	M		24	C
80255	6	H6	19	17	C	80264	23	L6	24	20	B
80256	153	L3	20–25	10–26	B	80265	7	H6	19	17	C
80257	8	H5	17	15	B/C	80266	9	H6	19	17	B/C
80258	4	M		17–21	B/C	80267	24	H4	19	16	C
80259	20	E5		0–1	B/C	80268	3	L5	24	20	B/C
80260	7	H5	18	16	C						
80261	61	L6	24	20	B	TIL					
80262	32	H6	19	17	C	82403	49	Eu		43–58	A

TABLE B.—Meteorites listed by class and source area in numerical sequence (fractions of grams weight dropped unless total weight is less than 1 gram).

Specimen number	Weight (g)	Class and type	Degree of weathering	Degree of fracturing	Specimen number	Weight (g)	Class and type	Degree of weathering	Degree of fracturing
				CHONDRITES					
ALHA77306	19	C2	A	A	ALHA79023	68	H4	B/C	C
ALHA78261	5	C2	A	A	ALHA79035	37	H4	B	B
ALHA81002	14	C2	A	B	ALHA79039	108	H4	B	B
ALHA81004	4	C2	A/B	A	ALHA80106	432	H4	C	B
ALHA82100	24	C2	A	A	ALHA80121	39	H4	B/C	C
ALHA77307	181	C3	A	A	ALHA80128	138	H4	B	B/C
ALHA77003	779	C3	A	A	ALHA80131	19	H4	B	B
ALHA77029**	1	C3	A/B		ALHA81022	912	H4	B/C	A
ALHA82101	29	C3	A	A/B	ALHA81041	728	H4	C	C
ALHA81003	10	C3	A/B	A/B	ALHA81043	106	H4	B/C	C
RKPA80241	0.6	C3	B	B	ALHA81044	386	H4	C	C
ALHA77156**	17	E4	B		ALHA81045	90	H4	C	B/C
ALHA77295	141	E4	B		ALHA81046	16	H4	C	B/C
RKPA80259	20	E5	B/C	B	ALHA81047	81	H4	B/C	B/C
ALHA81021	695	E6	A	B	ALHA81048	190	H4	B/C	B/C
ALHA77299	260	H3	A	A	ALHA81049	8	H4	B/C	B
OTTA80301	35	H3	B/C	B	ALHA81050	25	H4	C	C
RKPA80205	53	H3	B	B	ALHA81051	43	H4	B/C	B
ALHA77004	2230	H4	C	C	ALHA81052	28	H4	C	B
ALHA77009	235	H4	C	A	ALHA81056	1	H4	B	A
ALHA77010	295	H4	C	A	ALHA81057	8	H4	B	A
ALHA77056**	12	H4	A/B		ALHA81058	66	H4	C	C
ALHA77190	387	H4	C	C	ALHA81068	23	H4	B	A
ALHA77191	642	H4	C	B/C	ALHA81073	3	H4	B/C	A
ALHA77192	845	H4	C	C	ALHA81074	7	H4	B	B
ALHA77208	1733	H4	C	C	ALHA81092	15	H4	B	A
ALHA77221	229	H4	C	A	ALHA81095	58	H4	B/C	C
ALHA77222**	125	H4	A/B		ALHA81097	79	H4	B	A
ALHA77223	207	H4	C	C	ALHA81104	183	H4	C	C
ALHA77224	786	H4	C	C	ALHA81105	92	H4	C	B/C
ALHA77225	5878	H4	C	C	ALHA81109	1	H4	B	A
ALHA77226	15323	H4	C	C	ALHA81114	79	H4	B/C	B/C
ALHA77232	6494	H4	C	C	ALHA81117	32	H4	B	B/C
ALHA77233	4087	H4	C	B	META78001	624	H4	B/C	B
ALHA77262	861	H4	B/C	B	RKPA78002	8483	H4	B	A/B
ALHA77286	245	H4	C	B	RKPA78004	166	H4	A	A
ALHA78053	179	H4	C	B	RKPA80232	80	H4	B	A
ALHA78077	330	H4	C	B	RKPA80237	22	H4	C	B
ALHA78084	14280	H4	B/C	B	RKPA80267	24	H4	C	A
ALHA78134	458	H4	B/C	B/C	ALHA79004	34	H5	B/C	B
ALHA78193	13	H4	B/C	A	ALHA77007**	99	H5	B	
ALHA78196	11	H4	B/C	B	ALHA77012	180	H5	C	A
ALHA78223	6	H4	B	B	ALHA77014	308	H5	C	B/C
					ALHA77016**	78	H5	B	
					ALHA77017**	77	H5	B	

TABLE B.—Continued

Specimen number	Weight (g)	Class and type	Degree of weathering	Degree of fracturing	Specimen number	Weight (g)	Class and type	Degree of weathering	Degree of fracturing
ALHA77018**	51	H5	B/C		ALHA77124	4	H5	C	A
ALHA77021	16	H5	C	A	ALHA77125**	18	H5	A/B	
ALHA77022**	16	H5	A		ALHA77126**	25	H5	A/B	
ALHA77023**	21	H5	B		ALHA77129**	1	H5	B	
ALHA77025	19	H5	C	B	ALHA77130**	24	H5	A	
ALHA77038**	18	H5	A/B		ALHA77132**	115	H5	A/B	
ALHA77039**	8	H5	A/B		ALHA77136**	3	H5	A/B	
ALHA77042**	20	H5	A/B		ALHA77138**	2	H5	A	
ALHA77045**	17	H5	A		ALHA77139**	65	H5	A/B	
ALHA77051**	15	H5	A		ALHA77142**	3	H5	A/B	
ALHA77054**	10	H5	B		ALHA77143**	39	H5	A/B	
ALHA77058**	3	H5	B		ALHA77151**	16	H5	A	
ALHA77061	12	H5	B	A	ALHA77152**	17	H5	A	
ALHA77062	16	H5	B	B	ALHA77153**	12	H5	A	
ALHA77063**	2	H5	B		ALHA77158**	19	H5	B	
ALHA77064	6	H5	B	B	ALHA77161**	6	H5	B	
ALHA77066**	4	H5	A		ALHA77168**	24	H5	B	
ALHA77070**	18	H5	B		ALHA77171**	23	H5	A/B	
ALHA77071	10	H5	B	B	ALHA77173**	25	H5	B	
ALHA77073**	10	H5	A/B		ALHA77174**	32	H5	A	
ALHA77074	12	H5	B	B	ALHA77177	368	H5	C	A
ALHA77076**	1	H5	B		ALHA77181**	33	H5	B	
ALHA77078**	7	H5	B		ALHA77182	1134	H5	C	B
ALHA77079**	7	H5	A		ALHA77184**	127	H5	B	
ALHA77082**	12	H5	A/B		ALHA77186**	122	H5	A/B	
ALHA77084**	44	H5	A/B		ALHA77187**	52	H5	A/B	
ALHA77085**	45	H5	B		ALHA77188**	109	H5	A/B	
ALHA77086	19	H5	C	B	ALHA77193**	6	H5	A	
ALHA77087**	30	H5	B		ALHA77195**	4	H5	A	
ALHA77088	51	H5	C	B	ALHA77201**	15	H5	A	
ALHA77091**	4	H5	B/C		ALHA77202**	2	H5	B	
ALHA77092**	45	H5	A		ALHA77205**	3	H5	B	
ALHA77094**	6	H5	B		ALHA77207**	4	H5	A/B	
ALHA77096**	2	H5	A		ALHA77213**	8	H5	A	
ALHA77098**	8	H5	B		ALHA77220**	69	H5	B	
ALHA77100**	8	H5	A/B		ALHA77227**	16	H5	A	
ALHA77101**	3	H5	B		ALHA77228**	19	H5	B	
ALHA77102	12	H5	B	B	ALHA77235**	4	H5	A/B	
ALHA77104**	6	H5	A		ALHA77237**	4	H5	A	
ALHA77106**	7	H5	A/B		ALHA77240**	25	H5	A	
ALHA77108**	0.7	H5	A/B		ALHA77242**	56	H5	B	
ALHA77112**	21	H5	A		ALHA77245**	33	H5	A/B	
ALHA77113**	2	H5	B		ALHA77247**	44	H5	A/B	
ALHA77114**	44	H5	B		ALHA77253**	23	H5	A/B	
ALHA77118	7	H5	C	B	ALHA77259	294	H5	C	B
ALHA77119	6	H5	C	B	ALHA77264	11	H5	A/B	A
ALHA77120**	3	H5	A/B		ALHA77265**	18	H5	B	
ALHA77122**	4	H5	B		ALHA77266**	108	H5	B	

TABLE B.—Continued

Specimen number	Weight (g)	Class and type	Degree of weathering	Degree of fracturing	Specimen number	Weight (g)	Class and type	Degree of weathering	Degree of fracturing
ALHA77268	272	H5	C	C	ALHA79029	505	H5	C	B/C
ALHA77274	288	H5	C	A	ALHA79031	2	H5	C	B
ALHA77275**	24	H5	A		ALHA79032	2	H5	C	B
ALHA77279**	174	H5	A		ALHA79036	20	H5	B	B
ALHA77287	230	H5	C	A	ALHA79038	49	H5	C	B
ALHA77291**	5	H5	A		ALHA79040	13	H5	B	A
ALHA77294	1351	H5	A	A	ALHA79041	20	H5	B	B
ALHA77300	234	H5	C	B	ALHA79042	11	H5	B	A
ALHA78004*	35	H5			ALHA79046	89	H5	B	B
ALHA78027*	29	H5			ALHA79047	19	H5	B	B
ALHA78047*	130	H5	B	B	ALHA79048	36	H5	B	B
ALHA78052*	97	H5	C	B	ALHA79050	27	H5	C	B
ALHA78075	280	H5	B/C	B	ALHA79051	24	H5	C	A
ALHA78081*	17	H5			ALHA79053	86	H5	B/C	B
ALHA78085	219	H5	B	B	ALHA79054	36	H5	B	A
ALHA78088*	5	H5			ALHA80111	42	H5	B	A
ALHA78090*	7	H5			ALHA80123	27	H5	C	A
ALHA78092*	16	H5			ALHA80124	11	H5	B	B
ALHA78094*	4	H5			ALHA80127	47	H5	B	A
ALHA78096*	7	H5			ALHA80129	93	H5	B	A
ALHA78098*	2	H5			ALHA80132	152	H5	B	B
ALHA78102	336	H5	B/C	B	ALHA81015	5489	H5	B	B
ALHA78107	198	H5	C	A	ALHA81019	1051	H5	B/C	B
ALHA78108	172	H5	B	B	ALHA81020	1352	H5	B	A
ALHA78110	160	H5	B/C	B	ALHA81033	252	H5	C	C
ALHA78111	126	H5	B/C	A	ALHA81034	254	H5	B	B
ALHA78116*	127	H5	B	B	ALHA81036	252	H5	C	A
ALHA78121*	30	H5			ALHA81039	205	H5	A/B	B
ALHA78128	154	H5	C	B/C	ALHA81042	534	H5	C	C
ALHA78139*	17	H5			ALHA81062	0.5	H5	C	A
ALHA78160*	16	H5			ALHA81063	4	H5	B/C	B
ALHA78209	12	H5	B/C	B	ALHA81064	191	H5	C	A/B
ALHA78221	5	H5	B	A	ALHA81067	227	H5	C	B
ALHA78225	4	H5	B	A	ALHA81070	3	H5	B/C	A
ALHA78227	2	H5	B/C	B	ALHA81071	2	H5	B	A
ALHA78233	1	H5	B/C	B	ALHA81072	3	H5	B/C	A
ALHA79006	40	H5	B/C	B	ALHA81075	15	H5	B	A
ALHA79008	12	H5	B	B	ALHA81077	4	H5	B	A
ALHA79009	75	H5	C	A	ALHA81080	16	H5	A/B	A
ALHA79010	25	H5	B/C	B	ALHA81081	5	H5	B	A
ALHA79011	14	H5	B/C	A	ALHA81082	5	H5	B	A
ALHA79012	191	H5	C	B	ALHA81083	6	H5	B	A
ALHA79013	28	H5	C	B	ALHA81084	15	H5	B	A
ALHA79014	10	H5	B	A	ALHA81088	3	H5	B	A
ALHA79015	64	H5	B	B	ALHA81089	11	H5	B	A
ALHA79021	29	H5	B	A	ALHA81090	9	H5	B	A
ALHA79025	1208	H5	C	A	ALHA81091	12	H5	B	B
ALHA79026	572	H5	B	B	ALHA81100	154	H5	B	A

TABLE B.—Continued

Specimen number	Weight (g)	Class and type	Degree of weathering	Degree of fracturing	Specimen number	Weight (g)	Class and type	Degree of weathering	Degree of fracturing
ALHA81108	69	H5	B	B	ALHA77149**	25	H6	A/B	
ALHA81110	3	H5	B/C	A	ALHA77157**	88	H6	A/B	
ALHA81113	111	H5	B/C	C	ALHA77183	288	H6	C	A
ALHA81115	154	H5	C	A/B	ALHA77200**	0.9	H6	C	
ALHA81116	1	H5	B	A	ALHA77209**	31	H6	B	
ALHA81118	84	H5	B/C	A	ALHA77212**	16	H6	A/B	
ALHA81120	13	H5	B/C	B	ALHA77239**	19	H6	B	
ALHA81124	9	H5	B	A	ALHA77246**	41	H6	B	
ALHA81125	10	H5	B	A	ALHA77248**	96	H6	B/C	
ALHA81126	21	H5	B	A	ALHA77258	597	H6	B/C	A/B
ALHA81136	1	H5	B	A/B	ALHA77271	609	H6	C	A
ALHA81158	2	H5	B/C	A	ALHA77285	271	H6	C	B
EETA79007	199	H5	B	B	ALHA77288	1880	H6	C	B
META78010	233	H5	B	A	ALHA78076	275	H6	B	B
RKPA79004	370	H5	B/C	B	ALHA78086*	9	H6		
RKPA79014	77	H5	B/C	B	ALHA78115	847	H6	B	A
RKPA80210	10	H5	B/C	B	ALHA78135*	130	H6	B	B
RKPA80217	7	H5	C	A	ALHA78211	11	H6	B	B
RKPA80218	6	H5	C	A	ALHA78213	9	H6	B	B
RKPA80220	124	H5	B/C	B/C	ALHA78215	6	H6	B/C	B
RKPA80223	25	H5	C	B	ALHA78229	1	H6	B	B
RKPA80227	7	H5	B/C	A	ALHA78231	1	H6	B/C	B
RKPA80230	58	H5	B	B	ALHA79002	222	H6	C	B
RKPA80233	413	H5	B/C	B	ALHA79005	60	H6	B	B
RKPA80236	15	H5	B/C	B	ALHA79016	1146	H6	B/C	B
RKPA80240	61	H5	C	A	ALHA79019	12	H6	B	A
RKPA80243	3	H5	C	A	ALHA79020	4	H6	B/C	B
RKPA80244	14	H5	C	B	ALHA79024	21	H6	C	B
RKPA80245	36	H5	B/C	B	ALHA79028	16	H6	B	B
RKPA80247	1	H5	C	B	ALHA79034	12	H6	B	A
RKPA80249	9	H5	B/C	A	ALHA79037	14	H6	B	B
RKPA80250	3	H5	B/C	A	ALHA79049	54	H6	C	B
RKPA80251	29	H5	B	B	ALHA79055	15	H6	B/C	B
RKPA80257	8	H5	B/C	B	ALHA80118	2	H6	B	A
RKPA80260	7	H5	C	B	ALHA80122	49	H6	B/C	B
					ALHA80126	34	H6	A/B	A
ALHA78147*	30	H5, 6			ALHA80130	5	H6	B/C	A
ALHA76006	1137	H6	C	B	ALHA81035	256	H6	C	A/B
ALHA76008	1150	H6	B/C	B	ALHA81037	320	H6	B	A
ALHA77046**	7	H6	A/B		ALHA81038	229	H6	C	B
ALHA77111**	52	H6	A/B		ALHA81054	2	H6	B	B
ALHA77131**	25	H6	A/B		ALHA81055	4	H6	B	A
ALHA77133**	18	H6	A		ALHA81076	10	H6	B	A
ALHA77134**	19	H6	A		ALHA81078	5	H6	B/C	B
ALHA77144	7	H6	B	A	ALHA81079	7	H6	C	A
ALHA77146**	18	H6	A/B		ALHA81086	5	H6	B	B
ALHA77147**	18	H6	A/B		ALHA81093	271	H6	A/B	A/B
ALHA77148	13	H6	C	B	ALHA81094	152	H6	C	B

TABLE B.—Continued

Specimen number	Weight (g)	Class and type	Degree of weathering	Degree of fracturing	Specimen number	Weight (g)	Class and type	Degree of weathering	Degree of fracturing
ALHA81096	83	H6	B	B	ALHA77166**	138	L3	C	
ALHA81102	196	H6	B/C	A/B	ALHA77167	611	L3	C	B/C
ALHA81103	136	H6	B/C	B/C	ALHA77170**	12	L3	B/C	
ALHA81111	210	H6	B/C	B	ALHA77175**	23	L3	B/C	
ALHA81112	150	H6	B/C	A	ALHA77176**	54	L3	B	
ALHA81127	15	H6	B/C	B	ALHA77178**	5	L3	B/C	
ALHA81154	1	H6	B	B	ALHA77185**	28	L3	A/B	
MBRA76001	4108	H6	B	B	ALHA77197**	20	L3	A/B	
MBRA76002	13773	H6	B	B	ALHA77211**	26	L3	B/C	
META78006	409	H6	C	B	ALHA77214	2111	L3	C	C
META78007	174	H6	B/C	B	ALHA77215	819	L3	B	B/C
RKPA79003	182	H6	B	A	ALHA77216	1470	L3	A/B	B/C
RKPA79009	55	H6	C	B	ALHA77217	413	L3	B	B/C
RKPA79012	12	H6	B	B	ALHA77241**	144	L3	C	
RKPA80201	813	H6	B	A	ALHA77244**	39	L3	B/C	
RKPA80203	3	H6	C	A	ALHA77249	503	L3	C	C
RKPA80206	46	H6	C	B	ALHA77252	343	L3	B	C
RKPA80208	10	H6	B	A	ALHA77260	744	L3	C	C
RKPA80211	2	H6	C	B	ALHA77303**	78	L3	B/C	
RKPA80213	19	H6	B/C	B	ALHA78038	363	L3	C	C
RKPA80214	4	H6	C	B	ALHA78188	0.9	L3	C	B
RKPA80221	51	H6	C	B/C	ALHA79001	32	L3	C	A
RKPA80231	238	H6	C	B/C	ALHA79045	115	L3	C	B
RKPA80254	68	H6	C	B/C	ALHA80133	3	L3	B	B
RKPA80255	6	H6	C	B	ALHA81024	797	L3	C	B
RKPA80262	32	H6	C	B	ALHA81025	379	L3	C	B
RKPA80265	7	H6	C	B	ALHA81030	1851	L3	B/C	B/C
RKPA80266	9	H6	B/C	B	ALHA81031	1594	L3	C	B/C
ALHA77081	8	H?	B	A	ALHA81032	726	L3	C	A
					ALHA81053	2	L3	C	B
ALHA77011	291	L3	C	A	ALHA81060	28	L3	C	B
ALHA77013**	23	L3	B		ALHA81061	23	L3	B/C	A
ALHA77015	411	L3	C	B	ALHA81065	13	L3	B/C	B
ALHA77031**	0.5	L3	B/C		ALHA81066	8	L3	C	B
ALHA77033	9	L3	C	B	ALHA81069	7	L3	B/C	A
ALHA77034**	1	L3	B/C		ALHA81085	16	L3	C	B
ALHA77036**	8	L3	B		ALHA81087	8	L3	B/C	B
ALHA77043**	11	L3	B/C		ALHA81121	88	L3	B	B
ALHA77047**	20	L3	C		RKPA79008	73	L3	B	B
ALHA77049**	7	L3	B/C		RKPA80207	17	L3	C	B
ALHA77050**	84	L3	B/C		RKPA80256	153	L3	B	A
ALHA77052**	112	L3	B/C		ALHA79022	31	L3,4	A/B	B
ALHA77115**	154	L3	B/C						
ALHA77140	78	L3	C	B	ALHA77230	2473	L4	C	B
ALHA77160	70	L3	C	B	ALHA77304	650	L4	B	B
ALHA77163**	24	L3	B/C		ALHA78044	164	L4	B/C	B
ALHA77164	38	L3	C	C	ALHA81040	194	L4	B/C	A
ALHA77165	30	L3	C	C	ALHA81119	107	L4	B	B

TABLE B.—Continued

Specimen number	Weight (g)	Class and type	Degree of weathering	Degree of fracturing	Specimen number	Weight (g)	Class and type	Degree of weathering	Degree of fracturing
RKPA80216	44	L4	B	B	ALHA77292	199	L6	B	A
RKPA80242	7	L4	B/C	B	ALHA77293**	109	L6	B	
					ALHA77296	963	L6	A/B	A
ALHA77002	235	L5	B	A/B	ALHA77297	951	L6	A	B
ALHA77117**	20	L5	A/B		ALHA77301**	55	L6	A	
ALHA77127**	3	L5	B		ALHA77305	6444	L6	B/C	B
ALHA77218**	45	L5	A		ALHA78039	299	L6	B	B
ALHA77254	245	L5	A/B	A	ALHA78042	214	L6	B	A
ALHA77267**	103	L5	A		ALHA78043	680	L6	B	B
ALHA78142**	31	L5			ALHA78045	396	L6	B/C	B
ALHA81017	1434	L5	B	A	ALHA78048	190	L6	A/B	B
ALHA81018	2236	L5	B	B	ALHA78050	1045	L6	B	B
ALHA81023	418	L5	B	A/B	ALHA78074	200	L6	B	B
ALHA81153	4	L5	B	A	ALHA78078	290	L6	A/B	A
EETA79009	140	L5	B	B	ALHA78103	589	L6	B	B
RKPA79013	11	L5	B/C	B	ALHA78104	672	L6	B	A
RKPA80209	9	L5	C	B	ALHA78105	941	L6	B	A
RKPA80228	11	L5	C	B	ALHA78106	464	L6	A/B	A
RKPA80268	3	L5	B/C	B	ALHA78112	2485	L6	B	B
					ALHA78114	808	L6	B/C	B
ALHA76001	20151	L6	A	A	ALHA78125*	18	L6	B	B
ALHA76003	10495	L6	A	A	ALHA78126	606	L6	B	B
ALHA76007	410	L6	B	A	ALHA78127	194	L6	B/C	B
ALHA76009	407000	L6	B	B	ALHA78130	2733	L6	B/C	B
ALHA77001	252	L6	B	B	ALHA78131	268	L6	B/C	A
ALHA77008**	93	L6	A		ALHA78251	1312	L6	B	A
ALHA77019**	59	L6	B/C		ALHA79007	142	L6	A/B	B
ALHA77026**	20	L6	B/C		ALHA79018	120	L6	B/C	A/B
ALHA77027**	3	L6	B/C		ALHA79027	133	L6	B	A
ALHA77069**	0.8	L6	B/C		ALHA79033	208	L6	B	A
ALHA77089**	7	L6	B		ALHA79043	62	L6	C	B
ALHA77150	58	L6	C	B	ALHA79052	22	L6	B/C	B
ALHA77155	305	L6	A/B	A	ALHA80101	8725	L6	B	B
ALHA77159**	17	L6	A/B		ALHA80103	535	L6	B	A
ALHA77162**	29	L6	A		ALHA80105	445	L6	B	B
ALHA77180	190	L6	C	A	ALHA80107	177	L6	B	B
ALHA77198**	7	L6	B		ALHA80108	124	L6	B	B
ALHA77231	9270	L6	A/B	A/B	ALHA80110	167	L6	B	B
ALHA77251**	68	L6	B		ALHA80112	330	L6	B	B
ALHA77261	411	L6	B	B	ALHA80113	312	L6	B	B/C
ALHA77269	1045	L6	B	A	ALHA80114	232	L6	B	B
ALHA77270	588	L6	A/B	B	ALHA80115	306	L6	B	A
ALHA77272	674	L6	B/C	B	ALHA80116	191	L6	B/C	B
ALHA77273	492	L6	B	B	ALHA80117	89	L6	B	A
ALHA77277	142	L6	A/B	A	ALHA80119	33	L6	B	B
ALHA77280	3226	L6	B	B/C	ALHA80120	60	L6	B	B
ALHA77281	1231	L6	B	B	ALHA80125	139	L6	B/C	B
ALHA77282	4127	L6	B	B	ALHA81016	3850	L6	B	A
ALHA77284	376	L6	A/B	B					

TABLE B.—Continued

Specimen number	Weight (g)	Class and type	Degree of weathering	Degree of fracturing	Specimen number	Weight (g)	Class and type	Degree of weathering	Degree of fracturing
ALHA81026	515	L6	B	A	RKPA80225	8	L6	C	A
ALHA81027	3835	L6	C	A/B	RKPA80252	11	L6	A/B	A
ALHA81028	80	L6	B	B	RKPA80261	61	L6	B	A
ALHA81029	153	L6	C	A	RKPA80264	23	L6	B	B
ALHA81099	151	L6	A/B	A	ALHA78015*	34	LL(?L)3		
ALHA81106	48	L6	B	B	ALHA76004	305	LL3	A	A
ALHA81107	139	L6	B	A	ALHA77278	312	LL3	A	A
ALHA81122	20	L6	B	B	ALHA79003	5	LL3	B	B
BTNA78001	160	L6	B	B	ALHA81251	158	LL3	B/C	B
BTNA78002	4301	L6	B	A	ALHA77060**	64	LL5	A	
EETA79003	435	L6	B	B	ALHA78109	233	LL5	A/B	A
EETA79010	287	L6	B	C	RKPA80234	136	LL5	B	B
META78002	542	L6	B	A	RKPA80253	4	LL5	A/B	A
META78003	1726	L6	B	B	ALHA77041**	16	LL6	A	
META78005	172	L6	B	B	ALHA78153	151	LL6	B/C	B
META78028	20657	L6	B	B	ALHA81123	2	LL6	B	A
RKPA78001	234	L6	C	B	BTNA78004	1079	LL6	B	A
RKPA78003	1276	L6	C	B	PCA82500	90	LL6	B	C
RKPA79001	3006	L6	B	C	RKPA80222	6	LL6	B	B
RKPA79002	203	L6	B	B	RKPA80235	261	LL6	A/B	B
RKPA80202	544	L6	B	A	RKPA80238	18	LL6	A/B	A
RKPA80215	9	L6	C	B	RKPA80248	11	LL6	A/B	A
RKPA80219	21	L6	B	A					

	Class and type	*Class weight (g)*
Subtotals:	C2	66
	C3	1000
	E5	20
	E6	695
	E4	158
	H3	348
	H4	69549
	H5	25301
	H5,6	30
	H6	31453
	H?	8
	L3	20667
	L3,4	31
	L4	3637
	L5	5385
	L6	53889
	LL(L)3	34
	LL3	780
	LL5	437
	LL6	1634
Total:		215122

TABLE B.—Continued

Specimen number	Weight (g)	Class and type	Degree of weathering	Degree of fracturing	Specimen number	Weight (g)	Class and type	Degree of weathering	Degree of fracturing
				ACHONDRITES					
ALHA81005	31	Anorthositic breccia	A/B	A	ALHA81012	36	Eu	A/B	A
					EETA79004	390	Eu	B	B
ALHA78113	298	Au	A/B	A	EETA79005	450	Eu (polymict)	A	B
					EETA79011	86	Eu (polymict)	B	B
ALHA77256	676	Di	A/B	A	PCA82501	54	Eu (unbrecciated)	A	A
EETA79002	2843	Di	B	B	PCA82502	890	Eu (unbrecciated)	A	A
ALHA76005	1425	Eu (polymict)	A	A	RKPA80204	15	Eu	A	A
ALHA77302	235	Eu (polymict)	A	A	RKPA80224	8	Eu (unbrecciated)	A/B	A
ALHA78040	211	Eu (polymict)	A	A	TIL82403	49	Eu (brecciated)	A	A
ALHA78132	656	Eu (polymict)	A	A					
ALHA78158	15	Eu (polymict)	A	A	ALHA78006	8	Ho	A	A
ALHA78165	20	Eu (polymict)	A	A	EETA79006	716	Ho	B	B
ALHA79017	310	Eu (polymict)	A	A	EETA82600	247	Ho	A	B
ALHA80102	471	Eu (polymict)	A	B	ALHA77005	482	Sh	A	A
ALHA81001	52	Eu (anomalous)	A	B	EETA79001	7942	Sh	A	A
ALHA81006	254	Eu (polymict)	A	A/B					
ALHA81007	163	Eu (polymict)	A/B	A	ALHA77257	1995	Ur	A	B
ALHA81008	43	Eu (polymict)	A/B	A/B	ALHA78019	30	Ur	B/C	C
ALHA81009	229	Eu	A	A	ALHA78262	26	Ur	B/C	A
ALHA81010	219	Eu (polymict)	A	A	ALHA81101	119	Ur	A/B	B
ALHA81011	405	Eucritic breccia	A/B	A	RKPA80239	5	Ur	B	B

	Class and type	*Class weight (g)*
Subtotals:	Anorthositic breccia	31
	Aubrite	298
	Diogenite	3519
	Eucrite	6686
	Howardite	971
	Shergottite	8424
	Ureilite	2175
Total:		22104

Specimen number	Weight (g)	Class and type	Degree of weathering	Degree of fracturing	Specimen number	Weight (g)	Class and type	Degree of weathering	Degree of fracturing
				IRONS					
ALHA81013	17727	Hexahedrite			ALHA77250	10555	IA		
ALHA81014	188	Octahedrite			ALHA77263	1669	IA		
ALHA80104	882	Ataxite			ALHA77283	10510	IA		
ALHA77255	765	Ataxite (anom)			ALHA77289	2186	IA		
ALHA76002	1510	IA			ALHA77290	3784	IA		

TABLE B.—Continued

Specimen number	Weight (g)	Class and type	Degree of weathering	Degree of fracturing	Specimen number	Weight (g)	Class and type	Degree of weathering	Degree of fracturing
PGPA77006	19068	IA			DRPA78006	389	IIB		
ALHA78100	85	IIA			DRPA78007	11800	IIB		
DRPA78001	15200	IIB			DRPA78008	59400	IIB		
DRPA78002	7188	IIB			DRPA78009	138100	IIB		
DRPA78003	144	IIB			ALHA78252	2789	IVA		
DRPA78004	133	IIB			RKPA80226	160	Octahedrite		
DRPA78005	18600	IIB			*Total:*	322832			
					STONY-IRONS				
ALHA81098	70	M	C	B/C	RKPA80246	5	M	C	C
ALHA77219	637	M	B	B	RKPA80258	4	M	B/C	B
ALHA81059	539	M	C	B/C	RKPA80263	16	M	C	B
RKPA79015	10022	M	A/B	A	*Total:*	11307			
RKPA80229	14	M	C	B/C					

TABLE C.—Meteorites from common falls tentatively identified as paired specimens (t = field relations; v = physical similarities; w = petrographic similarities; x = metallography; y = bulk chemistry; z = trace element chemistry).

Pair no.	Paired specimens	Criteria
	EUCRITES	
1	ALHA76005, 77302, 78040, 78132, 78158, 78165, 79017, 80102, 81006, 81007, 81008, 81010	v, w
2	ALHA81009, 81012	v, w
	UREILITES	
3	ALHA78019, 78262	v, w
	C2 CHONDRITES	
4	ALHA77306, 78261, 81002, 81004	w
	L3 CHONDRITES	
5	ALHA77011, 77015, 77031, 77033, 77034, 77036, 77043, 77047, 77049, 77050, 77052, 77115, 77140, 77160, 77163, 77164, 77165, 77166, 77167, 77170, 77175, 77178, 77185, 77211, 77214, 77241, 77244, 77249, 77260, 77303, 78038, 78188, 79001, 79045, 80133, 81025, 81030, 81031, 81032, 81053, 81060, 81061, 81065, 81066, 81069, 81085, 81087, 81121	w
6	ALHA77215, 77216, 77217, 77252	t, v, w
	L4 CHONDRITES	
7	RKPA80216, 80242	w
	L5 CHONDRITES	
8	ALHA81017, 81018, 81023	w
	L6 CHONDRITES	
9	ALHA77001, 77150, 77180, 77292, 77293, 77296, 77297, 77305	t, v, w
10	ALHA77231, 77269, 77270, 77272, 77273, 77277, 77280, 77281, 77282, 77284	t, v, w
11	ALHA78043, 78045	w
12	ALHA78103, 78104, 78105	t, w
13	ALHA78112, 78114	w
14	ALHA78126, 78130, 78131	w
15	ALHA78105, 78251	v
16	ALHA80101, 80103, 80105, 80107, 80108, 80110, 80112, 80113, 80114, 80115, 80116, 80117, 80119, 80120, 80125	v, w
17	ALHA81027, 81028, 81029	w
18	BTNA78001, 78002	v, w
19	RKPA78001, 78003, 79001, 79002, 80202, 80219, 80225, 80252, 80261, 80264	w
	LL3 CHONDRITES	
20	ALHA76004, 81251	w
	LL6 CHONDRITES	
21	RKPA80222, 80238, 80248	w

TABLE C.—Continued

Pair no.	Paired specimens	Criteria
	H4 CHONDRITES	
22	ALHA77004, 77190, 77191, 77192, 77208, 77222, 77223, 77224, 77225, 77226, 77232, 77233	t, w
23	ALHA78084, 81022	w
24	ALHA78193, 78196, 78223	t, x
25	ALHA81041, 81043, 81044, 81045, 81046, 81047, 81048, 81049, 81050, 81051, 81052	w
	H5 CHONDRITES	
26	ALHA77014, 77264	t
27	ALHA77021, 77025, 77061, 77062, 77064, 77071, 77074, 77086, 77088, 77102	t, w
28	ALHA77118, 77119, 77124	t
29	ALHA78209, 78221, 78225, 78227, 78233	t, x
30	ALHA79031, 79032	w
31	ALHA80111, 80124, 80127, 80129, 80132	w
32	RKPA80217, 80218	w
33	RKPA80220, 80223	w
34	RKPA80250, 80251	w
	H6 CHONDRITES	
35	ALHA77144, 77148	t
36	ALHA77271, 77288	t
37	ALHA78211, 78213, 78215, 78229, 78231	t, x
38	ALHA80122, 80126, 80130	w
39	ALHA81035, 81038, 81103, 81112	w
40	RKPA80203, 80206, 80208, 80211, 80213, 80214, 80221, 80231, 80254, 80255, 80262, 80265, 80266	w
	E4 CHONDRITES	
41	ALHA77156, 77295	w
	MESOSIDERITES	
42	ALHA81059, 81098	w
43	RKPA79015, 80229, 80246, 80258, 80263	w
	IRONS	
44	ALHA76002, 77250, 77263, 77289, 77290	t, x, y, z
45	DRPA78001, 78002, 78003, 78004, 78005, 78006, 78007, 78008, 78009	t, v, x, y